The Design and Synthesis of MRI Contrast Agents for Imaging Cancer and Hypoxia.

Eleanor F Grimes, MChem.

Thesis submitted to the University of Nottingham for the degree of Doctor of Philosophy

March 2014

Abstract

The aim of this thesis was to develop a series of gadolinium(III) contrast agents based on the DOTA and AAZTA molecules used widely in the literature that will locate preferentially in hypoxic tumour cells. Three contrast agents were synthesised with alkyne tags, by adapting compounds already produced in the literature.

Whilst contrast agents in the clinic locate preferentially in cancer cells over normal tissues, they do not have the ability to inform a clinician about the type, or the environment of the cancer. One cancer environment that often leads to poor patient prognosis is hypoxia, as hypoxic tumours are both chemotherapy and radiotherapy resistant, whilst also promoting metastasis at a cellular level.

Under hypoxic conditions nitro-aromatic compounds can be enzymatically reduced to either the hydroxylamine or amine compounds. Once this has occurred either a leaving group can be lost, or partial ring breakdown occurs, which can then be attacked by molecules within the cell such as glutathione to form a covalent bond. This tethers the hypoxic marker within the hypoxic cell. Currently this technology is only used with nuclear medicine techniques, whilst this thesis outlines how this principle is to be used in conjunction with MRI technology.

The hypoxia markers were synthesised with azide functionalities to allow the two halves of these molecules to be conjugated using the copper (I)-catalyzed azide-alkyne cycloaddition. The conjugation occurred as the last step to produce a series of final compounds.

Once synthesised these contrast agents were characterised using NMR relaxivity calculations, to prove their effectiveness as contrast agents. They were also to undergo enzymatic tests using xanthine oxidase and glutathione to see if the nitro-aromatics can be reduced under hypoxic conditions, and thus their ability to locate within the hypoxic region of a tumour. Unfortunately this last step wasn't completed due to time constraints.

.

Acknowledgements

First I'd like to thank Prof Neil Thomas and Dr Walter Köckenberger for allowing me to undertake this project, followed by Cancer Research UK and The University of Nottingham.
Secondly I'd like to thank all past and present members of the Neil Thomas group and everyone who worked on A/C-Floor with me with note to David for proof reading my thesis. Special mention goes to the following:
Andrew and Austin for keeping me entertained and occasionally covering me in acetone!
James and Terry for teaching me the rules of football against my will.
Sarentha for having the kindest heart I've ever known.
Will for all the help advice and chats.
Stef also for all the help but also for the holidays and fun times.
Shailesh, Sarah, Andrea, Gavin, Dan, and Dave thanks for all the help, advice and Friday's down the pub!
All the technicians who've kept us up and running, notably Graham, Lee, Dane, Shaz, Kevin and Huw who've always been free to lend a hand when I've most needed it.
The CBS ski group – Lee/Chrissy/Ross/Hutch etc for giving me something to look forward to each year.
Finally Indi and Aditi, the 2 people who've kept me wanting to turn up even on the worst of days, and then taken me out for a Nando's to cheer me up. I wouldn't be here without your friendship.
Next I'd like to thank the many other friends I've had over the years, in particular the group from Cloister, Sophie/Ellie/Sara/Paulina/Hsu and Zoe.
Also for helping me retain my sanity I must thank both Notts Uni water polo and Hucknall Ladies water polo. I may never want to see the inside of Crisis again but I will miss you all, in particular Chari, Hannah, Ellie, Becky, Maxine, Katy and Naomi.
Finally I'd like to thank my family, Mum/Dad/Aunty Sheila and Saffy! You've always been supportive and I couldn't have done it without you.

Contents

List of Figures

List of Schemes

List of Tables

List of Equations

Abbreviations

2D	2 Dimensions
3D	3 Dimensions
AAZTA	1,4-*Bis*(hydroxycarbonylmethyl)-6-[*bis*(hydroxycarbonylmethyl)]amino-6-methyl-perhydro-1,4-diazepine
Ac	Acetate
ADEPT	Antibody directed enzyme prodrug therapy
ATP	Adenosine triphosphate
ATSM	Diacetyl-*bis*(N^4-methylthiosemicarbazone)
BAPTA	1,2-*Bis*(*o*-aminophenoxy)ethane-*N,N,N',N'*-tetraacetic acid
BOC	*tert*-Butyloxycarbonyl
BOLD	Blood oxygen level dependent
bs	Broad singlet
C	Concentration
C1	Complex 1
CDI	1,1'-Carbonyldiimidazole
CEST	Chemical exchange saturation transfer
CT	Computed tomography
d	Doublet
DBU	1,8-Diazabicyclo[5.4.0]undec-7-ene
DCC	Dicyclohexycarbodiimide
DCM	Dichloromethane
dHb	Deoxyhaemoglobin
DIBAL-H	Diisobutylaluminium hydride
DIPEA	Diisopropylethylamine
DMAP	4-Dimethylaminopyridine
DMF	Dimethylformamide
DNA	Deoxyribonucleic acid
DO3A	1,4,7-Triscarbonylmethyl-1,4,7,10-tetraazacyclododecane

DOTA	1,4,7,10-Tetraazacyclododecanetetraacetic acid
DPDP	Dipyridoxal-diphosphate
DPPA	Diphenylphosphoryl azide
DSPC	1,2-Diastearoyl-*sn*-glycerol-3-phosphocholine
DTPA	Diethylenetriaminopentacetic acid
E.coli	*Escherichia coli*
EDC	1-Ethyl-3-(3-dimethylaminopropyl) carbodiimide
EF5	2-(2-Nitro-1*H*-imidazol-1-yl)-*N*-(2,2,3,3,3-pentauoropropyl) acetamide
EI	Electron impact
ESI	Electrospray ionisation
Et	Ethyl
FLOOD	Flow and oxygen dependent contrast
FMISO	F-misonidazole
Fmoc	9-Fluorenylmethyloxycarbonyl
GSH	Glutathione
h	Plancks constant (6.626×10^{-34}Js)
Hb	Haemoglobin
HBTU	*O*-Benzotriazol-1-yl-*N,N,N′,N′*-tetramethyluronium hexafluorophosphate
HIF-1	Hypoxia inducing factor 1
HOBt	Hydroxybenzotriazole
HOPO	Hydroxypyridinone
HPLC	High performance liquid chromatography
HRMS	High resolution mass spectrometry
I	Intensity on MRI scan
IR	Infrared spectroscopy
K_d	Dissociation constant
K_{ex}	Exchange constant
LD_{50}	50% of lethal dose
Ln	Lanthanide metal

M	Magnetism present and Molar
m	Multiplet
M_s	Spin quantum number
Me	Methyl
M_o	Net magnetism
MOM	Methoxy methyl ether
mp	Melting point
MRI	Magnetic resonance Imaging
Ms	Mesyl
$N_{+1/2}$	Number of protons in the +1/2 spin state
$N_{-1/2}$	Number of protons in the -1/2 spin state
NMR	Nuclear magnetic resonance
PAMAM	Polyamidoamine
PBS	Phosphate buffered saline
PE	Petroleum ether
PEG	Polyethylene glycol
PET	Positron emission tomography
PO_2	Oxygen partial pressure
q	Number of water molecules bound to the central ion
q	quartet
QDOTAMA	1-(*N*-Quinolin-8-yl-acetamide)-4,7,10-tris(acetic acid)-1, 4,7,10-tetraazacyclododecane
r_1	Relaxivity
$R_{1,\ CA}$	Contrast agent relaxation rate
$R_{1,\ obs}$	Observed relaxation rate
$R_1,^{\ outer}$	Outer-sphere contribution to relaxation rate
$R_{1,\ tissue}$	Tissue relaxation rate
$R_1,^{inner}$	Inner-sphere contribution to relaxation rate
R_{1p}	Longitudinal paramagnetic relaxation rate

R_{2p}	Transverse paramagnetic relaxation rate
RF	Radiofrequency pulse
RNA	Ribonucleic acid
s	Singlet
SA	Square antiprismatic
siRNA	Small interfering RNA
S_N2	Substitution Nucleophilic Biomolecular
SPECT	Single photo-emission tomography
SPIO	Superparamagnetic iron oxide
Su	Succinimide
T	Temperature
t	Triplet
T_1	Longitudinal relaxation time
$T_{1,obs}$	Observed T1
$T_{1,tissue}$	Tissue T1
T_2	Transverse relaxation time
T_2*	Transverse relaxation time constant
TBAF	Tetra-*n*-butylammonium fluoride
TBS	*tert*-Butyl dimethylsilyl
TBTA	Tris(triazolyl)benzylamine
*t*Bu	*tert*-Butyl
TEA	Triethylamine
TFA	Trifluoroacetic acid
THF	Tetrahydrofuran
THPTA	Tris(hydroxypropyltriazolyl)methylamine
Ts	Tosyl
TSA	Twisted square antiprismatic
TV	Targeting vector
UV	Ultra-violet

β	Pulse angle
B_o	Applied magnetic field
γ	Gyromagnetic ratio ($2.7 \times 10^{8} rads^{-1}T^{-1}$ for a proton)
δ_C	Carbon NMR shift
ΔE	Energy difference
δ_H	Proton NMR shift
κ	Boltzmann constant ($1.38 \times 10^{-23} JK^{-1}$)
μ_{spin}	Magnetic moment
ν_{max}	Frequency maximum
τ_p	Pulse length
τ_R	Rotational correlation time
ω_1	Pulse frequency
ω_o	Larmour frequency

Chapter 1 - Introduction

1.1 Magnetic Resonance Imaging

Non-invasive imaging of the human body is a valuable tool in modern medicine, with a range of techniques in clinical use. The major imaging system used today is X-ray technology that was originally invented in 1895 by Wilhelm Röentgen. [(1)] Though other imaging systems including computed tomography (CT), nuclear medicine such as positron emission tomography (PET) and single photon emission computed tomography (SPECT), ultrasound and magnetic resonance imaging (MRI) are also widely available.

Without these techniques, clinicians would struggle to diagnose many serious diseases, such as multiple sclerosis, foetal spina bifida and certain cancers. These diseases would typically have been diagnosed only when they became much more advanced, resulting in a poorer prognosis and requiring patients to undergo significantly more invasive procedures.

MRI is a favourable method of visualising the body for three major reasons: its non-invasive nature; good spatial resolution of ≤10 μm in 3D; and lack of adverse effects from either the magnetic field or the radiofrequency (RF) pulses used clinically, even to foetuses. [(2)]

The magnetic resonance phenomenon was discovered independently by Bloch and Purcell in 1946, but it was not until 1973 that the first image was produced. [(3)] In 1971 Damadian proved that natural and certain pathogenic tissues had different proton relaxation times, yet it took until 1977 for Damadian, Minkoff and Goldsmith to produce the first human scan using this technology. Although

this initial scan took five hours to complete, imaging has since been reduced to mere seconds and in 1999 the first portable MRI technology produced by Magne Vu (TM) became commercially available. (4)

1.1.1 NMR Principles

MRI is based on the same principles as nuclear magnetic resonance (NMR), though most medical MRI uses the protons within the body to produce an image.

The nucleus of a hydrogen atom is a single positively charged proton that precesses constantly around an axis. Like all other nuclei a proton has its own magnetic field, called its magnetic moment, or μ_{spin}.

If an external magnetic field is applied to a proton, the nucleus will experience a force that is called torque as it is forced to align with the applied field (B_o). The precession that the proton undergoes now it is aligned with the external magnetic field is proportional to the external field and described by the Larmor frequency (ω_o) in Equation 1. (5)

$$\omega_{\mathrm{O}} = \gamma \times B_{\mathrm{O}}$$

Equation 1 The relationship between precession of a proton and the external magnetic field. γ is the gyromagnetic ratio (2.7 x 10^8rads^{-1}T^{-1} for a proton). (5)

During the application of the external field the proton will either align parallel or antiparallel with the field, thus creating two different proton spin-states. These spin states are both thermodynamically stable but differ slightly in energy. This difference is characterised by the spin quantum number m_s, though the extent of the energy difference is dependent on the extent of the external magnetic field, as seen in Figure 1. (6)

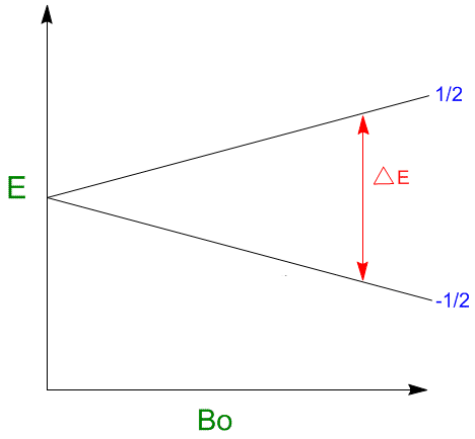

Figure 1. The relationship between *ΔE* and B_o for spin up and spin down protons. [6]

The energy difference in Hertz (Hz) can be calculated using Equation 2.

$$\Delta E = \frac{\gamma h B_o}{2\pi}$$

Equation 2 The difference in energy between parallel and antiparallel aligned protons with regards to the magnetic field, gyromagnetic ratio and Plancks constant. (*h* (6.626 x 10^{-34}Js)). [6]

The ratio between the populations of protons in each of these states is not equal, instead there are marginally more protons to be found in the +1/2 spin state compared to the -1/2 at room temperature, and the ratio of these spin states can be calculated using a Boltzmann equation (Equation 3).

$$\frac{N_{+1/2}}{N_{-1/2}} = exp\ \frac{-\Delta E}{\kappa T} = exp\ \frac{-h\gamma B_o}{2\pi\kappa T}$$

Equation 3 The ratio between the number of protons found in the spin up and the spin down state. [6]

At equilibrium the protons precess at an angle out of phase in the z axis in the magnetic field (Figure 2).

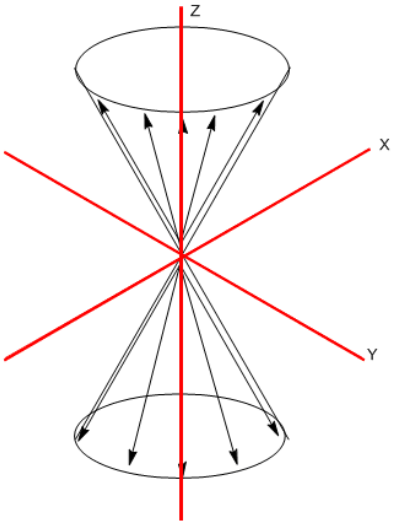

Figure 2 The angle of proton precession when in an external magnetic field. [6]

When the net magnetism (M_o) is calculated it is found to be aligned with the main field B_o in the z axis (Figure 3).

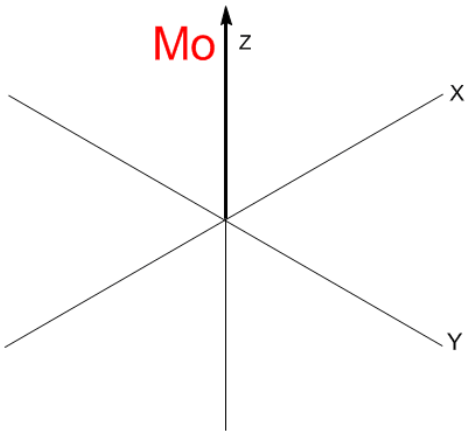

Figure 3 Direction of the averaged total magnetism. [6]

It is impossible to measure the net magnetism when the protons are in equilibrium with the external field, as the net magnetism is in the order of microtesla (μT), and thus negligible when compared to the external field, which is in the region of 3-5 tesla (T). The net magnetism can be measured when it is rotated into the transverse x,y plane, and a transverse plane detector is used. The precession towards the x,y plane in the direction of the y axis can be caused by applying a RF pulse created by a coil placed along the x-axis (Figure 4).

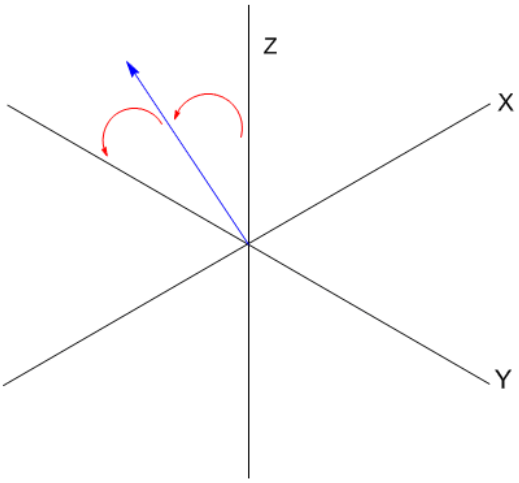

Figure 4 The precession of M_o after RF pulse is applied. [6]

The angle through which the RF pulse can rotate is related to Equation 4. Most MRI scanners calculate the length of the pulse so that the pulse angle (β) is equal to $\pi/2$ (90^o) or π (180^o).

$$\beta = \omega_1 t_p$$

Equation 4 The relationship between the frequency and length of the pulse to produce the desire pulse angle. RF pulse (ω_1), length of the pulse (t_p). [6]

After the pulse has been removed, the protons start to relax back to their equilibrium state. There are two types of relaxation, both independent of each other, longitudinal relaxation and transverse relaxation.

The longitudinal relaxation time (T_1) is inversely dependent on the field strength. During the RF pulse the population of protons in the spin up and spin down positions in the x,y plane is equal. Once the RF is removed the imbalance found at equilibrium is restored. This longitudinal relaxation can take up to a few seconds to equilibrate. [6]

The transverse relaxation time (T_2), also known as the spin-spin relaxation time is independent of field strength, and involves the loss of magnetism in the x,y plane back to zero at equilibrium. Compared to the T_1 relaxation time, T_2 is very quick and only requires milliseconds to reach equilibrium. For example the T_1 for fluids is 1500-2000 ms, whilst the T_2 is 700-1200 ms, and the T_1 for lipids is 192 ms, compared to 10-100 ms for the T_2. [2]

1.1.2 Applying NMR Principles to MRI.

Since clinical MRI uses protons to produce an image, it relies on the fact that the human body is composed of between 55% and 78% water depending on the tissue type. [7] These water molecules are found within three main environments: the fluids, such as blood and lymph; the water based tissues, including muscles and the brain; and finally the fat based tissues, such as the

adipose and bone marrow. The protons present in these environments have different relaxation times, with fat based tissue protons having a much shorter relaxation times than the fluid protons. Due to this effect an image in grey scale can be built up with regards to the magnetism at the point of acquisition.

The other factor that affects the intensity of the image shown is the concentration of protons at the specific location. This relationship is shown in Equation 5.

$$I = C \times M$$

Equation 5 The relationship between the concentration of the contrast agent and the magnetism present to produce the intensity seen on the MRI scan. [8]

During a typical MRI scan, the RF pulse is repeated at a constant rate and the overall data is averaged. This can help improve contrast as those protons in environments with long relaxation times will not fully relax in between pulses creating a lower intensity. Scans are either T_1 or T_2 weighted; the main difference between them is that in T_1 weighted scans protons with a longer relaxation time appear darker whilst in T_2 weighted images they appear brighter. T_2 weighted images can also have less picture clarity as shorter T_2 relaxation times produce broader line widths, and if they get too broad this becomes indistinguishable from background noise. [8]

1.2 MRI Contrast Agents

MRI can detect different tissues due to variations in relaxivity of the protons in these environments. The same is the case with pathogenic tissues versus normal tissues as proven by Damadian in 1977. [9] However, in some cases the

pathogenic defects vary only slightly from the normal tissues, such as in the case of cerebral lesions of the blood brain barrier. In this instance a contrast agent is used as it allows for visualisation of tissue changes not easily seen on a standard magnetic resonance image.

The total effect a contrast agent can have on improving the images can be calculated by measuring the relaxation rate using a MRI scanner. It must be remembered that the observed relaxation rate consists of contributions from both the intrinsic relaxation rate of the tissue, and the relaxation rate of the contrast agent, as seen in Equation 6.

$$R_{1,obs} = R_{1,tissue} + R_{1,CA}$$

Equation 6 An equation to show how the observed relaxation is the sum of relaxation rate contributions from both the underlying tissue and the contrast agent. [10]

Since the relaxation rate of the contrast agent is dependent on both the intrinsic relaxivity and the concentration of the contrast agent,

Equation **7** can be produced.

$$R_{1,CA} = r_1 \times [CA]$$

Equation 7 An equation to show how the relaxation rate of the contrast agent is dependent on both the inherent relaxivity of the contrast agent, and its localised concentration. [10]

As R_1 is equal to $1/T_1$ this leads to Equation 8 that shows the concentration of contrast agent is linearly proportional to the relaxivity.

$$\frac{1}{T_{1,obs}} = \frac{1}{T_{1,tissue}} + (r_1 \times [CA])$$

Equation 8 An equation to show the relationship between the observed T_1, the T_1 of the tissue and the relaxivity of the contrast agent. [10]

This equation illustrates that the two previously mentioned factors, concentration of protons and local relaxation, affect the intensity seen on the MR image. Since increasing proton density at specific locations is impractical, the best option is to add a compound that affects the relaxation time of the local protons. The current method of choice involves the use of a paramagnetic metal ion complex that enhances imaging by greatly decreasing T_1, this is usually a gadolinium(III) based complex which contains seven unpaired electrons. These ions increase the relaxation rate of the surrounding and interchangeable water molecules, and thus increase the intensity in T_1 weighted images producing a bright white area (Figure 5). [10]

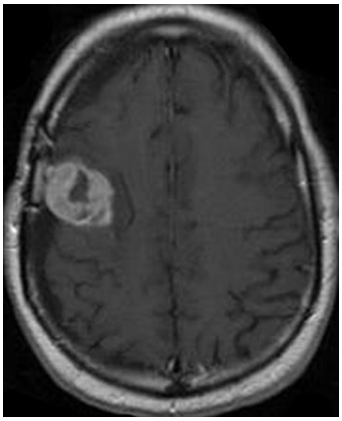

Figure 5 A T_1 weighted image using a contrast agent to show a brain lesion.

Reprinted with permission from [11]. Copyright (2009) American Journal of Roentgenology

The complexed paramagnetic ion is surrounded by three types of water molecule. The inner-sphere water molecules are bound directly to the paramagnetic ion, these can interchange with the surrounding bulk water and produce the greatest effect on the overall relaxivity due to it proximity to the paramagnetic ion. The second-sphere water molecules, are hydrogen bonded to the organic chelate binding the paramagnetic ion. They undergo rapid exchange with the surrounding bulk water and their relaxivity is much less affected, due to the larger distance to the metal ion and the shorter period of time they reside on the complex before undergoing exchange. The final outer-sphere or bulk water comprises of the water surrounding the complex as the contrast agent diffuses through the tissue (Figure 6). All of these spheres contribute to the total relaxation rate of the contrast agent as seen in Equation 9. [12]

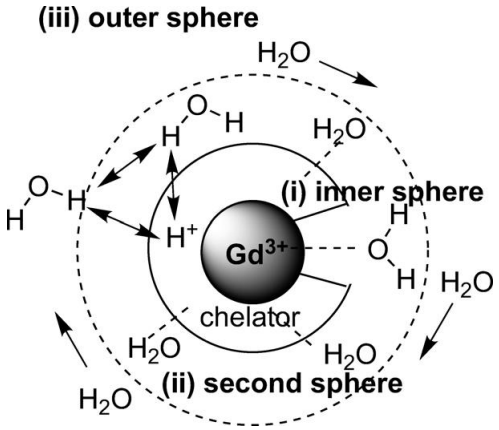

Figure 6 The three types of water molecule which undergo a change in relaxivity when in proximity to a paramagnetic ion.

$$R_{1,CA} = R_1^{inner} + R_1^{outer}$$

Equation 9 An equation to show how the overall relaxation rate of the contrast agent is comprised of contributions from both inner sphere and outer sphere relaxation. [10]

The mechanism of exchange found for the inner-sphere water molecules is a dissociative one, where the present molecule leaves the central gadolinium ion to form an eight coordinate complex in most cases, before another water molecule can coordinate to reform the parent structure. [8]

Although paramagnetic ions such as gadolinium(III) effectively reduce T_1 relaxation time, the metal must be complexed sufficiently with organic ligands, as the metal ion itself has a high toxicity at the dose administered to patients. This is due to gadolinium(III)'s similar size and donor ability to calcium(II). Therefore, free gadolinium(III) can bind to serum proteins at calcium sites and irreversibly enter bone. To prevent these side effects the chelator must strongly bind to the gadolinium(III) in a thermodynamically and kinetically stable manner. [10]

1.2.1 Current Contrast Agents

There are several gadolinium(III) based contrast agents on the market, the most common of which are; Magnevist (**1**) (Bayer HealthCare Pharmaceuticals), [13] Omniscan (**2**) (GE Healthcare) [14] and Prohance (**3**) (Bracco Diagnostics) [15]. These compounds are all administered intravenously (0.1 mmol/Kg dose) and are excreted *via* the kidneys within 24 hours. [16] They effectively visualise vasculature in the brain, spine and associated tissues, with regards to viewing lesions and abnormalities within these structures, however

there are many pathogenic tissues, such as certain tumours that are difficult to visualise effectively with the current contrast agents.

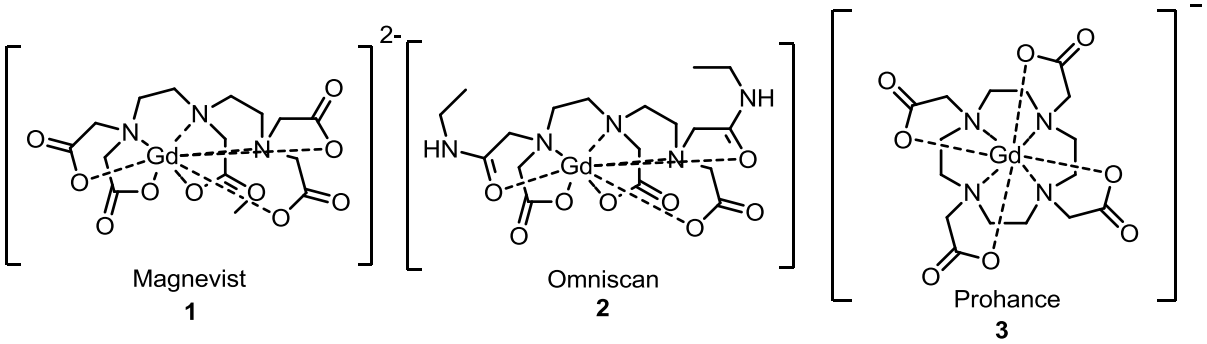

Figure 7 Contrast agents currently on the market.[13-15]

These commercially available compounds are not perfect and are in need of optimisation. Due to the need for strong chelation, all of the commercially available compounds routinely used are octadentate, leaving only one free site for inner-sphere water molecules, and are therefore more dependent on second-sphere binding. They also are far from optimal with regards to inner-sphere water molecule lifetimes, with a proton lifetime of 230 ns (Prohance) instead of the calculated optimal of 13 ns. [17] The other phenomenon affecting relaxivity is a property called reorientation correlation time (molecular tumbling), in which the slower the tumbling, the greater the increase in relaxivity. This effect is best observed in large rigid molecules, and thus the relatively small commercial contrast agents benefit little from molecular tumbling.

Nephrogenic Systemic Fibrosis

The most severe side effect of gadolinium(III) contrast agents is nephrogenic systemic fibrosis. This disease can cause fibrosis of the skin, joints, eyes and internal organs, which if severe enough can even lead to the death of the patient. Whilst first described in 2000, it was not until 2006 that the connection

between the disease and gadolinium (III) based contrast agents was made. The contrast agent most associated with this disease is Omniscan, a non-ionic linear agent, which has poor kinetic stability for gadolinium(III), and a K_d value of 1.4×10^{-17} M, [18] and is thus more likely to release into the blood, unlike Prohance which is more stable, due to its crown based structure, [19] with a K_d value of 1.5×10^{-24} M. [18] As the pH in the kidneys is lower than that of the surrounding tissues the gadolinium(III) is more likely to be released by the chelators with poor kinetic stability. For this reason the disease is seen almost exclusively in patients with acute or chronic renal failure, who due to their slower glomerular filtration rate have the contrast agent lingering longer in their bodies, and thus the gadolinium(III) is more likely to separated from the chelate. Since this connection has been made, gadolinium(III) based contrast agents have been withheld from patients with a glomerular filtration rate of <30 mL min^{-1}, resulting in there being no new reported cases of the disease since 2008. [20]

1.2.2 Experimental Contrast Agents

There are relatively few contrast agents that have passed into clinical usage: however, there are many novel therapeutics in the literature that are aimed to produce more effective and targeted contrast agents to be used in conjunction with MRI. These experimental ideas can be categorised with regards to how they try and improve upon the commercially available contrast agents, with the main areas of research outlined below.

Increased inner-sphere water molecules

By doubling the number of inner-sphere water molecules, you can double the number of water molecules affected by the paramagnetic ion.

Hydroxpyridinone ligands

Hydroxypyridinone (HOPO) complexes are a series of molecules designed to replace the current eight coordinated nitrogen and oxygen donor chelators on the market today. The HOPOs are chelators that consist of just oxygen donors, and since they occupy fewer sites on the central gadolinium(III) ion an extra water molecule can bind forming a $q = 2$ (q = number of water molecules bound to the central ion,) chelate instead of the usual $q = 1$. Unlike other current contrast agents, the HOPO molecules do not require a change of conformation to achieve the eight coordinated intermediate, reducing the energy required for water exchange. This increased exchange rate results in a greatly increased relaxivity with values of 10.5 $mM^{-1}s^{-1}$, compared to 4-5 $mM^{-1}s^{-1}$ (20 MHz 298 K), for those compounds already on the market. Poor solubility was a problem with these compounds which has been partially solved by the addition of polyethylene glycol (PEG) to the terephthalamide ligand of the Gd-TREN-*bis*HOPO-TAM complex (**6**) (Figure 8). [21]

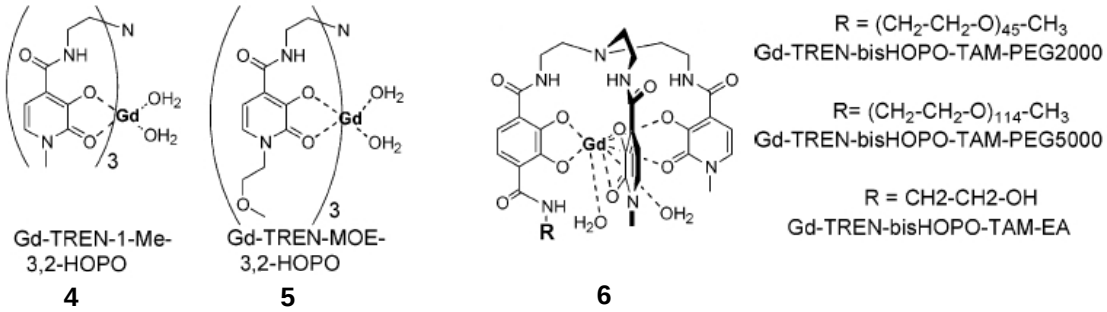

Figure 8 HOPO based complexes.

Reprinted with permission from [21]. Copyright (2005) American Chemical Society

Increased gadolinium concentration at site

The sensitivity of MRI is very low, so to combat this, a high concentration of contrast agent is required. One way to produce this high concentration is to synthesise molecules capable of carrying a high payload.

Fullerene ligands

A recent development now available is the use of fullerenes to contain a payload of gadolinium(III) ions. Originally only 4 % of gadolinium(III) endohedrals were of the soluble $Gd@C_{82}$ fullerene, since then it has been possible to produce a series of $Gd@C_{60}$ fullerenes that are highly soluble and air stable. These are $Gd@C_{60}[C(COOH)_2]_{10}$ **7** and $Gd@C_{60}[C(COOCH_2CH_3)_2]_{10}$, (Figure 9) and they have been proven to have similar relaxivities to the commercial contrast agents with values of 4.6 mM^{-1} s^{-1} (20 MHz, 298 K) despite relying on outer sphere contributions. These compounds also prevent any release of gadolinium(III) ions, and thus reduce the risk of nephrogenic systemic fibrosis. [22] Other gadofullerenes such as $Gd_3N@C80(OH)_{26}$ $(CH_2CH_2COOH)_{16}$ have shown relaxivity values of up to 282 mM^{-1} s^{-1} (0.47 T, 298 K) at 2.4 T, which is over fifty times greater than that seen for the commercial contrast agents. [23]

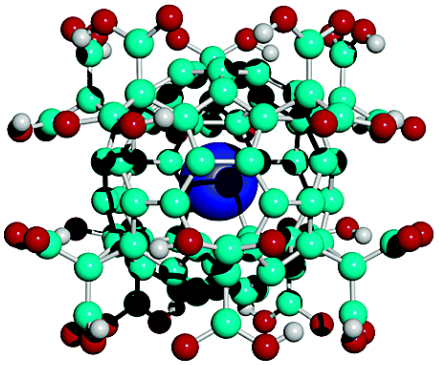

$Gd@C_{60}[C(COOH)_2]_{10}$

7

Figure 9 A gadolinium fullerene complex (7).

Reprinted with permission from [22]. Copyright (2003) American Chemical Society

Liposomes

A series of liposomes containing chelated gadolinium(III) ions have been synthesised. The liposome technology is well established and can carry significantly larger payloads than a single chelator. Since they have already been generally optimised with regards to stability, circulation times and membrane composition, liposomes of between 5-500 nm in size can be easily modified to include MRI active paramagnetic ions, or a fluorescent molecule for imaging and targeting vectors for localisation. A typical MRI contrast liposome can be seen in Figure 10. [24]

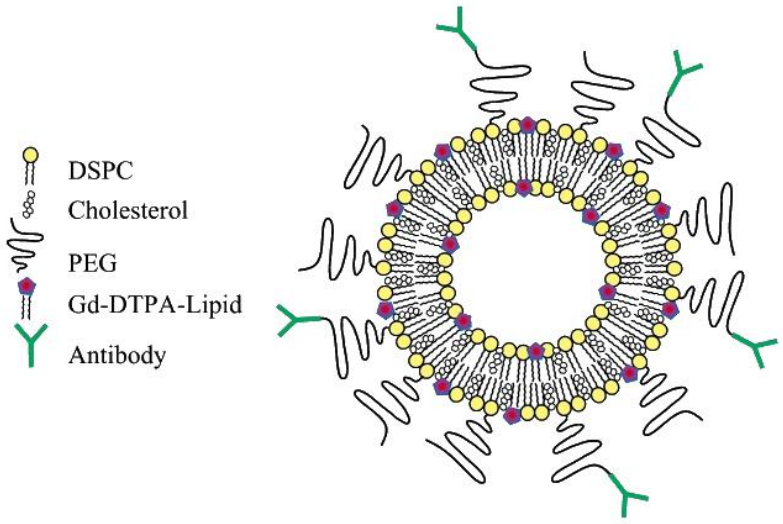

8

Figure 10 A gadolinium(III) contrast agent liposome.

Reprinted with permission from [24]. Copyright (2004) American Chemical Society

One specific use of the contrast liposomes has been to target sites of apoptosis (programmed cell death). When tumour cells react to radiation and chemotherapy they usually undergo apoptosis, and by measuring this *via* a medium such as MRI, a patients response to a specific treatment can be visualised. When a cell undergoes apoptosis, the lipid phosphatidylserine translocates to the external layer of the cell membrane, which can then be detected *via* conjugation to the proteins annexin A5 or synaptotagmin I in the presence of calcium(II). Targets for these proteins can be incorporated into the liposome bilayer allowing for liposome localisation at the tumour site. [25] Other interesting targeting molecules such as the peptide $\alpha_v\beta_3$ integrin (a marker for angiogenesis) can be added *via* conjugation to the head of 1,2-diastearoyl-*syn*-glycerol-3-phosphocholine (DSPC) *via* a PEG linker. [26]

Decreased molecular tumbling

Decreasing the molecular tumbling rate has been shown to increase relaxivity of the contrast agents at clinical imaging fields (0.5-1.5 T). The best way to achieve this is by significantly increasing the molecular weight of the contrast agent.

Contrast agents attached to dendrimers

Dendrimers are three dimensional oligomeric structures based on a single repeating unit. They produce structures that have a uniform surface chemistry, and due to their rigidity when compared to linear polymers of a similar nature, they can decrease the tumbling properties of the gadolinium(III) ion, thus increasing its effect on T_1 relaxivity. One of the basic dendrimeric structures is the starburst polyamidoamine (PAMAM) dendrimer **9** (Figure 11). These dendrimeric structures can chelate many gadolinium(III) ions in a single macromolecule allowing for a higher concentration of the paramagnetic ion, and therefore a greater effect on relaxivity can be seen. [27] The major issue with these contrast agents is their inability to cross membranes into surrounding tissues, thus limiting their usage to visualising vascular targets. There have also been questions raised about their toxicity, this time from the polyamide ligand. [28]

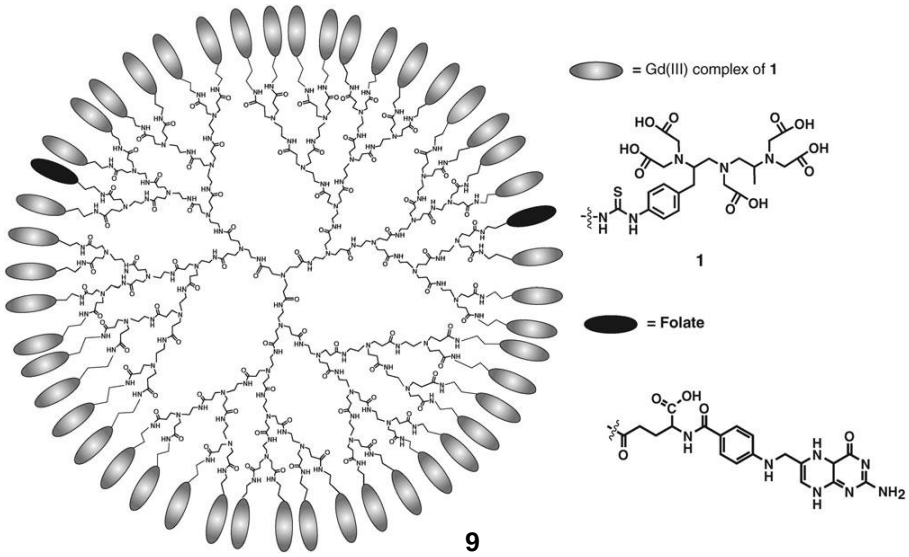

Figure 11 A PAMAM dendrimer structure.

Reproduced from Ref. [27] with permission from the Centre National de la Recherche Scientifique (CNRS) and The Royal Society of Chemistry.

Gadolinium dimers

It has been discovered that a dimer with increased rigidity between the two metal centres has a greater increase in relaxivity than expected by doubling the number of free water molecule binding sites. This is due to decreasing the tumbling rate of the contrast agent. A dimer with a xylene based rigidity core, and a heptadentate chelator allowing for two water molecules to bind to each individual gadolinium(III) ion has been synthesised (**10**) (Figure 12). [29] Another similar molecule has been synthesised, this time with an iron terpyridine core and two terminal diethylenetriamine-*N,N,N'',N''*-tetraacetate gadolinium(III) complexes (**11**) (Figure 12). Although this complex has greater rigidity and thus greater relaxivity, the thermodynamic stability of the complex is greatly reduced. [30]

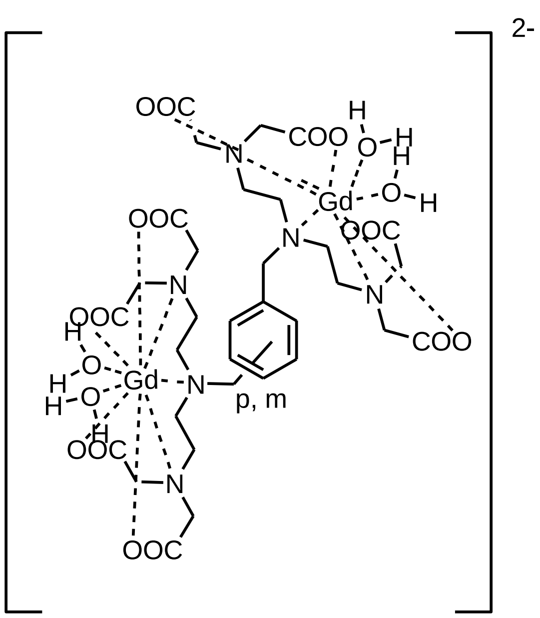

10

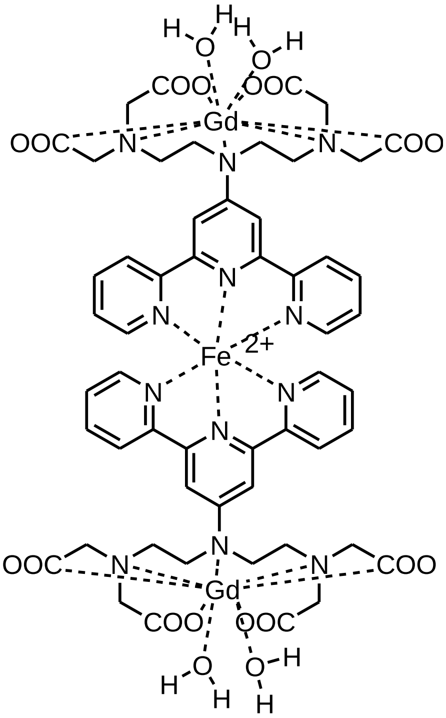

11

Figure 12 The double gadolinium(III) ion complex with a xylene based core (10). The double gadolinium(III) ion complex with an iron terpyridine core (11). [29-30]

"Smart" MRI contrast agents

Intelligent contrast agents that change their level of activity only in targeted regions can be synthesised. This can occur *via* one of two methods, by changing the *q* value, usually by losing masking group from the central gadolinium ion [31] or by having an effect on molecular tumbling. [32]

ADEPT MRI contrast agents

The first MRI contrast agents sensors designed and synthesised were by Moats *et al.* [33] and were activated using *β*-galactosidase an enzyme associated with the Antibody Directed Enzyme Prodrug Therapy (ADEPT) system. This technique uses a non-endogenous enzyme that has been conjugated to an antibody fragment that targets a receptor found primarily on tumour cells. This

complex is administered initially and allowed to localise, before a prodrug contrast agent is administered. The non-endogenous enzyme then cleaves a group attached to the central gadolinium(III) ion to produce the active contrast agent with a free water binding site, which can be used to decrease the relaxivity of the surrounding bulk water (Figure 13). [34]

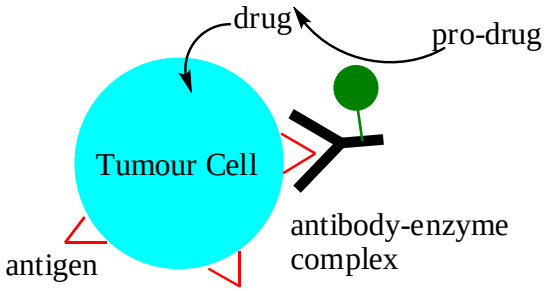

Figure 13 Antibody-enzyme conjugate. [34]

The enzyme *β*-galactosidase cleaves the sugar *β*-galactopyranosides from the contrast agent (**12**) to produce a free site on the gadolinium(III) ion for a water molecule to bind (Scheme 1)

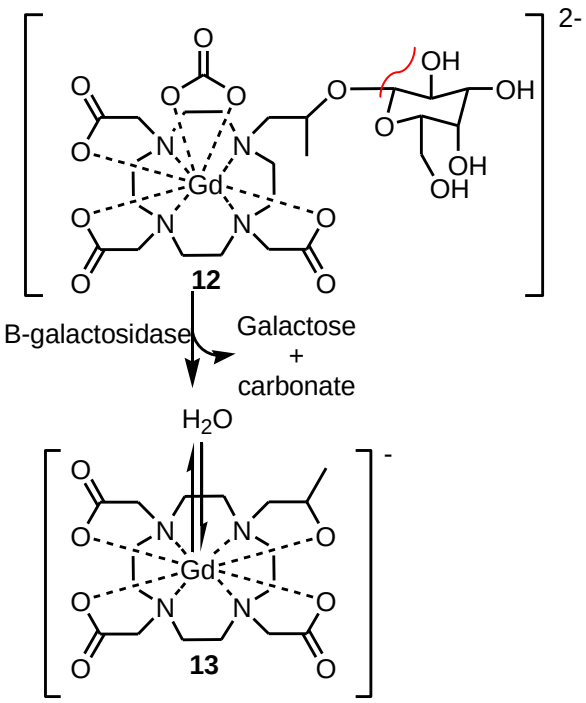

Scheme 1 The release of *β*-galactopyranoside and carbonate to produce a water binding site in the presence of *β*-galactosidase. [35]

Other work in this area uses the *β*-glucoronidase enzyme, which has also been used to release free sites on the gadolinium(III) opening it up for inner-sphere water binding. [31] Yet more recent work has taken this principle to mask albumin binding groups, thus resulting in an increased relaxivity due to slowing the molecular tumbling. [36]

Metal ion sensor contrast agents

Metal ion sensors are of great importance as ions like calcium(II) are widely used for regulation in humans, whilst other metals including copper are associated with disease states such as Wilson's disease. [37] The greatest challenge with these types of sensors is making the ligand specific enough for the metal to prevent false positive activation from other similar metals. To do this scientists must tune the ligands to force the selectivity, using properties

such as a preference for hard or soft donor atoms, and preferred co-ordination numbers. [32]

A method to study biological copper has been developed that allows for a MRI contrast agent to become active in the presence of copper. Thus, cellular copper accumulation and trafficking can be monitored. A DO3A-based chelate is attached to a pyridine moiety with side chains containing copper binding groups (O, N, S) (**14**). When inactive the pyridine binds to the gadolinium(III) and blocks the two free water binding sites, whilst in the presence of copper, the pyridine and its side chain bind the copper, allowing for two water molecules to bind to gadolinium's inner-sphere (**15**) (Scheme 2). This structure has a dual effect on decreasing the T_1 relaxation, as there are two inner-sphere binding sites instead of the usual one, and the copper binding increases overall molecular weight thus decreasing molecular tumbling. The major problem so far regarding this technique is specificity, as the contrast agents are often activated by other biological metals including zinc, although work is continuing to solve this. [38] To an extent this problem has been improved upon using other ligands to bind the copper as developed by Li *et al.* [39] with the Gd-QDOTAMA complex and Que *et al*. [37] who developed a chelate with a sulfur based ligand.

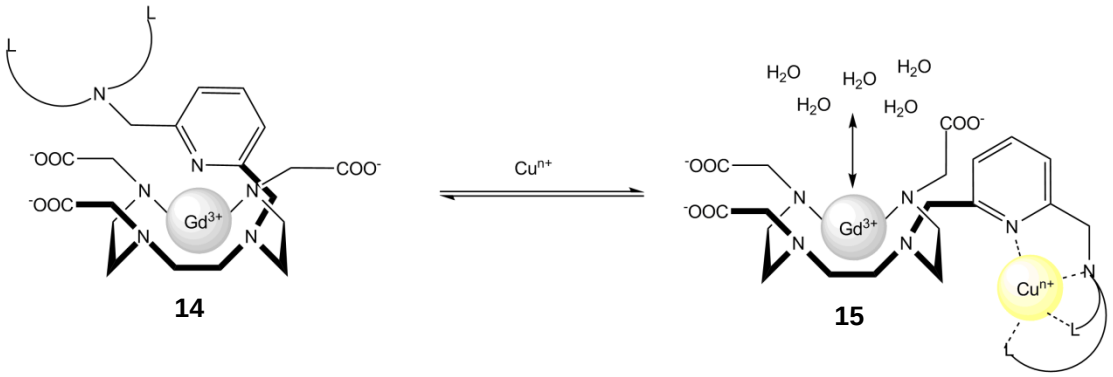

Scheme 2 Copper activation of a "smart" MRI contrast agent. [37]

The first calcium(II) sensors were also developed by Li *et al*. [40] and used a BAPTA ligand (**16**) that caused a *q* value change once calcium(II) had bound and could be used to measure intracellular calcium fluctuations. The acetate functionalities have since proven to be necessary for selectivity over magnesium(II) during the development of extracellular calcium(II) sensors. [41] These *bis*polyazamacrocyclic sensors (**17**) have since shown a 50% increase in relaxivity in extracellular brain models (Figure 14).

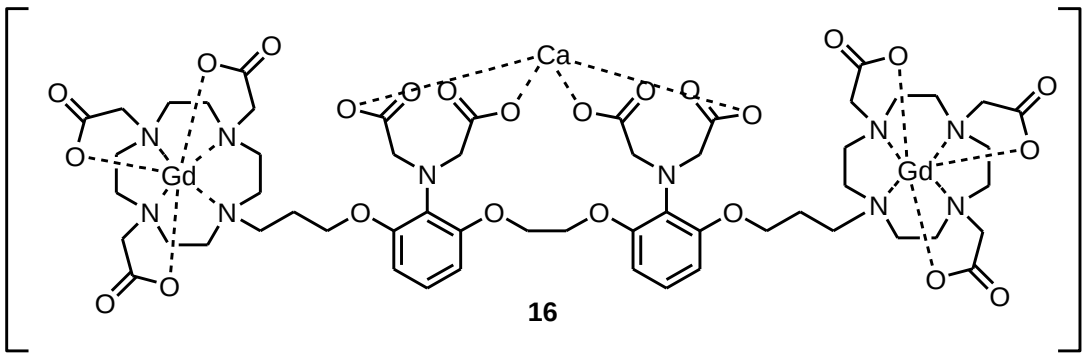

16

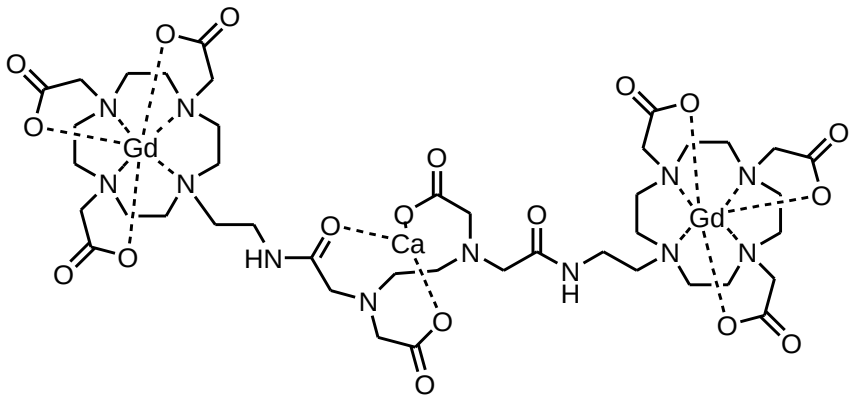

17

Figure 14 Gd-DOTABAPTA 16 [40] and the *bis*polyazamacrocyclic sensor (17). [41]

Other metal sensors have been worked on, most predominantly with zinc in which elevated levels have been associated with Alzheimer's disease. [12] Sensors for metals including potassium, [42] magnesium, [43] and iron [44] have also had varied success in terms of metal selectivity and change in relaxivity.

pH and redox sensor contrast agents

It has been noted that in certain tumours physical changes occur within the cells, this includes a reduction in pH and a change of reducing potential, these tumours can then be targeted using "smart" contrast agents.

The major difficulty with pH sensors is in keeping the result independent of concentration of the contrast agent, something which is often difficult to determine *in vivo*. The first to achieve this was Aime *et al*. in 2006, [45] in which

he produced a slow tumbling complex that produced pH sensitivity by measuring the ratio between the transverse (R_{2p}) and longitudinal (R_{1p}) paramagnetic relaxation rate contributions. This can be seen in Figure 15.

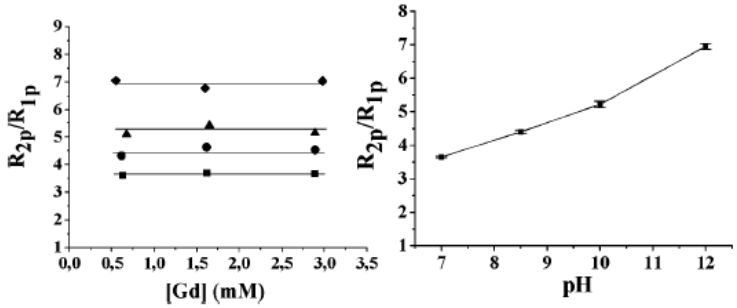

Figure 15 Graphical representation of how the ratio between transverse and longitudinal relaxation rates are concentration independent but pH dependent.

Reprinted with permission from [45]. Copyright (2006) American Chemical Society.

Whilst this technique works well in principle the sensitivity required for *in vivo* imaging is not reached and thus other techniques have been explored. The inclusion of sulfonamide groups for pH sensitivity was first reported in 2001 by Lowe *et al*. [46] and has since been employed by Gianolio *et al*. [47] in a dual MRI/SPECT sensor. This is useful as the SPECT sensor can act as a measure of local concentration, whilst the changes in relaxivity from the gadolinium(III) report the local pH measurements.

Contrast agents designed to be redox sensors usually exploit the reduction of disulfides to thiols caused by up regulation of the anti-oxidant response element seen in many cancers. Unusually these sensors work by showing a reduction in contrast in areas of high reducing potential. This is because the gadolinium(III) contrast agents are bound to structures either held together by disulfide bonds [48] (Figure 16) or directly bound to a large protein by a disulfide linker, [49] thus

once the disulfide bond is broken the molecular tumbling dramatically increases, reducing the overall relaxivity.

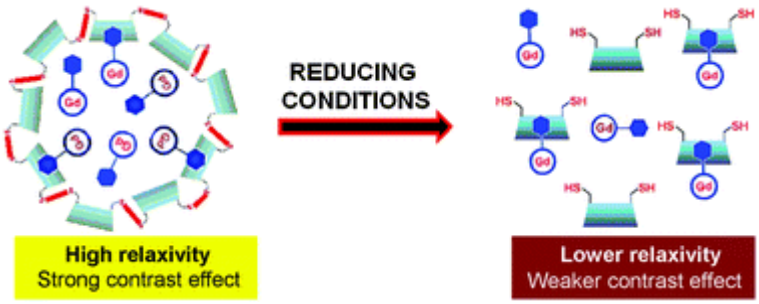

18 **19**

Figure 16 The breakdown of the large cyclodextran macromolecule on thiol reduction. Reproduced from Ref. [48] with permission from The Royal Society of Chemistry.

A more recent alternate contrast agent for measuring hypoxia is the $4NO_2$2MeOSAGd "smart" MRI sensor developed by Nagano *et al*. [50] (**20**) (Scheme 3). This contrast agent blocks the two free sites of the DO3A complex with a nitro-aromatic sulfonamide under normoxic conditions. Yet under the reducing hypoxic conditions, the nitro group is reduced to an amine, which causes a shift in acidity of the nitrogen in the sulphonamide, allowing for the nitrogen to become protonated so it no longer co-ordinates to the central gadolinium(III) ion, thus leaving two free sites for water to bind.

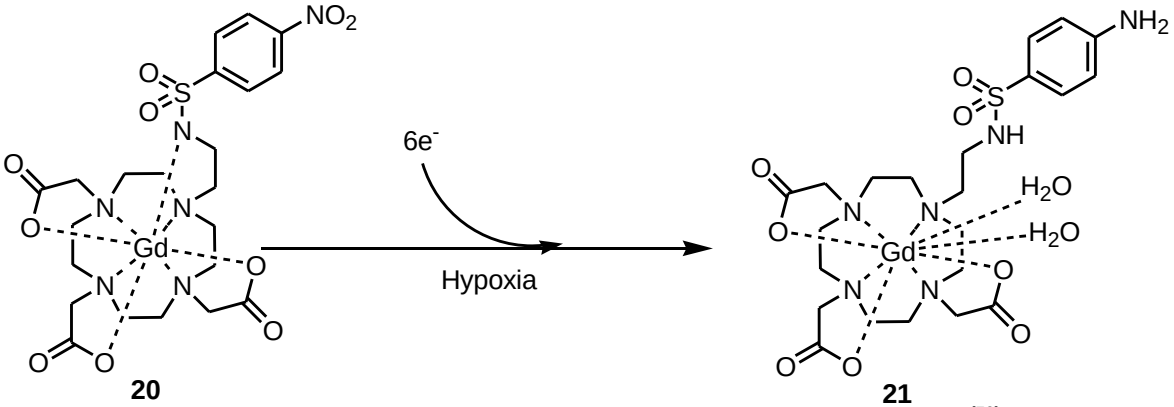

20 **21**

Scheme 3 Activation of $4NO_2$2MeSAGd under hypoxic conditions. [50]

Alternative paramagnetic ions

Gadolinium(III) is not the only suitable paramagnetic ion with regards to MRI. Alternatives such as superparamagnetic iron nanoparticles and manganese have also been explored.

Superparamagnetic iron oxide particles

Although gadolinium(III) is a good ion for affecting the T_1 of water molecules, it does not affect the T_2 relaxation. For this purpose superparamagnetic iron oxide (SPIO) particles have been used. Introduced in 1985 shortly after the use of gadolinium complexes, the SPIO particles are becoming increasingly popular. [51] This is due to several reasons; firstly per unit of metal, SPIO causes the greatest change of relaxivity in comparison with other paramagnetic metals; secondly the iron itself is biodegradable and can be reused and recycled by the body's metabolic processes; and finally the dextran or dextran-based coating can be easily manipulated to incorporate other ligands and groups. [52] These particles have therefore also been used instead of gadolinium(III) in many of the previously mentioned techniques, *i.e.* in the liposome technology (Figure 17). [24]

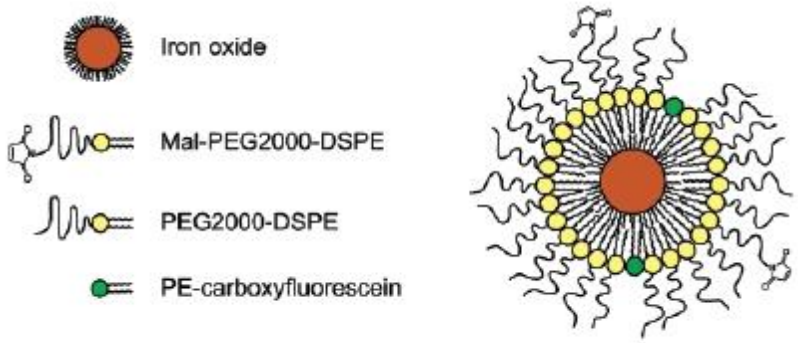

22

Figure 17 A liposome contrast agent with a SPIO core 22.

Reprinted with permission from [24]. Copyright (2004) American Chemical Society

Another potential iron nanoparticle complex is the protein ferritin **23**, a biological iron storage complex that consists of 24 subunits and can accommodate up to 4500 iron atoms in the form of ferric oxyhydroxide. The iron can be removed from this carrier *via* dialysis to produce the protein shell apoferritin **24** leaving a central cavity with a diameter of approximately 7-8 nm. In a similar manner to the liposome technology this protein complex can be filled with SPIO, magnesium(II) or gadolinium(III) nanoparticles. The popular way of encapsulating the nanoparticles is to dissociate the apoferritin protein at pH 2 **(25)**, before reforming the shell in a nanopartical rich environment at pH 7 **(26)** as seen in (Figure 18). [53]

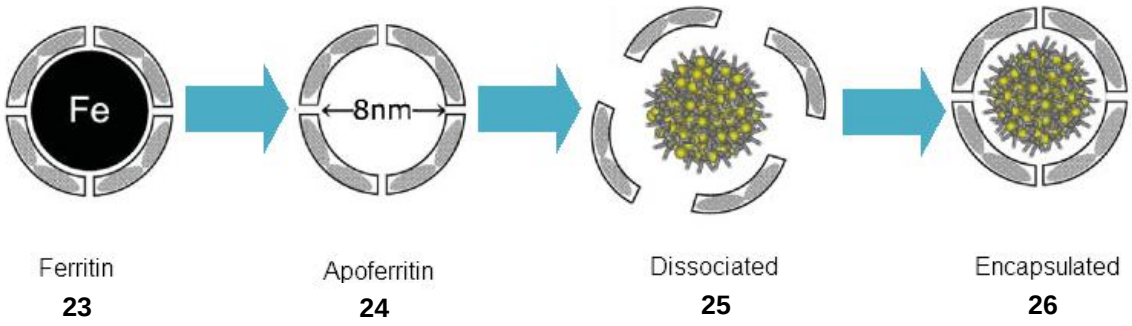

Figure 18 Insertion of nanoparticles into a ferritin shell.

Reprinted with permission from [54]. Copyright (2008) John Wiley and Sons

The major advantages of the apoferritin complex **24** are its capability of carrying a large payload, whilst having little or no immunogenic effect. It also has the potential to become a multimodal contrast agent if other imaging functionalities are conjugated to the apoferritin's outer surface.

It has been mentioned that these coatings covering the SPIO nanoparticle can be easily manipulated so that targeting vectors or alternative imaging agents can also be incorporated. Thus one of the major new developments for this technology is in the synthesis of new theranostic molecules, usually SPIO nanoparticles that also contain a drug delivery mechanism, allowing for localisation, imaging and then treatment of a disease area. [55] This technology works as the nanoshell surrounding the iron oxide core can be conjugated to a series of different moieties, including targeting vectors, near infrared dyes (example Cy5.5) and drugs such as the cancer drugs doxorubicin, [56] docetaxel [57] or siRNA for RNA interference. [58]

Manganese as an imaging agent

Manganese is paramagnetic due to its five unpaired electrons; therefore under magnetic resonance conditions it shows similar properties to gadolinium(III) and decreases the relaxation times for T_1 scans.

Manganese(II) ions have similar properties to calcium(II), and during brain ischemia, there is an increased influx of calcium(II) and consequently manganese(II). This influx of calcium(II) is due to the fact that during brain ischemia the sodium/potassium ATPase pumps stop, causing depolarisation of the cell due to increased sodium levels.

The result is the opening of calcium(II) channels, hence when calcium(II) and consequently manganese(II) enter the cell they begin to accumulate. This accumulation of manganese(II) can be detected by T_1 weighted MRI images, as the manganese(II) decreases the relaxation of the surrounding protons (Figure 19). This technique however has little clinical usage, as for manganese(II) to enter the brain, mannitol must be used to osmotically open the blood brain

barrier. The similarity of manganese(II) to calcium(II) means it is both neuro- and cardiotoxic. [59]

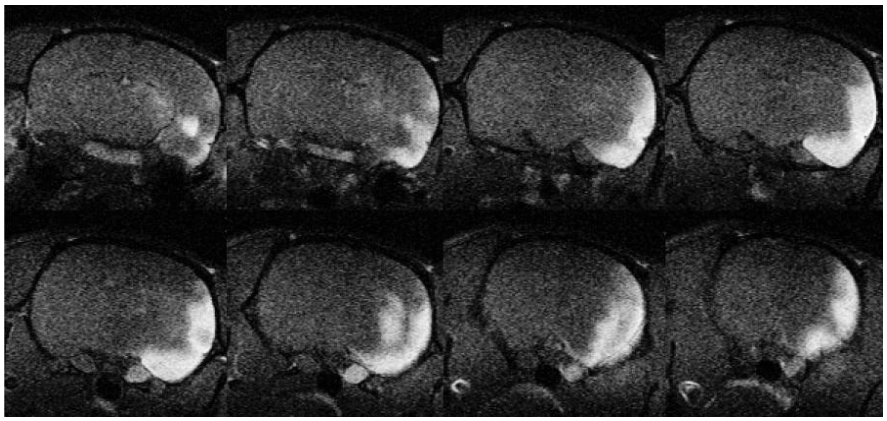

Figure 19 Manganese enhancement in a rat brain after brain ischemia.

Reprinted with permission from [59]. Copyright (2003) John Wiley and Sons

Manganese(II) is also being used in a similar manner to gadolinium(III), for example when complexed with ligands such as diethylenetriaminopentacetic acid (DTPA). The manganese(II) can also be conjugated to a variety of targeting vectors and contrast enhancing moieties, including dendrimers. [60] In 2000 manganese(II) dipyridoxal-diphosphate (Mn-DPDP) **27** was cleared for clinical use in liver imaging (Figure 20). [61] Toxicologically Mn-DPDP is superior to Gd-DTPA with a LD_{50} of 540 mmol Kg^{-1} compared to 60-100 mmol Kg^{-1} shown by Gd-DTPA. It also shows a dramatic increase in relaxivity in tissues such as the liver and kidney compared to the blood, which reduces background noise. [62]

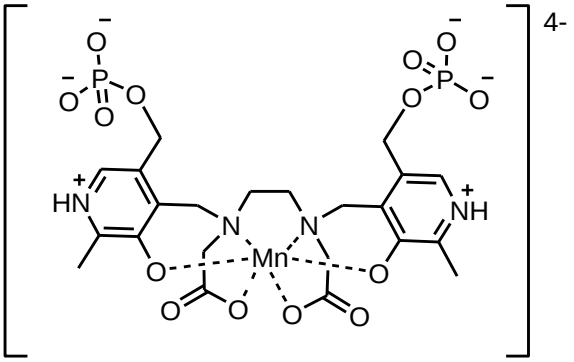

27

Figure 20 Mn-DPDP 27. [62]

Chemical exchange saturation transfer agents (CEST)

A CEST agent creates contrast in an image by intensifying the darkness of the surrounding bulk water *via* proton or atom exchange. For these agents to work the compound must be in a constant state of chemical exchange in which there is a difference in chemical shift between the different states. A good example of this is a hydroxyl proton, constantly exchanging with bulk water protons.

Initially, a state of saturation must be reached in pool B (the CEST agent's protons), this is when the number of protons in the spin up state equal the number of protons in the spin down state, creating a net magnetism of 0. This is achieved by applying a soft irradiation pulse specific to the pool B protons. Once saturation has been reached a transfer of spins begin with a transfer of spin down protons from pool B to pool A (the bulk water protons), and spin up protons from pool A to pool B. The overall result of this is to transfer saturation from pool B to pool A, thus reducing the signal from the bulk water and intensifying the darkness of the background (Figure 21).

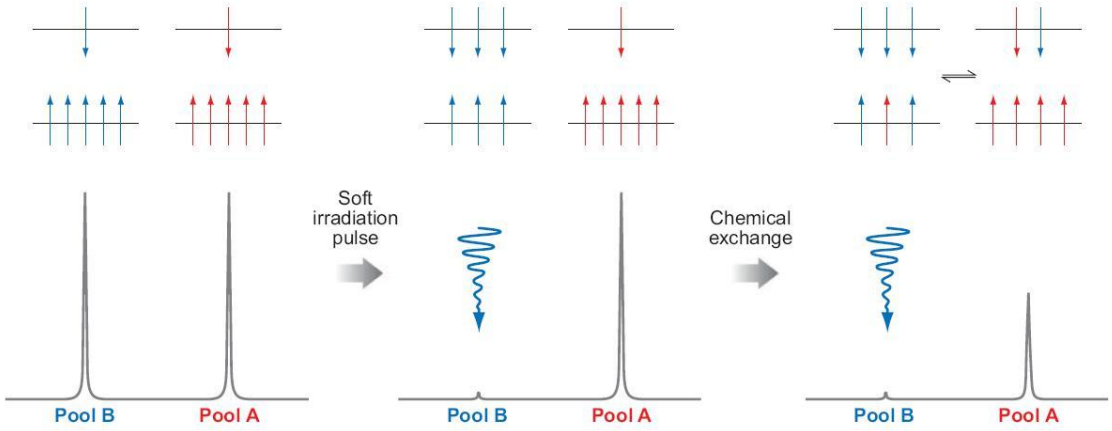

Figure 21 Distribution of spins in two distinct pools before and after a CEST irradiation pulse.

Reprinted with permission from [63]. Copyright (2008) Annual Reviews

This technology has major implications in cellular MRI, for use of endogenous CEST agents such as the hydroxyls in glucose can allow for tracking of the distribution, breakdown and synthesis of glycogen. Knowledge of these processes can greatly improve the diagnosis of diseases including diabetes.

Of the exogenous CEST agents, those with the most promise appear to be the paramagnetic CEST agents. These use an anisotropic lanthanide such as europium(III) to create a difference in proton shift of the bound water molecule. Gadolinium(III) is not suitable as it is isotropic with seven unpaired electrons in seven f-orbitals, and it has an inner-sphere water lifetime that is too short. For optimum CEST the lifetime must be 0.5 ms, and not in the nanosecond range required for T_1 relaxation. Other exchangeable protons available for CEST enhancement include co-ordinating hydroxyl or amide protons, and even the non-co-ordinating amides in close proximity to the metal. [63]

1.2.3 The gadolinium (III) chelators that form the basis of the work in this thesis.

DOTA ligand

The gadolinium(III) DOTA complex (**28**) is currently one of the clinical contrast agents in use today under the name Dotarem™ [64]. With a central crown like structure and four acetate functionalities the ligand forms an octadentate complex with gadolinium(III) which has exceptional thermodynamic and kinetic stability. A common analogue of DOTA is DO3A (**29**), which only has three acetate functionalities, allowing the fourth nitrogen to be covalently bonded to a linker moiety that allows for further modifications.

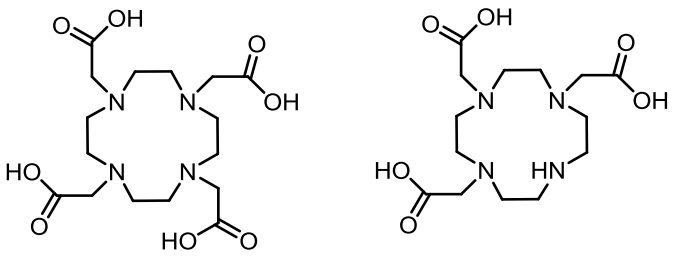

Figure 22 DOTA (28) and DO3A (29). [65]

These compounds have been used in the contrast agent field since 1986, [66] and since then have been used as the basis of many experimental contrast agents, including metal sensors, [67] dendrimers, [27] ADEPT agents [35] and even CEST agents. [63]

The unmodified DOTA chelator (**28**) has a relaxivity value of 3.5 mM^{-1} s^{-1} at 20 MHz and 312K, [68] yet this value is produced as an average between the relaxivity values of two different DOTA conformers. Crystallographic studies

have shown that Ln(DOTA) can be found in either the square antiprismatic (SA) **30** or the twisted square antiprismatic (TSA) **31** geometries as seen in Figure 23. These structures differ in the twist angle between two square planes of the antiprism. These different structures are important as the TSA geometry has a significantly faster water exchange rate than that of a SA geometry. [65] Mechanistic studies have shown that the difference in the exchange rate between the two is up to 50 fold with the SA having a k_{ex} (exchange constant) value of $8.3x10^3$ s^{-1}, compared to $327x10^3$ s^{-1} for the TSA geometry. Therefore even though the SA conformation is 4.5 times more prevalent in solution than the TSA, 90% of the relaxation is produced by the TSA conformer. [69]

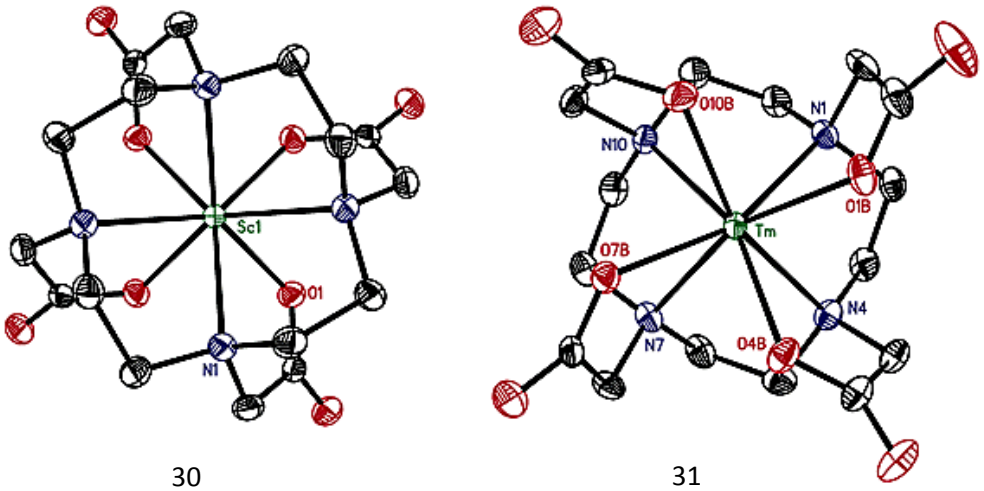

30 31

Figure 23 The SA and TSA [LnDOTA]$^-$ (Ln = Sc(III) on left, Tm(III) on right) conformers. Reprinted with permission from [65]. Copyright (2003) American Chemical Society

Whilst in theory [GdDO3A] should have almost double the relaxivity value of [GdDOTA]$^-$ due to the extra water coordination site, this hasn't shown to be the case, with a relaxivity value of 4.8 $mM^{-1}s^{-1}$ at 20 MHz and 312 K. This is because the coordination environment occupied by the two water molecules is suitable for binding of anionic ligands found within biological conditions,

including phosphates and citrates. [70] Thus the overall relaxivity value is significantly lower than expected.

Gadolinium(III) containing DOTA complexes were initially synthesised by Margastadt *et al.* in 1986. [71] This synthetic route included the formation of cyclen using the method developed by Richman *et al.* [72] (Scheme 4) This involves reacting the bisulfonamide sodium salt of ((tosylazanediyl)bis(ethane-2,1-diyl))bis(tosylamide) **32** with (tosylazanediyl)bis(ethane-2,1-diyl) dimethanesulfonate **33** to produce the tosyl protected cyclen ring **34**, which undergoes acid hydrolysis to form the unprotected cyclen **35**. This can then undergo the addition of the acetate functionalities using *tert*-butyl bromoacetate followed by gadolinium(III) insertion to produce the Gd(III)DOTA complex.

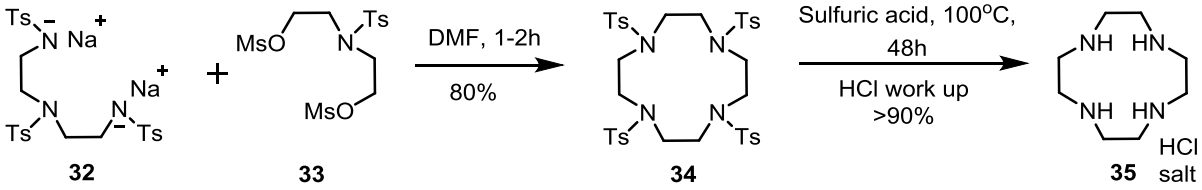

Scheme 4 Cyclen 35 formation used by Richman *et al.* [72]

The synthesis of the DO3A based complexes are significantly more intricate as the reaction must be stopped after the addition of the third acetate functionality. Within the Thomas group DO3A gadolinium(III) complexes were synthesised using a six step process involving a series of orthogonal protections to produce the final DO3A complex (**40**) as outlined in Scheme 5. [8] This synthetic route is discussed in further detail in Chapter 3.

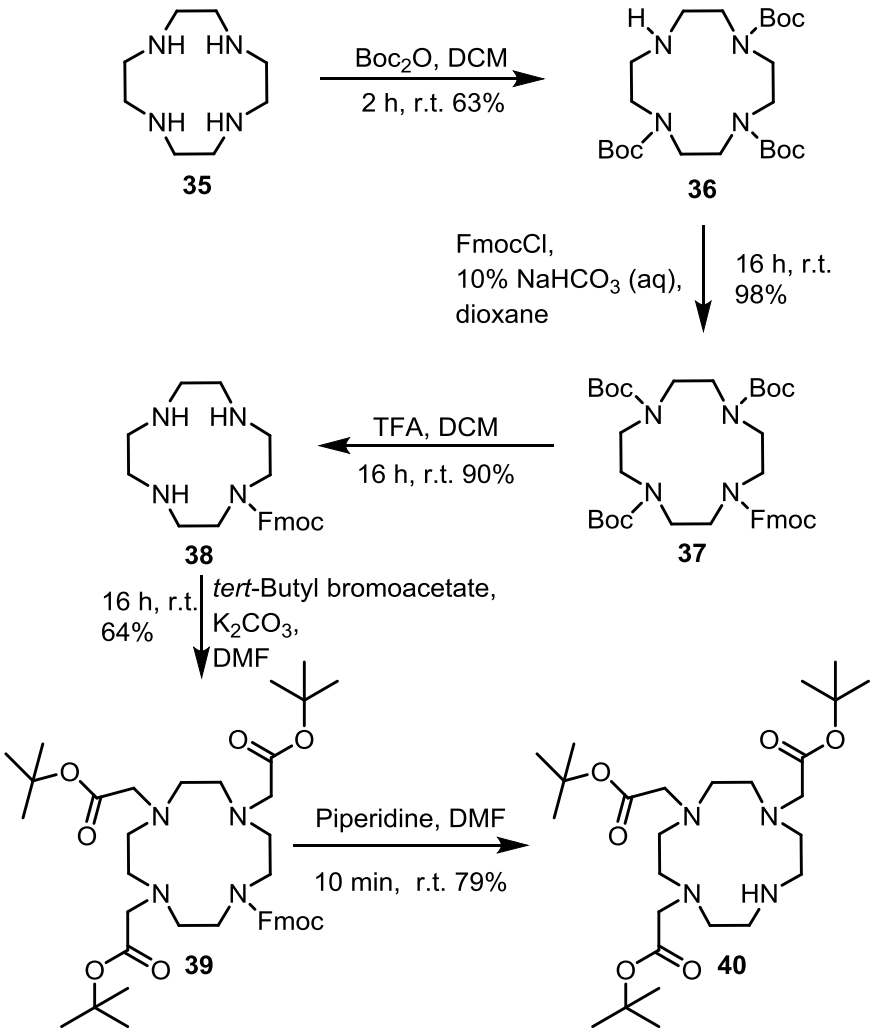

Scheme 5 Synthesis of the protected DO3A complex (40) as developed by the Thomas group. [8]

This synthesis has since been streamlined within the literature with Machitani, *et al.* [73] forming the HBr salt of the DO3A complex (**40**) in a single step using strict equivalences of *tert*-butyl bromoacetate and at a high dilution (Scheme 6).

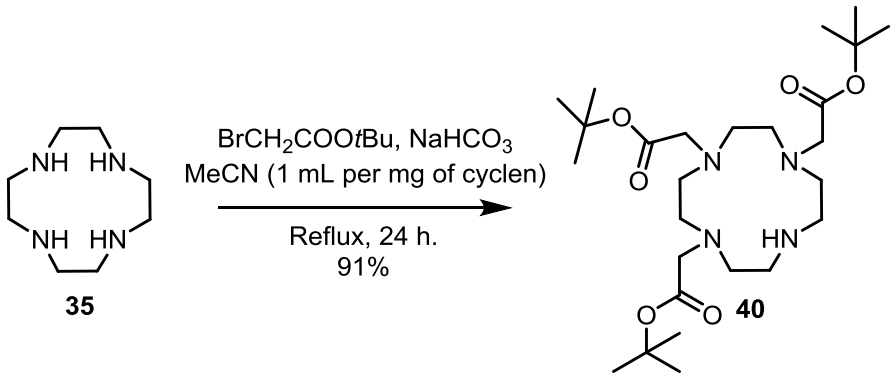

Scheme 6 Formation of protected DO3A 40 developed by Machitani *et al*. [73]

The propargyl containing DOTA based complex with a potential for use in copper (I) mediated cycloaddition has been developed by Viguier *et al.* [74] This synthesis takes the DO3A starting material **40** and reacts it with 2-bromo-*N*-(prop-2-yn-1-yl)acetamide **41** and base to produce the protected version of the desired compound **42** in a 78% yield before *tert*-butyl deprotection and Eu(III) insertion as seen in Scheme 7.

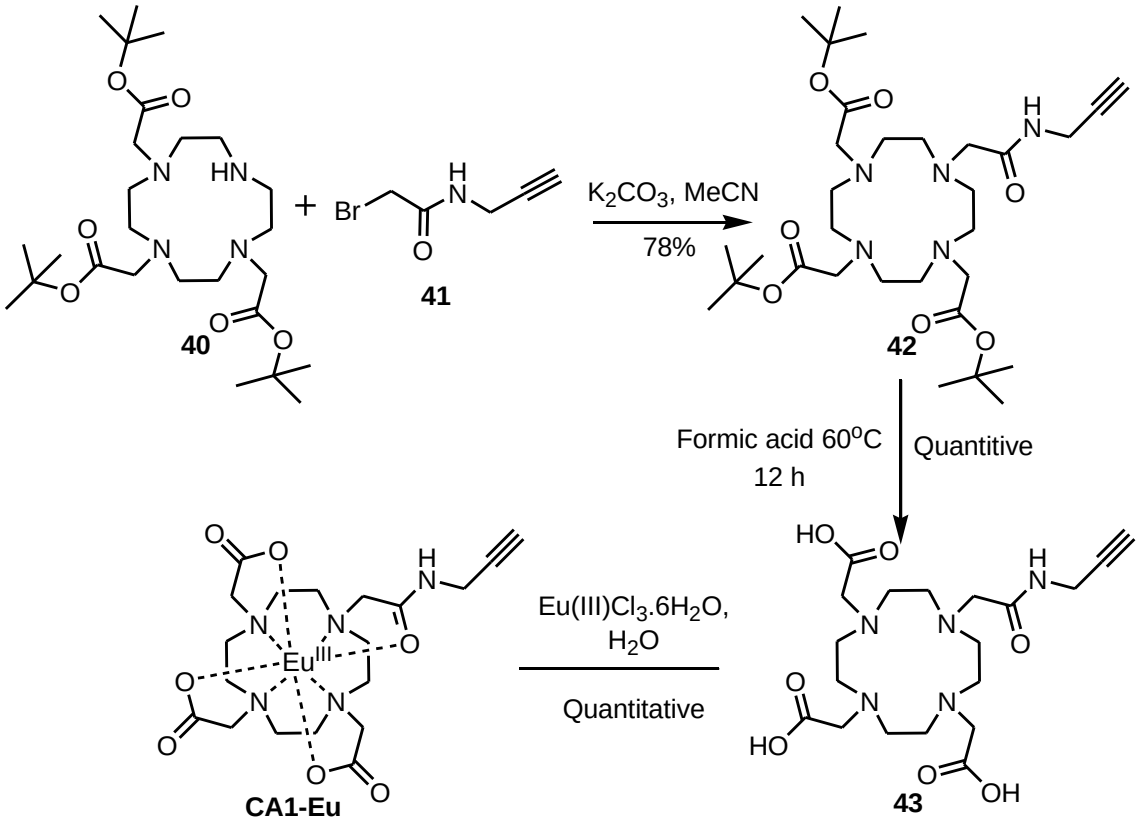

Scheme 7 Formation of the Europium(III) propargyl DOTA complex CA1-Eu. [74]

AAZTA ligand

The 1,4-*bis*(hydroxycarbonylmethyl)-6-[*bis*(hydroxycarbonylmethyl)]amino-6-methyl-perhydro-1,4-diazepine (AAZTA) ligand (**44**) is a heptadentate ligand reported to produce stable complexes with gadolinium(III) (Figure 24). Due to this extra coordination site for water, the relaxivity of the complex is almost double compared to Dotarem™. If the gadolinium(III) AAZTA complex is conjugated to a slow tumbling molecule the relaxivity can be dramatically increased.

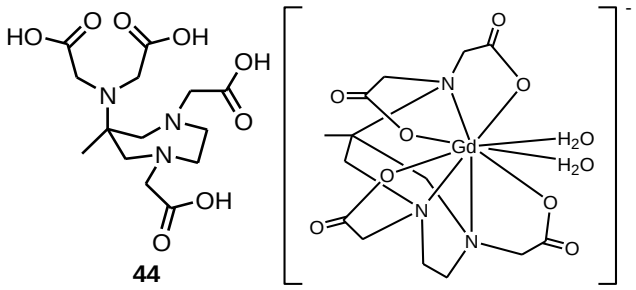

Figure 24 The AAZTA ligand (44). [75]

The gadolinium(III) complex of AAZTA is significantly more thermodynamically stable than the gadolinium(III) complex of DTPA. [76] This stability of the AAZTA complex is based on the location of the three nitrogen atoms, with the two in the ring and the third on the sp^3 carbon. Due to their close spatial relationship there is no possibility of coordination extension and therefore the gadolinium(III) is held tightly. Despite this high stability, AAZTA only takes up seven of gadolinium(III)'s nine coordination sites. Yet unlike [GdDO3A] the area occupied by the exchanging water molecules is not suitable for the binding of more kinetically stable anionic biomolecules, all of this contributing to the relaxivity value of 7.1 mM^{-1} s^{-1} at 20 MHz and 298 K. [77]

With regards to modifying AAZTA the obvious site is the methyl group on the sp^3 carbon. This position has been converted into a C17 alkyl chain, having the overall effect of producing AAZTA micelles and dramatically increasing the relaxivity of the compound to 30 $mM^{-1}s^{-1}$ (20 MHz, 298 K) due to effects on molecular tumbling. [78] Insertion of an alcohol group in the methyl position produces similar relaxivity properties to the parent compound (**44**), whilst producing a handle for further modification. [79] (Figure 25)

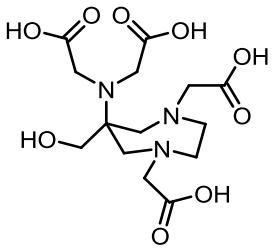

45

Figure 25 A modified AAZTA ligand (45) at the *sp*^{3} carbon. [79]

The overall synthesis of the AAZTA ligand is relatively short, being only four steps for the parent compound, yet this is still three steps longer than the synthesis of DOTA or DO3A. The synthesis starts with a Mannich reaction, followed by a hydrogenation to convert the nitro functionality into an amine (**50**). The synthesis then proceeds with the addition of the acetate functionalities *via* an S_N2 reaction (**51**) before a final deprotection to yield the final ligand (**44**), [80] as shown in Scheme 8.

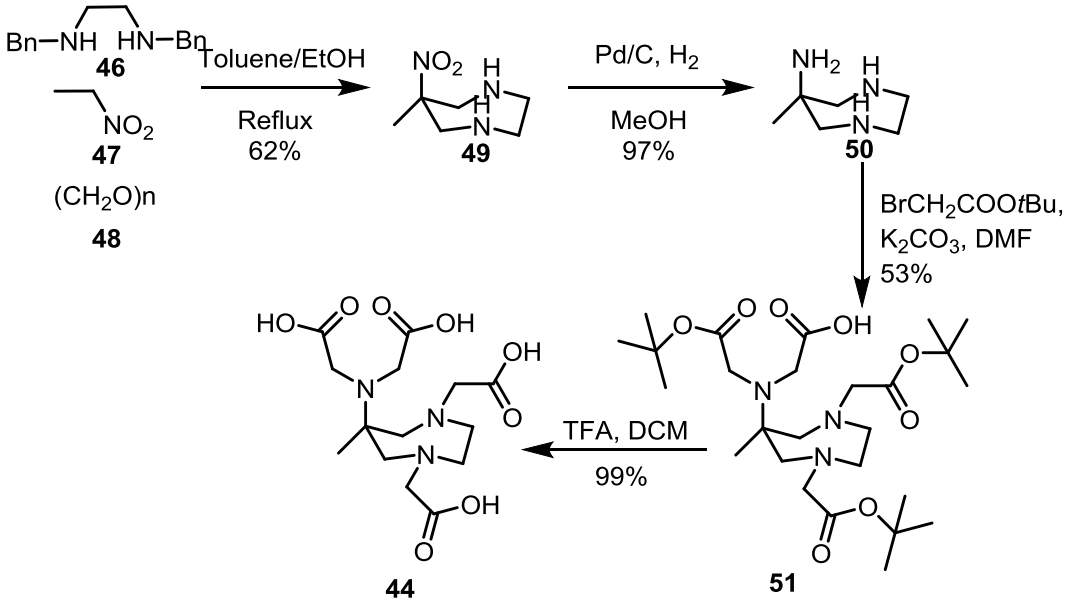

Scheme 8 Synthesis of the AAZTA ligand (44). [79]

1.3 Hypoxia and 2-Nitroimidazole

1.3.1 Hypoxia

Hypoxia is a microenvironment within the body in which an area is deprived of oxygen and can no longer undergo normal metabolic processes. This microenvironment is formed in some solid tumours, as during the rapid growth of the pathogenic cells the vasculature is not formed properly, preventing much needed oxygen and nutrients from reaching certain areas. Hypoxia can also be found during a stroke, a myocardial infarction and as a consequence of poor blood perfusion in diabetic limbs and arthritic joints. [81]

Hypoxic regions in tumours cause major problems with regards to oncological treatment, as these areas are resistant to radiotherapy and chemotherapy. This is due to poor vascular delivery in conjunction with a reduced cell cycle, which in turn lessens chemotherapeutic effects, as most of the drugs in the clinic are anti-proliferation agents and not anticancer agents.The efficacy of radiotherapy however is not reduced because of poor vascular perfusion, but because the cytotoxic effect of this type of treatment relies on the presence of intracellular oxygen.

The treatment resistance of the hypoxic region is not the only reason for poor patient prognosis with hypoxic tumours. Unlike normal human tissue, tumour cells are capable of adapting to the hypoxic conditions *via* a pathway induced by hypoxia inducing factor 1 (HIF-1). HIF-1 is a protein that consists of two proteins HIF-1α and HIF-1β. Under normoxic conditions HIF-1α is hydroxylated by oxygen, which leads to ubiquitination and degradation. Yet under hypoxic conditions, HIF-1α translocates to the nucleus and forms a dimer with HIF-1β to

form HIF-1. This dimer acts as a transcription factor to induce the production of over 100 proteins. These proteins include those essential for glycolysis (a method of producing energy anaerobically), growth, neovascularisation, prevention of apoptosis, proteolytic enzymes that degrade the extracellular matrix promoting metastases and even proteins that down-regulate the immune response. [81]

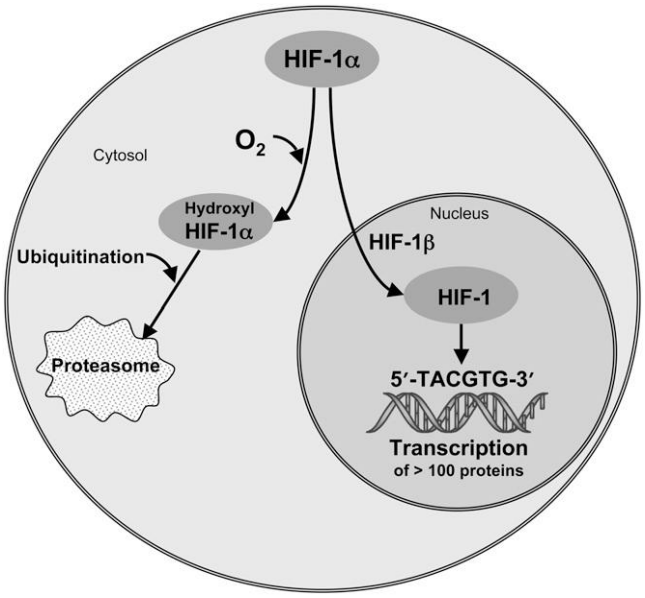

Figure 26 Pathways taken by HIF-1 in normoxic and hypoxic conditions.

Reprinted with permission from [81]. Copyright (2008) Society of Nuclear Medicine, Inc.

Due to the increased treatment resistance and the up regulation of proteins that contribute to factors including metastases, patient prognosis is dramatically reduced when a hypoxic region is produced in a solid tumour. [82] Thus effective methods of treatment and visualisation are required to improve patient survival.

1.3.2 Visualising hypoxia – 2-Nitroimidazole

Currently, major methods for visualising hypoxic cells use compounds based on the 2-nitroimidazole structure, a known marker of hypoxic tissues [81], [83]. The main reason for this is that under hypoxic conditions the nitro group undergoes

an irreversible reduction and activation, due to a lack of oxygen to perform the reoxidation step. Once this occurs the molecule is trapped inside the cell as this reduction leads to a chain reaction that produces a suitable leaving group from the (imidazol-5-yl)methyl position (**53**) which is eliminated leaving a methide group (**54**) that is electrophilic enough to covalently bind to molecules inside the cell. [84]

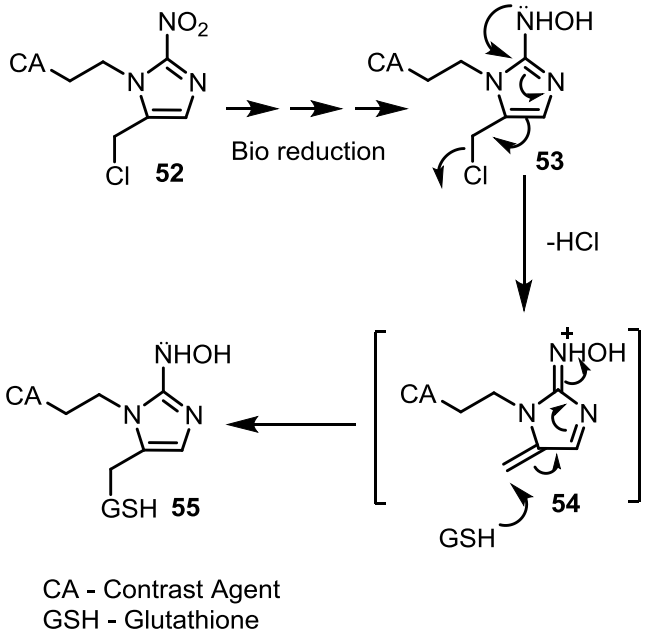

Scheme 9 The reaction undertaken by 2-nitroimidzole once under hypoxic conditions resulting in cell localisation.

The initial cytochrome P_{450} reductase catalysed single electron transfer to the nitro compound is the rate determining step, as it is reversible under aerobic conditions, however under hypoxic conditions this radical is not converted by an oxygen molecule back to the parent compound. Instead it undergoes a series of conversions which lead to the formation of an amine (Scheme 10).

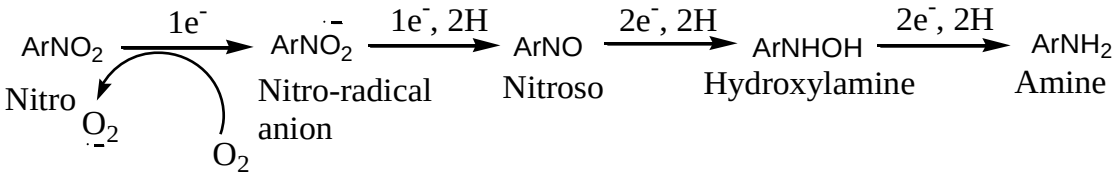

Scheme 10 The enzymatic conversion of a nitro group to an amine under hypoxic conditions. [85]

2-Nitroimidazole is the most widely used of the nitroimidazole compounds, as it has a steady uptake into the cells and good retention, unlike the 4- or 5-nitroimidazole which have a better uptake into cells, but are rapidly removed again before localisation can take place. This is because there are slight differences in redox potential between the 2- and 4-/5-nitroimidazoles, which affects the rate of reduction of the nitro group. The value of the redox potential of 2-nitroimidazole is -243 to -398 mV, whilst for 4- or 5-nitroimidazole the redox potential is below -400 mV. [86]

A positron emission tomography (PET) agent commonly used to measure hypoxia is ^{18}F–misonidazole (FMISO) **56**. This is injected into patients and allowed to localise for one and a half hours before using a PET scanner to image the tumour. The timing is chosen as it allows for the ^{18}F–FMISO to equilibrate and localise within the tissue, whilst also taking into account the ^{18}F half life of one hundred and nine minutes. [87] Since ^{18}F requires a cyclotron to be produced the supply is limited and expensive.

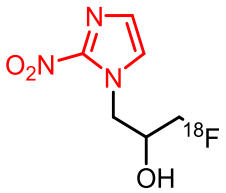

56

Figure 27 ^{18}F-FMISO 56. [81]

Whilst optical imaging is not practical *in vivo,* these probes have been widely successful for accurately measuring hypoxia in an *in vitro* setting. One of the major 2-nitroimidazole based compounds in this group is pimonidazole **57**. [88] Commercially available as Hydroxyprobe-1™, pimonidazole staining has been shown to not only view hypoxic regions immunohistologically, but when normoxia is returned the staining of pimonidazole is seen to dramatically decrease.

Assays used to measure radiobiological hypoxia include the comet assay and antibody binding to EF5 **58** another 2-nitroimidazole based compound. The comet assay involves exposing tumours to irradiation followed by electrophoresis. The DNA that has been broken by irradiation migrates faster to produce a comet-like tail that lengthens proportionally to the number of DNA breaks. This technique was used to validate pimonidazole as an accurate measure of hypoxia. Antibodies have been produced to bind to adducts of EF5, these antibodies can contain a fluorescent tag, which allows for quantitative histological staining of the hypoxic tissue. [89]

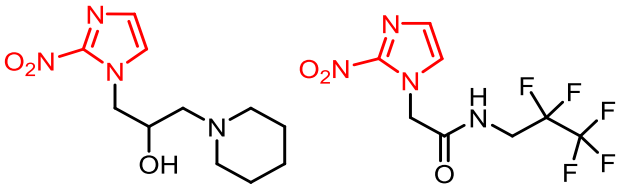

Figure 28 Optical 2-nitroimidazole based hypoxia markers. [88] [89]

The final type of hypoxia marker based on 2-nitroimidazole are the fluorine MRI markers. So far three ^{19}F labelled 2-nitroimidazole structures have been synthesised for use in ^{19}F MRI, including trifluoroethoxy-misonidazole. Whilst

^{19}F MRI is similar to proton MRI in sensitivity, it has a much greater signal to noise ratio as there is very little natural fluorine in human tissue. Although these compounds are advantageous in comparison with PET agents, as they avoid the radioactivity and limited shelf-life problems associated with ^{18}F, the dose required for good quality images using ^{19}F is 400-1,600 mg/m^2 in comparison with the 15 μg/m^2 required for ^{18}F-FMISO. (90) The sensitivity of the ^{19}F MRI is also reduced as the 2-nitroimidazole forms several adducts once activated, producing a broadened signal, and reducing the signal to noise ratio produced.

1.3.3 Alternative hypoxia markers

An alternative PET agent that can be used for hypoxia imaging is ^{64}Cu-ATSM **59**. Diacetyl-*bis*(*N*^{4}-methylthiosemicarbazone) (ATSM), has anti-tumour properties that are enhanced by chelation with Cu(II), the complex is taken up more rapidly than ^{18}F –FMISO **56**, and the normoxic-hypoxic ratio seen is greater. The method by which Cu-ATSM is up-taken and located in hypoxic cells is thought to be related to the lipophilicity of Cu(II)-ATSM, whilst Cu(I)-ATSM is charged and can be trapped within cells *via* irreversible intracellular reduction. Yet this mechanism doesn't explain the differences seen in variable tumour types, so more work needs to be done to understand this compound further. (91)

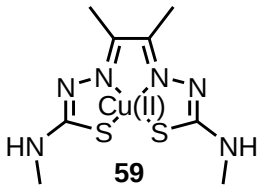

59

Figure 29 Cu-ATSM 59. (91)

As hypoxia is just a state of low oxygen partial pressure ($_PO_2$), electrodes such as the Eppendorf $_PO_2$ Histograph™, can be used to directly measure the level

of oxygen in the tumour. The relationship between this value and poor tumour prognosis due to the effects of hypoxia has been proven using this type of technology for cervical carcinomas. [92] The major disadvantages of this technology is that only a specific part of the tumour can be monitored at any one time, and unlike general imaging techniques the probes are invasive.

Another direct method of measuring hypoxia is to use a MRI method called BOLD (blood oxygen level dependent). This technique exploits the fact that deoxyhaemoglobin (dHb) is paramagnetic, unlike oxyhaemoglobin (O_2Hb), and thus can be seen on T_2*-weighted images. For dHb decreases the relaxation rate of blood water, and is directly related to vascular oxygenation. The disadvantages with this technique are that, for smaller blood vessels, the partial-volume effects can produce inaccurate results, as can the flow effects of the blood. One method to solve the latter problem is a technique called FLOOD (flow and oxygen dependent contrast) which uses pulse sequences to decouple the flow effects from the static effects of the relaxation. This technique is valuable due to its non-invasive application, allowing for easy repetition of the test, complimented by the high spatial and temporal resolution of the technique. [81]

Whilst 2-nitroimidazole is the most commonly used, it is not the only compound able to undergo activation in hypoxic conditions. Nitro aromatics, aromatic and aliphatic *N*-oxides, quinones and metal complexes can all accept electrons, irreversibly causing a significant change in their intrinsic properties. These compounds have yet to be exploited for use in tumour imaging, but they have been used experimentally as prodrugs for cancer treatment.

Nitrobenzyl compounds are activated *via* an identical mechanism to the nitroimidazole compounds, however whilst the nitroimidazole drugs are often activated by uncontrolled fragmentation of the ring structure, the nitrobenzyl compounds are more commonly associated with the controlled release of known cancer drugs such as mustards (**60**) (Figure 30) [93] and paclitaxel (**61**) (Figure 30). [94]

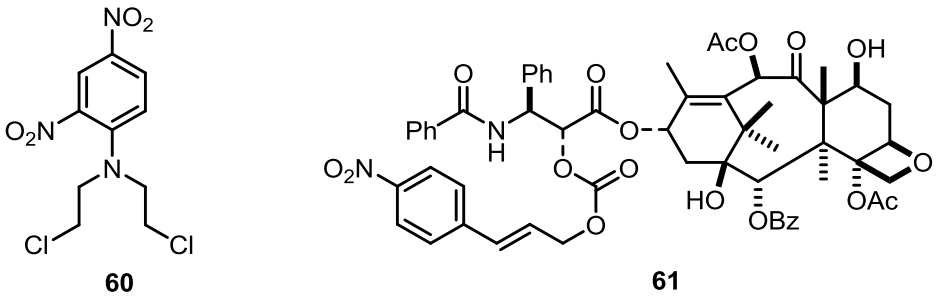

60 **61**

Figure 30 Nitrobenzyl based cancer prodrugs (60,61). [93] [94]

For the nitrobenzyl compounds to be reduced under hypoxic conditions it is best if they have reduction potentials between -330 and -450 mV. [95] The best way to achieve this is by reducing the electron density of the ring itself, most commonly by putting in extra electron withdrawing groups including nitro groups in both the *ortho* and *para* positions. Electron withdrawing groups however can reduce the potency of the cytotoxic agent, so a balance must be struck. [96]

Aromatic *N*-oxides contain one of the first potential hypoxia selective tumour activating drugs, tirapazamine **62** (Figure 31). These compounds accept two electrons in the *N*-4 position *via* a single electron transfer mechanism to produce the deoxygenated form and a hydroxyl radical. This radical attacks the C-4' position of the ribose site in DNA causing cleavage. The DNA can then undergo oxidation and form a covalent adduct with tirapazamine. [97]

Unfortunately whilst tirapazamine showed a 200-fold selectivity for hypoxic tissues its use is limited as it can be metabolised to the radical species preventing diffusion through tissues. [98] Derivatives of tirapazamine have been synthesised with the *N*-2 replaced with a C-CN functionality, [99] which showed a retention in hypoxic selectivity, yet these were unsuccessful therapeutically due to their short half lives and low solubility. [100]

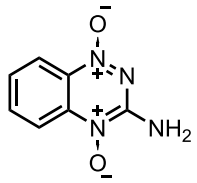

62

Figure 31 Tirapazamine 62. [97]

Unlike the aromatic *N*-oxides, the aliphatic *N*-oxides do not undergo a single electron process, yet reduction to the corresponding tertiary amine is inhibited due to competition between oxygen and the drug for binding in the CYP3A cytochrome C enzyme. This is best seen in the drug AQ4N **63** (Figure 32), which once activated binds tightly to DNA and inhibits topoisomerase II. Whilst not totally successful on its own, the drug showed more promise when potentiated by radiotherapy. [96]

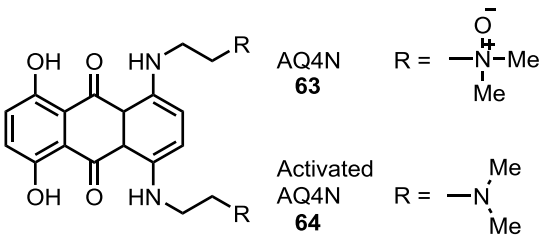

Figure 32 AQ4N 63 and its hypoxia activated form (64). [96]

Quinones are reduced *via* a single electron transfer to form the semiquinone radical anion. Groups have been added in the C-2 position that under hypoxic conditions will leave to form a reactive methide intermediate that can crosslink to DNA *via* the guanine-guanine crosslinks in the major groove. [101] *In vivo* these compounds showed little selectivity for hypoxic tissue, due to the quinines being good substrates for DT diphorase, a two-electron reductase that is not reversible in the presence of oxygen. [102]

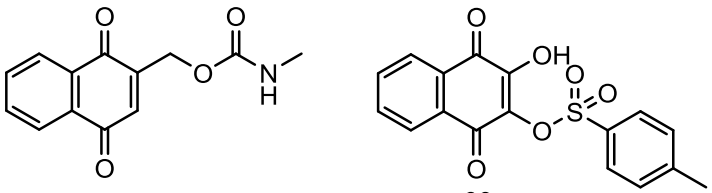

Figure 33 Hypoxia activated quinone based drugs (65 and 66). [101]

The final group are the metal complexes, and in particular cobalt, although complexes with rhenium [103] and palladium [104] have also been synthesised. These complexes work on the principle that whilst cobalt(III) is relatively inert, cobalt(II) is very labile and readily releases its ligands. This occurs as cobalt(III) is in a d^6 low-spin electron state, whilst cobalt(II) is in a d^7 high spin, and the energy required for this interconversion is -200 to -400 mV, and thus in the range of cellular reductants. [85] To exploit this, chemotherapeutic agents such as 8-hydroxyquinolines [105] and nitrogen mustards, [106] have been chelated to the cobalt (III) complex. Whilst they showed promise in *in vitro* studies the selectivity for hypoxic cells was decreased in *in vivo* studies, and thus none of these drugs have reached the clinic. One way to try and combat this lack of stability is to increase the stability of the initial cobalt(III) complex by using tri-

dentate nitrogen mustards (**67**) (Figure 34) instead of a mono or bi-dentate, as of yet no candidates have reached the clinic.

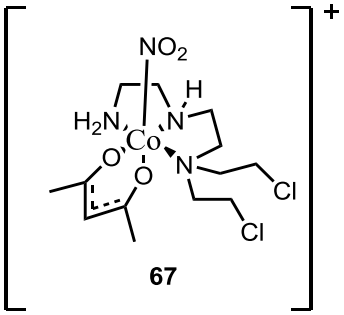

67

Figure 34 a Tri-dentate Co(III) mustard complex (67) [106]

Chapter 2 Aims and Objectives

The overall aim of this thesis was the synthesis of a MRI contrast agent that will accumulate in hypoxic tumour cells. Although ^{1}H MRI contrast agents in the clinic accumulate preferentially in cancer cells over normal tissues, there are no known compounds that accumulate specifically in hypoxic cancer cells. Clinically PET is the most commonly used technique to image hypoxic cells, [81] however this requires the patient to be dosed with small amounts of radiation, which is more harmful for patients than MRI.

The envisioned contrast agent was supposed to contain a gadolinium(III) central ion, with as high a *q* value as possible whilst still maintaining thermodynamic and kinetic stability *in vivo*. To enhance the relaxivity of the contrast agent, a high *q* value is desirable as the final molecules are too small to enable enhanced relaxation due to slower molecular tumbling. [78] The newly designed contrast agent was then to be conjugated to a known hypoxia targeting vector *via* a rigid linker.

The linker chosen was a triazole, formed by the copper(I) catalysed azide-alkyne cycloaddition, [107] with the azide and alkyne moieties able to react orthogonally to any other groups present within the complexes allowing for easy assembly (Figure 35). [108]

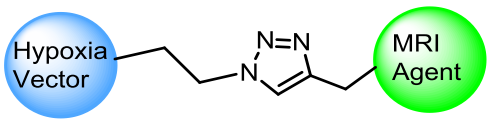

68

Figure 35 Short triazole linker used to conjugate the MRI contrast agent to the hypoxia targeting vector.

The DOTA-based contrast agents are the most widely reported in the literature. [39] [66] [109] This is because the eight coordinate structure possesses highly favoured thermodynamic and kinetic properties making it unlikely to release the gadolinium(III) payload in an *in vivo* system. [70] These compounds are also easily manipulated to contain groups for conjugation. As an example the alkyne containing compound (**CA1**) has been synthesised by Viguier *et al.* [74] As **CA1** already carries the desired alkyne moiety this served as a starting molecule to be taken and adapted for use in this project. Furthermore, the synthesis the di-propargyl containing DOTA based structure (**CA2**) was performed (figure 37).

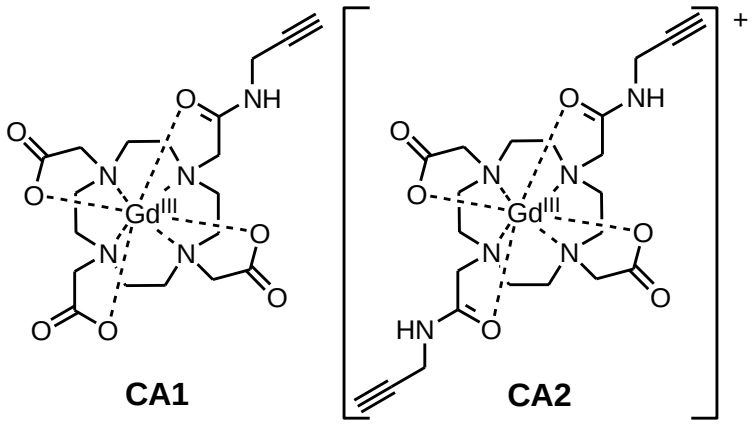

Figure 36 DOTA based contrast agents to be synthesised. (CA1/CA2)

As an alternative to the widely used DOTA based complexes a contrast agent based on the AAZTA structure was chosen to be synthesised for this project (Figure 38). This has a longer synthetic route, and fewer sites for adaptation, however the parent compound has been shown to have better relaxivity properties than the DOTA based complexes (**CA1** and **CA2**) as it has a higher *q* value of 2, whilst still maintaining good metal retention properties *in vivo*. [80]

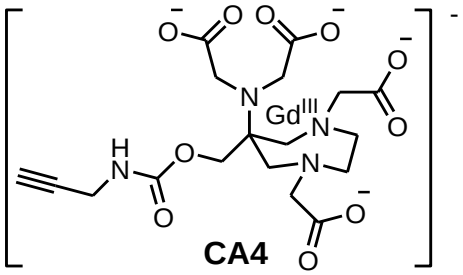

Figure 37 [GdAAZTA]$^-$ based contrast agent to be synthesised. (CA4)

Table 1 Comparison between the [GdDOTA]$^-$ and [GdAAZTA]$^-$ complexes with regards to relaxivity and transmetallation. [68] [80] [110] [111] [112]

	[GdDOTA]$^-$	[GdAAZTA]$^-$
Structure	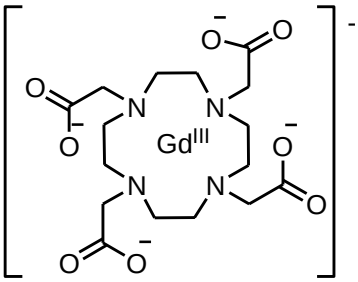 **57**	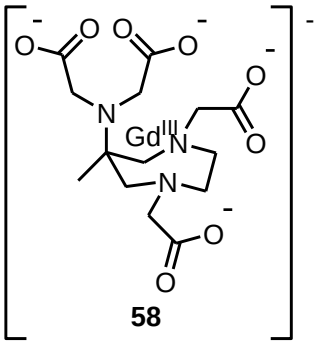 **58**
q Value	1	2
Water Exchange rate	240 ns, k_{ex} 0.41 x 10^7 s^{-1}	90 ns, k_{ex} 0.87 x $10^7 s^{-1}$
Rotational Correlation times	77 ps	74 ps
Relaxivity	4.2 $mM^{-1}s^{-1}$ @ 20 MHz 298 K	7.1 $mM^{-1}s^{-1}$ @ 20 MHz 298 K
Resistant to transmetallation	✓	✓

Regarding the hypoxia targeting vector, 2-nitroimidazole based compounds are the most widely used in the clinic, [113] so the logical first step was to synthesise

a simple 2-nitroimidazole based targeting vector containing a short carbon chain connected to an azide moiety. It has to be considered that if the carbon chain is too short the targeting vector has the potential to be highly explosive. The compound with a 2-carbon chain between the 2-nitroimidazole and the azide functionality **TV1** has been reported in the literature, [114] providing the initial starting place (Figure 39).

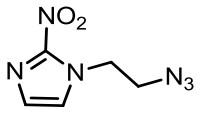

TV1

Figure 38 Initial 2-nitroimidazole based targeting vector to be synthesised. (TV1)

As an alternative to the 2-nitroimidazole based targeting vector, a series of nitro-benzyl compounds were also synthesised (**TV3-5**). Unlike with 2-nitroimidazole, a leaving group must be present if the reduction of the nitro group is to lead to the contrast agent being tethered within the hypoxic cell, for the ring is not capable of the partial breakdown seen in the imidazole structure. The leaving group has to be attached to a methylene group in the *ortho* or *para* position with regards to the nitro functionality, otherwise it can not be released due to the resonance within the aromatic system (Scheme 11). [93]

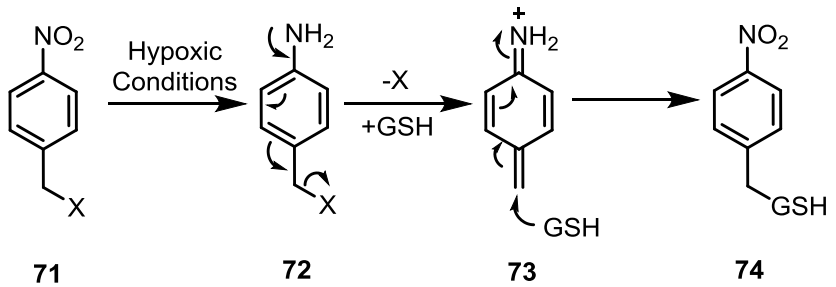

Scheme 11 The release of a leaving group to produce a reactive methylene functionality in nitro benzene based compounds under hypoxic conditions.

Whilst these compounds have less favourable electron potential values for enzymatic nitroreduction, (-600 to -400 mV [95] compared to -250 to -400 mV [86] for the 2-nitroimidazole based compounds) it has been shown that they can be reduced using human DT-Diaphorase. [115] The synthetic route toward these compounds is relatively simple having adapted a paper by Jiang *et al.* [116], to insert the side chain containing both an azide group and a suitable leaving group, in this case a chloride ion (Figure 40).

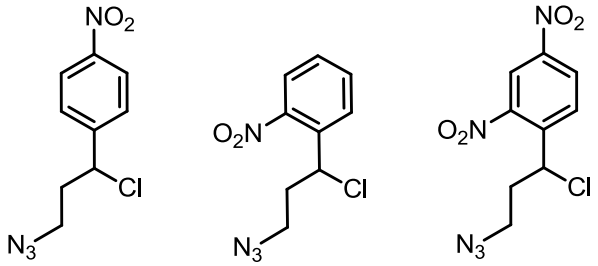

TV3 **TV4** **TV5**

Figure 39 The nitrobenzyl based targeting vectors to be synthesised. (TV3/TV4/TV5)

The final envisioned targeting vector **TV6** combines both the desirable 2-nitroimidazole central structure with the substituent produced for the nitrobenzyl compounds. This should allow the nitro group to be reduced and the molecule to be attached indefinitely to structures within the hypoxic cell without requiring a temporary partial breakdown of the central ring structure. For this to occur the substituent must be in the 5- position on the imidazole, to allow for the flow of electrons to remove the chloride leaving group as seen in Scheme 12.

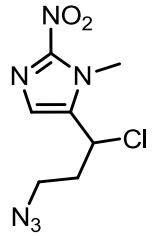

TV6

Figure 40 2-nitroimidazole based targeting vector to be synthesised (TV6).

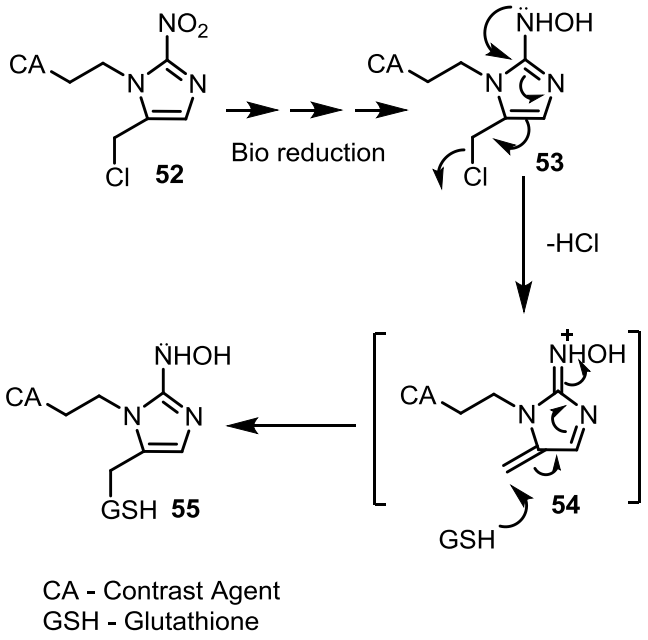

Scheme 12 Mechanism by which the reduced nitro group will bind irreversibly in the hypoxic cell

Once all of the separate components have been synthesised the aim was to fuse both sides together to create a series of hypoxia targeting contrast agents. It is also to be noted that the di-propargyl DOTA based contrast agent (**CA2**) will be conjugated to both a hypoxia targeting vector and a fluorescent dye (**DYE1**) making the final product multi modal. The fluorescent dye chosen is a pro fluorescent coumarin dye widely used in the Thomas group.

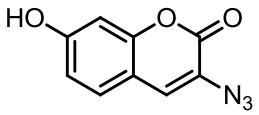

DYE 1

Figure 41 Coumarin dye to be synthesised. (DYE1)

Table 2 Table of final compounds to be synthesised. (C1-7)

Contrast Agent	Targeting Vector	Final Compound
CA1	TV1	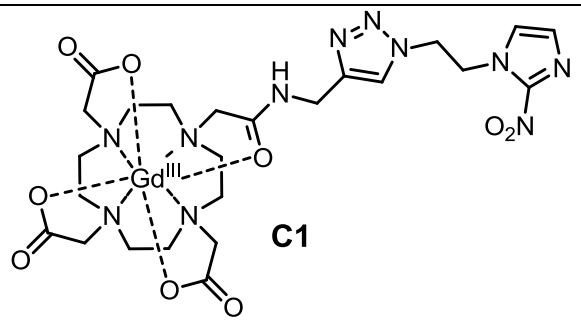 **C1**
CA1	TV3	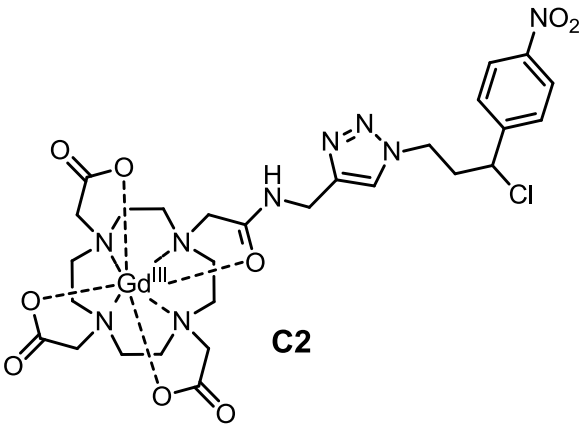 **C2**
CA1	TV4	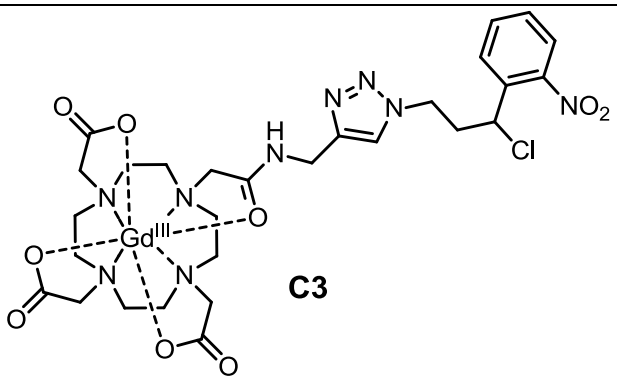 **C3**

CA1	TV5	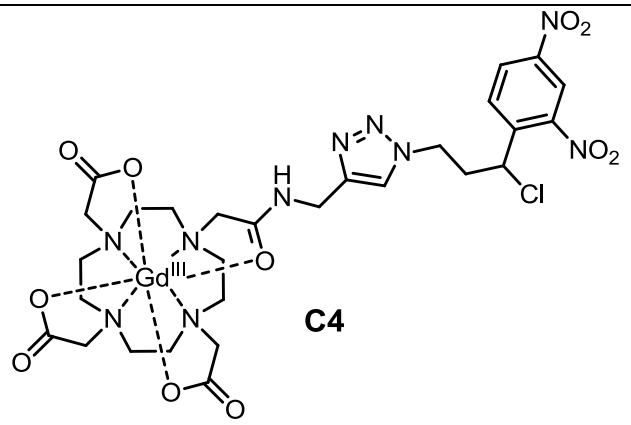 **C4**
CA2	TV1/DYE1	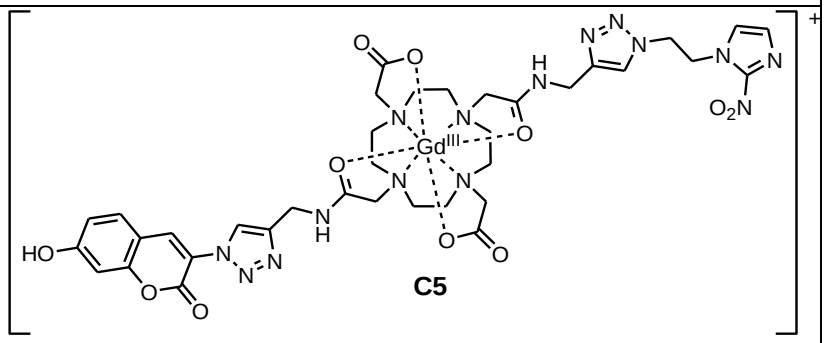 **C5**
CA4	TV1	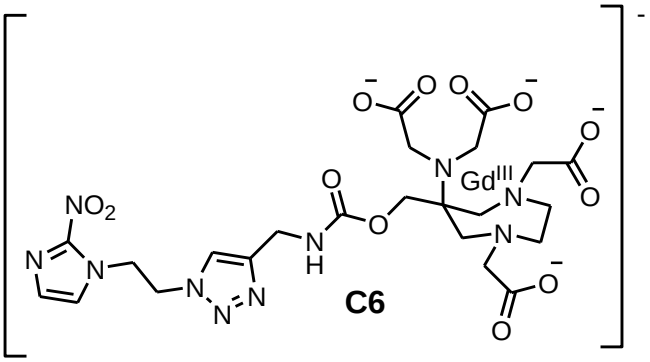 **C6**
CA4	TV3	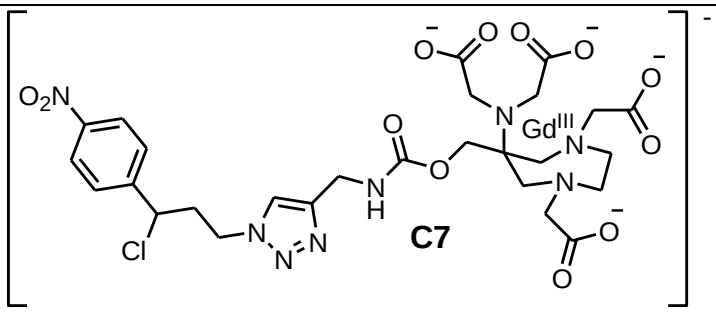 **C7**

Once all the complexes were synthesised they were to be tested with regards to their relaxivity properties and their ability to be reduced specifically under hypoxic conditions.

The relaxivity testing was performed using a series of known concentrations of the complexes. These were then subjected to an inversion recovery pulse sequence to produce a MRI scan of the tube from which the signal strength could be extrapolated. Using the equation below (Equation 10) a reciprocal T_1 value could be deduced which was then plotted against the concentration of the complex. The gradient of this graph produces a relaxivity value in $mM^{-1}s^{-1}$ for the complex. [117]

$$S_t = S_o(1 - 2exp^{\frac{-t}{T_1}})$$

Equation 10 Equation used to calculate the T_1 value from the signal intensity.

The activity under hypoxic conditions was monitored using the enzyme *Xanthine oxidase*. The aim was to use the protocol set out by Bejot *et al.* [118] which uses xanthine and the azole complex as the reducing and oxidising substrates respectively. This reaction could be monitored at time points using UV spectroscopy as there should be a noted reduction in the absorption at 325 nm, which corresponds to the absorption maximum of the nitro group containing chromophore.

Chapter 3 - Results and Discussion

3.1 Synthesis of Contrast Agent 1.

The initial aim of the project was to synthesise a gadolinium(III) chelate containing a propargyl linker. This novel class of compound has the unique advantage of a synthetic handle for orthogonal diversification – the alkyne group. 'Click' chemistry was then used to attach the chelate to a variety of azides which allows the chelate to be targeted to biological areas of interest, for example, hypoxic environments (typically associated with diseases such as cancer). The first complex **CA1** was based on the DO3A gadolinium(III) complex which has the shortest synthetic route of the chelating agents, and is widely used in literature. [119] [109] [74] It will therefore acts as a good comparative standard with other technologies. It is also to be noted that the europium(III) derivatives were also synthesised, for use in NMR characterisation of the compounds, as NMR spectra can not be produced for the gadolinium compounds.This is due to the extensive paramagnetic nature of the gadolinium(III) having a deleterious effect on the NMR spectra as the signal is broadened beyond useful recognition.

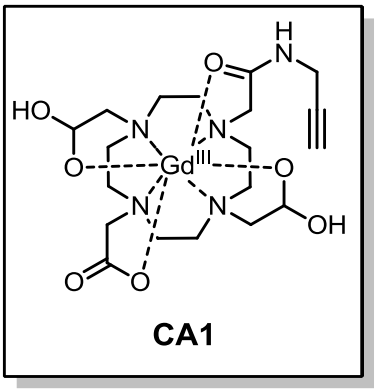

Figure 42 Contrast Agent 1.

This complex (**CA1**) has already been reported in the literature by Viguier *et al.* [74] whic is based on the pivotal *tert*-butyl protected DO3A compound. Initially this intermediate was to be synthesised *via* a method developed within the Thomas group, which was reported to give an overall yield of 31% (Scheme 13). [8] This method involved the formation of the tri-Boc substituted cyclen ring **60** in 49% yield, before protecting the remaining free nitrogen with an orthogonal Fmoc group **61**. The Boc group was then removed and replaced with three *tert*-butyl acetate groups **63**, and then finally the Fmoc group was deprotected to produce the protected DO3A compound **64**. However, both the introduction of the *tert*-butyl arms and the Fmoc deprotection proceeded in much lower yields, resulting in an overall yield of 7% (Scheme 13). As considerable quantities of the key intermediate (**40**) were required, an alternative route that was more robust was sought.

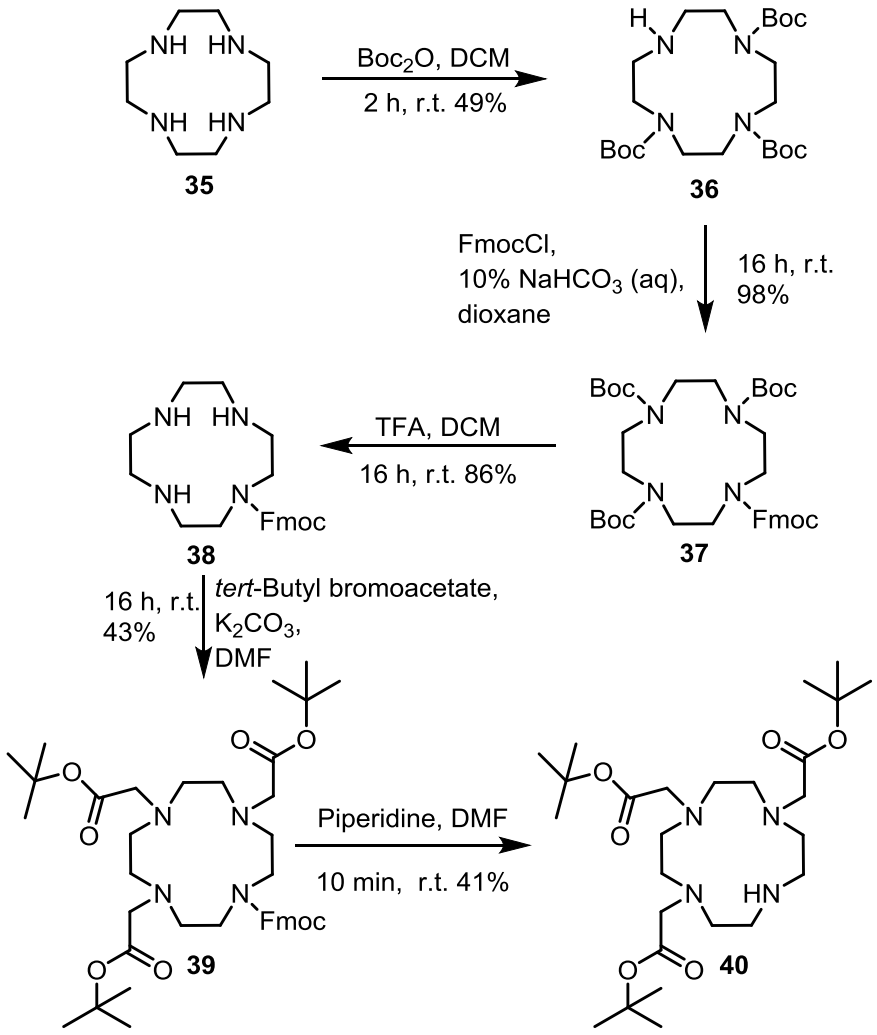

Scheme 13 Initial synthesis of *tert*-butyl protected DO3A (40).

Following an established synthesis by Machitani *et al*. [73] it was observed that the three fold addition of the *tert*-butyl acetate substituents onto the cyclen could be controlled using exactly three equivalents and large dilutions (1 mg of cyclen **35** per 1 mL of acetonitrile) to give 85% yield, similar to the 91% reported in the initial paper (Scheme 14).

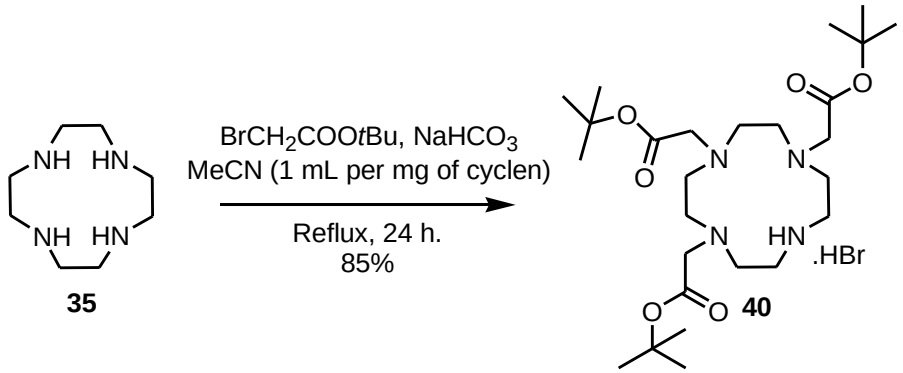

Scheme 14 Used synthesis of tri-protected DO3A (40).

Once the tri-protected DO3A (**40**) had been synthesised, a variety of methods were investigated for the addition of the fourth substituent containing a free carboxylic acid group (**76**) (Scheme 15). Once in place, the carboxylic acid could be conjugated to propargyl amine to form the final contrast agent.

Adapting literature reports by Miranda-Vera *et al.* a benzyl protected acetate group was introduced (**75**). [120] Cyclen based compounds are notorious for being unstable on silica, [121] so purification of the benzyl compound was difficult. A possible reason for this instability is that the compounds sit on the silica for an extended period of time as long columns are required to separate out the product from impurities.

The synthesis was continued on the crude material with the aim to remove the impurities at a later stage. However classic benzyl deprotection strategies like the hydrogenation at atmospheric pressure or two methods of basic saponification could not deprotect the compound. [122] Acid hydrolysis was not attempted as it would also remove the *tert*-butyl protection groups. A second route in which the carboxylic acid group was added directly, [121] was successful but required HPLC purification. This proved to be impractical with regards to both time and scale.

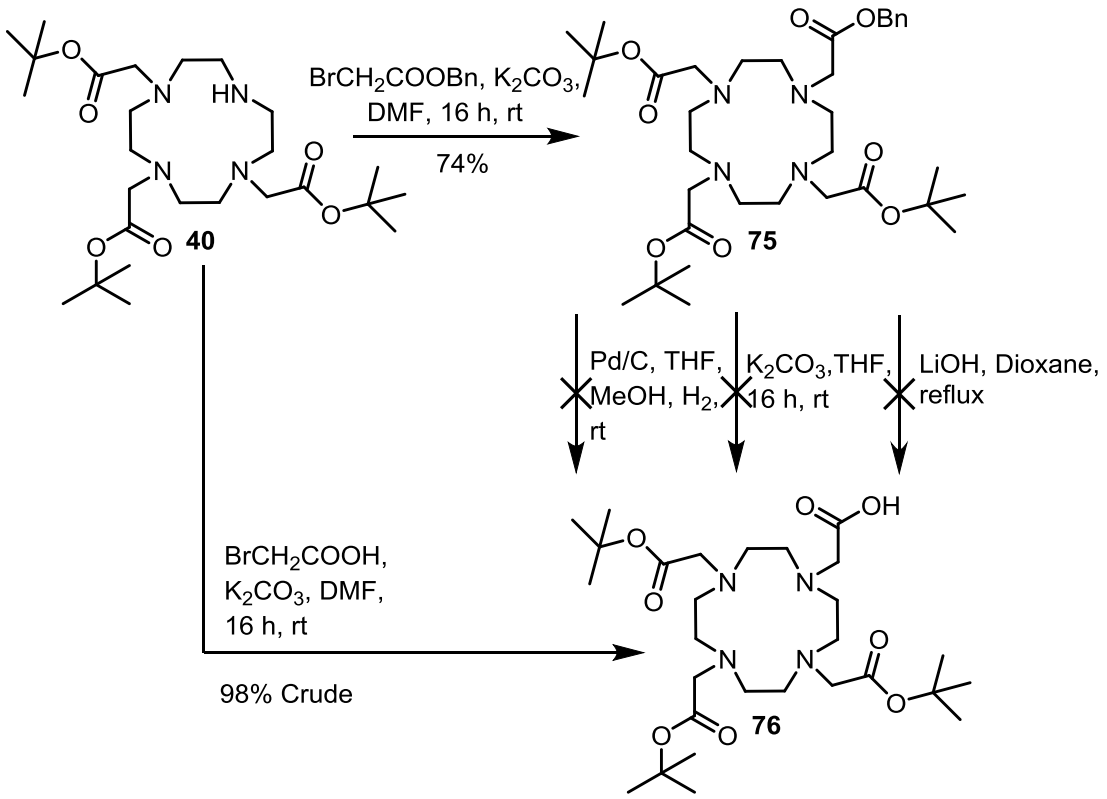

Scheme 15 Synthesis of the carboxylic acid derivative of the tri-protected DOTA complex (76).

As an alternative route to the desired product, a methyl ester protected acetate functionality was added in a 79% yield (**77**) and then deprotected using lithium hydroxide. Whilst this yielded the free carboxylic acid (**76**) removal of the excess lithium salt produced poor yields of <20% (Scheme 16). [122]

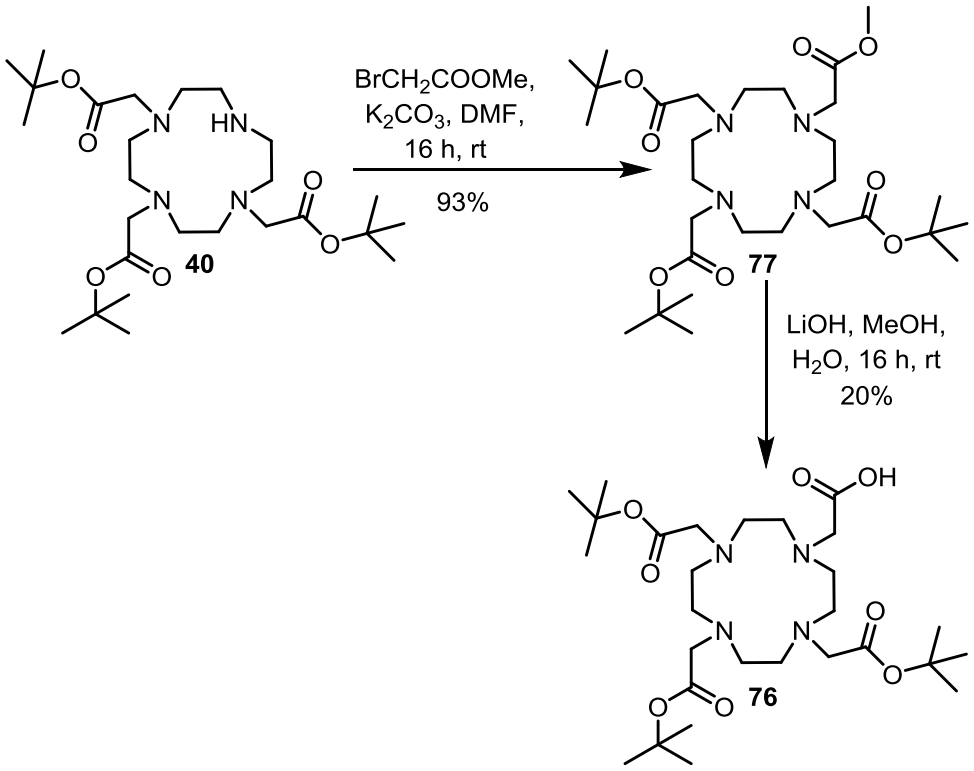

Scheme 16 Methyl acetate route to the free carboxylic acid intermediate (76).

To complete the synthesis of **CA1** a dicyclohexylcarbodiimide (DCC) coupling with propargyl amine was attempted following work done by Heppeler *et al.* [123] However, this only resulted in a mixture of unreacted starting materials, thus *O*-benzotriazole-*N,N,N′,N′*-tetramethyl-uronium-hexafluoro-phosphate (HBTU) was used as the coupling agent. [124] Whilst this produced the desired product (**78**) by mass spectrometry, separation from aromatic impurities proved impossible.

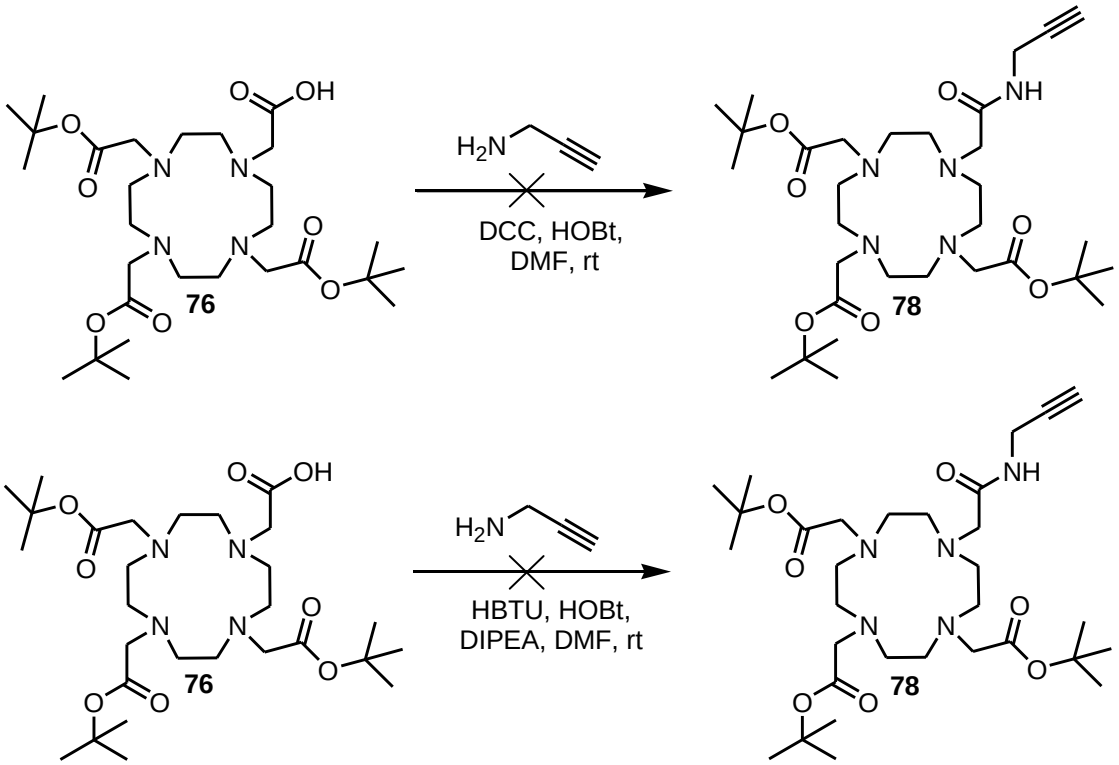

Scheme 17 Attempts to introduce the propargyl group using standard peptide coupling methods.

Instead of carrying out an exhaustive exploration of the many alternative coupling agents, a procedure by Mani *et al.* [125] was adapted. In this protocol propargyl amine is mono-coupled *via* an elimination-addition mechanism to bromo-acetylbromide **79** (Scheme 18), before addition of the acetamide (**80**) to the tri-protected cyclen ring (**40**) (Scheme 19).

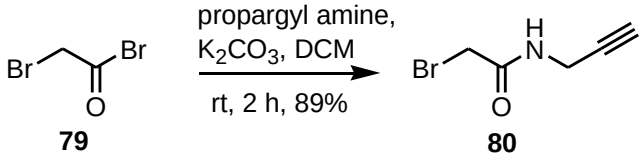

Scheme 18 Synthesis of 2-bromo-N-(prop-2-yn-1-yl)acetamide 80

Initially this reaction was carried out in DMF, which produced a 55% yield, yet when the reaction was run in acetonitrile the yield was improved to 77%. The *tert*-butyl

groups were then removed using hydrochloric acid as this produced a crystalline salt which was easier to handle than the standard trifluoroacetic acid (TFA) salt. The gadolinium(III) and europium(III) ions were then introduced using a procedure by Ferreira *et al.* [126] to give an overall yield of 45% for the gadolinium(III) chelate **CA1** from the cyclen starting material (**35**) and 44% for the europium(III) complex **CA1-Eu** (Scheme 19).

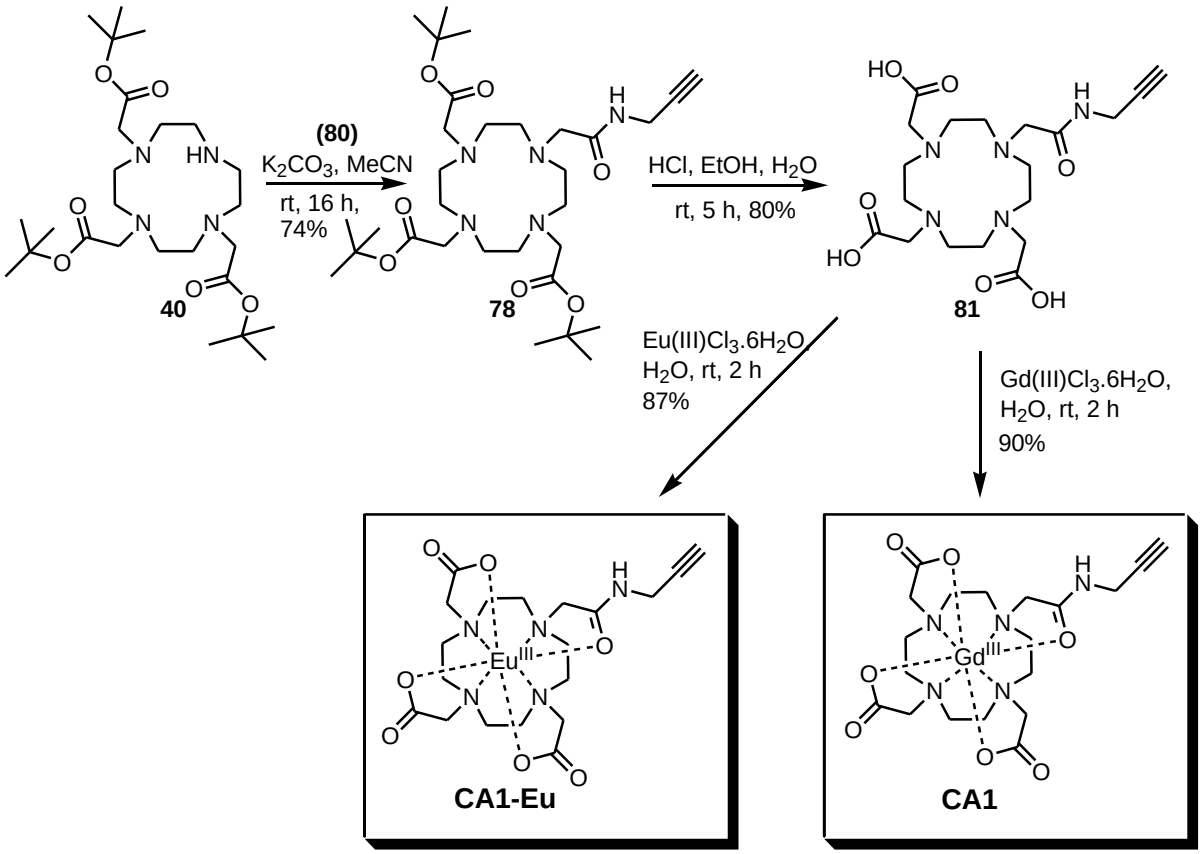

Scheme 19 Final synthesis route for complex 1 (CA1)

3.2 Synthesis of Contrast Agent 2

The next complex synthesised was a DOTA-based complex with two functionalised alkyne substituents **CA2**. This compound has the advantage of being able to attach two moieties with different functionality. This technology

could be used to create a multimodal contrast agent with a hypoxia targeting vector, and either a fluorescence or PET probe covalently attached to the gadolinium(III) contrast agent (Figure 43).

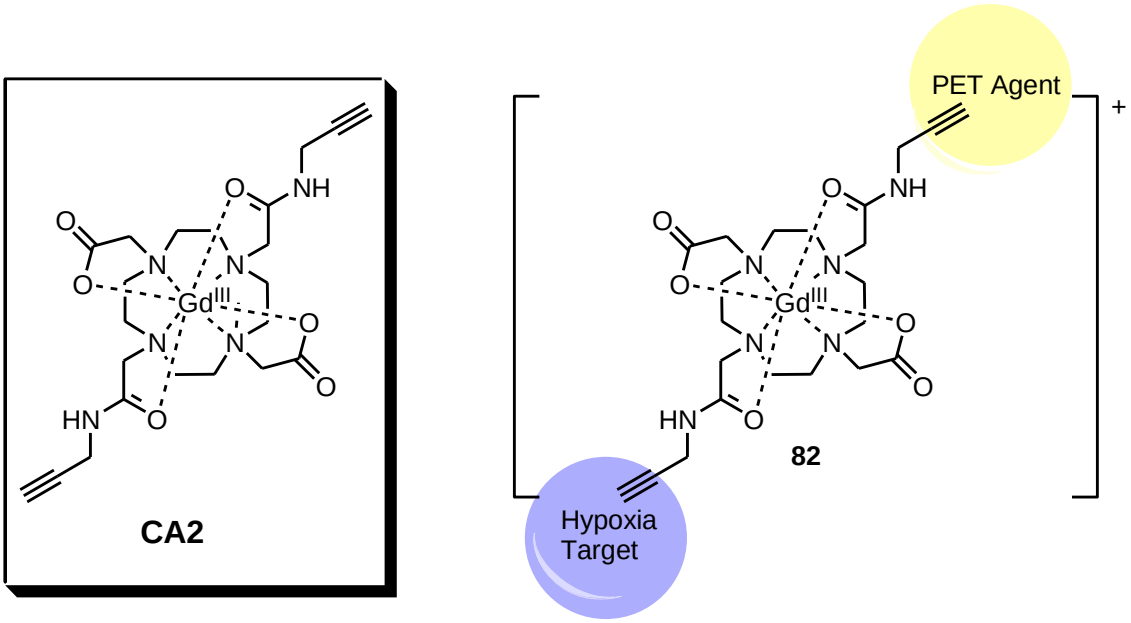

Figure 43 Contrast Agent 2 CA2 and a potential multimodal contrast agent 72.

The synthesis started with a double Boc protection (Scheme 20). This was achieved by adapting a synthesis developed by Miranda-Vera *et al*. [120] which used Boc-oxysuccinimide instead of Boc-anhydride to produce the trans-*bis* product preferentially over the tri substituted product. This occurs as the cyclen ring **35** has two available electron pairs on N1 and N7, as the H-atoms on these amines are directed towards the centre of the ring, whilst the H-atoms on N4 and N10 are directing outwards, a phenomenon that has been determined by X-ray crystallographic studies. [127] This also affects the basicity of the protons as the pKa values of the four amino groups are 10.5, 9.5, 1.6 and 0.8 respectively. This is important as if the basicity of the leaving group is comparable to or higher than that of the unprotected amine groups on the

cyclen ring it will act as a base and promote the formation of the tri and tetra substituted cyclen ring. However if a weakly basic leaving group such as an oxysuccinimide (pKa 7.8) derivative is used only the di-protected cyclen ring will be formed.

As this compound was synthesised in parallel with the previous compound, similar optimisation problems were encountered. A benzyl group was the initial orthogonal protection group used but the di-benzyl, di-*tert*-butyl substituted complex (**86**) could not be purified in acceptable yields due to instability on the silica column. (Scheme 20)

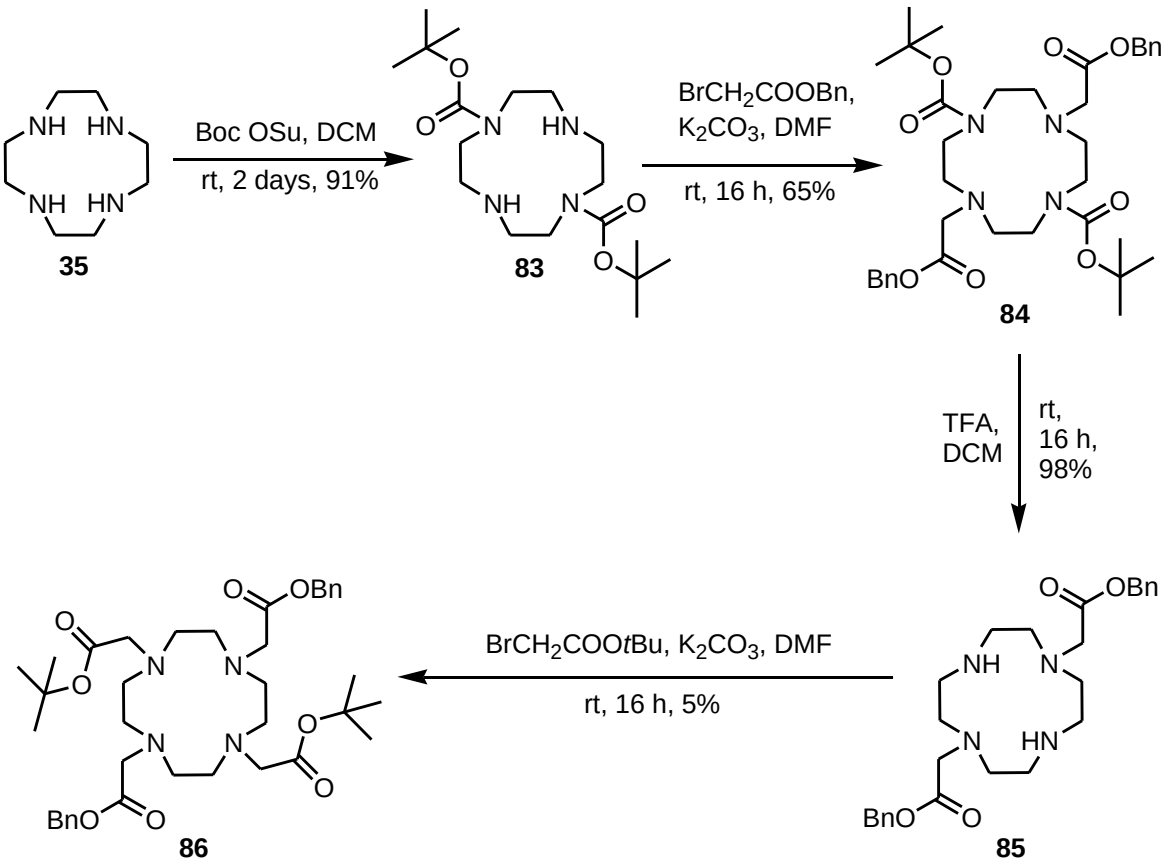

Scheme 20 Route 1 towards the synthesis of a bifunctional chelator (86).

Two synthetic routes to the methyl ester protected intermediate (**88**) were developed . Interestingly, the shorter synthesis (Scheme 21) that introduced the ester directly *via* methyl bromoacetate had a lower overall yield of 37% compared with 55% for the longer synthetic route (Scheme 22). However in either case, deprotection of the methyl ester with LiOH again gave disappointing yields of only 15%.

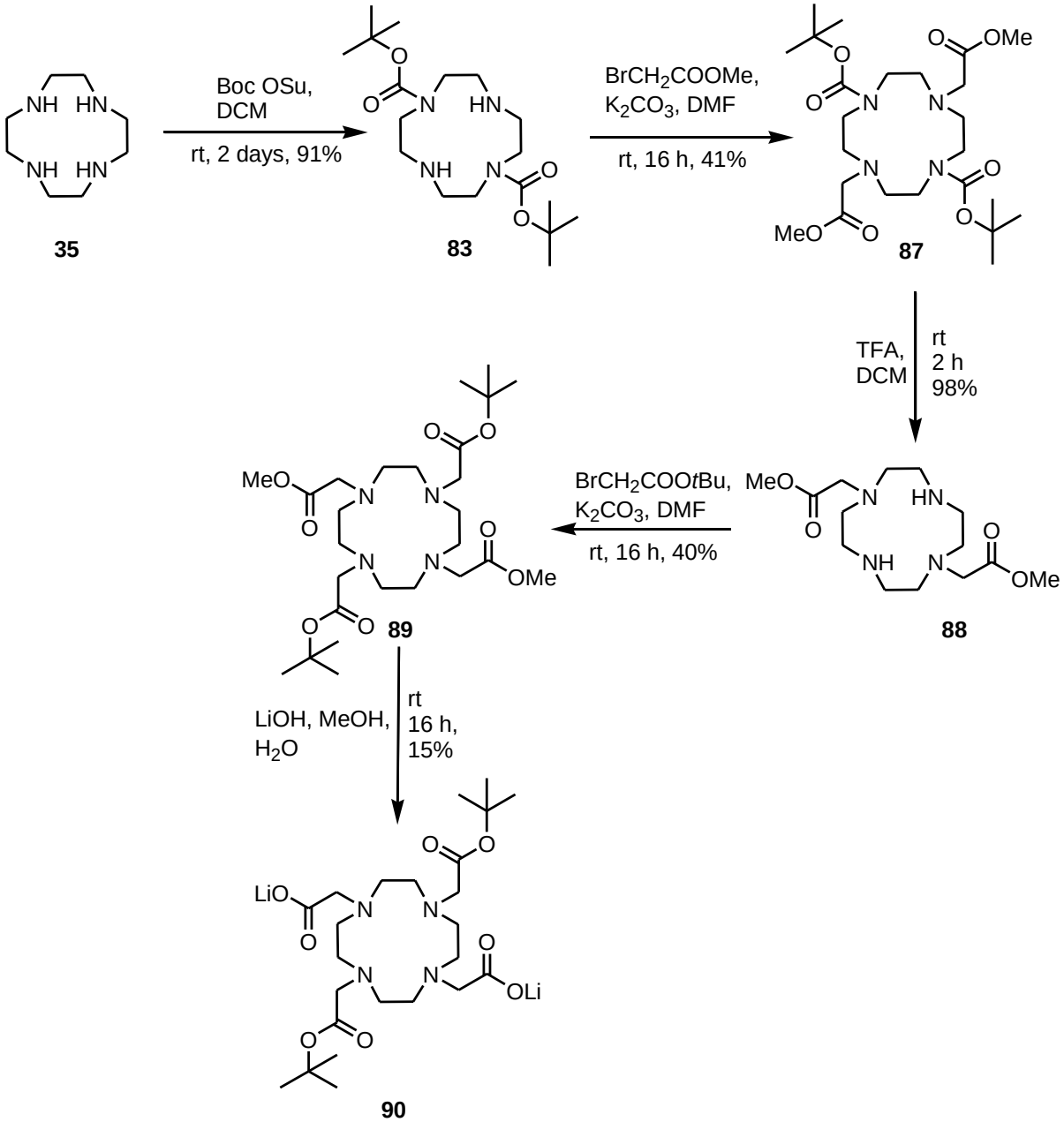

Scheme 21 Route 2 towards the synthesis of a bi-functional chelator (CA2).

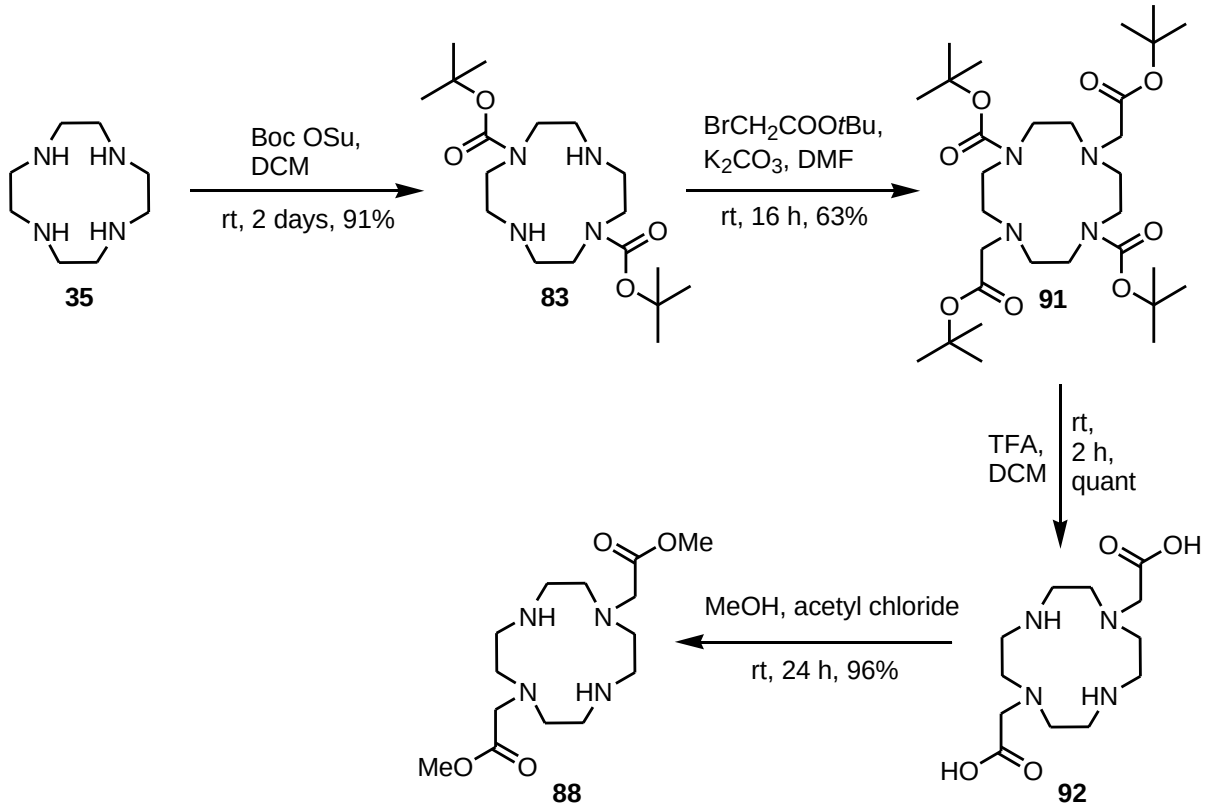

Scheme 22 Second synthesis of the *bis*-methylacetate substituted cyclen (88).

The procedure already used before by Mani *et al.* [125] was then applied to form the bi-functional complex (**96**). This successfully yielded both the europium(III) (**CA2-Eu**) and the gadolinium(III) complexes (**CA2**) in overall yields of 8 and 12% respectively (Scheme 23).

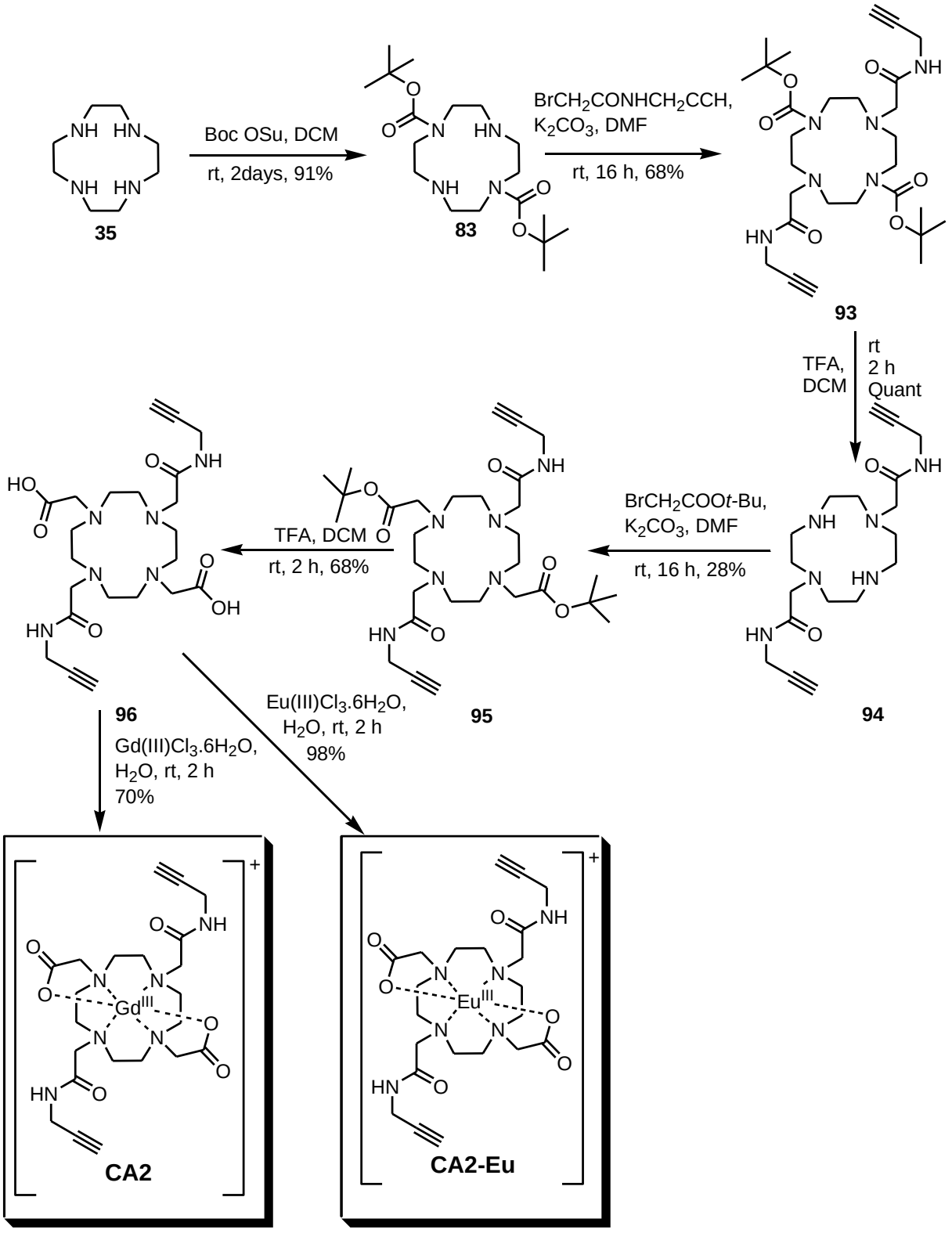

Scheme 23 Final synthesis of the bi-functional chelator (86) and the respective lanthanide complexes CA2 and CA2-Eu.

3.3 Synthesis of Contrast Agent 3

The synthesis of the Gd(III)DO3A-*N*-α-aminopropionate complex **CA3** was undertaken as an alternative to the Gd(III) DO3A based complex (**CA1**). This complex has optimised water exchange rates, with a k_{ex} of 4.0 $x10^{-7}$ s^{-1}, compared to 0.46 $x10^{-7}$ s^{-1} for $[Gd(DOTA)(H_2O)]^-$, even though less than 2% of DO3A-*N*-α-aminopropionate was found to be in the favourable TSA form. This acceleration of the water exchange is postulated to be due to steric crowding caused by the propionate group facilitating the departure of the water molecule from the central ion. [126]

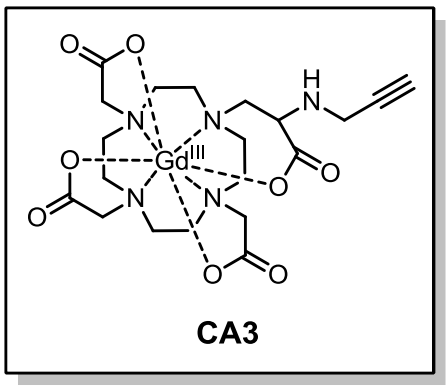

Figure 44 Contrast Agent 3.

This synthesis uses dehydroalanine **100** in a Michael addition onto the cyclen **35** instead of the standard S_N2 addition used for the acetate functionality. This is due to the instability of the orthodox bromo and tosyl serine derivatives seen by Ferreira *et al.* [126] The dehydroalanine **100** was synthesised from protected serine (**99**), [122] [128] *via* a dehydration reaction using copper(I) and a dicarbodiimide as reported by Zhu *et al.* (Scheme 24) [129]

Originally the aim was to synthesise the target compound by reacting the dehydroalanine **100** with *tert*-butyl protected DO3A **40** synthesised previously, yet this reaction yielded only starting materials (Scheme 24).

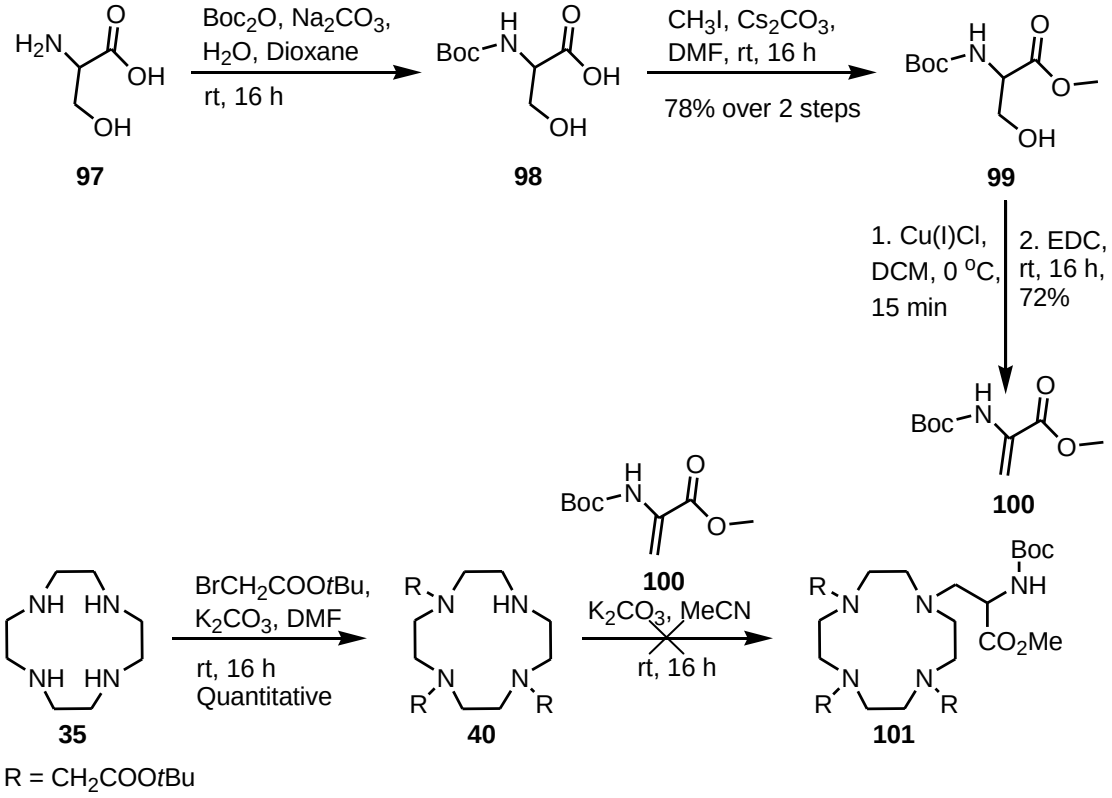

Scheme 24 Synthesis towards a DO3A-*N*-α-aminopropinate based chelator CA3.

Mono addition onto an unfunctionalised cyclen ring **35** however yielded the expected compound, just in much lower yields than in the literature, 50% compared to 77% (Scheme 25). [126] The yield was highly capricious and often a maximum of 10% yield was attainable, despite the majority of cyclen **35** being converted according to mass spectrometry detection. This poor yield can be attributed to retention and breakdown of the complex on silica as seen with other cyclen based compounds. As the cyclen **35** starting material is relatively expensive, and the dehydroalanine **100** difficult to handle, the synthesis of this compound was abandoned.

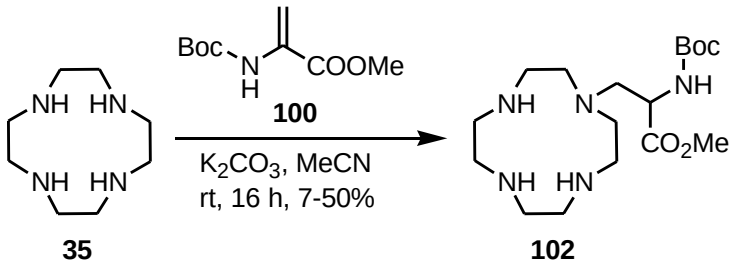

Scheme 25 Michael addition of the dehydroalanine 100 onto the unsubstituted cyclen 35.

3.4 Synthesis of Contrast Agent 4.

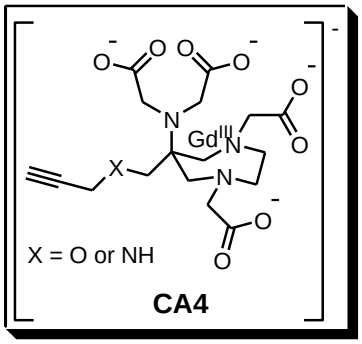

Figure 45 Contrast Agent 4

An alternative gadolinium(III) chelator to DOTA is the AAZTA complex. As explained previously AAZTA has significant advantages over DOTA for despite having similar thermodynamic properties it occupies fewer co-ordination sites on the central gadolinium(III) ion. Thus two water molecules are free to coordinate to gadolinium(III), which in turn improves overall relaxivity. [77]

The synthesis starts with a nitro-Mannich reaction to produce the 1,4-diazepine ring with both amines protected by benzyl groups (**103**). This reaction was completed using a method developed by Gugliotta *et al.* [79] and obtained a quantitative yield, identical to that reported. Compound **103** was to then undergo a hydrogenation reaction to simultaneously remove both benzyl groups and reduce the nitro group to an amine. Initially the procedure by

Gugliotta *et al.* [79] which used ammonium formate and formic acid as the hydrogen source, yielded a small amount of compound **104** which was inseparable from degradation products of the starting material (**103**). Two atmospheric pressure hydrogenations were then attempted, one with and one without the addition of acetic acid. [122] [130] The acetic acid method was to try and prevent catalytic poisoning from the primary and secondary amines produced. After 24 hours the hydrogenation containing acid had degraded to unidentifiable materials, whilst the hydrogenation without acid only underwent one de-benzylation after 24 hours and after 72 had degraded completely. To solve this problem a modified version of the parr hydrogenation used by Sengar *et al*. [75] was attempted. The reaction was undertaken at room temperature instead of 60 °C and for 48 hours due to equipment limitations. It was then observed that if the filtered solution was concentrated *in vacuo* at 40 °C, the resultant product (**104**) was a crude pale yellow oil, obtained in 85%. However, if the solution was concentrated *in vacuo* at room temperature to remove the ethanol, and then freeze dried to remove the water the resultant product (**104**) was a colourless oil obtained in 98%. The acetate group addition was achieved using a modified version of the method published by Sengar *et al*. to yield a pale yellow oil (**105**) as expected in an identical yield of 56% (Scheme 26).

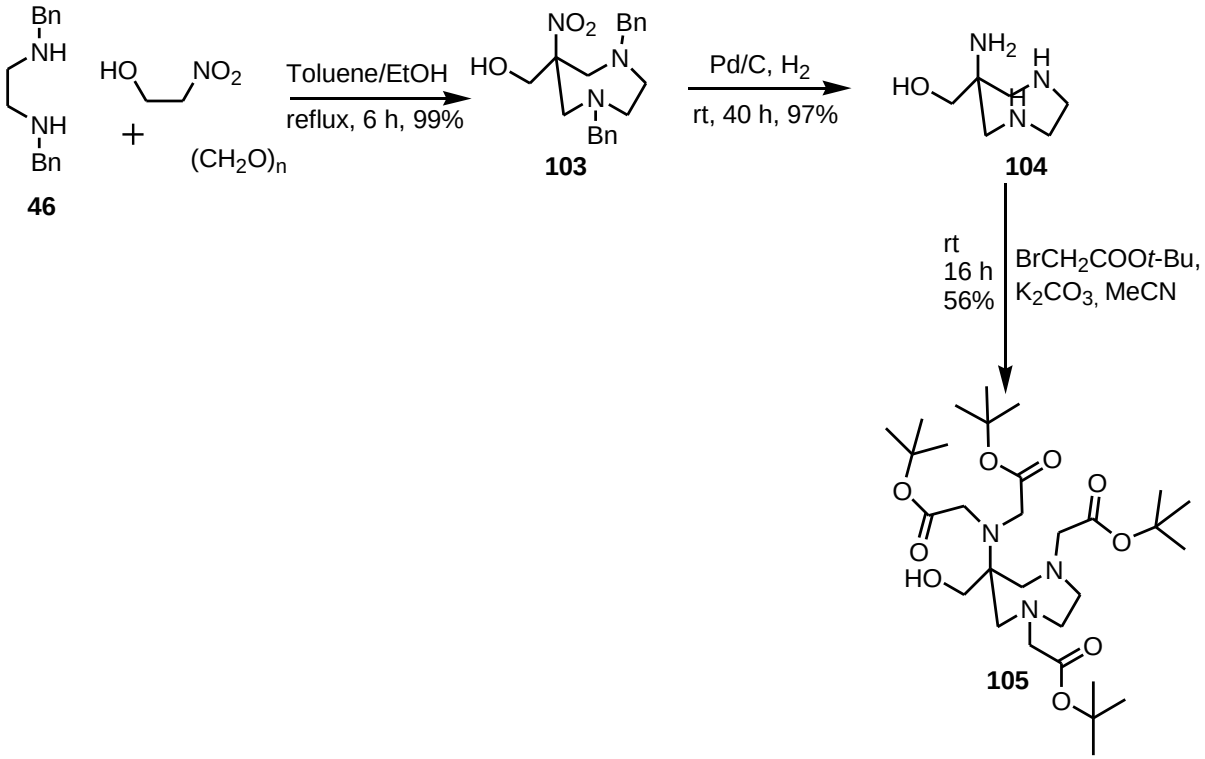

Scheme 26 Synthesis of key intermediate 105 of the AAZTA based complex CA4.

Once compound **105** was synthesised on gram scale a range of reactions were attempted to insert propargyl functionality at the hydroxyl position. Initially a mesylation was attempted, [131] yet this yielded an unidentifiable material that was later proved to be the chlorinated product (**106**) as well as a small amount of the known cyclised material (**107**) by mass spectrometry (Scheme 27).

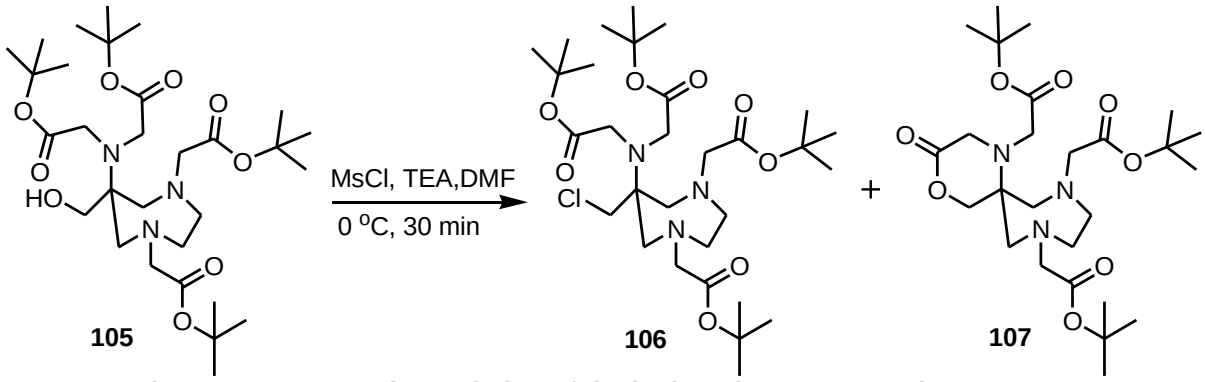

Scheme 27 Attempted mesylation of the hydroxyl AAZTA complex 105.

The cyclised material (**107**) has been widely reported in the literature to occur in the presence of acid or base, as the configuration of the hydroxyl in relation to

one of the acetate functionalities allows for the hydroxyl to attack the carbonyl to produce a *tert*-butoxide ion and a stable 6-membered ring as shown in Scheme 28. [75] [79]

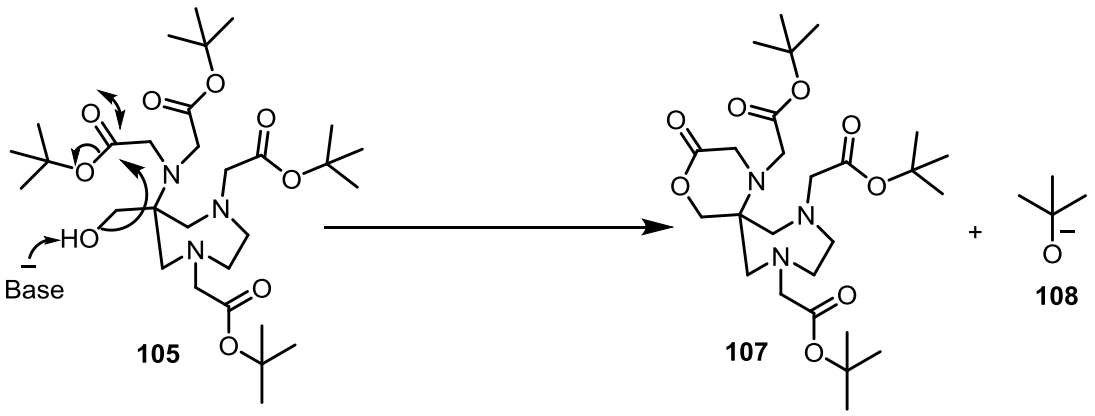

Scheme 28 Formation of [8,11-*bis*-*tert*-butoxy carbonylmethyl-3-oxo-4-oxa-1,8,11-triaza-spiro[5.6]dodec-1-yl]]-aceticacid *tert*-butyl ester 107 in the presence of a base.

Synthesis of the ether linked compound (**109**) was then attempted *via* an S_N2 reaction using propargyl bromide. When triethylamine was used as a base only starting material (**105**) was observed by mass spectrometry (Scheme 29). When sodium hydride was used the compound was seen to almost entirely cyclise (**107**). Whilst a judicious choice of base with an intermediate pK_a between these two extremes may have permitted the desired reaction, such optimisation was deemed to be too time-consuming to be practical. Thus the ether linker route was abandoned for other potential linkers.

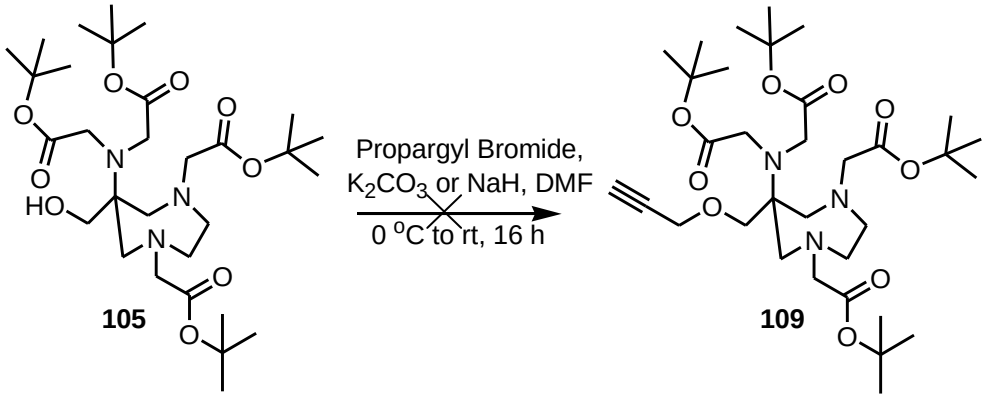

Scheme 29 Attempt to form an ether linkage 109 using propargyl bromide.

Conversion of the hydroxyl group to a chlorine (**106**) was achieved using thionyl chloride. The crude material was taken onto the S_N2 reaction using propargyl amine, triethylamine and acetonitrile to allow for insertion of the propargyl group into the AAZTA structure (**110**). [79] When carried out on a small scale (100 mg), the reaction yielded the expected product in a low 35% yield, yet when performed on a larger scale (1 g) one of the *tert*-butyl groups was removed and this product was produced in a 40% yield. This was inconsequential as the next step was the removal of the *tert*-butyl groups. Unfortunatly during the removal of the *tert*-butyl groups half the compound cyclised to form the amide derivative of the cyclised structure, and despite following literature procedure [79] the attempt to hydrolyse this using sodium hydroxide yielded only degraded material (Scheme 30).

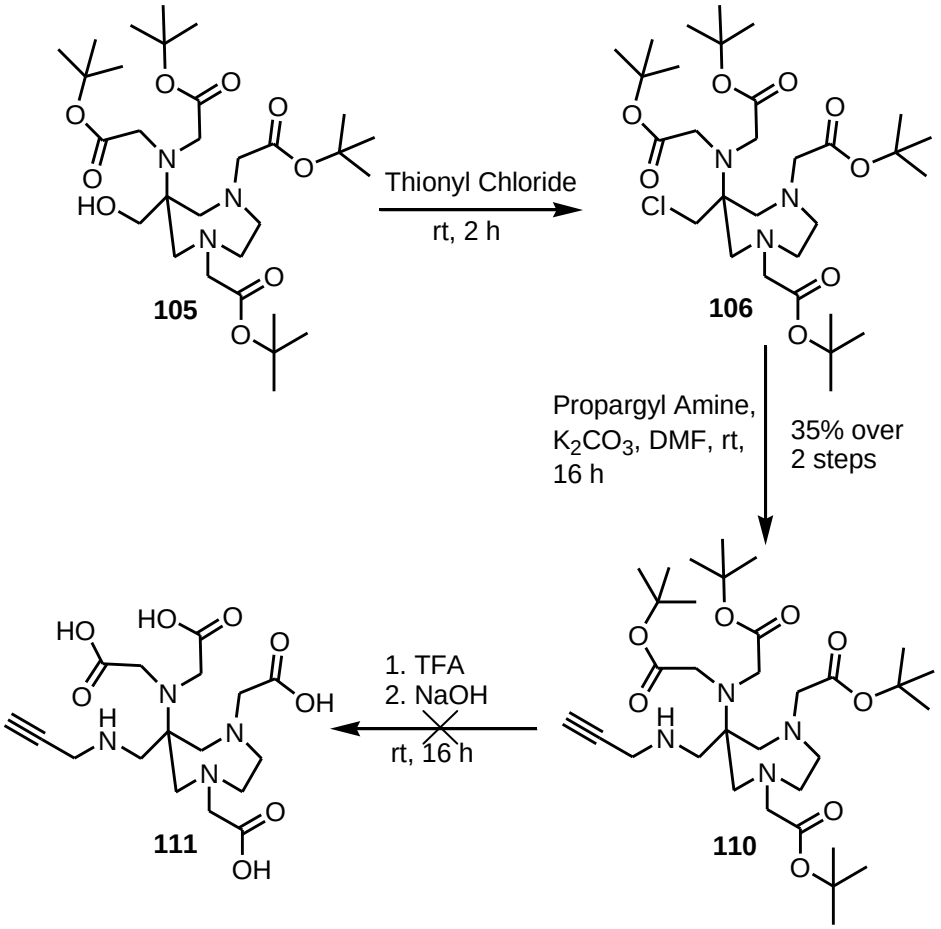

Scheme 30 Attempted synthesis of the AAZTA based contrast agent CA4 using a nitrogen bridge.

A recent paper by Gugliotta *et al.* [79] reacted the primary alcohol of the AAZTA (**105**) with isocyanates to produce carbamate compounds that were stable enough to withstand *tert*-butyl cleavage conditions (TFA), without producing any cyclised side product (**107**). *Via* a Curtius rearrangement [132] the isocyanate of propiolic acid (**113**) was generated *in situ* before addition of the free alcohol (**105**), to try and produce the carbamate (**114**). Whilst all of the AAZTA starting material (**105**) was consumed by mass spectrometry, the end product was unidentifiable (Scheme 31).

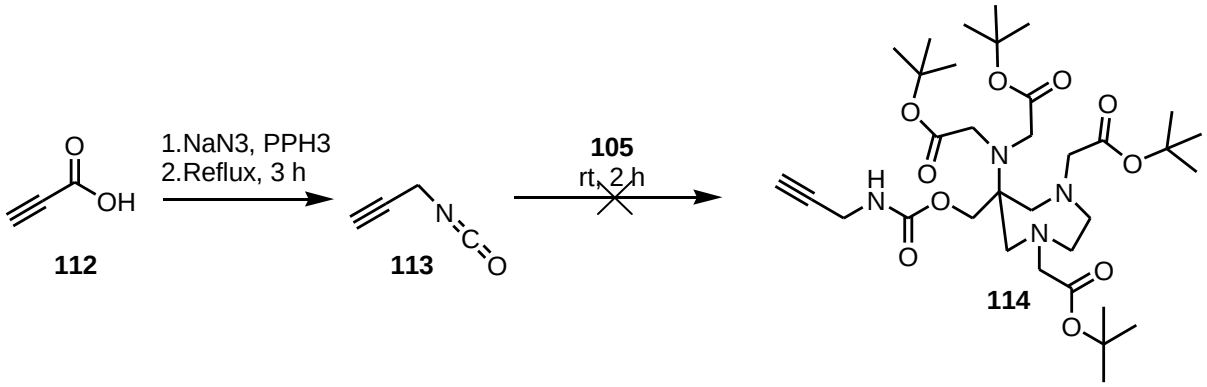

Scheme 31 Attempt to form the carbamate derivative 114 using the Curtius rearrangement

Thus the synthesis was modified and the chloroformate AAZTA derivative (**114**) was produced using triphosgene. This was then reacted with propargyl amine to yield the corresponding carbamate in a yield of 32%. [133] The carboxylate groups were then deprotected using TFA, to yield the tetra TFA salt (**115**), before undergoing metal insertion using the same method as for the DOTA based complexes (**CA1** and **CA2**). This produced the europium(III) complex (**CA4-Eu**) in an overall yield of 12% and the gadolinium(III) complex (**CA4**) in 9% (Scheme 32).

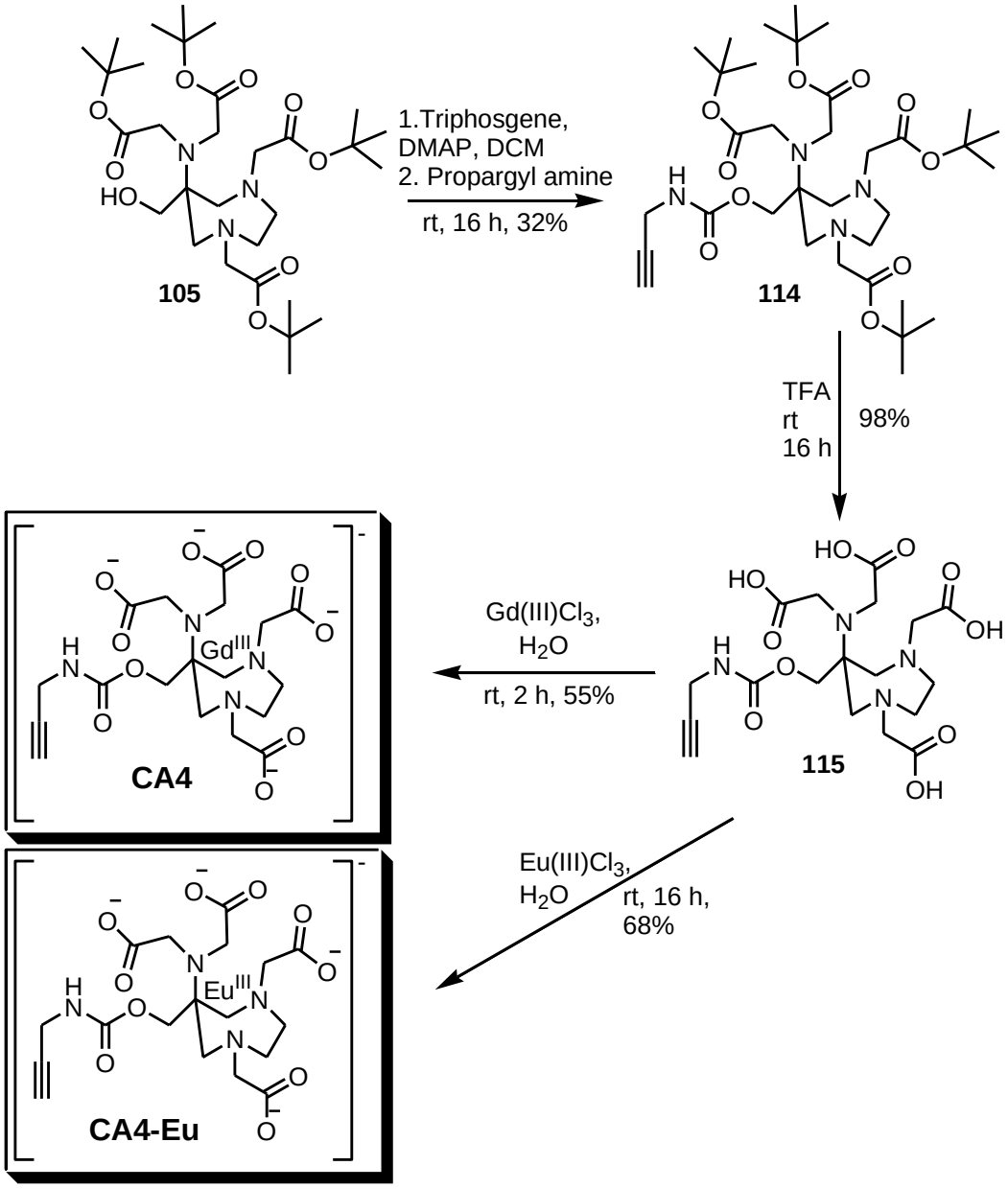

Scheme 32 Synthesis of the AAZTA based complex CA4.

3.5 Synthesis of Targeting Vector 1.

To target the MRI contrast agents to hypoxic tumours a targeting vector must be conjugated via the alkyne functionality in the complexes. The initial vector synthesised consists of the known 2-nitroimidazole targeting vector conjugated to an azide moiety **TV1**. The azide is required to react with the alkyne on the contrast agents to form the triazole linker using 'click' chemistry. [108]

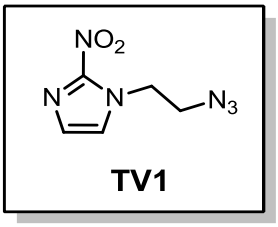

Figure 46 Targeting Vector 1 TV1.

2-Nitroimidazole **117** was synthesised from 2-aminoimidazole hemisulfate **116**, via a diazatisation and subsequent displacement method developed by Takuma *et al.* [134] This occurred in a 70% yield comparable to a literature yield of 76%. The 2-nitroimidazole **117** was then to be conjugated to the azide functionality via an S_N2 reaction with dibromoethane as previously undertaken by Chu *et al.* [135] Whilst the corresponding product was confirmed by mass spectrometry the product **118** could never be isolated and confirmed by NMR. (Scheme 33)

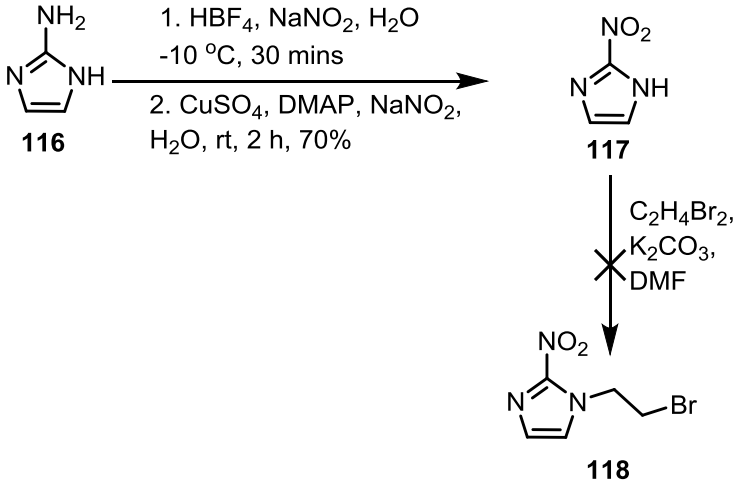

Scheme 33 Route 1 towards the synthesis of the 2-nitroimidazole based targeting vector TV1.

As an alternative to the S_N2 reaction, an epoxide was used to form the ethyl linker as suggested by Bejot *et al.* [118]. The epoxide used was propylene oxide which had the potential to yield two regioisomers (**119a** and **b**)(Figure 47).

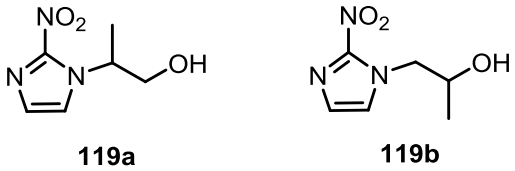

119a **119b**

Figure 47 The two possible regioisomers after propylene oxide opening.

Whilst not the originally intended compound propylene oxide is significantly less expensive and easier to handle than ethylene oxide. It also has the advantage of inserting an extra carbon into what could potentially be an explosive compound. During purification only the **119b** regioisomer was isolated and characterised. A Mitsunobu reaction as outlined by Sen *et al.* [136] was then attempted to convert the hydroxyl group to an azide, yet this yielded only starting material (**119b**) by mass spectrometry and IR spectroscopy (Scheme 34).

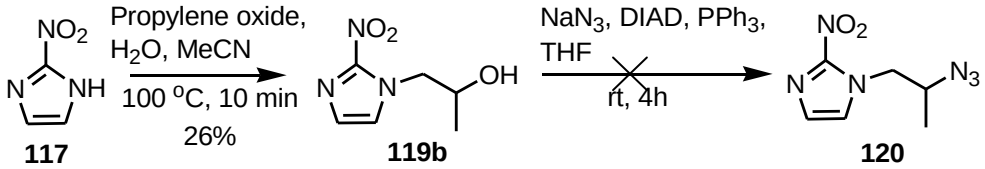

117 **119b** **120**

Scheme 34 Route 2 towards the synthesis of the 2-nitroimidazole based targeting vector TV1.

Thus a route *via* a mesylate intermediate followed by displacement with an azide was explored (Scheme 35). (131) Whilst the mesylate was formed (**121**) and confirmed by NMR, yields were <10%, and azidation using sodium azide to

displace the mesylate (**120**) was unsuccessful as proven by mass spectrometry and IR spectroscopy.

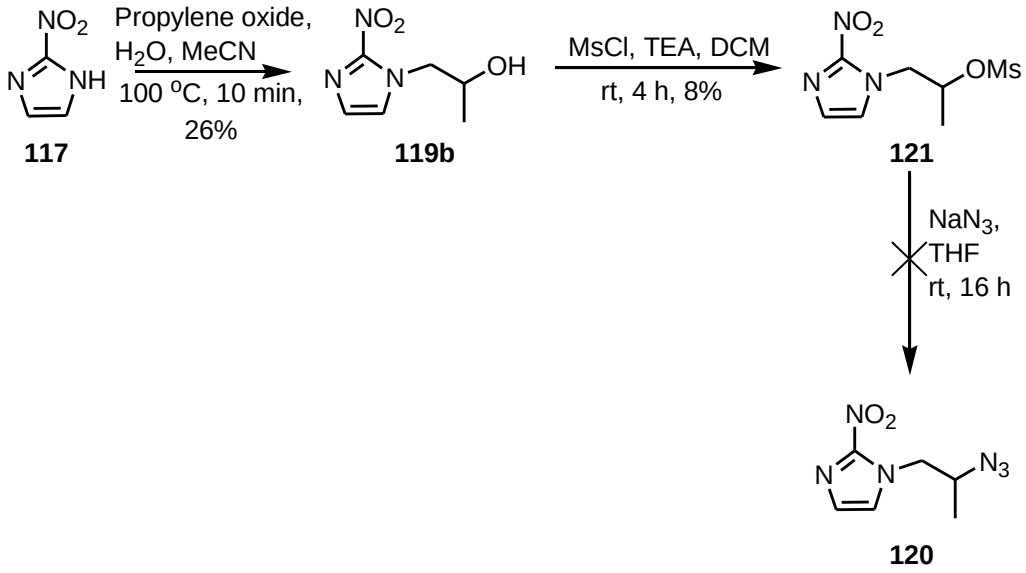

117 **119b** **121** **120**

Scheme 35 Route 3 towards the synthesis of the 2-nitroimidazole based targeting vector TV1.

Finally inspired by a patent which produced similar compounds but with a PEG linker between the imidazole and the azide a method was deduced to produce the final compound **TV1**. [(114)] Initially 2-nitroimidazole **117** was conjugated to a tosyl protected ethanol group using ethylene glycol *bis*-*p*-toluenesulfonate and triethylamine (**122**). When run overnight the maximum isolatable yield was 11%, yet when left for 4 days this increased to 86%. The tosyl group was then displaced using sodium azide at room temperature to produce the final compound (**TV1**) in a 58% overall yield from 2-aminoimidazole hemisulfate **116** (Scheme 36).

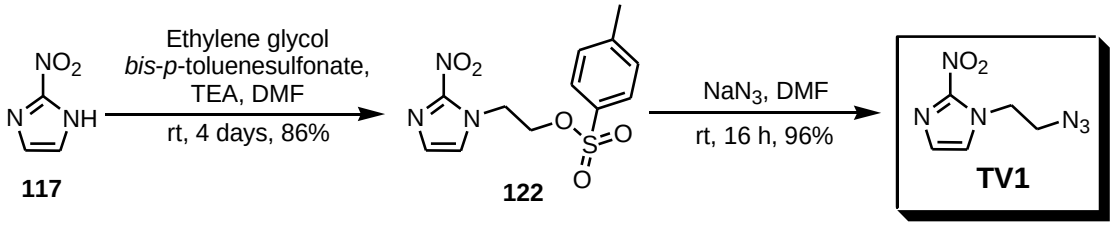

Scheme 36 Completed synthesis of a simple 2-nitroimidazole targeting vector TV1.

3.6 Synthesis of targeting vectors 2-4

An alternative targeting vector to the 2-nitroimidazole is the nitrobenzyl series of compounds. For the leaving group to be activated successfully the nitro functionality must be in either the *ortho* or *para* position regarding the leaving group of choice. [137] Otherwise the resonnance will not allow the leaving group to leave and produce the reactive methylene. These compounds have been demonstrated to be successful with regards to hypoxia activated pro-drugs in the literature, even if they are not as widely used in comparison to the nitroimidazoles. [94] [138] [139] [140] [141] [142]

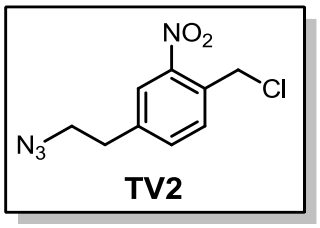

Figure 48 Targeting vector 2

The initial alternative target vector was TV2 (Figure 48). Despite numerous efforts at optimisation, the key Friedel-Crafts acylation/alkylation (Scheme 37) failed to produce the desired product (**126**), due to the deactivating effect of the nitro group.

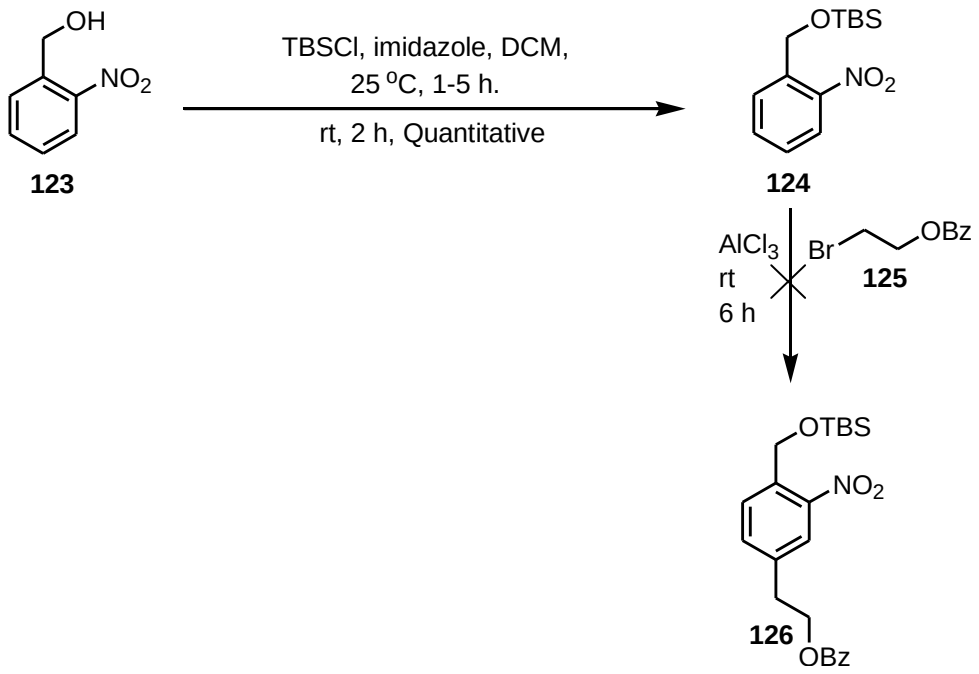

Scheme 37 Route 1 for the synthesis of an alternative targeting vector based on 2-Nitrobenzene (TV2).

Thus two alternative target compounds were developed, still containing all the necessary functionalities, just in a different configuration (Figure 49).

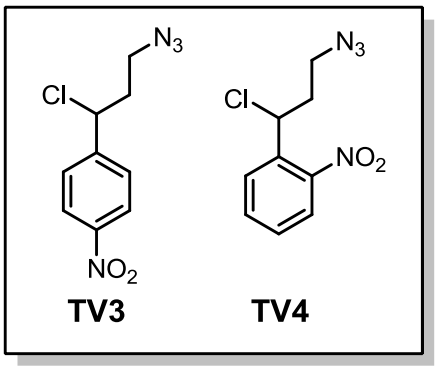

Figure 49 Modified targeting vectors 3 and 4

These compounds were based on those designed by Jiang *et al.* [116] for ADEPT activation of cancer prodrugs using *Escherichia coli* nitroreductase. These compounds are still able to release a leaving group to form an activated

methylene, and still contain the azide linker, which will allow for the 'click' reaction to the contrast agent.

The synthesis of both compounds (**TV3** and **TV4**) was initiated with a standard Grignard addition using vinyl magnesium bromide, followed by a methoxy methyl ether (MOM) protection of the alcohol produced (**131/2**). The Grignard (**129/30**) produced significantly lower yields (76% and 26% respectively compared to 95% for the *para* complex (**129**) in the literature) with the exceptionally low yield for the *ortho* compound (**130**) attributed to steric hinderance from the nitro functionality. A MOM protection in compatible yields was then undertaken followed by a hydroboration to allow for the anti-Markovnikov hydroxylation product (**133/4**). This reaction also produced significantly lower yields than those suggested in the original paper 55/56% respectively for the *para* (**133**) and *ortho* compound (**134**) compared to 78% in the literature. Once this intermediate was obtained the synthesis deviated from the paper by Jiang *et al.* [116] and the free alcohol was converted to an azide using diphenylphosphoryl azide (DPPA), DBU and sodium azide. [143] Whilst the desired product was obtained in excellent yields (97%) for the *para* compound (**135**), the *ortho* compound (**136**) produced a mixture containing product and an unknown aromatic impurity, which was separated after the next step despite dramatically reducing the yield (20% over 2 steps). The MOM group was removed using standard acid hydrolysis to leave the free secondary alcohol (**137/8**) for conversion to a suitable leaving group. [122] The leaving group chosen was a chloride ion, and was initially to be introduced using an Appel chlorination. [144] This procedure however produced only starting material (**137/8**), so thionyl chloride was used to successfully produce the chloride in a

reasonable 60% yield for the *para* compound (**TV3**) and a 43% yield for the *ortho* (**TV4**), [145] respectively to give an overall yields of 17% and 2% over 6 steps, as seen in Scheme 38.

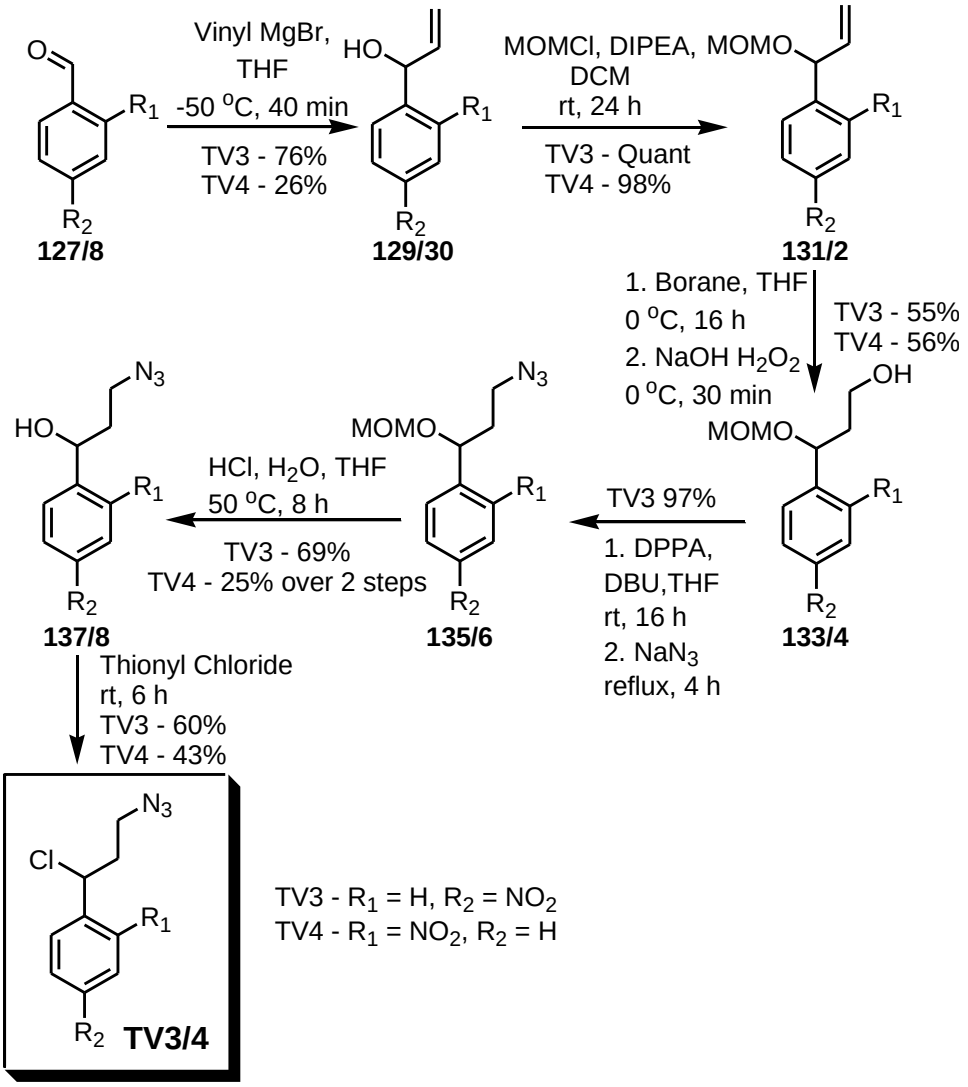

Scheme 38 Synthesis of *para* and *ortho*-nitrobenzyl targeting vectors TV3 snd TV4.

During the synthesis of all the nitrobenzyl compounds, MOM chloride became temporarily unavailable, thus a slightly altered route was attempted, during which the hydroboration occurred on the free alcohol compound (**130**) to produce the diol (**139**), before selectively tosylating the primary alcohol over the secondary using stoichiometric control (**140**). The tosyl group could then be

displaced by an azide (**138**) using sodium azide. The final chlorination could then occur as before as seen in Scheme 39 to yield the product (**TV4**) in an overall yield of 1% (Scheme 39).

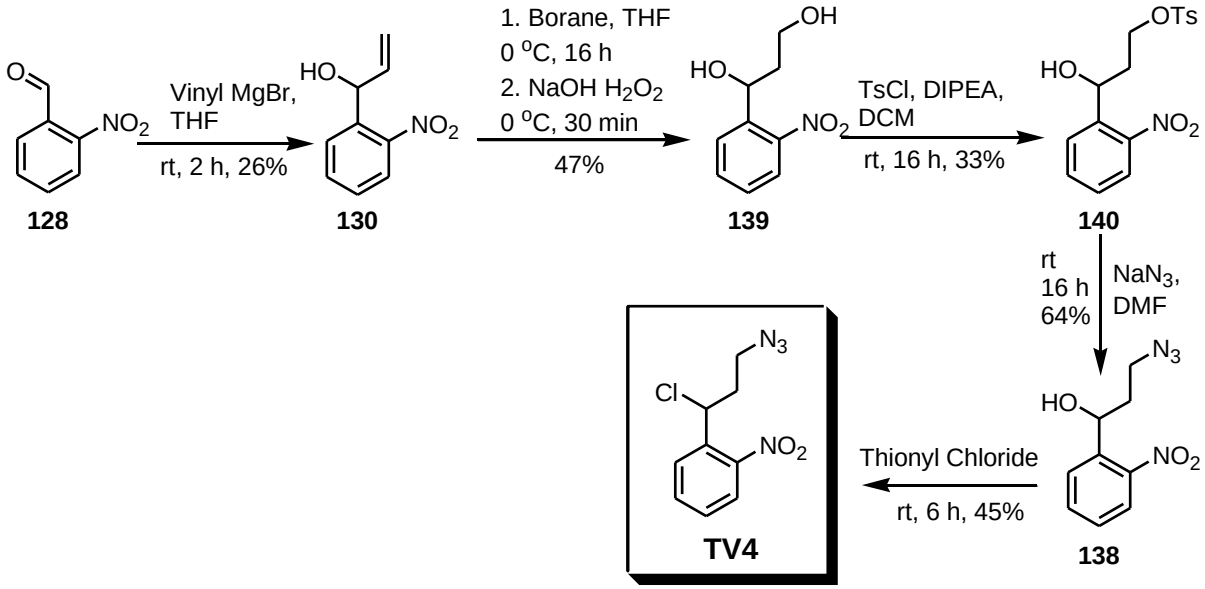

Scheme 39 Alternative synthesis of the *ortho*-nitrobenzyl targeting vector TV4.

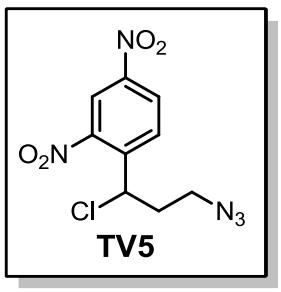

Figure 50 Targeting vector 5.

Another nitro-benzyl targeting vector is the 2,4-dinitrobenzyl complex **TV5**. It has been widely used experimentally for ADEPT purposes [146] [147] [148] using *E.coli* nitroreductase, it can also be reduced by both rat and human DT diaphorase under hypoxic conditions. [149] [150] There is however a 5-fold

reduction in the rate of reaction when human DT diaphorase is used compared to rat DT diaphorase. [115] These compounds also have a more favourable redox potential compared to the mono-nitro compounds, as the di-nitro mustard compounds have a redox potential of -450mV compared to -620mV for the *para*-nitro compound. [93]

Synthesis of this complex (**TV5**) was carried out in an identical manner to the original nitrobenzyl compounds, with most yields around 50% per step most likely due to the steric hindrance caused by the nitro group in the *ortho*-position (Scheme 40).

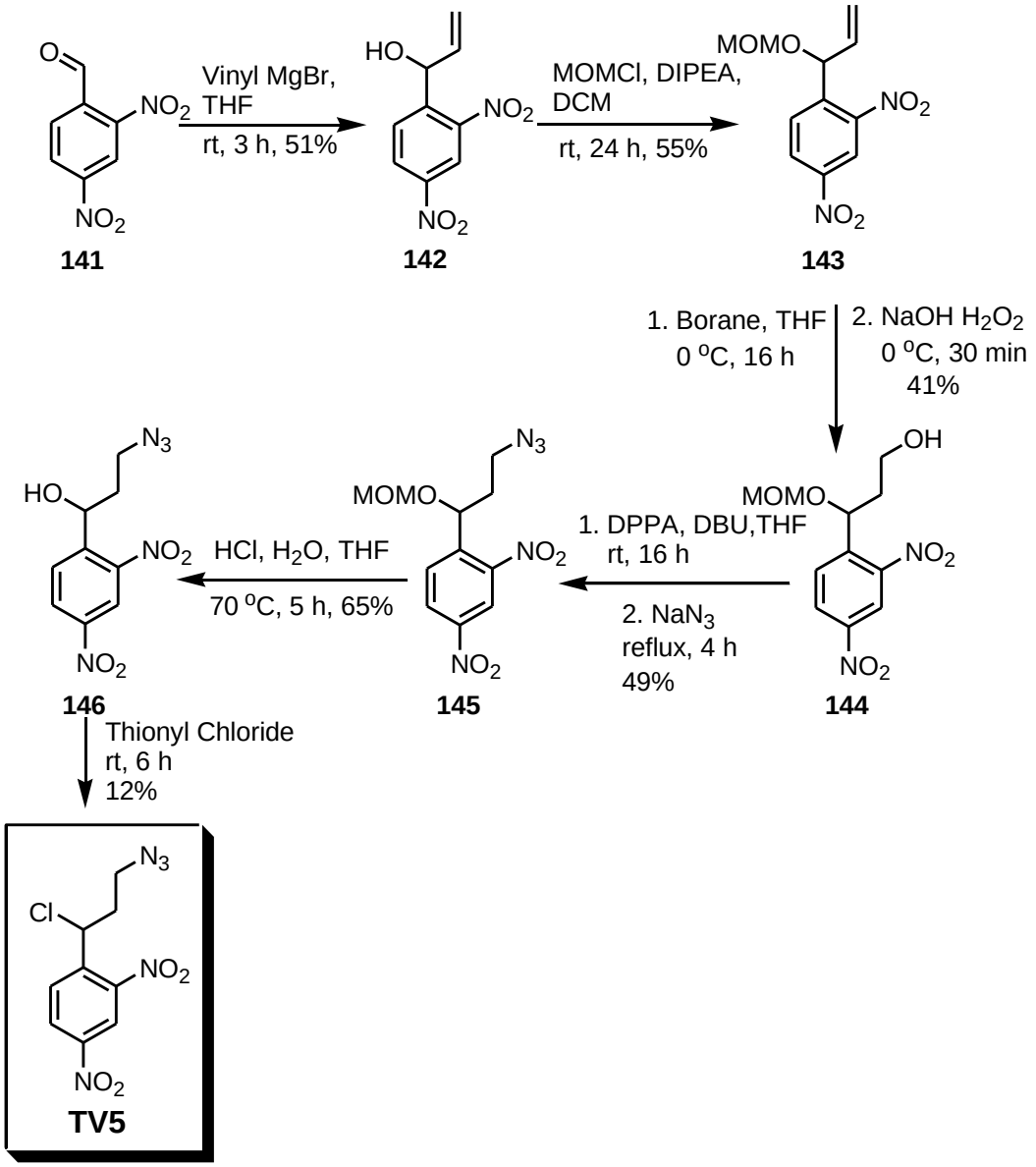

Scheme 40 Synthesis of the 2,4-dinitrobenzyl targeting vector TV5.

3.7 Synthesis of targeting vector 6

The final targeting vector **TV6** (Figure 51), was a 2-nitroimidazole based compound with the leaving group and azide containing side chain in the 5 position. This allows for the reactive methylene to be formed under hypoxic conditions due to the resonance throughout the ring. This compound is considered to be an optimum combination of the technology used for targeting

vectors 2-4 with the more electronically favourable 2-nitroimidazole heteroaromatic system.

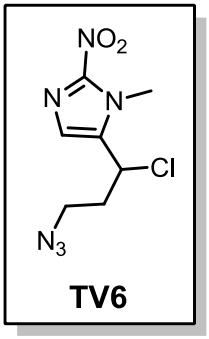

Figure 51 Targeting vector 6

The initial synthesis of these complexes involved the construction of the central heterocyclic structure as seen in Scheme 41. These steps were performed according to patents by Matteucci *et al*. in which the imidazole (**149**) is built up from sarcosine methyl ester **147**, ethyl formate and cyanoamine in a reported 45% yield over 2 steps [151] [152]. The patents proposes two different methods, one used potassium carbonate for the initial formylation of the sarcosine methyl ester (**147**) and sodium hydride for the second formylation, whilst the other used sodium hydride to achieve both formylations in one step. Both methods were tried, with the potassium carbonate method achieving a yield of 45%, whilst the yield for the sodium hydride method was 29%. The overall yield was drastically improved however if the initial formylation using potassium carbonate was left for 3 days rather than the suggested 16 hours, as this pushed the yield for the ring formation up to 75% (Scheme 41).

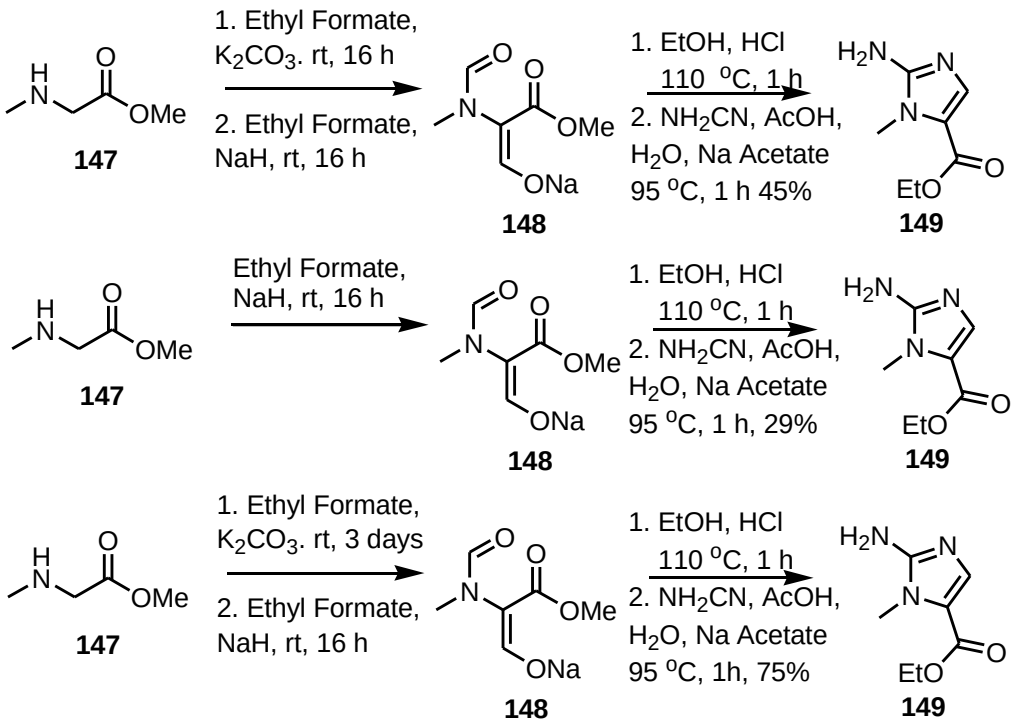

Scheme 41 Synthesis of the functionalised 2-aminoimidazole heterocycle (149).

The next step was the diazotisation of the 2-position in the ring before inserting a nitro group. This was attempted using a variety of methods, initially following the patent by Matteucci *et al*. [(151)] which used acetic acid as the proton source. Unfortunately, this method did not deliver the desired product (**150**). A method by Takuma *et al.* used previously on the 2-aminoimidazole hemisulfate (**116**), was also unsuccessfull. [(134)] A review of the original literature revealed a method by Cavaller *et al*. using fluoroboric acid, with a copper powder catalyst. [(153)] This method produced a pure yellow solid (**150**), but the yield was less than 5%, so a similar procedure by Lancini *et al*. was followed. [(154)] This method was identical to the Cavaller method, but the extraction solvent was changed from ethyl acetate to diethyl ether. However the material obtained was unidentifiable. Finally a method by Asato *et al.* [(155)] using sulphuric acid as the proton source

and no copper catalyst was used, and this resulted in a 43% crude yield of **150** as seen in Scheme 42.

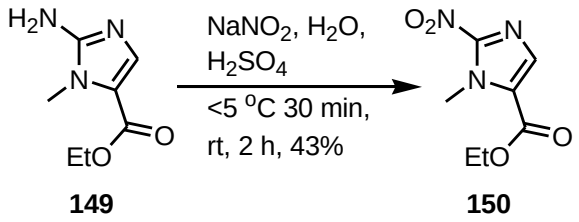

149 **150**

Scheme 42 Diazatisation of the substituted 2-aminoimidazole (149).

Once the nitro group was in place (**150**) the aim was to reduce the ester in the 5-position to an aldehyde (**151**). This was initially attempted with DIBAL-H at -78 °C, yet after a reaction time of 8 hours with 2 batches of DIBAL-H the reaction had only reached 6% conversion by NMR and there were signs of degradation. [156] Stronger reducing agents were then used to convert the ester (**150**) to the alcohol (**152**) using either $LiAlH_4$ [157] or $LiBH_4$, [152] yet both of these yielded degradation products. The ester (**150**) was therefore hydrolysed to the carboxylic acid (**153**) in a 70% yield using sodium hydroxide. [151] The carboxylic acid (**153**) was then initially reduced using borane (1M in THF), in 45% yield to produce the corresponding alcohol (**152**). [158] This reaction was highly capricious and the initial yield could not be repeated, so a method that formed an anhydride using CDI before reducing with $NaBH_4$ was explored, but also proved to be unsuccessful (Scheme 43). [159]

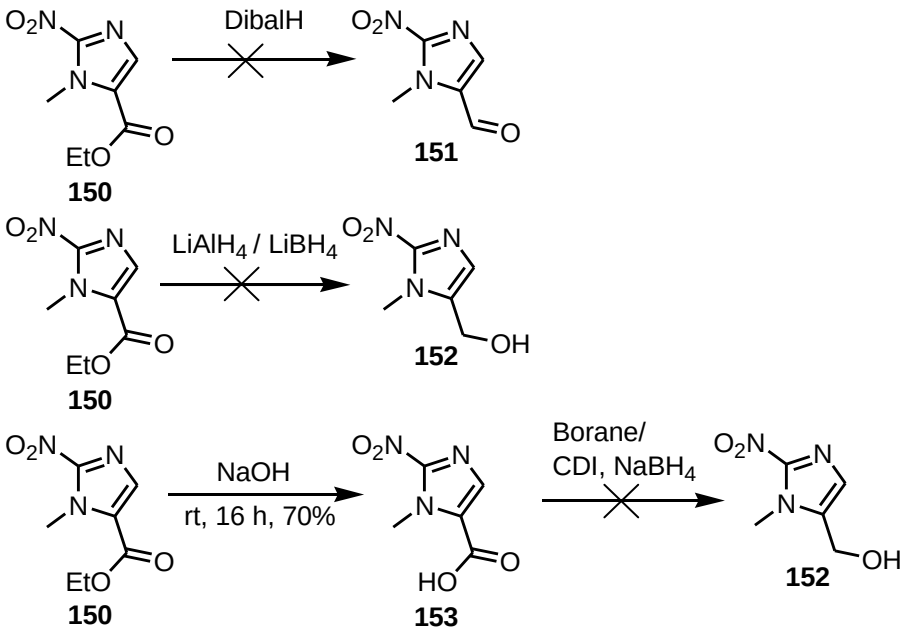

Scheme 43 Attempted synthesis of 1-methyk-2-nitro-imidazole-5-carbaldehyde 151.

An alternative route to the aldehyde (**151**) was then attempted. This method was inititated by a nitration of 4(5)-imidazolecarboxaldehyde **154** with nitric acid at room temperature as referenced by Ballani *et al*. [160] This produced the 2-nitro-4(5)-imidazolecarboxaldehyde as **155** expected. However the aldehyde (**155**) could not be subjected to the Grignard conditions used in the nitro-benzyl syntheses, [116] due to its insolubility in any solvent other than water or methanol. Thus 1-methyl-imidazole-5-carbaldehyde **156**, was nitrated after refluxing in nitric acid, but the same solubility issues arose, so the route was abandoned (Scheme 44).

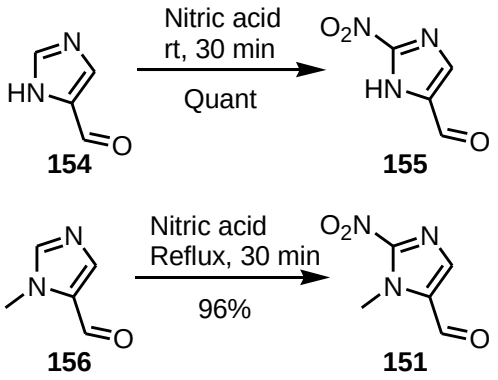

Scheme 44 Alternative synthesis of 2-nitro-4(5)-imidazolecarboxaldehyde 155 and 1-methyl-2-nitro-imidazole-5-carbaldehyde 151

3.8 Conjugation of the contrast agent to the targeting vector.

To form the completed complexes, the Copper(I)-catalyzed Azide-Alkyne Cycloaddition was used. [107] Initial optimisation reactions were run to 'click' contrast agent 1 **CA1** to targeting vector 3 **TV3** (Scheme 46).

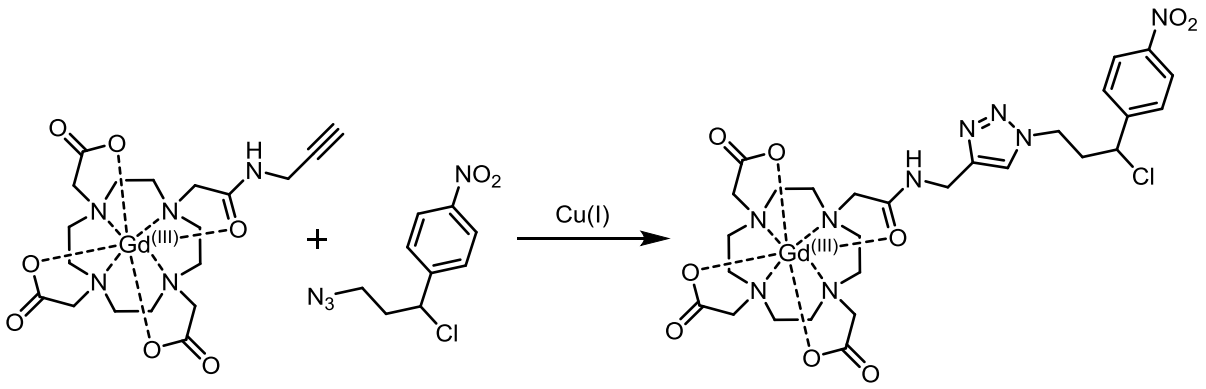

Scheme 45 "Click reaction between contrast agent 1 CA1 and targeting vector 3 TV3.

The reactions were monitored by HPLC and the key peak areas analysed using mass spectrometry. It was deduced that the most successful reactions would be those with the largest peak area for the targeted compound.

An inital screen was run to identify the best solvent system for the reaction as it was noted that the targeting vector had poor solubility in water. Whilst the reaction did occur in 100% water it was found that using either a methanol or *tert*-butanol co-solvent increased product formation as seen in table 3.

Table 3 Table summarising the solvent optimisation of the 'click' reaction.

Reaction Solvent	Amount and source of catalyst and reducing agent.	Product peak area %
Water	$Cu(II)SO_4$ 100% + sodium ascorbate 100%	65
1:1 MeOH:H_2O	$Cu(II)SO_4$ 100% + sodium ascorbate 100%	80
1:1 tBuOH:H_2O	$Cu(II)SO_4$ 100% + sodium ascorbate 100%	78

All of these reactions were run at room temperature for 24 h in 1mL of solvent.

The next step was to screen the source of copper and the amounts used as seen in table 4.

Table 4 Table summarising the catalyst optimisation of the 'click' reaction.

Reaction Solvent	Amount and source of catalyst and reducing agent.	Product peak area %
1:1 MeOH:H_2O	$Cu(II)SO_4$ 100% + sodium ascorbate 100%	80
1:1 MeOH:H_2O	$Cu(II)SO_4$ 10% + sodium ascorbate 10%	23
1:1 MeOH:H_2O	$[Cu(I)(MeCN)_4]PF_6$10%	0

All of these reactions were run at room temperature for 24 h in 1mL of solvent.

Overall the best conditions were determined to be stoichemetric amounts of copper and sodium ascorbate, yet when the reactions were purified a large amount of green by-product (containing a small amount of product by mass spectrometry) was produced, and then lost when filtering the solution for HPLC purification, resulting in only an 8% yield.

To try and improve purification a method inspired by work reported by Mindt *et al*. was used. [161] In this strategy the 'click' reaction takes place before the *tert*-butyl groups had been removed and gadolinium (III) has been inserted (Scheme 47). It was hoped that using standard silica chromatography would produce a higher yield as any product caught in the precipitate could also be loaded onto the column. Initial tests using the protected DO3A based contrast agent (**78**) and the 2-nitroimidazole based targeting vector (**TV1**) proved unsuccessful and no product was isolated.

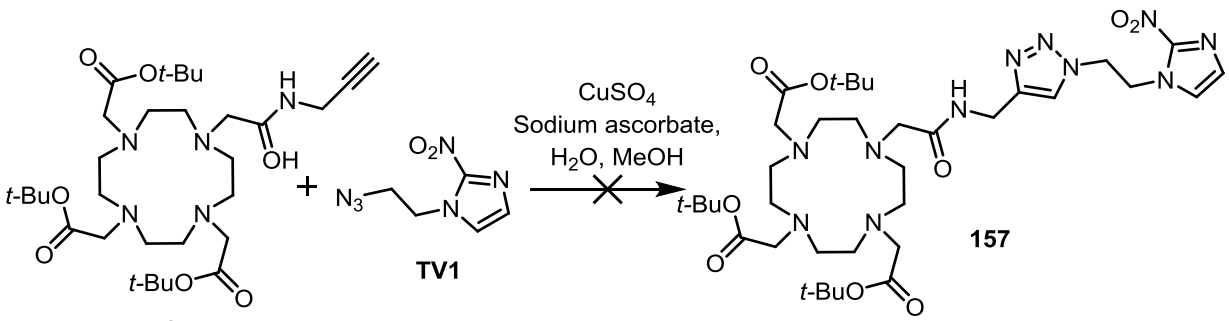

78

Scheme 46 Attempts at the 'click' reaction using the protected DO3A complex 78 and targeting vector 1 TV1

For further optimisation coumarin dye **DYE1** (Figure 52) was used instead of a hypoxia targeting vector. This had an advantage as the reaction could then be monitored using UV, for the coumarin dye used only fluoresces once the

triazole ring has been formed. It also prevented waste of the precious targeting vectors that had been synthesised in house and discussed earlier.

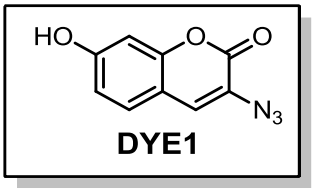

Figure 52 Coumarin Dye DYE1

The coumarin dye **DYE1** was synthesised following a route developed by Sivakumar *et al.* which used 2,4-dihydroxybenzaldehyde **158** and *N*-acetyl glycine refluxed in acetic anhydride to produce the intermediate 3-(Acetamino)-2-oxo-2*H*-chromen-7-yl acetate **159** as a yellow solid. [162] This then underwent acetate removal by acid hydrolysis followed by a diazatisation to produce the final coumarin dye **DYE1** as a brown solid in an overall yield of 9%. This yield is much lower than the quoted 54% with most of the material lost during the initial step, which had a maximum achieved yield of 11% (Scheme 48). [162]

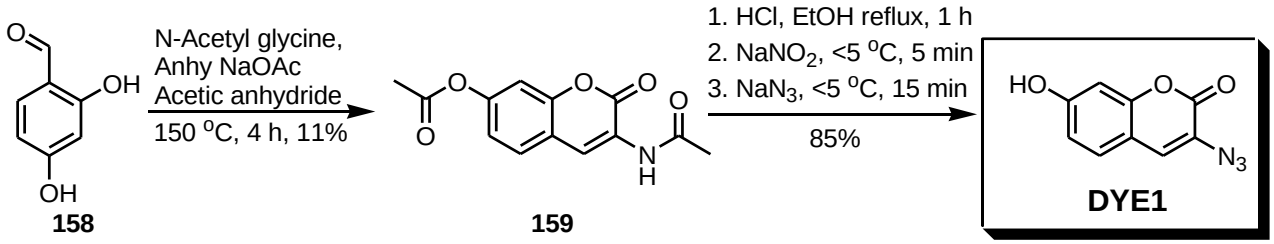

Scheme 47 Synthesis of azido coumarin dye DYE1.

To help prevent any copper displacing the gadolinium(III), copper(I) ligands THPTA **160** and TBTA **161** were used in the hope it would produce higher overall yields. [163]

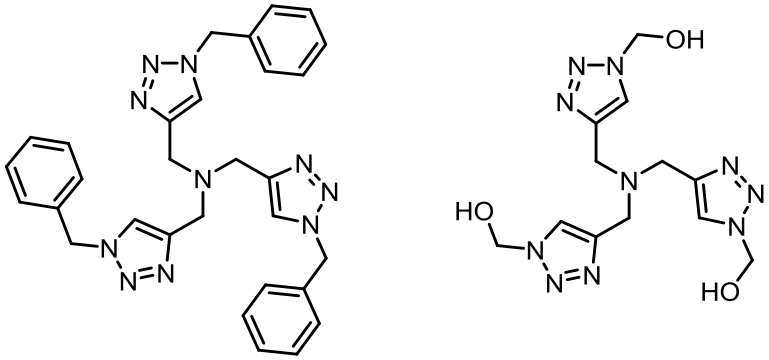

TBTA **160** THPTA **161**

Figure 53 Copper (I) ligands TBTA and THPTA. [163]

When THPTA **160** was used it appeared to produce a brighter fluorescence than when TBTA **161** or no copper (I) ligand was used to the naked eye suggesting more formation of product. Yet when the reaction was analysed by HPLC it appeared that the number of side products dramatically increased, some of which were also UV active, and purification became more difficult.

As the completed contrast agents run almost at the solvent front on a C18 silica HPLC column, it was decided to investigate reverse phase silica chromatography as a method of purifiying these compounds. By monitoring the purification using reverse phase TLC, it was discovered that the column could be washed initially with methanol, which would remove any unreacted targeting vector, before flushing with water to elute the final compound. Assuming all of the contrast agent starting material had been consumed in the reaction the water fraction was pure. These compounds were then tested with xylenl orange to prove there was no free gadolinium(III) in the fractions. The yields for the compounds successfully synthesised have been summarised in table 4.

Table 4 Yields for the 'click' reaction used to produce the final compounds.

Compound Name	Compound Produced	Yield
C1	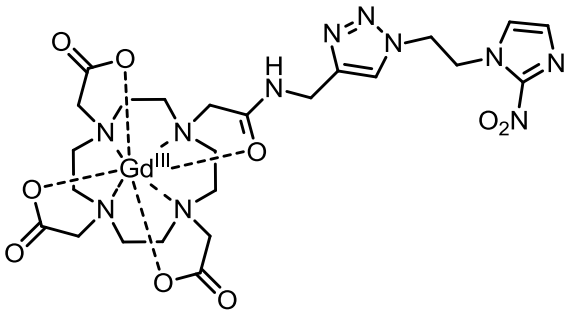	42%
C2	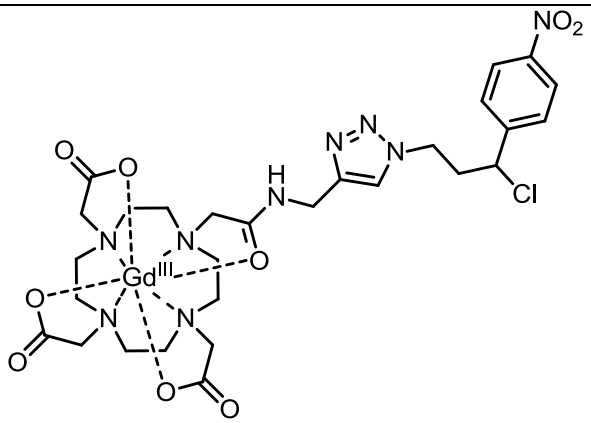	8%, purified by HPLC.

C3	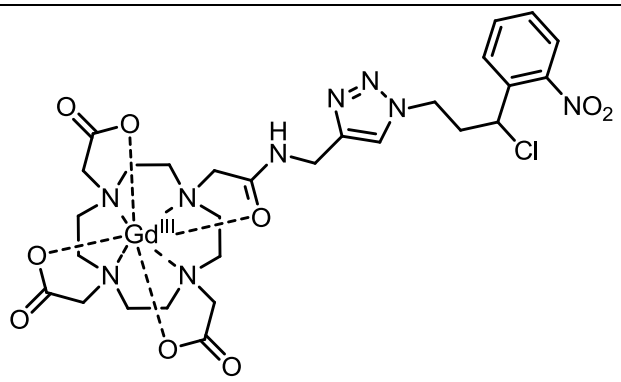	21%
CA1-DYE	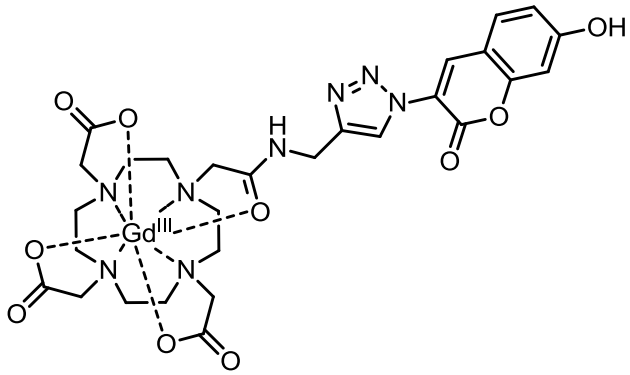	19%
C4	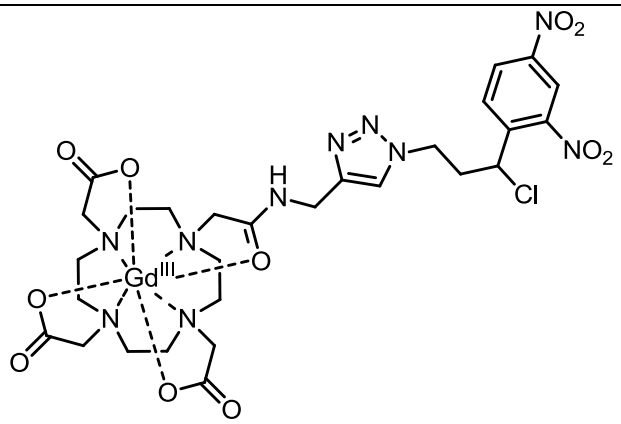	Not synthesised due to limited time constraints.
C6	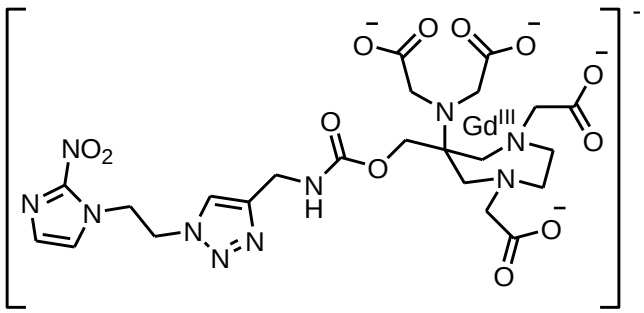	Not synthesised due to limited time constraints.

C7	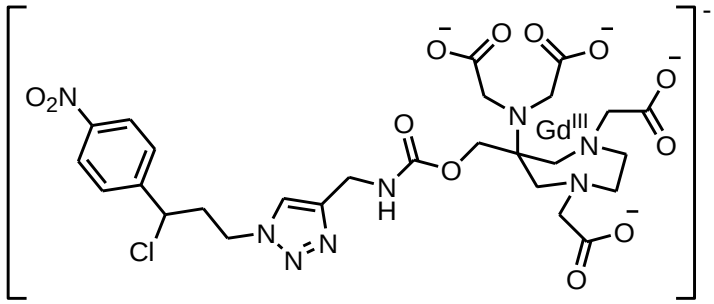	Not synthesised due to limited time constraints.

3.9 NMR Relaxivity testing

A series of eight known contrast agent concentrations between 0.1 and 2.5 mM were used to calculate the relaxivity value of the contrast agents synthesised. The samples were made up in milli q water rather than the standard phosphate buffer due to the small quantities synthesised, and the need to recover the complexes for further testing. Whilst this prevents the results from being directly comparable with the literature any difference in relaxivity should be negligible for DOTA and AAZTA based compounds at physiological pH. [(70)] [(164)] These samples were then subjected to an inverse recovery pulse sequence used to record the NMR relaxivity data. This sequence begins with an initial 180º (π) pulse which rotates the magnetism so it aligns with the –Z axis. This then undergoes longitudinal relaxation and the magnetism realigns with the +Z axis., however before this equilibrium is reached a 90º (π/2) pulse is applied rotating the magnetism so it aligns in the X-Y plane. The time difference between these pulses is very short (t = 20-2500 ms) and the strength of the resulting magnetism seen in the X-Y plane is directly related to the T_1 relaxation time. [(117)] The spectrometer was run at 20 MHz at 298K (Figure 54).

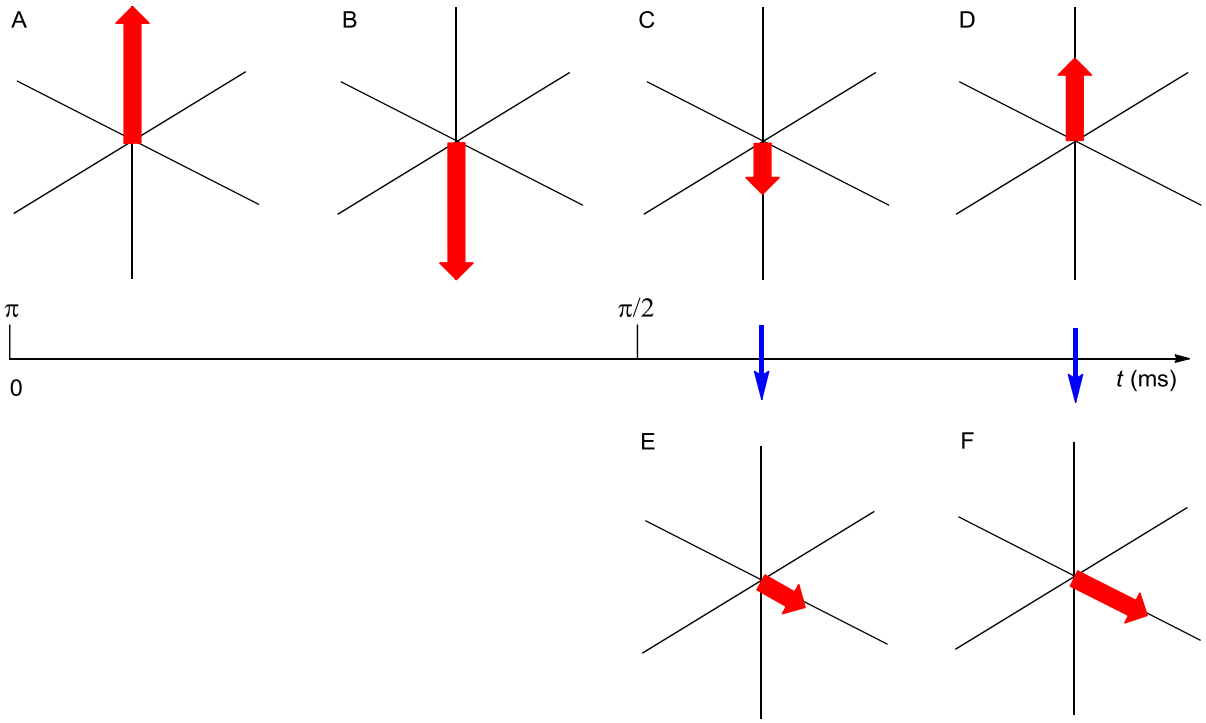

Figure 54 Inversion recovery pulse sequence. [117]

The data recorded from these experiments is a MRI graphic (Figure 55). The intensity of each sample tube in this graphic is averaged and extrapolated using Matlab computer software. This data is then plotted as an exponential showing intensity as a function of time (Figure 56).

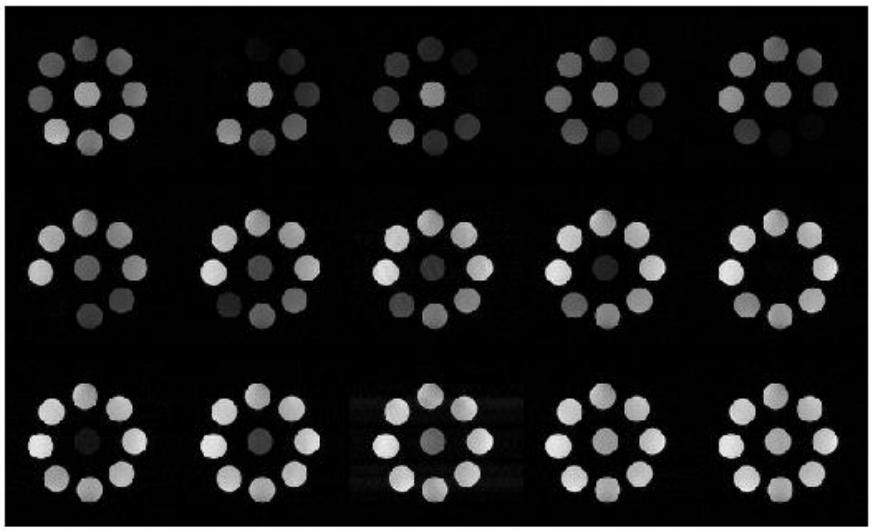

Figure 55 A T_1 weighted composite image of the DO3A complex with inversion times of 20 to 2500 ms.

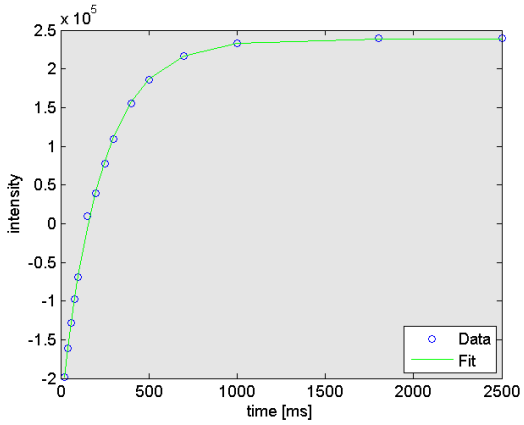

Figure 56 A typical evaluation of MR scan v's time needed to calculate T_1.

The exponential inversion recovery function $S_{(t)} = S_{(0)}(1\text{-}2\exp^{(-t/T_1)})$ was fitted by a non-linear Levenberg–Marquardt algorithm to provide $S_{(0)}$ and the T_1 value, the reciprocal of which is then plotted against concentration (Figure 57). The gradient of this plot gives the relaxivity (r_1) of the contrast agent in $mM^{-1}s^{-1}$. The results of which are shown in table 5.

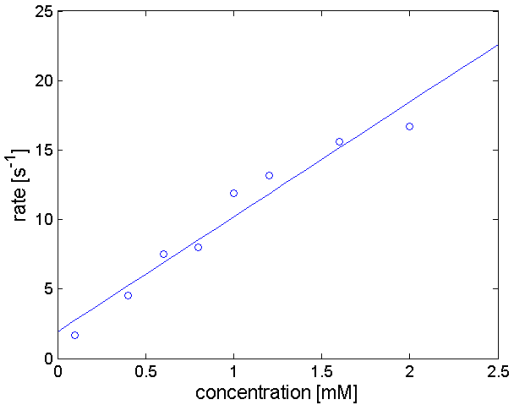

Figure 57 The correlation between calculated T_1 and Concentration for Gd(III)DO3A (CA1).

Table 5 Relaxivity values of the compounds tested.

Name and structure of Compound	Relaxivity Value at 20MHz, 298K.
Gd(III)-DO3A 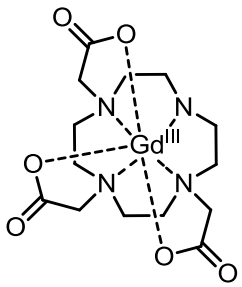	8.3 ± 0.8 $mM^{-1}s^{-1}$
CA1 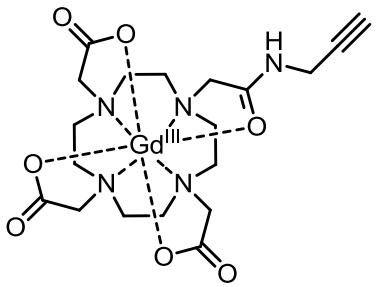	4.1 ± 0.4 $mM^{-1}s^{-1}$

CA2 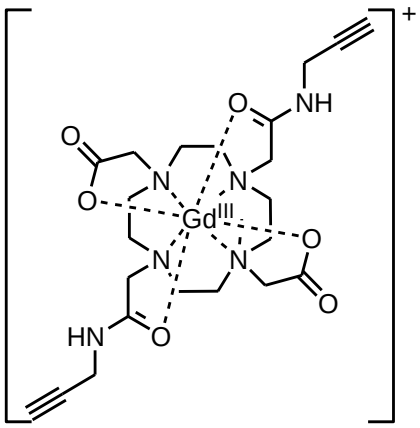	3.4 ± 0.3 $mM^{-1}s^{-1}$
CA4 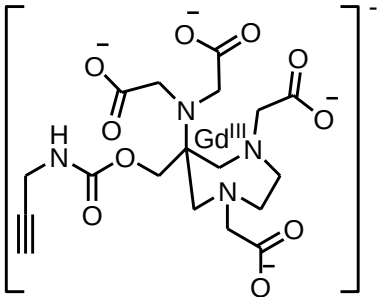	7.0 ± 0.5 $mM^{-1}s^{-F1}$
C1 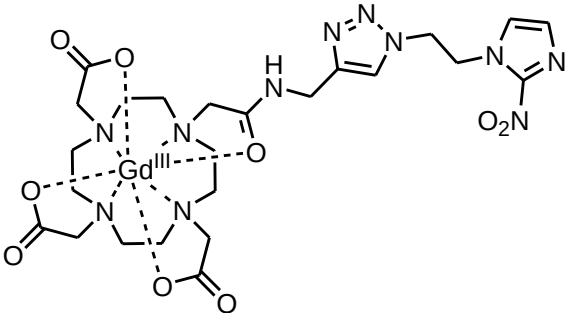	5.3 ± 0.7 $mM^{-1}s^{-1}$

C2 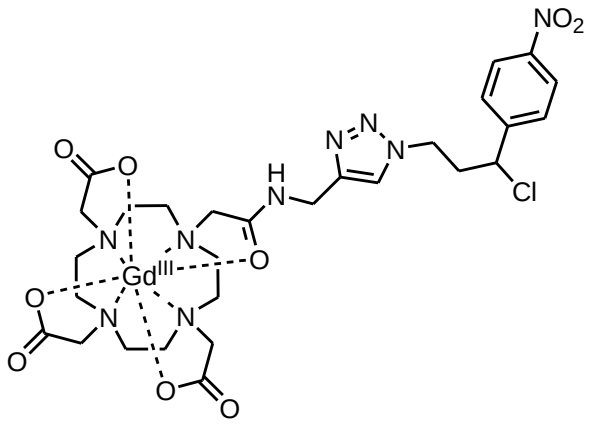	1.4 ± 0.06 $mM^{-1}s^{-1}$

Initially the relaxivity of Gd(III)-DO3A was calculated so the data could be compared to that in the literature, however as the samples were analysed in pure water rather than a buffer this value was high at 8.3 $mM^{-1}s^{-1}$, almost double the literature value of 4.8mM^{-1} s^{-1} at 20 MHz and 312 K. This is because the angle at which the two water molecules bind is suitable for binding of much stronger molecules including phosphates found in biological systems and the buffers commonly used. [70] However **CA1,2** and **4** which are the propargyl derivatives of the parent DOTA and AAZTA compounds were found to have comparable relaxivities to their parent compounds. For **CA1** and **CA2** reported values of 4.1 and 3.4 $mM^{-1}s^{-1}$ which corresponded to the DOTA value of 3.5 $mM^{-1}s^{-1}$ [68], and **CA4** has a reported value of 7.0 $mM^{-1}s^{-1}$ compared to 7.3 $mM^{-1}s^{-1}$ [79] for the hydroxyl AAZTA derivative. As for the final compounds, whilst **C1** showed promise with a relaxivity value of 5.3 $mM^{-1}s^{-1}$, **C2** had a very poor relaxivity value of 1.4 $mM^{-1}s^{-1}$ suggesting there are potential impurities, possibly the oxidised sodium ascorbate as this had a similar R_f-value on the HPLC column.

3.10 Enzymatic testing for activation of the targeting vectors under a hypoxic environment.

To determine if the compounds synthesised were activated under hypoxic conditions a modified version of the assay developed by Bejot *et al*. was adopted. [165] This assay uses the enzyme *Xanthine oxidase* which converts xanthine **162** into uric acid **163**. This oxidation requires a single electron transfer from the xanthine to an electron acceptor. [166] In normoxic conditions this acceptor is usually molecular oxygen, though under hypoxic conditions nitroimidazoles can be used as suitable alternatives. This then allows for the reduction of the nitro functionality to the hydroxylamine or the final amine compound (Scheme 49).

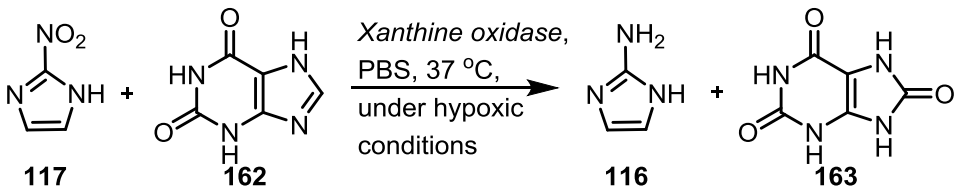

Scheme 48 Conversion of Xanthine 162 and 2-nitroimidazole 117 using *Xanthine oxidase* and hypoxic conditions.

The amount of enzyme in the assay had to be reduced compared to the literature precedence as the initial amount produced a rate too fast to be monitored by the UV spectrometer available. To confirm the validity of this assay a series of controls were run using 2-nitroimidazole **117** as the oxidising agent. This was chosen as the molecule is easily synthesised (as seen in Scheme 33) and known for its ability to be reduced under a hypoxic environment. [167] Whilst the aerobic assays worked as expected there were difficulties purging oxygen from the system using the methods suggested in the literature, as outlined in table 6.

Table 6 The methods used to try and achieve a hypoxic environment.

Method for obtaining the hypoxic conditions.	**Rate of conversion of xanthine to uric acid, and reduction of nitroimidazole.**
Aerobic conditions.	Xanthine consumed 0.78 $mMmin^{-1}U^{-1}$ ±0.025, Uric Acid formed 0.88 $mMmin^{-1}U^{-1}$ ±0.06. No reduction of 2-nitroimidazole
Pre gassing the solution with nitrogen, before purging using a vacuum pump. Repeated >5 times. (Adapted from paper by Tatsumi *et al*. [168])	Xanthine consumed 0.76 $mMmin^{-1}U^{-1}$, uric acid formed 1.29 $mMmin^{-1}U^{-1}$. No reduction of 2-nitroimidazole
Bubbling humidified argon through the substrate and enzyme buffer solutions for >20 minutes. (Adapted from Bejot *et al.* [165])	Xanthine consumed 0.50 $mMmin^{-1}U^{-1}$, uric acid formed 0.79 $mMmin^{-1}U^{-1}$. No reduction of 2-nitroimidazole
Bubbling nitrogen through the substrate and enzyme buffer solutions for >20 minutes. (Adapted from Clarke *et al.* [169])	Xanthine consumed 0.76 $mMmin^{-1}U^{-1}$, uric acid formed 0.76 $mMmin^{-1}U^{-1}$. No reduction of 2-nitroimidazole
Freeze substrate and enzyme buffer solutions. Put under vacuum and allow to defrost. Purge with argon. Repeat >4 times.	Xanthine consumed 0.20 $mMmin^{-1}U^{-1}$, uric acid formed 0.23 $mMmin^{-1}U^{-1}$. No reduction of 2-nitroimidazole

Due to technological difficulties and time constraints this assay could not be taken further.

Chapter 4 Conclusions and Future Work.

The initial aim of this thesis was to synthesise a series of building blocks containing either an alkyne or azide functionality to allow for copper(I) mediated cycloaddition to produce a series of final complexes.

Overall three contrast agent units containing an alkyne functionality were synthesised. These then had their relaxivity values calculated, and all produced similar results to those seen by the parent compounds.

In the end only the DO3A based contrast agent CA1 was conjugated to any of the hypoxia targeting vectors. This was due to it being the contrast agent available in the largest quantities as it had the shorter synthetic route. Hence it was used in most of the test conjugations and purifications, and when time ran out these were compounds used for final testing.

With regards to the hypoxia targeting vector, four potential compounds were synthesised. One was based on a central 2-nitroimidazole structure, whilst the other three used a central nitro-benzene based structure. Unfortunately the assay to prove their effectivity under hypoxic conditions was not completed. To do so would require time to improve the seal on the UV cuvette, hopefully leading to a properly degassed soloution, before the addition of the *Xanthine Oxidase*. An alternative assay would use HT1080 cells cultured under both normoxic and hypoxic conditions, in which the uptake of the hypoxia targeting vectors could be calculated by measuring their concentration in the lysed cells.

Of the targeting vectors synthesised the 2-nitroimidazole based compound (**TV1**) is by far the simplest synthetically, and would probably have the most favourable hypoxic retention, based on similar compounds in the literature.

Only 2 final complexes were synthesised, **C1**, which combined the DO3A based contrast agent (**CA1**) with the 2-nitroimidazole based targeting vector (**TV1**). This produced a similar relaxivity value to the parent **CA1** complex. Thus it can be concluded that there is no interference from the 2-nitroimidazole or the triazole linker with regards to the relaxation rate produced by the bound gadolinium(III) ion. **C2**, synthesised from **CA1** and the para-nitrobenzyl derivative targeting vectore (**TV2**), however produced a disappointingly low result, assumed to be due to contamination of the sample.

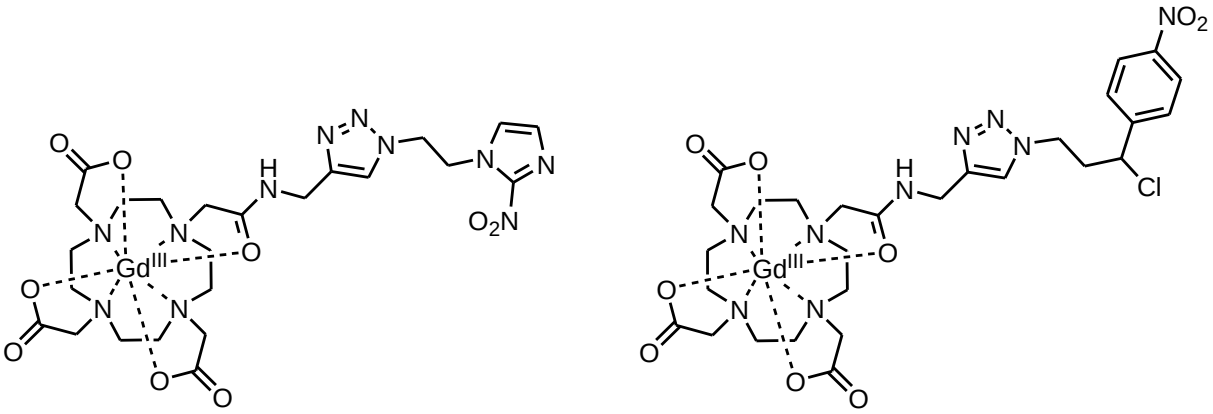

Figure 58 Final complexes synthesised.

Whilst the methods outlined in Chapter 3 allowed for the production of the desired contrast agents, some of which were successfully completed, this has not been the most expedient way of conjugating a hypoxia targeting vector to a gadolinium based contrast agent. The reason for this is down to

the inclusion of the copper(I) mediated cycloaddition based linker, which caused significant synthetic problems, not only in the incorporation of either an alkyne or an azide into the original components, but also in the final conjugation to produce the targeted contrast agents.

In the future I would design the compounds with a simple ethylene diamine linker, which in the case of the DOTA based structures would be easy enough to encorporate by producing the amine based analogue of the targeting vector (**165**) and reacting it with bromo acetylbromide, to produce the bromoacetamide (**166**) which can then be reacted with the protected DO3A (**40**) to form the protected complex (**167**) (Scheme 60). This could then undergo TFA deprotection of the tert-butyl protection groups and insertion of the gadolinium (III) ion to produce the final complex.

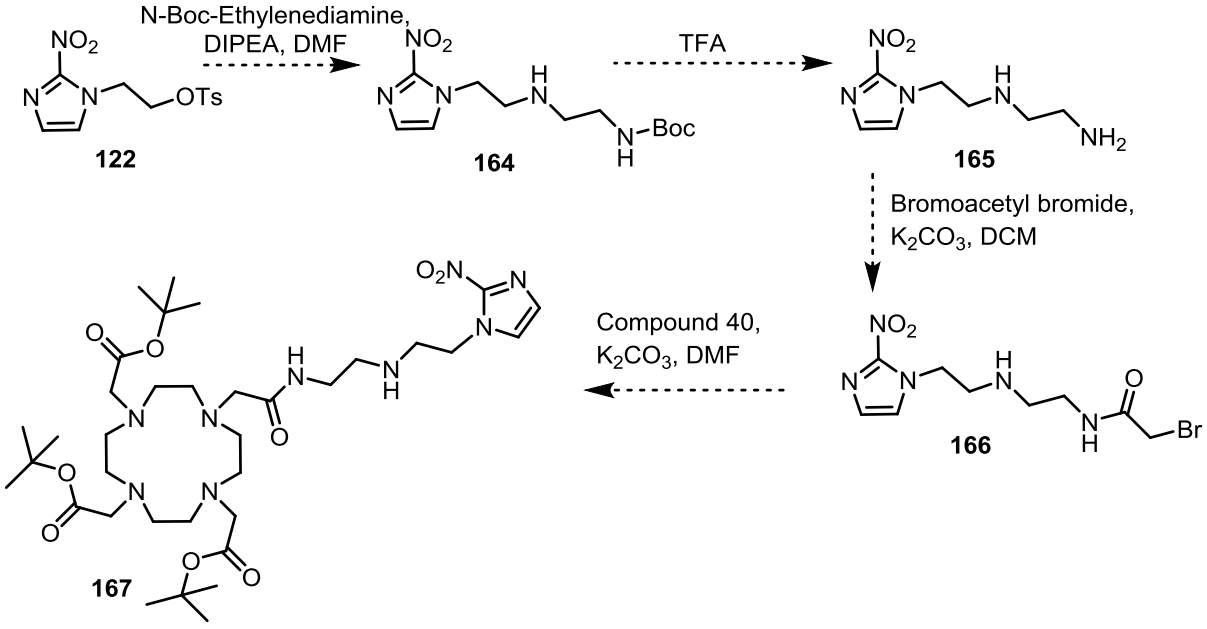

Scheme 49 Potential route to the protected amine DOTA derivative (167).

As for the AAZTA derivatives the amine based analogue of the targeting vector (**165**) would also be used, and conjugated to AAZTA via the carbamate linker used in this thesis to incorporate the alkyne functionality.

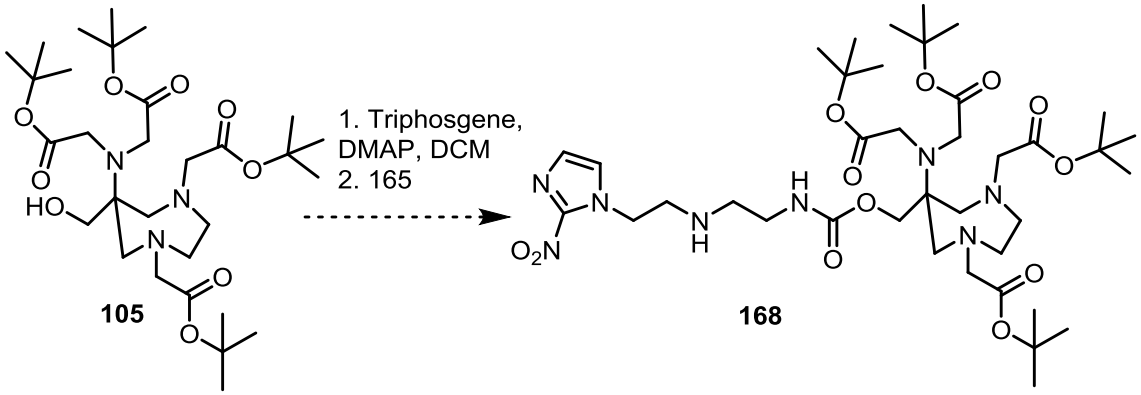

Scheme 50 Potential conjugation of the AAZTA complex 105 to a targeting vector with an ethylene diamine linker.

Those compounds produced in this thesis had NMR relaxivities comparible with the parent DOTA or AAZTA based complexes and it is assumed that the alternative complexes suggested above would have similar properties as the groups co-ordinating to the central gadolinium ion would be the same, the only differences would come from potential steric effects caused by the more flexible linker.

Chapter 5 Experimental

General Experimental

All ^{1}H NMR spectra were recorded on a Bruker AV 400 FT at 400 MHz and at 298 K. Data are reported as follows: chemical shifts in ppm relative to residual protic solvent shift on the δ scale $CDCl_3$ (7.26 ppm), D_2O (4.79 ppm), CD_3OD (3.31 ppm), d_6 DMSO (2.50 ppm) or CD_3COCD_3 (2.05 ppm), integration, multiplicity (s = singlet, d = doublet, t = triplet, q = quartet, m = multiplet, b = broad), coupling constants (*J*, Hz) and assignment. All multiplicity and coupling constants are reported as viewed. ^{13}C NMR spectra were recorded on a Bruker AV 400 at 100 MHz, and at 298 K. Data are reported as follows: chemical shifts in ppm relative to residual $CDCl_3$ (77.1 ppm), CD_3OD (49.0 ppm), d_6 DMSO (39.5 ppm), or CD_3COCD_3 (29.9 ppm) on the δ scale. Assignments were made using DEPT 135 and DEPT 90 (pulse experiments), HMBC and HSQC experiments.

All electrospary ionisation accurate mass spectrometry was recorded on a Bruker MicrOTOF time of flight spectrometer. All electron ionisation was recorded on either a VG AutoSpec magnetic sector spectrometer or a Bruker Apex IV 4.7 T ICR FTMS an ion cyclotron resonance fourier transform spectrometer with a 4.7 tesla magnet.

DCM, DMSO, acetone and piperidine were dried by distillation from calcium hydride or sodium and stored over preactivated 4 Å molecular sieves. Dry DMF was purchased from Alfa Aesar. All other reagents were purchased from either Sigma Aldrich Chemicals, Alfa Aesar, Fisher, Fluka and Strem Chemicals and used as supplied unless otherwise stated. Thin layer chromatography was

performed using Merck Kieselgel 60 F254 plates. Visualisation was by UV light and staining with potassium permanganate, vanillin or phosphomolybdic acid (PMA) with heating. Column chromatography was performed using Merck Kieselgel 35-70μ, 60 Å unless otherwise stated. Reverse phase column chromatography was performed using Fluka Silica gel 100 C_{18}-Reversed phase, and the corresponding TLC's were run on Merck HX615476 RP-18 F_{254s} plates.

All HPLC was run on an Aglient 1200 system, using either a Zorbax Eclipse XBD-C18 analytical column 4.6 x 150 mm, 5 μm pore size or a Zorbax Eclipse XBD-C18 semi-prep column 9.4 x 250 mm, 5 μm pore size. Solvent A was milli Q water and solvent B was acetonitrile.

All centrifugation was run on a Beckman GS-15R centrifuge for 5 minutes at 3000 rpm, 25 °C.

All chemical names were generated using ChemBioDraw Ultra 12.0.

Chemical Experimental

1,4,7,10-Tetraaza-cyclododecane-1,4,7-tricarboxylic acid-tri-*tert*-butyl ester **(36)**.

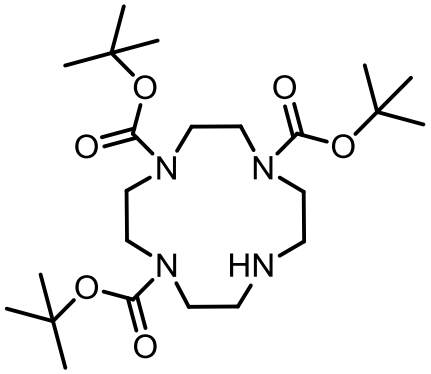

A solution of di-*tert*-butyl dicarbonate (9.5 mL, 41.4 mmol, 2.4 equiv) was added to a stirred solution of cyclen **(35)** (3.0 g, 17.4 mmol, 1 equiv) in dichloromethane (20 mL) at room temperature and under a nitrogen atmosphere. The solution was stirred for 2 h before concentrating *in vacuo*. The residue was purified by flash chromatography on silica (DCM/MeOH, 96/4) to yield the protected amine as a colourless foam **(36).** Reproduced from Gaillard [8] (4.0 g, 49%).

mp, 56 – 57 $^{\circ}$C (Lit, [168] 54 – 55 $^{\circ}$C); ν_{max} ($CHCl_3$)/cm^{-1}, 1681 (C=O); δ_H (400 MHz; $CDCl_3$) 1.43 (18H, s, C(CH_3)$_3$), 1.45 (9H, s, C(CH_3)$_3$), 2.83-3.64 (16H, m, NCH_2CH_2N); δ_C (100 MHz; $CDCl_3$) 28.6, 28.4 (C(*C*H_3)$_3$), 50.8, 49.5, 49.2, 45.5 (N*C*H_2*C*H_2N), 79.3, 79.2 (*C*(CH$_3$)$_3$), 155.6, 155.4 (*C*=O); HRMS *m/z* (+ ESI): Found $[MH]^+$, 473.3334. $C_{23}H_{45}N_4O_6$ requires $[MH]^+$, 473.3334.

1,4,7,10 Tetraaza-cyclododecane-1,4,7,10-tetra carboxylic acid tri-*tert*-butyl ester 9*H*-fluoren-9-ylmethyl ester **(37).**

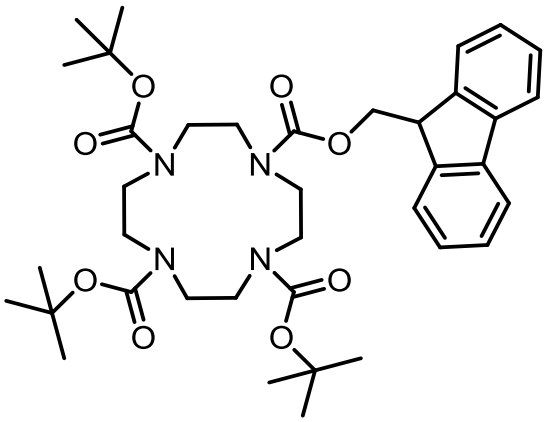

A suspension of 1,4,7,10-tetraaza-cyclododecane-1,4,7-tricarboxylic acid tri-*tert*-butyl ester **(36)** (4.01 g, 8.5 mmol, 1 equiv) and 10% aqueous sodium hydrogen carbonate (10 mL) in 1,4-dioxane (10 mL) was treated with 9-fluorenylmethoxycarbonyl chloride (3.22 g, 12.7 mmol, 1.5 equiv). The suspension was stirred at room temperature for 16 h. Water (10 mL) was added and the aqueous layer was extracted with chloroform (3 x 20 mL). The combined organic extracts were dried over magnesium sulfate, filtered and concentrated *in vacuo* to yield the amine as a colourless foam **(37).** Reproduced from Gaillard [8](5.80 g, 98%).

mp, 84 °C (Lit, [8] 94-96 °C); ν_{max} ($CHCl_3$)/cm^{-1}, 3068 (CHAr), 1686 (C=O); δ_H (400 MHz; $CDCl_3$) 1.46 ppm (18H, s, $C(CH_3)_3$), 1.50 (9H, s, $C(CH_3)_3$), 3.00-3.60 (16H, m, NCH_2CH_2N), 4.25 (1H, t, *J* = 5.5 Hz, $COOCH_2CH$), 4.55 (2H, bs, $COOCH_2CH$), 7.37 (2H, td, *J* = 7.4 Hz, 1.0 Hz, CHAr), 7.42 (2H, t, *J* = 7.4 Hz, CHAr), 7.62 (2H, d, *J* = 7.4 Hz, CHAr), 7.78 (2H, d, *J* = 7.4 Hz, CHAr); δ_C (100 MHz; $CDCl_3$) 28.4, 28.5 ppm ($C(CH_3)_3$), 47.3 ($COOCH_2CH$), 49.5-51.0 (bs,

N*C*H_2*C*H_2N), 67.0 (COO*C*H_2CH), 80.0 (*C*(CH_3)$_3$), 127.7, 127.2, 124.7, 120.0 (*C*HAr), 144.0,141.4 (*C*Ar), 156.2 (*C*=O); HRMS *m/z* (+ ESI): Found $[MH]^+$, 695.3982 $C_{38}H_{55}N_4O_8$ requires $[MH]^+$, 695.4020.

1,4,7,10-Tetraaza-cyclododecane-1-carboxylic acid 9*H*-fluoren-9-ylmethyl ester **(38)**.

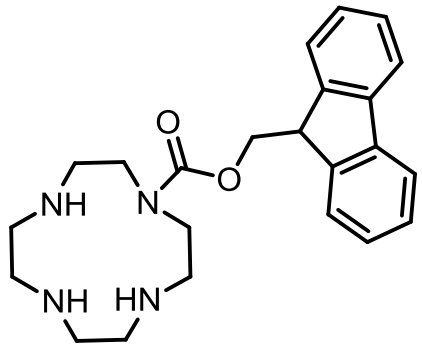

A solution of 1,4,7,10 tetraaza-cyclododecane-1,4,7,10-tetracarboxylic acid tri-*tert*-butyl ester 9*H*-fluoren-9-ylmethyl ester **(37)** (5.80 g, 8.3 mmol, 1 equiv) in dichloromethane (25 mL) was treated with trifluoroacetic acid (15 mL) at room temperature and stirred for 16 h. The solution was then concentrated *in vacuo* with dichloromethane (2 x 10 mL) to yield the triamine as an orange oil **(38)**. Reproduced from Gaillard [8](2.82 g, 86%).

ν_{max} ($CHCl_3$)/cm^{-1}, 3662 (NH), 1666 (C=O); δ_H (400 MHz; $CDCl_3$), 2.59-3.41 (16H, m, NC*H*$_2$C*H*$_2$N), 4.19 (1H, t, *J* = 2.0 Hz, COOCH$_2$C*H*), 4.69 (2H, s, COOC*H*$_2$CH), 7.32 (2H, t, *J* = 7.3 Hz, C*H*Ar), 7.39 (2H, t, *J* = 7.3 Hz, C*H*Ar), 7.51 (2H, d, *J* = 7.3 Hz, C*H*Ar), 7.73 (2H, d, *J* = 7.3 Hz, C*H*Ar); δ_C (100 MHz; $CDCl_3$), 47.8 (COOCH$_2$*C*H), 44.9, 45.1, 46.9, 53.4 (N*C*H$_2$*C*H$_2$N), 66.9 (COO*C*H$_2$CH), 120.0, 125.0, 127.4, 128.0 (CHAr), 141.4, 143.4 (*C*Ar), 160.6

(*C*=O); HRMS *m/z* (+ ESI): Found $[MH]^+$, 395.2427 $C_{23}H_{32}N_4O_2$ requires $[MH]^+$ 395.2447;

4,7,10-Tris-*tert*-butoxycarbonylmethyl-1,4,7,10-tetraaza-cyclododecane-1-carboxylic acid 9*H*-fluoren-9-ylmethyl ester **(39)**.

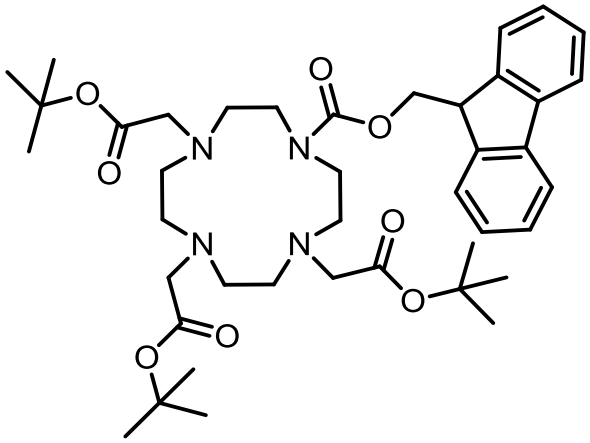

A solution of 1,4,7,10-tetraaza-cyclododecane-1-carboxylic acid 9*H*-fluoren-9-ylmethyl ester **(38)** (2.82 g, 7.1 mmol, 1 equiv) in dimethylformamide (15 mL) was added dropwise to a stirred solution of *tert*-butyl bromoacetate (4.7 mL, 32.0 mmol, 4.5 equiv) and potassium carbonate (4.80 g, 34.7 mmol, 5 equiv) in dimethylformamide (5 mL) at room temperature under a nitrogen atmosphere. The suspension was stirred for 16 h at room temperature and then filtered. The filtrate was concentrated *in vacuo* and the residue was purified by column chromatography (DCM/MeOH, 100/0 – 9/1 gradient) to yield the triester as a yellow oil **(39)**. Reproduced from Gaillard [8] (2.26 g, 43 %).

ν_{max} ($CHCl_3$)/cm^{-1}, 1726, 1692 (C=O); δ_H (400 MHz; $CDCl_3$), 1.21 (18H, s, C(C*H*$_3$)$_3$), 1.24 (9H, s, C(C*H*$_3$)$_3$), 2.40-3.45 (22H, m, NC*H*$_2$C*H*$_2$N, NC*H*$_2$COO),

3.98 (1H, t, *J* = 5.9 Hz, $COOCH_2CH$), 4.23 (2H, d, *J* = 5.9 Hz, $COOCH_2CH$), 7.07 (2H, td, *J* = 7.4 Hz, C*H*Ar), 7.15 (2H, t, *J* = 7.4 Hz, C*H*Ar), 7.35 (2H, d, *J* = 7.4 Hz, C*H*Ar), 7.52 (2H, d, *J* = 7.4 Hz, C*H*Ar); HRMS *m/z* (+ ESI): Found $[MH]^+$, 737.4480 $C_{41}H_{62}N_4O_8$ requires $[MH]^+$, 737.4484.

(4,10-*Bis*-*tert*-butoxycarbonylmethyl-1,4,7,10-tetraaza-cyclododec-1-yl)-acetic acid *tert*-butyl ester **(40)**.

Method 1

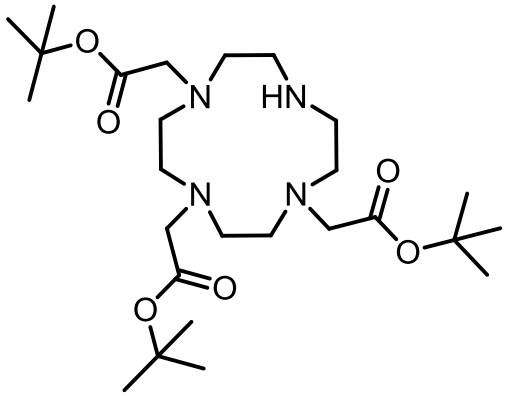

A solution of piperidine in dimethylformamide (piperidine/DMF, 1/9, 10 mL) was added dropwise to 4,7,10-tris-*tert*-butoxycarbonylmethyl-1,4,7,10-tetraaza-cyclododecane-1-carboxylic acid 9*H*-fluoren-9-ylmethyl ester **(39)** (2.26 g, 3.1 mmol, 1 equiv). The resulting solution was stirred at room temperature for 10 min prior to concentration *in vacuo*. The residue was triturated with diethyl ether and the resulting solid filtered and dried under vacuum to yield the triester as a white solid **(40)**. Reproduced from Gaillard [8] (0.65 g, 41%).

HRMS *m/z* (+ ESI): Found $[MH]^+$, 515.3783 $C_{26}H_{52}N_4O_6$ requires $[MH]^+$, 515.3803.

(4,10-*Bis*-*tert*-butoxycarbonylmethyl-1,4,7,10-tetraaza-cyclododec-1-yl)-acetic acid *tert*-butyl ester .HBr salt **(40)**.

Method 2

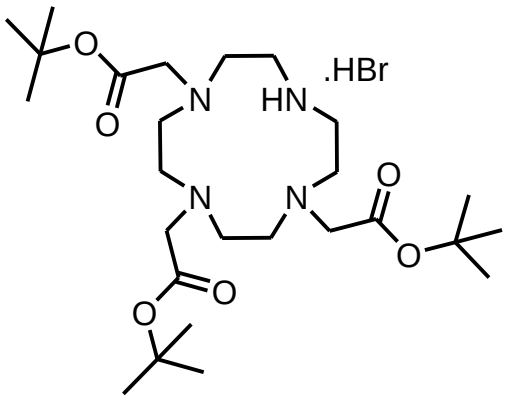

To a solution of cyclen **(35)** (200 mg, 1.3 mmol, 1 equiv) in acetonitrile (150 mL), sodium bicarbonate (350 mg, 4.2 mmol, 3 equiv) was added. This was then stirred for 15 min at room temperature under a nitrogen atmosphere. A solution of *tert*-butyl bromoacetate (800 mg, 4.2 mmol, 3 equiv) in acetonitrile (50 mL) was stirred at room temperature under a nitrogen atmosphere. The cyclen solution was added dropwise to the *tert*-butyl bromoacetate solution and stirred for 30 min at ambient temperature, prior to reflux at 80 °C for 24 h. The precipitate was filtered and the solution concentrated *in vacuo*. The residue was recrystallised from toluene, and washed in diethyl ether to yield the HBr salt as a white solid **(40)**. Reproduced from Machitani *et al.* [73] (589 mg, 85%).

mp, 186-188 °C (Lit: 190-191 °C [169]);ν_{max} ($CHCl_3$)/cm^{-1}, 1728 (C=O); δ_H (400 MHz; $CDCl_3$), 1.40 (9H, s, C(C*H*$_3$)$_3$), 1.41 (18H, s, C(C*H*$_3$)$_3$), 2.75-3.12 (16H, m, NC*H*$_2$C*H*$_2$N), 3.24 (2H, s, NC*H*$_2$COO), 3.33 (4H, s, NC*H*$_2$COO); δ_C (100 MHz $CDCl_3$): 27.4, 27.8 (C(*C*H$_3$)$_3$), 30.7, 35.8 (*C*H$_2$COO), 41.8-56.1 (NCH$_2$*C*H$_2$N), 80.5, 81.2 (*C*(CH$_3$)$_3$), 162.3, 170.5 (*C*=O); HRMS *m/z* (+ ESI): Found $[MH]^+$, 515.3804 $C_{26}H_{52}N_4O_6$ requires $[MH]^+$, 515.3803.

(4,7,10-Tris-*tert*-butoxycarbonylmethyl-1,4,7,10-tetraaza -cyclododec-1-yl)acetic acid benzyl ester **(75)**.

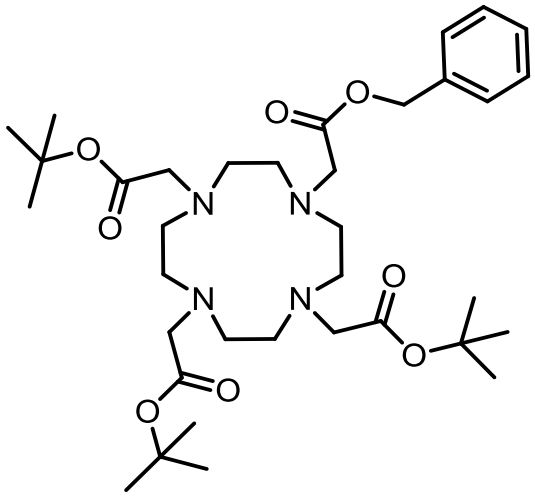

To a solution of (4,10-*bis*-*tert*-butoxycarbonylmethyl-1,4,7,10-tetraaza-cyclododec-1-yl)-acetic acid *tert*-butyl ester .HBr **(40)** (200 mg, 0.3 mmol, 1 equiv) in dimethylformamide (4 mL) potassium carbonate (64 mg, 0.5 mmol, 1.7 equiv) was added and this was stirred at room temperature under a nitrogen atmosphere. A solution of benzyl bromoacetate (172 mg, 0.8 mmol, 2.7 equiv) in dimethylformamide (1 mL) was added dropwise to the suspension and stirred for 16 h. The precipitant was filtered from the reaction and the solution was

concentrated *in vacuo* to yield the crude amine as a white solid **(75)**. Reproduced from Wangler *et al.* [121] (196 mg).

HRMS *m/z* (+ ESI): Found $[MH]^+$, 663.4315 $C_{35}H_{58}N_4O_8$ requires $[MH]^+$, 663.4327.

(4,7,10-Tris-*tert*-butoxycarbonylmethyl-1,4,7,10-tetraaza -cyclododec-1-yl)acetic acid (tris-*t*-Bu-DOTA) **(76)**.

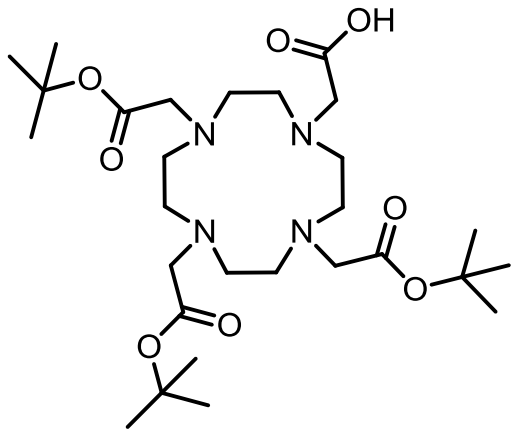

To a solution of 4,10-*bis*-*tert*-butoxycarbonylmethyl-1,4,7,10-tetraaza-cyclododec-1-yl)acetic acid *tert*-butyl ester .HBr **(40)** (100 mg, 0.15 mmol, 1 equiv) in dimethylformamide (4 mL), potassium carbonate (60 mg, 0.5 mmol, 3.3 equiv) and this was stirred under a nitrogen atmosphere at ambient temperature. A solution of bromoacetate (32 mg, 0.2 mmol, 1.3 equiv) in dimethylformamide (1 mL) was added dropwise to the suspension prior to stirring for 16 h. The reaction was then filtered to remove precipitate and the solution was concentrated *in vacuo* to yield the crude amine as a white solid **(76)**. Adapted from Wangler *et al.* [121] (126 mg).

HRMS *m/z* (+ ESI): Found $[MH]^+$ 573.3858 $C_{28}H_{52}N_4O_8$ requires 573.3858.

(1,4,7-Tris-*tert*-butoxycarbonylmethyl-10-prop-2-ynyl carbamoylmethyl-1,4,7,10- tetraaza-cyclododec-1-yl)-acetic acid *tert*-butyl ester **(78)**.

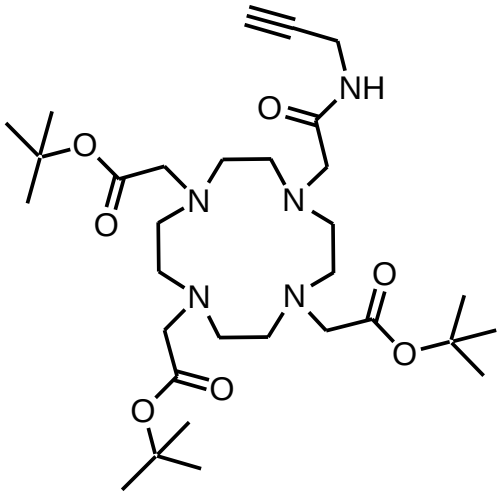

To a suspension of (4,7,10-tris-*tert*-butoxycarbonylmethyl-1,4,7,10-tetraaza -cyclododec-1-yl)acetic acid **(76)** (50 mg, 0.08 mmol, 1.3 equiv), propargyl amine (3 mg, 0.06 mmol, 1 equiv), *o*-(benzotriazol-1-yl)-*N,N,N′,N′*-tetramethyluronium hexafluorophosphate (43 mg, 0.08 mmol, 1.3 equiv) and 1-hydroxybenzotriazole hydrate (10 mg, 0.08 mmol, 1.3 equiv) in dimethylformamide (3 mL) diisopropylethyl amine (17 µL, 0.08 mmol, 1.3 equiv) was added. This was stirred at ambient temperature for 2 h before being concentrated *in vacuo*, to obtain the crude product as an off white solid **(78)**. Adapted from Montalbetti *et al.* [172]

HRMS m/z (+ ESI): Found $[MH]^+$, 610.4164, $C_{31}H_{55}N_4O_8$ requires $[MH]^+$, 610.4174

(4,10-*Bis*-*tert*-butoxycarbonylmethyl-7-methoxycarbonylmethyl-1,4,7,10tetraaza-cyclododec-1-yl)-acetic acid *tert*-butyl ester **(77)**.

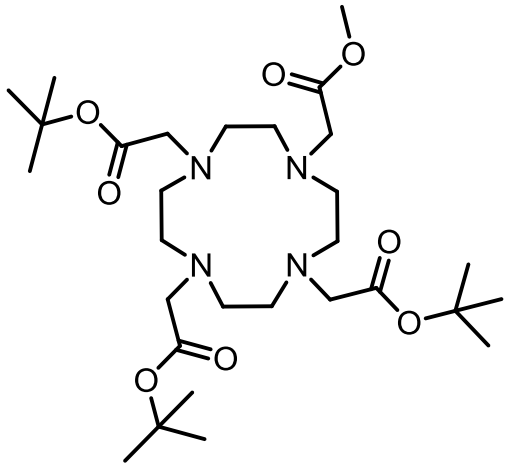

To a suspension of (4,10-*bis*-*tert*-butoxycarbonylmethyl-1,4,7,10-tetraaza-cyclododec-1-yl)-acetic acid *tert*-butyl ester .HBr **(40)** (100 mg, 0.15 mmol, 1 equiv) and potassium carbonate (30 mg, 0.21 mmol, 1.4 equiv) in dimethylformamide (2 mL), methyl bromoacetate (33 mg, 0.21 mmol, 1.4 equiv) was added. The reaction was stirred overnight at room temperature under a nitrogen atmosphere. The product was then concentrated *in vacuo* and purified using column chromatography (DCM/MeOH, 95/5) to yield the amine as a yellow oil **(77)**. Adapted from Wanger *et al.* [121] (79 mg, 93%)

δ_H (300 MHz; $CDCl_3$): 1.42 (27H, s, C*H*$_3$), 2.00-3.60 (24H, m, C*H*$_2$), 3.67 (3H, s, OC*H*$_3$); δ_C (100 MHz $CDCl_3$): 27.9 (C(*C*H$_3$)$_3$), 51.9 (O*C*H$_3$), 53.5, 54.7, 55.6, 55.7 (*C*H$_2$), 82.0 (*C*(CH$_3$)$_3$), 172.9, 173.0, 174.0 (*C*=O); HRMS *m/z* (+ ESI): Found $[MH]^+$, 587.4015 $C_{29}H_{54}N_4O_8$ requires $[MH]^+$, 587.4014.

(4,7,10-Tris-*tert*-butoxycarbonyl methyl-1,4,7,10-tetraaza-cyclododec-1-yl)-acetic acid **(76)**.

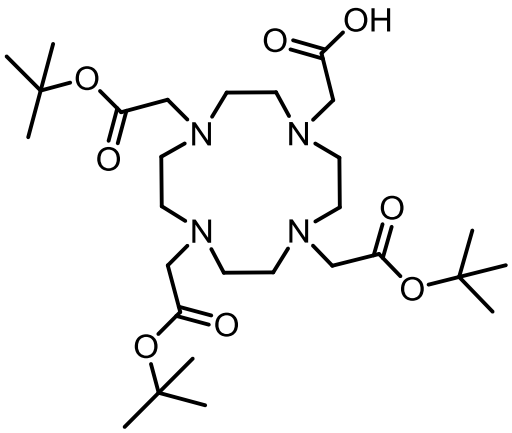

To a solution of (4,10-*bis*-*tert*-butoxycarbonylmethyl-1,4,7,10-tetraaza-cyclododec-1-yl)-acetic acid *tert*-butyl ester **(77)** (71 mg, 0.12 mmol, 1 equiv) in methanol (3 mL) and water (1 mL), lithium hydroxide (30 mg, 0.61 mmol, 5 equiv) was added. The solution was stirred overnight at room temperature under a nitrogen atmosphere, before being neutralised with hydrochloric acid (1 M), and concentrated *in vacuo*. The residue was then taken up in methanol and filtered to yield the free carboxylic acid as a yellow oil **(76)**. Adapted from Green *et al.* [122] (13 mg, 19%).

ν_{max} ($CHCl_3$)/cm^{-1}, 3433 (OH), 1585 (C=O); δ_H (300 MHz; MeOD): 1.46 (27H, s, C(CH_3)$_3$), 2.24-3.05 (24H, m, CH_2); δ_C (75 MHz MeOD): 27.1 (C(*C*H_3)$_3$), 50.3, 53.3, 55.4, 59.2 (*C*H_2), 81.0 (*C*(CH$_3$)$_3$), 179.15 (*C*=O); HRMS *m/z* (+ ESI): Found $[MH]^+$, 573.3862 $C_{28}H_{52}N_4O_8$ requires $[MH]^+$, 573.3858.

2-Bromo-*N*-(prop-2-yn-1-yl) acetamide **(80)**.

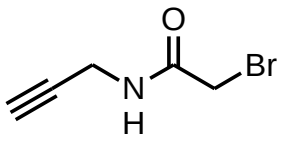

A suspension of bromo acetylbromide **(79)** (500 mg, 2.5 mmol, 1.1 equiv) and potassium carbonate (622 mg, 4.5 mmol, 2 equiv) in anhydrous dichloromethane (5 mL) was cooled to 0 °C and stirred for 15 mins under a nitrogen atmosphere. Propargyl amide (124 mg, 2.3 mmol, 1 equiv) was then added dropwise over half an hour, before the suspension was brought to room temperature and stirred for 2 h before quenching with water (20 mL). The product was then extracted with dichloromethane (3 x 10 mL), and washed with citric acid (5% solution, 10 mL) and water (10 mL), before concentrating *in vacuo* to yield the amine as a brown solid **(80)**. Reproduced from Mani *et al*. [125] (386 mg, 89%).

ν_{max} ($CHCl_3$)/cm^{-1}, 3422 (NH), 2944, 2837 (CH), 2255 (Alkyne), 1671 (C=O); δ_H (400 MHz; $CDCl_3$): 2.27 (1H, t, *J* = 2.6 Hz, CH_2CCH), 3.88 (2H, s, $BrCH_2$), 4.75 (2H, dd, J = 5.3, 2.6 Hz, CH_2CCH), 6.98 (1H, bs, NH); δ_C (100 MHz $CDCl_3$): 28.7 ($BrCH_2$), 29.9 ($NHCH_2$), 72.2 (CH_2CCH), 78.6 (CH_2CCH), 165.3 (C=O); HRMS *m/z* (+ ESI): Found $[MNa]^+$, 197.9517 $C_5H_6BrNNaO$ requires $[MNa]^+$, 197.9524.

(1,4,7-Tris-*tert*-butoxycarbonylmethyl-10-prop-2-ynyl carbamoylmethyl-1,4,7,10- tetraaza-cyclododec-1-yl)-acetic acid *tert*-butyl ester **(78)**.

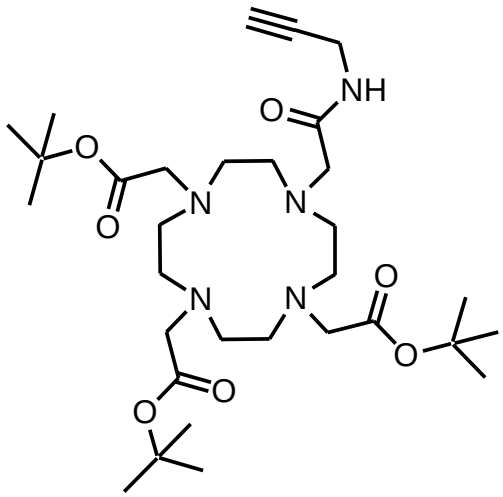

To a suspension of (4,10-*bis*-*tert*-butoxycarbonylmethyl-1,4,7,10-tetraaza-cyclododec-1-yl)-acetic acid *tert*-butyl ester .HBr **(40)** (242 mg, 0.35 mmol, 1 equiv) and potassium carbonate (70 mg, 0.52 mmol, 1.5 equiv) in dimethylformamide (2.5 mL), 2-bromo-*N*-(prop-2-yn-1-yl) acetamide **(80)** (92 mg, 0.52 mmol, 1.5 equiv) was added. The suspension was then stirred overnight at room temperature under a nitrogen atmosphere before concentration *in vacuo*. The residue was then purified using column chromatography (DCM/MeOH, 95/5) to yield the product as a colourless sticky solid **(78)**. Reproduced from Viguler *et al.* [74] (158 mg, 74%).

ν_{max} ($CHCl_3$)/cm^{-1}, 3439 (NH), 2976, 2825 (CH), 1676 (C=O); δ_H (400 MHz; $CDCl_3$): 1.46 (27H, s, $C(CH_3)_3$), 2.03 (1H, s, CH_2CCH), 1.80-3.80 (24H, m, NCH_2CH_2N, CH_2), 3.97 (2H, s, CH_2CCH), 8.80 (1H, t, J = 5.6 Hz, NH); δ_C (100 MHz $CDCl_3$): 28.0 ($C(CH_3)_3$), 28.5 (CH_2CCH), 55.7, 56.2 (NCH_2CH_2N, CH_2),

69.6 (CH_2CCH), 80.9 ($C(CH_3)_3$), 81.9 (CH_2CCH), 171.9, 172.3 (C=O); HRMS *m/z* (+ ESI): Found $[MH]^+$, 610.4154 $C_{31}H_{55}N_5O_7$ requires $[MH]^+$, 610.4174.

(1,4,7-Tris-carbonylmethyl-10-prop-2-ynyl carbamoylmethyl-1,4,7,10- tetraaza-cyclododec-1-yl)-acetic acid .3HCl **(81)**.

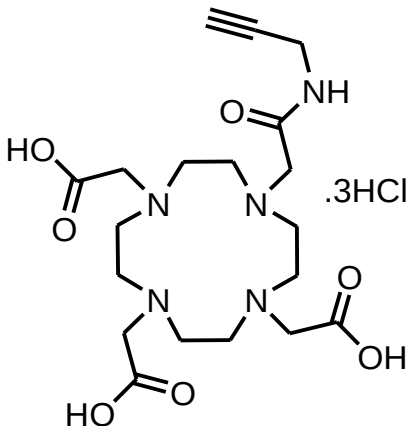

To a solution of (1,4,7-tris-*tert*-butoxycarbonylmethyl-10-prop-2-ynyl carbamoylmethyl-1,4,7,10-tetraaza-cyclododec-1-yl)-acetic acid *tert*-butyl ester **(78)** (858.9 mg, 1.4 mmol, 1 equiv) in ethanol (10 mL) and water (5 mL), hydrochloric acid (11.8 M, 5 mL) was added. The solution was stirred for 5 h at room temperature before concentration *in vacuo*, to yield the HCl salt as an off white solid **(81)**. Adapted from Prasuhn *et al.* [109] (614 mg, 80%).

ν_{max} ($CHCl_3$)/cm^{-1}, 3433 (OH), 2925 (CH), 1733, 1636 (C=O); δ_H (400 MHz; $CDCl_3$):, 2.64 (1H, b, CH_2CCH), 2.80-4.20 (24H, m, NCH_2CH_2N, CH_2), 3.96 (2H, b, CH_2CCH); δ_C (100 MHz $CDCl_3$): 28.3 (CH_2CCH), 48.6, 49.7, 51.5, 51.7 (NCH_2CH_2N, CH_2), 71.6 (CH_2CCH), 78.8 (CH_2CCH), 167.5, 172.6 (C=O); HRMS *m/z* (+ ESI): Found $[MH]^+$, 442.2306 $C_{19}H_{31}N_5O_7$ requires $[MH]^+$, 442.2296.

(1,4,7-Tris-carbonylmethyl-10-prop-2-ynyl carbamoylmethyl-1,4,7,10- tetraaza-cyclododec-1-yl)-acetic acid europium **(CA1-Eu)**.

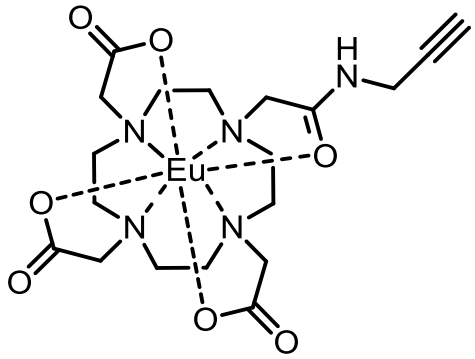

A solution of (1,4,7-tris-carbonylmethyl-10-prop-2-ynyl carbamoylmethyl-1,4,7,10- tetraaza-cyclododec-1-yl)-acetic acid .3HCl **(81)** (200 mg, 0.36 mmol, 1 equiv) in water (1.5 mL) was adjusted to pH 6 using potassium hydroxide solution (1 M in water), before addition of europium (III) chloride hexahydrate (133 mg, 0.36 mmol, 1 equiv) in water (0.5 mL). The solution was then readjusted to pH 6 with more potassium hydroxide solution and stirred for 2 h at room temperature. The pH was adjusted again to pH 6, before freeze drying. The residue was then suspended in ethanol, centrifuged and the supernatant was collected and concentrated *in vacuo* to yield the product as a colourless solid **(CA1-Eu)**. Reproduced from Viguier *et al.* [74] (184 mg, 87%).

ν_{max} ($CHCl_3$)/cm^{-1}, 3378 (OH), 1584 (C=O); HRMS *m/z* (+ ESI): Found $[MH]^-$, 590.1141 $C_{19}H_{27}{}^{152}EuN_5O_7$ requires $[MH]^-$, 590.1128.

(1,4,7-Tris-carbonylmethyl-10-prop-2-ynyl carbamoylmethyl-1,4,7,10- tetraaza-cyclododec-1-yl)-acetic acid gadolinium **(CA1)**.

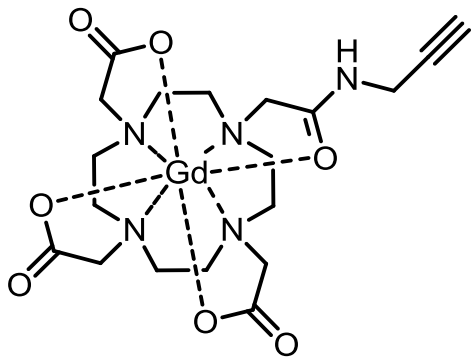

A solution of (1,4,7-tris-carbonylmethyl-10-prop-2-ynyl carbamoylmethyl-1,4,7,10- tetraaza-cyclododec-1-yl)-acetic acid .3HCl **(81)** (200 mg, 0.36 mmol, 1 equiv) in water (1.5 mL) was adjusted to pH 6 using potassium hydroxide solution (1 M in water), before addition of gadolinium (III) chloride hexahydrate (135 mg, 0.36 mmol, 1 equiv) in water (0.5 mL). The solution was then readjusted to pH 6 with more potassium hydroxide solution and stirred for 2 h at room temperature. The pH was adjusted again to pH 6, before freeze drying. The residue was then suspended in ethanol, centrifuged and the supernatant was collected and concentrated *in vacuo* to yield the product as a colourless solid **(CA1)**. Adapted from Viguier *et al.* [74] (194 mg, 90%).

ν_{max} ($CHCl_3$)/cm^{-1}, 3383 (OH), 1580 (C=O); HRMS *m/z* (+ ESI): Found $[MH]^-$, 596.1235 $C_{19}H_{28}{}^{158}GdN_5O_7$ requires $[MH]^-$, 596.1223.

1,4,7,10-Tetraaza-cyclododecane-1,7-dicarboxylic acid di-*tert*-butyl ester **(83)**.

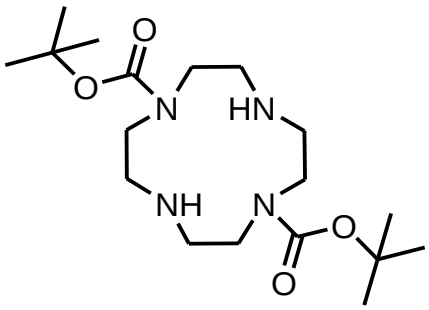

To a solution of cyclen **(35)** (100 mg, 0.56 mmol, 1 equiv), in methanol (5 mL) boc succinimide (242 mg, 1.12 mmol, 2 equiv) was added. The reaction was stirred for 48 hours and monitored by mass spectrometry. Once the reaction was completed the product was concentrated *in vacuo*, and saturated sodium hydrogen carbonate solution was added (10 mL) before extraction with chloroform (3 x 10 mL). The organic layer was dried with magnesium sulphate and concentrated *in vacuo* to yield the product as a colourless foam **(83)**. Reproduced from De Leon-Rodriguez *et al.* [120] (191 mg, 91%).

ν_{max} ($CHCl_3$)/cm^{-1}, 3351 (NH), 1686 (C=O); δ_H (400 MHz; $CDCl_3$): 1.39 (18H, s, $C(CH_3)_3$), 2.52-3.62 (16H, m, NCH_2CH_2N); δ_C (100M Hz; $CDCl_3$); 28.4 ($C(CH_3)_3$), 48.8-50.8 (CH_2), 80.2 ($C(CH_3)_3$), 155.7 (C=O); HRMS *m/z* (+ EI): Found $[MNa]^+$, 395.2643, $C_{18}H_{36}N_4O_4Na$ requires $[MH]^+$, 395.2629

4,10-*Bis*-benzyloxycarbonylmethyl-1,4,7,10-tetraaza-cyclododecane-1,7-dicarboxylic acid di-*tert*-butyl ester **(84)**.

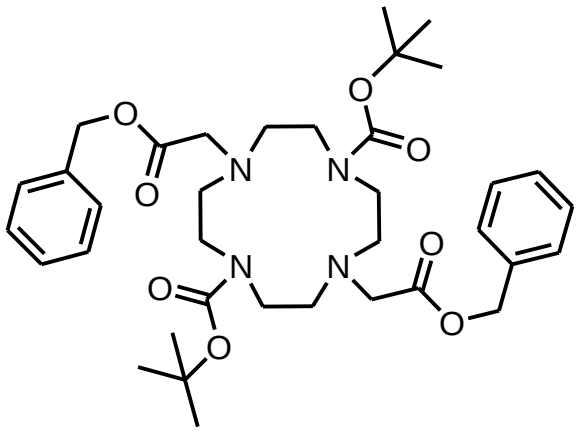

To a suspension of 1,4,7,10-tetraaza-cyclododecane-1,7-dicarboxylic acid di-*tert*-butyl ester **(83)** (100 mg, 0.3 mmol, 1 equiv), potassium dicarbonate (93 mg, 0.7 mmol, 2.5 equiv) in anhydrous dimethylformamide (6 mL), benzylbromoacetate (184 mg, 0.9 mmol, 3 equiv) was added dropwise. The reaction was stirred overnight at room temperature under a nitrogen atmosphere. The suspension was then concentrated *in vacuo*, and purified using column chromatography (DCM/MeOH, 99/1) to yield the amine as a yellow oil **(84).** Reproduced from De Leon-Rodriguez *et al.* [120] (110 mg, 65%).

ν_{max} ($CHCl_3$)/cm^{-1}, 1680 (C=O); δ_H (400 MHz; $CDCl_3$): 1.43 (9H, s, C(CH_3)$_3$), 2.34-3.89 (24H, m, CH_2), 7.31-7.54 (10H, m, CHAr); δ_C (100 MHz $CDCl_3$): 28.4 (C(CH_3)$_3$), 46.7, 47.4, 51.6, 54.4 (NCH_2CH_2N), 66.1, 66.4 (CH_2), 79.5, 79.8 (C(CH_3)$_3$), 128.3-128.7 (CHAr), 135.8 (CAr), 155.9, 171.1 (C=O); HRMS *m/z* (+ ESI): Found $[MH]^+$, 669.3856 $C_{36}H_{52}N_4O_8$ requires $[MH]^+$, 669.3858.

(7-Benzyloxy carbonyl methyl-1,4,7,10-tetraaza-cyclododec-1-yl)acetic acid benzyl ester .2TFA **(85)**.

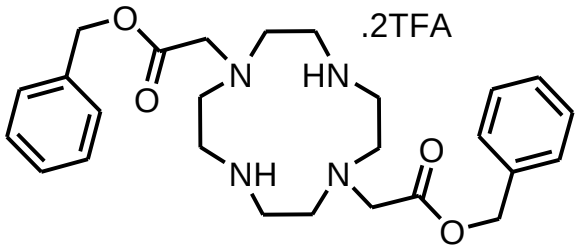

To a solution of 4,10-*bis*-benzyloxycarbonylmethyl-1,4,7,10-tetraaza-cyclododecane-1,7-dicarboxylic acid di-*tert*-butyl ester **(84)** (666 mg, 1 mmol, 1 equiv) in dichloromethane (6 mL), trifluoroacetic acid (0.6 mL) was added. The solution was then stirred overnight at room temperature, before being concentrated *in vacuo* to yield the TFA salt as a sticky orange oil **(85)**. Reproduced from De Leon-Rodriguez *et al.* [120] (697 mg, 98%).

ν_{max} ($CHCl_3$)/cm^{-1}, 1668 (C=O); δ_H (400 MHz; $CDCl_3$): 2.34-4.00 (24H, m, C*H*$_2$), 7.27-7.38 (10H, m, C*H*Ar); δ_C (100 MHz $CDCl_3$): 43.1, 49.9, 54.0, (N*C*H$_2$*C*H$_2$N), 67.8 (*C*H$_2$), 114.1, 116.9 (*C*Ar) 128.4,128.6, 128.7,134.5 (*C*HAr), 171.6 (*C*=O); HRMS *m/z* (+ ESI): Found $[MH]^+$, 469.2822 $C_{26}H_{36}N_4O_4$ requires $[MH]^+$, 469.2809.

(4,10-*Bis*-benzyloxycarbonylmethyl-7-*tert*-butoxycarbonyl methyl-1,4,7,10-tetraaza-cyclododec-1-yl)acetic acid *tert*-butyl ester **(86)**.

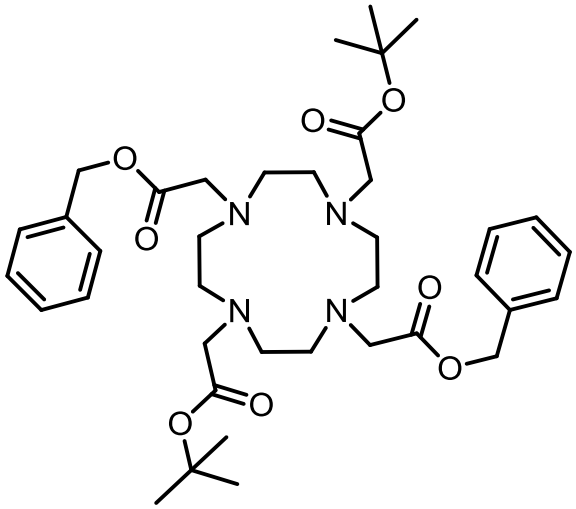

To a stirred suspension of (7-benzyloxy carbonyl methyl-1,4,7,10-tetraaza-cyclododec-1-yl)acetic acid benzyl ester .2TFA **(85)** (100 mg, 0.14 mmol, 1 equiv) and potassium carbonate (88 mg, 0.6 mmol, 4 equiv) in anhydrous dimethylformamide (10 mL), *tert*-butyl bromoacetate (87 mg, 0.4 mmol, 3 equiv) was added. The suspension was then stirred at room temperature, overnight under a nitrogen atmosphere. The suspension was then concentrated *in vacuo* and purified using column chromatography (DCM/MeOH, 99/1) to yield the product as a sticky yellow oil **(86)**. Reproduced from De Leon-Rodriguez *et al.* [120] (7 mg, 7%).

ν_{max} ($CHCl_3$)/cm^{-1}, 3018 (CAr), 1733 (C=O); δ_H (400 MHz; $CDCl_3$): 1.40 (18H, s, C(CH_3)$_3$), 2.60-4.00 (20H, m, CH_2), 5.14 (4H, s, CH_2), 7.29-7.40 (10H, m, CHAr); δ_C (100 MHz $CDCl_3$): 27.9 (C(CH_3)$_3$), 55.0, 55.8, 65.1, 66.9 (CH_2), 82.1 (C(CH_3)$_3$), 127-128 (CHAr), 173.2, 173.6 (C=O); HRMS *m/z* (+ ESI): Found $[MH]^+$, 697.4151 $C_{38}H_{57}N_4O_8$ requires $[MH]^+$, 697.4171.

4,10-*Bis*-*tert*-butoxycarbonylmethyl-1,4,7,10tetraaza-cyclododecane-1,7-dicarboxylicacid di-*tert*-butyl ester **(91)**.

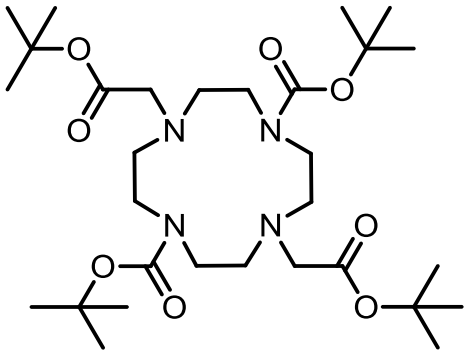

To a suspension of 1,4,7,10-tetraaza-cyclododecane-1,7-dicarboxylic acid di-*tert*-butyl ester **(83)** (100 mg, 0.3 mmol, 1 equiv) and potassium carbonate (64 mg, 0.6 mmol, 2.2 equiv) in anhydrous dimethylformamide (2 mL), *tert*-butyl bromoacetate (90 mg, 0.6 mmol, 2.2 equiv) was added dropwise. The suspension was stirred overnight at room temperature under a nitrogen atmosphere. The reaction was then concentrated *in vacuo* and purified using column chromatography (DCM/MeOH, 99/1) to yield the product as a brown oil **(91)**. Adapted from De Leon-Rodriguez *et al.* [120] (160 mg, 63%).

ν_{max} ($CHCl_3$)/cm^{-1}, 1721 (C=O); δ_H (300 MHz; $CDCl_3$): 1.43 (18H, s, C(CH_3)$_3$), 1.44 (18H, s, C(CH_3)$_3$), 2.87-3.35 (20H, m, CH_2); δ_C (75 MHz $CDCl_3$): 28.2, 28.5 (C(*C*H_3)$_3$), 46.6 (*C*H_2), 54.4-55.9 (*C*H_2), 79.3, 80.7 (*C*(CH$_3$)$_3$), 155.9, 170.5 (*C*=O); HRMS *m/z* (+ ESI): Found $[MH]^+$, 601.4152 $C_{30}H_{57}N_4O_8$ requires $[MH]^+$, 601.4171.

(7-Carboxymethyl-1,4,7,10tetraaza-cyclododec-1-yl)acetic acid .4TFA **(92)**.

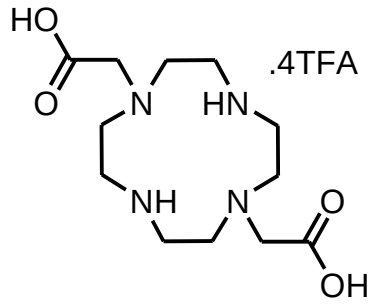

To a solution of 4,10-*bis*-*tert*-butooxycarbonylmethyl-1,4,7,10tetraaza-cyclododecane-1,7-dicarboxylicacid di-*tert*-butyl ester **(91)** (100 mg, 0.2 mmol, 1 equiv) in dichloromethane (2 mL), trifluoroacetic acid (1 mL) was added. The reaction was then stirred overnight at room temperature. The solution was then concentrated *in vacuo* to yield the trifluoroacetic acid salt as a sticky oil **(92)**. Adapted from Green *et al.* [122] (124 mg, quantitative)

ν_{max} ($CHCl_3$)/cm^{-1}, 3445 (NH), 3124 (OH), 1689 (C=O); δ_H (300 MHz; MeOD): 2.04-5.69 (20H, m, CH_2); δ_C (75 MHz MeOD): 42.5, 49.1, 53.1 (*C*H_2), 173.8 (*C*=O); HRMS *m/z* (+ ESI): Found $[MNa]^+$, 311.1696 $C_{12}H_{24}N_4O_4Na$ requires $[MNa]^+$, 311.1690.

(7-Methoxycarbonylmethy-1,4,7,10tetraaza-cyclododec-1-yl) acetic acid methyl ester **(88)**.

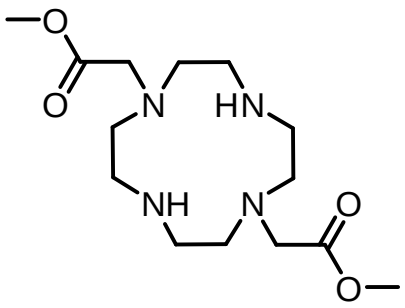

To a solution of (7-carboxymethyl-1,4,7,10tetraaza-cyclododec-1-yl)acetic acid .4TFA **(92)** (100 mg, 0.3 mmol, 1 equiv) in anhydrous methanol (4 mL), acetyl chloride (168 mg, 5.5 mmol, 16 equiv) was added dropwise at 0 °C. The solution was then stirred for 24 h under a nitrogen atmosphere at room temperature. The reaction was then concentrated *in vacuo* before being taken up in dichloromethane and filtered. The residue was then dried to yield the product as a yellow solid **(88)**. Adapted from Thomas *et al.* [173] (105 mg, 96 %).

ν_{max} ($CHCl_3$)/cm^{-1}, 3421 (NH), 1723 (C=O); δ_H (300 MHz; MeOD): 2.00-5.71 (26H, m, CH_2, CH_3); δ_C (75 MHz MeOD): 43.4, 49.9, 53.6 (*C*H_2), 52.1 (O*C*H_3), 173.7 (*C*=O); HRMS *m/z* (+ ESI): Found $[MH]^+$, 317.2179 $C_{14}H_{28}N_4O_4$ requires $[MH]^+$, 317.2183.

(4,10-*Bis*-*tert*-butoxycarbonylmethyl-7-methoxycarbonylmethyl-1,4,7,10tetraaza-cyclododec-1-yl)-acetic acid methyl ester **(89)**.

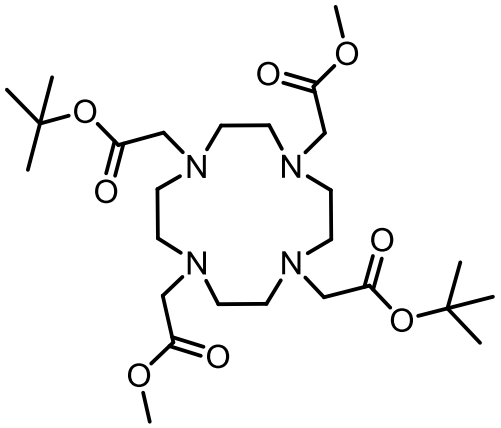

To a suspension of (7-methoxycarbonylmethyl-1,4,7,10tetraaza-cyclododec-1-yl) acetic acid methyl ester **(88)** (273 mg, 0.9 mmol, 1 equiv) and potassium carbonate (280 mg, 1.9 mmol, 2.2 equiv) in dimethylformamide (12 mL), *tert*-butylbromoacetate (168 mg, 1.9 mmol, 2.2 equiv) was added dropwise. The reaction was then stirred overnight under a nitrogen atmosphere at room temperature. The product was then concentrated *in vacuo* and purified using column chromatography (DCM/MeOH, 94/6) to yield the amine as a yellow oil **(89)**. Adapted from De Leon-Rodriguez *et al.* [120] (300 mg, 64%).

ν_{max} ($CHCl_3$)/cm^{-1}, 3018, 2951 (CH), 1737 (C=O); δ_H (400 MHz; $CDCl_3$): 1.39 (18H, s, CH_3), 1.40-3.60 (24H, m, CH_2), 3.65 (6H, s, OCH_3); δ_C (100 MHz $CDCl_3$): 27.1 (C(*C*H_3)$_3$), 52.0 (O*C*H_3), 47.3-57.0 (*C*H_2), 82.3 (*C*(CH$_3$)$_3$), 173.2, 174.0 (*C*=O); HRMS *m/z* (+ ESI): Found $[MNa]^+$, 567.3366 $C_{26}H_{48}N_4O_8Na$ requires $[MNa]^+$, 567.3364.

(4,10-*Bis*-*tert*-butoxycarbonyl methyl-7-carboxymethyl-1,4,7,10tetraaza-cyclododec-1-yl)-acetic acid **(90)**.

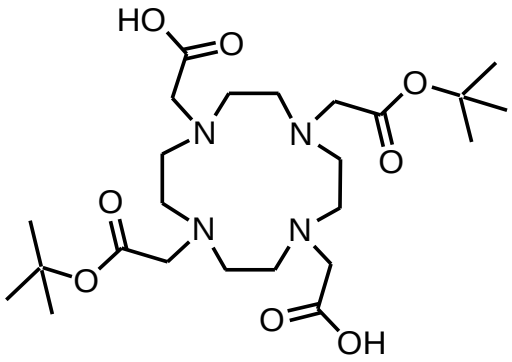

To a solution of (4,10-*bis*-*tert*-butoxycarbonylmethyl-7-methoxycarbonylmethyl-1,4,7,10tetraaza-cyclododec-1-yl)-acetic acid *tert*-butyl ester **(89)** (160 mg, 0.27 mmol, 1 equiv), in water (2.5 mL) and methanol (7.5 mL), lithium hydroxide (60 mg, 2.5 mmol, 9 equiv) was added at 0 °C. The reaction was stirred overnight at room temperature under a nitrogen atmosphere. The product was then concentrated *in vacuo*, before being up taken in dichloromethane and filtered. The filtrate was then concentrated *in vacuo* to yield the dicarboxylic acid as a yellow powder **(90)**. Adapted from Green *et al.* [122] (20 mg, 14%).

HRMS *m/z* (+ ESI): Found $[MH]^+$, 517.3225 $C_{24}H_{44}N_4O_8$ requires $[MH]^+$, 517.3232.

(7-*tert*-Butoxycarbonylmethyl-4,10-*bis*-prop-2-ynylcarbonylmethyl-1,4,7,10-tetraaza-cyclododec-1-yl)-acetic acid *tert*-butyl ester **(95)**.

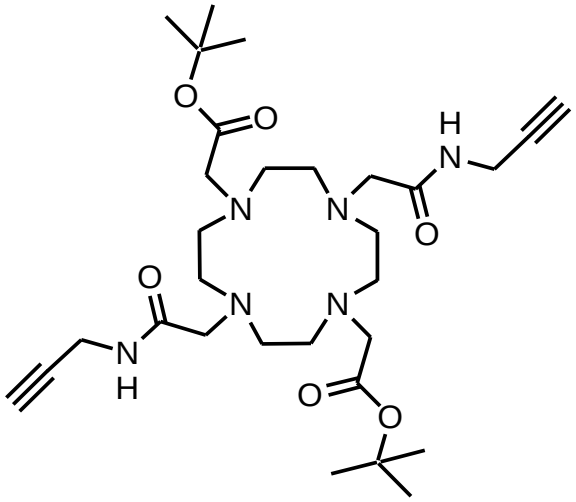

To a stirred solution of (4,10-*bis*-*tert*-butoxycarbonyl methyl-7-carboxymethyl-1,4,7,10tertaaza-cyclododec-1-yl)-acetic acid **(90)** (50 mg, 0.10 mmol, 1 equiv), *N*-hydroxybenzotriazole (29 mg, 0.05 mmol, 0.5 equiv) and [benzotriazol-1-yloxy(dimethylamino)methylidene]-dimethylazanium (81 mg, 0.22 mmol, 2.2 equiv) in dimethylformamide (2 mL), propargyl amine (12 mg, 0.22 mmol, 2.2 equiv) was added, before the addition of diisopropylethylamine (27 mg, 0.22 mmol, 2.2 equiv). The solution was then stirred at room temperature overnight. The solution was then concentrated *in vacuo* and purified via column chromatography (DCM/MeOH, 98/2) to yield the product as a brown oil **(95)**. Adapted from Montalbetti *et al.* [172] (7 mg, 12%).

HRMS *m/z* (+ ESI): Found $[MNa]^+$, 613.3688 $C_{30}H_{50}N_6NaO_8$ requires $[MNa]^+$, 613.3684.

7-Carbonylmethyl-4,10-*bis*-prop-2-ynylcarbonylmethyl-1,4,7,10-tetraaza-cyclododec-1-yl)-acetic acid .2TFA **(96)**.

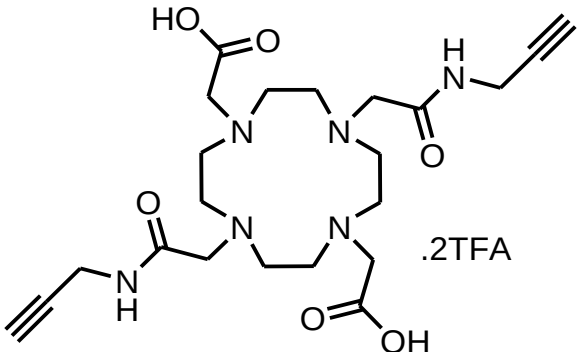

To a solution of (7-*tert*-butoxycarbonylmethyl-4,10-*bis*-prop-2-ynylcarbonylmethyl-1,4,7,10-tetraaza-cyclododec-1-yl)-acetic acid *tert*-butyl ester **(95)** (20 mg, 0.03 mmol, 1 equiv) in dichloromethane (1 mL), trifluoroacetic acid (0.4 mL) was added. The solution was then stirred overnight at room temperature before concentrating *in vacuo* to yield the TFA salt as a sticky brown oil **(96)**. Adapted from Green *et al.* [122] (15 mg, 68%).

HRMS *m/z* (+ ESI): Found $[MH]^+$, 479.2626 $C_{22}H_{35}N_6O_6$ requires $[MH]^+$, 479.2613.

4,10-*Bis*-methoxycarbonylmethyl-1,4,7,10-tetraaza-cyclododecane-1,7-dicarboxylic acid di-*tert*-butyl ester **(87)**.

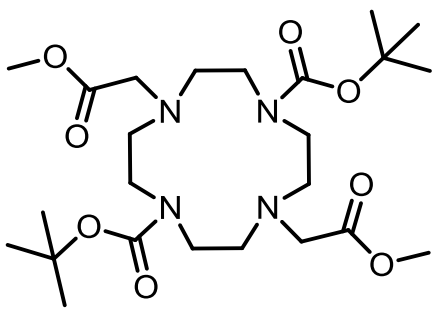

To a suspension of 1,4,7,10-t\etraaza-cyclododecane-1,7-dicarboxylic acid di-*tert*-butyl ester **(83)** (1.00 g, 2.7 mmol, 1 equiv) and potassium carbonate (800 mg, 5.9 mmol, 2.2 equiv) in dimethlformamide (5 mL), methyl bromoacetic acid (900 mg, 5.9 mmol, 2.2 equiv) was added dropwise. The reaction was stirred overnight at room temperature under a nitrogen atmosphere. The suspension was then concentrated *in vacuo*, and the residue was purified using column chromatography (DCM/MeOH, 99/1), to yield the product as a yellow oil **(87)**. Adapted from De Leon-Rodriguez *et al.* [120] (630 mg, 41%).

ν_{max} ($CHCl_3$)/cm^{-1}, 2973 (CH), 1737, 1682 (C=O); δ_H (300 MHz; $CDCl_3$): 1.43 (18H, s, C(C*H*$_3$)$_3$), 2.67-3.62 (20H, m, C*H*$_2$), 3.67 (6H, s, C*H*$_3$); δ_C (75 MHz $CDCl_3$): 28.5 (C(*C*H$_3$)$_3$), 46.5, 54.6, 54.9 (*C*H$_2$), 51.3 (*C*H$_3$), 79.5 (*C*(CH$_3$)$_3$), 155.9, 171.7 (*C*=O); HRMS *m/z* (+ ESI): Found $[MH]^+$, 573.3862 $C_{24}H_{44}N_4O_8$ requires $[MH]^+$, 573.3858.

7-Methoxycarbonylmethy-1,4,7,10-tetraaza-cyclododec-1-yl) acetic acid methyl ester .2TFA **(88)**.

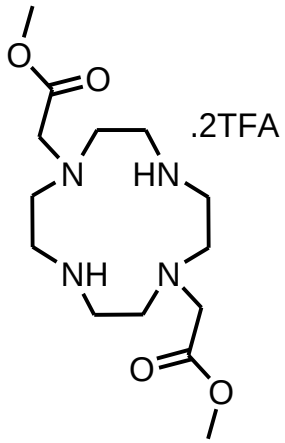

To a solution of 4,10-*bis*-methoxycarbonylmethyl-1,4,7,10-tetraaza-cyclododecane-1,7-dicarboxylic acid di-*tert*-butyl ester **(87)** (713 mg, 1.2 mmol, 1 equiv) in dichloromethane (5 mL), trifluoroacetic acid (2 mL) was added. The reaction was then stirred at room temperature overnight before concentrating *in vacuo* to yield the TFA salt as a sticky orange oil **(88)**. Adapted from De Leon-Rodriguez *et al.* [120] (665 mg, 98%).

ν_{max} ($CHCl_3$)/cm^{-1}, 3421 (NH), 1723 (C=O); δ_H (300 MHz; MeOD): 2.00-5.71 (26H, m, CH_2, CH_3); δ_C (75 MHz MeOD): 43.4, 49.9, 53.6 (*C*H_2), 52.1 (O*C*H_3), 173.7 (*C*=O); HRMS *m/z* (+ ESI): Found $[MH]^+$, 317.2179 $C_{14}H_{28}N_4O_4$ requires $[MH]^+$, 317.2183.

4,10-*Bis*-prop-2-ynylcarbonylmethyl-1,4,7,10-tetraaza-cyclododecane-1,7-dicarboxylic acid di-*tert*-butyl ester **(93)**. [73]

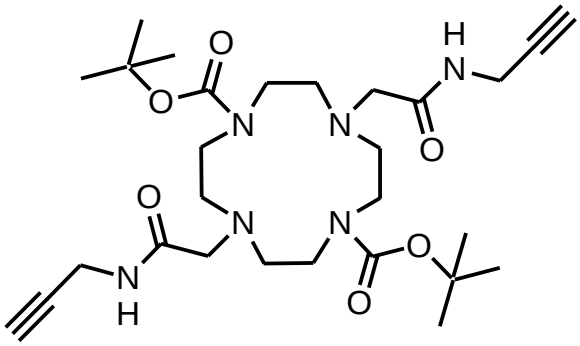

To a suspension of 1,4,7,10-tetraaza-cyclododecane-1,7-dicarboxylic acid di-*tert*-butyl ester **(83)** (100 mg, 0.27 mmol, 1 equiv) and potassium carbonate (81 mg, 5.6 mmol, 2.1 equiv) in dimethylformamide (2.5 mL), 2-bromo-*N*-(prop-2-yn-1-yl) acetamide **(80)** (92 mg, 5.6 mmol, 2.1 equiv) was added. The suspension was then stirred overnight at room temperature under a nitrogen

atmosphere before concentration *in vacuo*. The residue was then purified using column chromatography (DCM/MeOH, 95/5) to yield the product as a pale orange oil **(93)**. Adapted from Viguier *et al.* [74] (103 mg, 68%).

ν_{max} ($CHCl_3$)/cm^{-1}, 3400 (NH), 2990 (CH), 2250 (Alkyne), 1650 (C=O); δ_H (400 MHz; $CDCl_3$): 1.45 (18H, s, C(C*H*$_3$)$_3$), 2.18 (2H, t, *J* = 2.4 Hz, CH_2CCH), 2.70-3.70 (24H, m, NC*H*$_2$C*H*$_2$N, C*H*$_2$), 4.03 (4H, dd, *J* = 5.4, 2.4 Hz, C*H*$_2$CCH); δ_C (100 MHz $CDCl_3$): 28.5 (C(*C*H$_3$)$_3$), 28.7 (*C*H$_2$CCH), 48.4, 53.4, 55.3, 58.8 (NC*H*$_2$*C*H$_2$N, *C*H$_2$), 71.2 (CH_2CCH), 79.8 (*C*(CH$_3$)$_3$), 80.5 (CH_2CCH), 156.6, 170.9 (*C*=O); HRMS *m/z* (+ ESI): Found $[MH]^+$, 563.3543 $C_{28}H_{46}N_6O_6$ requires $[MH]^+$, 563.3552.

4,10-*Bis*-prop-2-ynylcarbonylmethyl-7-carboxymethyl-1,4,7,10tetraaza-cyclododec-1-yl)-acetic acid .2TFA **(94)**.

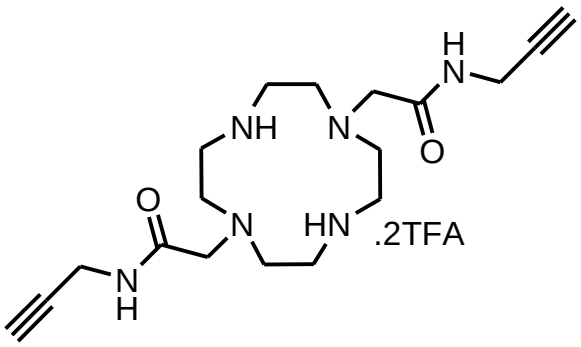

To a solution of 4,10-*bis*-prop-2-ynylcarbonylmethyl-1,4,7,10-tetraaza-cyclododecane-1,7-dicarboxylic acid di-*tert*-butyl ester **(93)** (514 mg, 0.9 mmol, 1 equiv) in dichloromethane (10 ml), trifluoroacetic acid (7 mL) was added. The reaction was stirred at room temperature overnight before concentration *in vacuo*, to yield the TFA salt as a sticky yellow oil **(94)**. Adapted from De Leon-Rodriguez *et al.* [120] (539 mg, quant).

ν_{max} ($CHCl_3$)/cm^{-1}, 3425 (NH), 2925 (CH), 1679 (C=O); δ_H (400 MHz; $CDCl_3$): 2.65 (2H, t, *J* = 2.5 Hz, CH_2CCH), 2.70-3.70 (20H, m, NCH_2CH_2N, CH_2), 4.03 (4H, d, *J* = 2.5 Hz, CH_2CCH); δ_C (100 MHz $CDCl_3$): 28.8 (CH_2CCH), 42.8, 43.3, 46.0, 49.5, 55.7, 66.5 (NCH_2CH_2N, CH_2), 72.0 (CH_2CCH), 79.6 (CH_2CCH), 172.4 (*C*=O); HRMS *m/z* (+ ESI): Found $[MH]^+$, 363.2512 $C_{18}H_{30}N_6O_2$ requires $[MH]^+$, 363.2503.

1,7-Tris-*tert*-butoxycarbonylmethyl-4,10-*bis*-prop-2-ynyl carbamoylmethyl-1,4,7,10- tetraaza-cyclododec-1-yl)-acetic acid *tert*-butyl ester **(95)**.

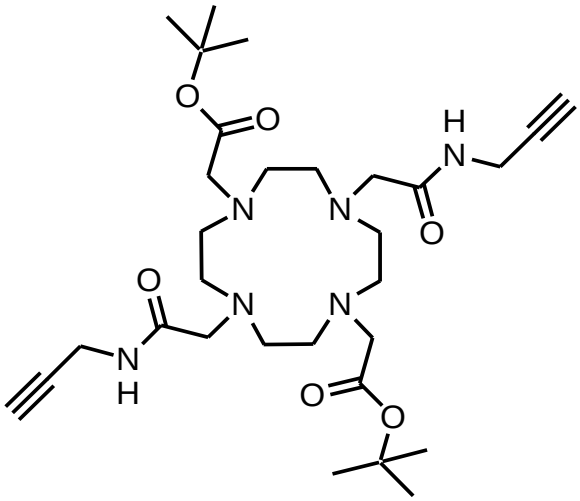

To a suspension of 4,10-*bis*-prop-2-ynylcarbonylmethyl-7-carboxymethyl-1,4,7,10tetraaza-cyclododec-1-yl)-acetic acid .2TFA **(94)** (331 mg, 0.9 mmol, 1 equiv) and potassium carbonate (277 mg, 2.0 mmol, 2.2 equiv) in dimethylformamide (5 mL), *tert*-butyl bromoacetate (391 mg, 2.0 mmol, 2.2 equiv) was added dropwise. The suspension was then stirred overnight at room temperature under a nitrogen atmosphere, before concentration *in vacuo.* The

residue was then purified using column chromatography (DCM/MeOH, 97/3) to yield the product as a colourless oil **(95)**. Adapted from De Leon-Rodriguez *et al.* [120] (151 mg, 28%).

ν_{max} ($CHCl_3$)/cm^{-1}, 3222 (NH), 2977, 2821 (CH), 1731, 1672 (C=O); δ_H (300 MHz; $CDCl_3$): 1.44 (18H, s, $C(CH_3)_3$), 2.65 (2H, t, *J* = 2.6 Hz, CH_2CCH), 2.30-3.80 (24H, m, NCH_2CH_2N, CH_2), 4.05 (4H, dd, *J* = 2.5, 5.2 Hz, CH_2CCH), 8.67 (2H, t, *J* = 5.0 Hz, NH); δ_C (75 MHz $CDCl_3$): 28.2 ($C(CH_3)_3$), 28.9 (CH_2CCH), 52.3, 55.6, 56.2, 58.4, (NCH_2CH_2N, CH_2), 71.1 (CH_2CCH), 80.1 ($C(CH_3)_3$), 81.9 (CH_2CCH), 170.2, 171.4 (C=O); HRMS *m/z* (+ ESI): Found $[MH]^+$, 591.3852 $C_{30}H_{50}N_6O_6$ requires $[MH]^+$, 591.3865.

1,7-Tris-carbonylmethyl-4,10-*bis*-prop-2-ynyl carbamoylmethyl-1,4,7,10- tetraaza-cyclododec-1-yl)-acetic acid .2TFA **(96)**.

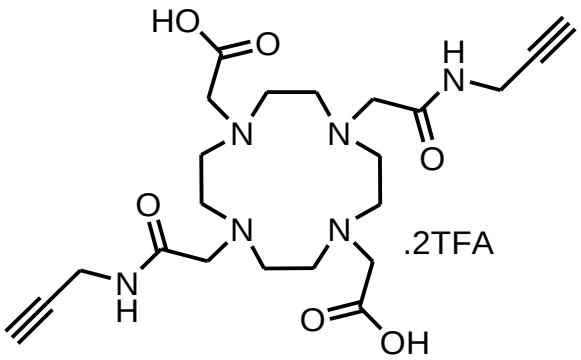

To a solution of 1,7-tris-*tert*-butoxycarbonylmethyl-4,10-*bis*-prop-2-ynyl carbamoylmethyl-1,4,7,10- tetraaza-cyclododec-1-yl)-acetic acid *tert*-butyl ester **(95)** (100 mg, 0.02 mmol, 1 equiv) in dichloromethane (5 mL), trifluoroacetic acid (3 mL) was added. The reaction was stirred overnight at room temperature

before concentration *in vacuo* to yield the TFA salt as a pale brown solid **(96)**. Adapted from Green *et al.* [122] (118 mg, 99%).

ν_{max} ($CHCl_3$)/cm^{-1}, 3406 (OH), 1671 (C=O); δ_H (300 MHz; $CDCl_3$):, 2.61 (2H, t, *J* = 2.3 Hz, CH_2CCH), 3.10-3.90 (24H, m, NCH_2CH_2N, CH_2), 4.02 (4H, d, *J* = 2.3 Hz, CH_2CCH); δ_C (100 MHz $CDCl_3$): 28.3 (CH_2CCH), 48.2, 48.4, 49.2, 50.6, 54.5, 54.8 (NCH_2CH_2N, CH_2), 71.1 (CH_2CCH), 79.1 (CH_2CCH), 161.7, 168.8 (C=O); HRMS *m/z* (+ ESI): Found $[MH]^+$, 479.2628 $C_{22}H_{34}N_6O_6$ requires $[MH]^+$, 479.2613.

1,7-Tris-carbonylmethyl-4,10-*bis*-prop-2-ynyl carbamoylmethyl-1,4,7,10- tetraaza-cyclododec-1-yl)-acetic acid europium **(CA2-Eu)**.

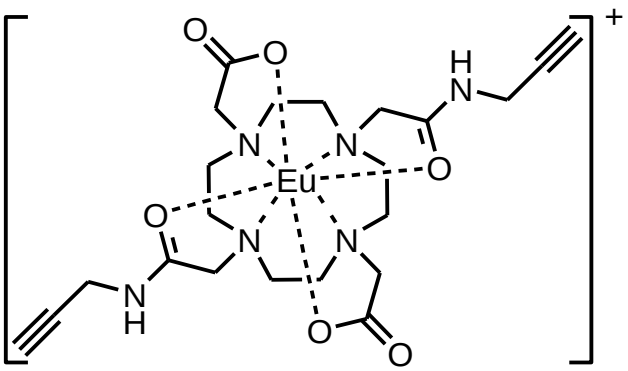

A solution of 1,7-tris-carbonylmethyl-4,10-*bis*-prop-2-ynyl carbamoylmethyl-1,4,7,10- tetraaza-cyclododec-1-yl)-acetic acid .2TFA **(96)** (239 mg, 0.3 mmol, 1 equiv) in water (1.5 mL) was adjusted to pH 6 using potassium hydroxide solution (1 M in water), before addition of europium (III) chloride hexahydrate (124 mg, 0.3 mmol, 1 equiv) in water (0.5 mL). The solution was then readjusted to pH 6 with more potassium hydroxide solution and stirred for 2 h at room temperature. The pH was adjusted again to pH 6, before freeze drying.

The residue was then suspended in ethanol, centrifuged and the supernatant was collected and concentrated *in vacuo* to yield the product as a colourless solid **(CA2-Eu)**. Adapted from Viguier *et al.* [74] (207 mg, 98%).

ν_{max} ($CHCl_3$)/cm^{-1}, 3262 (OH), 1683, 1631 (C=O); HRMS *m/z* (+ ESI): Found $[MH]^-$, 627.1467 $C_{22}H_{30}{}^{152}EuN_6O_6$ requires $[MH]^-$, 627.1445.

1,7-Tris-carbonylmethyl-4,10-*bis*-prop-2-ynyl carbamoylmethyl-1,4,7,10- tetraaza-cyclododec-1-yl)-acetic acid gadolinium **(CA2)**.

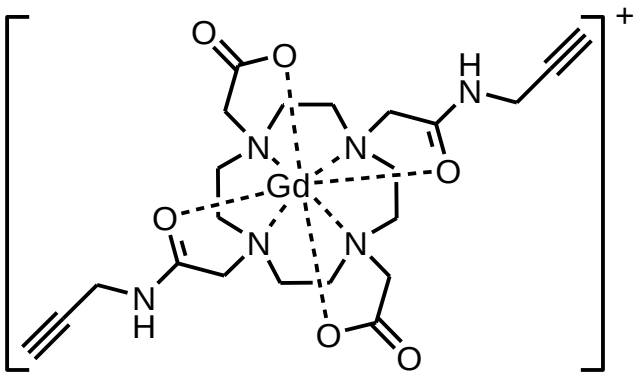

A solution of 1,7-tris-carbonylmethyl-4,10-*bis*-prop-2-ynyl carbamoylmethyl-1,4,7,10- tetraaza-cyclododec-1-yl)-acetic acid .2TFA **(96)** (239 mg, 0.3 mmol 1 equiv) in water (1.5 mL) was adjusted to pH 6 using potassium hydroxide solution (1 M in water), before addition of gadolinium (III) chloride hexahydrate (126 mg, 0.3 mmol, 1 equiv) in water (0.5 mL). The solution was then readjusted to pH 6 with more potassium hydroxide solution and stirred for 2 h at room temperature. The pH was adjusted again to pH 6, before freeze drying. The residue was then suspended in ethanol, centrifuged and the supernatant was collected and concentrated *in vacuo* to yield the product as a colourless solid **(CA2)**. Adapted from Viguier *et al.* [74] (148 mg, 69%).

ν_{max} ($CHCl_3$)/cm^{-1}, 3258 (OH), 1685, 1631 (C=O);); HRMS *m/z* (+ ESI): Found $[M]^+$, 634.1632 $C_{22}H_{30}{}^{158}GdN_6O_6$ requires $[M]^+$, 634.1619.

2-*tert*-Butoxycarbonylamino-3-hydroxy-propionic acid **(98)**.

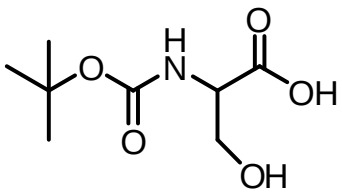

To a suspension of D/L serine **(97)** (100 mg, 1 mmol, 1 equiv) and sodium carbonate (200 mg, 2 mmol, 2 equiv) in water (3 mL) and dioxane (3 mL), Boc anhydride (228 mg, 1.1 mmol, 1.1 equiv) was added dropwise. This was stirred overnight at room temperature. The reaction mixture was then concentrated in vacuo and recrystallised in methanol to yield a colourless solid **(98)**. Repeated from Onisko *et al.* [128]

ν_{max} ($CHCl_3$)/cm^{-1}, 3405 (OH), 1690 (C=O); δ_H (400 MHz; D_2O): 1.38 (9H, s, $C(CH_3)_3$), 3.74 (1H, dd, *J* = 11.3, 3.8 Hz, CH_2), 3.78 (1H, dd, *J* = 11.3, 3.8 Hz, CH_2), 3.95 (1H, bs, CH); δ_C (100 MHz D_2O): 27.7 ($C(CH_3)_3$), 58.0 (CH), 62.4 (CH_2), 81.2 ($C(CH_3)_3$), 157.7, 177.2 (C=O); HRMS m/z (+ EI): Found $[MNa]^+$, 228.0839, $C_8H_{15}N_1O_5Na$ requires $[MNa]^+$, 228.0842

2-*tert*-Butoxycarbonylamino-3-hydroxy-propionic acid methyl ester **(99)**.

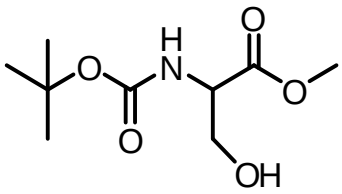

To a suspension of 2-*tert*-butoxycarbonylamino-3-hydroxy-propionic acid **(98)** (205 mg, 1 mmol, 1 equiv) and caesium carbonate (165 mg 0.5 mmol, 0.5 equiv) in anhydrous dimethylformamide (5 mL), iodomethane (273 mg, 1.9 mmol, 1.9 equiv) was added dropwise. This was stirred overnight at room temperature under a nitrogen atmosphere. Water (5 mL) was then added before extraction with ethyl acetate (3 x 10 mL). The organic layers were combined, washed with brine (30 mL) and concentrated *in vacuo* to produce a crude mixture. The residue was then purified via column chromatography (PE/EtOAc, 60/40) to yield the methyl ester as a pale yellow oil **(99)**. Repeated from Onisko *et al.* [128] (162 mg, 78% over both steps).

ν_{max} ($CHCl_3$)/cm^{-1}, 3399 (OH), 1747 (C=O); δ_H (400 MHz; $CDCl_3$): 1.42 (9H, s, C(C*H*$_3$)$_3$), 2.71 (1H, bs, O*H*), 3.69 (3H, s, OC*H*$_3$), 3.87 (1H, dd, *J* = 11.2, 3.7 Hz, C*H*$_2$), 3.94 (1H, dd, *J* = 11.2, 3.7 Hz, C*H*$_2$), 4.35 (1H, b, C*H*), 5.53 (1H, bs, N*H*); δ_C (100 MHz $CDCl_3$): 28.3 (C(*C*H$_3$)$_3$), 52.6 (O*C*H$_3$), 55.7 (*C*H), 63.4 (*C*H$_2$), 80.3 (*C*(CH$_3$)$_3$), 155.8, 171.4 (*C*=O); HRMS *m/z* (+ ESI): Found $[MNa]^+$, 242.0999 $C_9H_{17}N_1O_5Na$ requires $[MNa]^+$, 242.0999.

2-*tert*-Butoxycarbonylamino-acrylic acid methyl ester **(100)**.

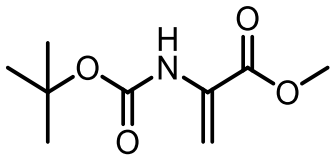

A suspension of 2-*tert*-butoxycarbonylamino-3-hydroxy-propionic acid methyl ester **(99)** (100 mg, 0.4 mmol, 1 equiv) and copper (I) chloride (54 mg, 0.5 mmol, 1.2 equiv) in anhydrous dichloromethane (4 mL) was stirred at 0 ºC under a nitrogen atmosphere in a covered flask. To this cooled green suspension 1-ethyl-3-(3-dimethylaminopropyl)carbodiimide (85 mg, 0.5 mmol, 1.2 equiv) was added. The flask was then purged with nitrogen, before being allowed to reach room temperature and stirred overnight. The solution turned dark green, and was then purified using column chromatography (DCM/MeOH, 99/1) to yield the amino acid as a colourless oil **(100)**. Repeated from Zhu *et al.* [(129)] (61 mg, 72%). Note this compound decomposes quickly even in a covered flask.

δ_H (300 MHz; $CDCl_3$): 1.48 (9H, s, $C(CH_3)_3$), 3.83 (3H, s, CH_3), 5.72 (1H, d, *J* = 1.5 Hz, CH_2), 6.15 (1H, s, CH_2), 7.00 (1H, bs, NH); δ_C (75 MHz $CDCl_3$): 28.2 ($C(CH_3)_3$), 52.8 (CH_3), 80.7 ($C(CH_3)_3$), 105.1 (CCH_2), 131.3 (CCH_2), 152.6, 174.4 (*C*=O); HRMS *m/z* (+ ESI): Found $[MNa]^+$, 224.0894 $C_9H_{15}N_1O_4Na$ requires $[MNa]^+$, 224.0893.

Methyl-2-[(*tert*-butoxycarbonyl)amino]-3-(1,4,7,10-tetraaza cyclododec-1-yl) propanoate **(102)**.

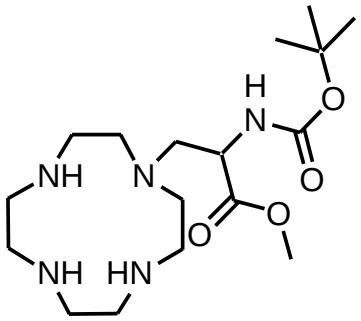

To a suspension of cyclen **(35)** (541 mg, 3.1 mmol, 1.1 equiv) and potassium carbonate (504 mg, 3.6 mmol, 1.3 equiv) in acetonitrile (9 mL), 2-*tert*-butoxycarbonylamino-acrylic acid methyl ester **(100)** (619 mg, 2.8 mmol, 1 equiv) was added. The suspension was stirred overnight at room temperature under a nitrogen atmosphere, before concentration *in vacuo*. The residue was then purified using column chromatography (DCM/EtOH/NH_4OH, 50/50/2) yield the product as a colourless oil **(102)**. Repeated from Molteni *et al.* [174] (180 mg, 17%).

ν_{max} ($CHCl_3$)/cm^{-1}, 3404 (NH), 2972, 2848 (CH), 1696, 1599 (C=O); δ_H (400 MHz; $CDCl_3$): 1.43 (9H, s, C(C*H*$_3$)$_3$), 2.50-2.90 (16H, m, NC*H*$_2$C*H*$_2$N), 3.46-3.75 (2H, m, C*H*$_2$CH), 3.76 (3H, s, OC*H*$_3$), 4.40 (1H, bs, CH_2C*H*), 5.99 (1H, b, N*H*); δ_C (100 MHz $CDCl_3$): 28.3 (C(*C*H_3)$_3$), 45.6, 45.9, 46.1, 47.2, 49.7, 50.6 (N*C*H_2*C*H_2N), 52.5 (O*C*H_3), 52.6 (*C*H_2CH), 53.3 (CH_2*C*H), 79.9 (*C*(CH_3)$_3$), 155.5, 172.7 (*C*=O); HRMS *m/z* (+ ESI): Found $[MH]^+$, 374.2777 $C_{17}H_{35}N_5O_4$ requires $[MH]^+$, 374.2762.

1,4-Dibenzyl-6-hydroxymethyl-6-nitroperhydro-1,4-diazepine **(103)**.

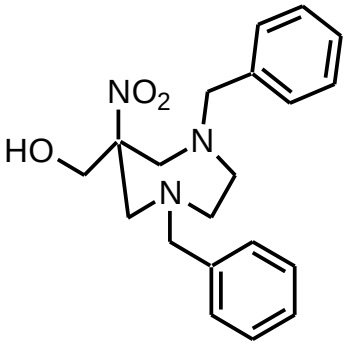

To a solution of *N,N'*-dibenzylethylendiamine diacetate **(46)** (1.08 g, 3.0 mmol, 1 equiv) and 2-nitroethanol (215 µL, 3.0 mmol, 1 equiv) in toluene (20 mL) and ethanol (20 mL), paraformaldehyde (320 mg, 10.7 mmol, 3.5 equiv) was added in portions. The suspension was then heated to reflux for 6 h before concentration *in vacuo.* The residue was then dissolved in dichloromethane (10 mL) and washed with water (3 x 10 mL) before drying with magnesium sulphate and concentration *in vacuo.* This residue was then purified using column chromatography (PE/EtOAc, 8/2) to yield the final product as a sticky colourless oil **(103)**. Repeated from Gugliotta *et al.* [79] (923 mg, 99.5%).

ν_{max} ($CHCl_3$)/cm^{-1}, 3401 (OH), 3026 (CHAr), 2821 (CH), 1538, 1349 (NO_2); δ_H (300 MHz; $CDCl_3$): 2.50-2.75 (4H, m, C*H*$_2$C*H*$_2$), 3.07 (2H, d, *J* = 14.3 Hz, C*H*$_2$C), 3.53 (2H, d, *J* = 14.3 Hz, C*H*$_2$C), 3.66 (2H, d, *J* = 13.1 Hz, C*H*$_2$Ph), 3.73 (2H, s, C*H*$_2$OH), 3.76 (2H, d, *J* = 13.1 Hz, C*H*$_2$Ph), 7.27-7.36 (10H, m, C*H*Ar); δ_C (75 MHz $CDCl_3$): 58.7, 59.2 (*C*H_2 ring), 63.7 (*C*H_2Ph), 65.8 (*C*H_2OH), 94.8 (*C*NO_2), 127.5, 128.5. 129.1 (*C*HAr), 138.9 (*C*Ar); HRMS *m/z* (+ ESI): Found $[MNa]^+$, 378.1797 $C_{20}H_{25}N_3O_3Na$ requires $[MNa]^+$, 378.1788.4

6-Amino-6-hydroxymethylperhydro-1,4-diazepine **(104)**.

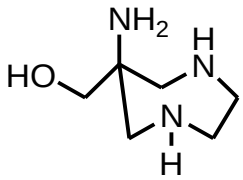

To a solution of 1,4-dibenzyl-6-hydroxymethyl-6-nitroperhydro-1,4-diazepine **(103)** (4.00 g, 11 mmol, 1 equiv) in ethanol (70 mL) and water (15 mL), 10% palladium on carbon (1.89 g) was added. The suspension was then hydrogenated at room temperature, under 60 psi of hydrogen for 40 h. The suspension was then filtered and concentrated *in vacuo* to remove the ethanol, and the freeze dried overnight to yield the amine as a colourless oil **(104)**. Adapted from Sengar *et al.* [75] (1.60 g, 98%).

ν_{max} ($CHCl_3$)/cm^{-1}, 3338 (OH); δ_H (400 MHz; D_2O): 2.65 (2H, d, *J* = 14.3 Hz, C*H*$_2$C), 2.78-2.91 (4H, m, C*H*$_2$C*H*$_2$), 2.85 (2H, d, *J* = 14.3 Hz, C*H*$_2$C), 3.42 (2H, s, C*H*$_2$OH); δ_C (100 MHz D_2O): 50.6 (*C*H$_2$*C*H$_2$), 55.5 (*C*H$_2$C), 57.4 (CH$_2$*C*) 66.5 (*C*H$_2$OH); HRMS *m/z* (+ ESI): Found $[MH]^+$, 146.1283 $C_6H_{15}N_3O$ requires $[MH]^+$, 146.1288.

1,4-*Bis*(*t*-butoxycarbonylmethyl)-6-[*bis*(*t*-butoxycarbonylmethyl)]amino-6-hydroxymethylperhydro-1,4-diazepine **(105)**.

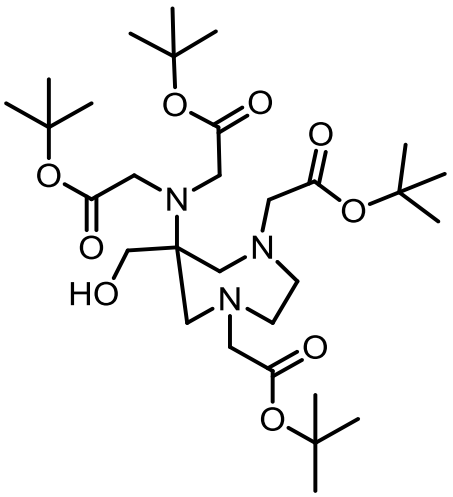

A suspension of 6-amino-6-hydroxymethylperhydro-1,4-diazepine **(104)** (1.42 g, 1.0 mmol, 1 equiv), potassium carbonate (9.40 g, 7.0 mmol, 7 equiv) and magnesium sulfate (approx 2 g) in acetonitrile (30 mL), was cooled to 0 °C and *tert*-butyl bromoacetate (7.78 g, 4.1 mmol, 4.1 equiv) was added dropwise. The suspension was then stirred overnight at room temperature under a nitrogen atmosphere, before filtration and concentration *in vacuo*. The residue was then purified using column chromatography (PE/EtOAc, 8/2) to yield the product as a pale yellow oil **(105)**. Repeated from Gugliotta *et al.* [79] (3.28 g, 56%).

ν_{max} ($CHCl_3$)/cm^{-1}, 3451 (OH), 1729 (C=O); δ_H (400 MHz; $CDCl_3$): 1.42 (18H, s, C(C*H*$_3$)$_3$), 1.42 (18H, s, C(C*H*$_3$)$_3$), 2.60-2.77 (4H, m, C*H*$_2$C*H*$_2$), 2.76 (2H, d, *J* = 14.3 Hz, C*H*$_2$C), 2.96 (2H, d, *J* = 14.2 Hz, C*H*$_2$C), 3.22 (2H, s, C*H*$_2$CO), 3.23 (2H, s, C*H*$_2$CO), 3.47 (2H, s, C*H*$_2$OH), 3.54 (4H, s, C*H*$_2$CO); δ_C (100 MHz $CDCl_3$): 28.2, 28.3 (C(*C*H$_3$)$_3$), 52.7, 58.9 (*C*H$_2$*C*H$_2$, CH$_2$C), 61.5, 62.1 (*C*H$_2$CO),

64.4 (*C*CH_2), 66.3 (*C*H_2OH), 80.9, 81.0 (*C*$(CH_3)_3$), 170.9, 172.7 (*C*=O); HRMS *m/z* (+ ESI): Found $[MH]^+$, 602.3991 $C_{30}H_{56}N_3O_9$ requires $[MH]^+$, 602.4011.

1,4-*Bis*(*t*-butoxycarbonylmethyl)-6-[*bis*(*t*-butoxycarbonylmethyl)]amino-6-chloromethylperhydro-1,4-diazepine **(106)**.

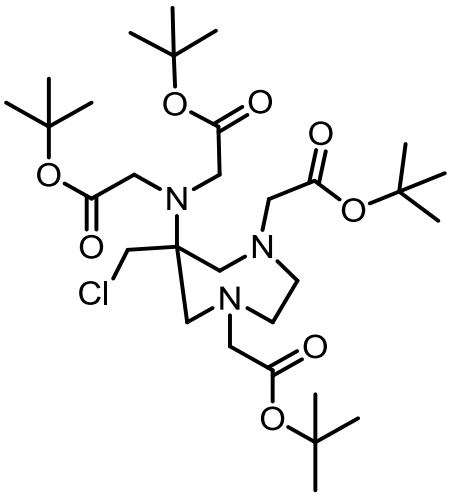

A solution of 1,4-*bis*(*t*-butoxycarbonylmethyl)-6-[*bis*(*t*-butoxycarbonylmethyl)] amino-6-hydroxymethylperhydro-1,4-diazepine **(105)** (100 mg, 0.2 mmol, 1 equiv) in thionyl chloride (3 mL) was stirred at room temperature under nitrogen for 2 h. The solution was then concentrated *in vacuo* to yield the crude HCl salt as a yellow solid **(106)**. Adapted from Aime *et al.* [80]

ESI *m/z* (+ ESI): Found $[MH]^+$, 620.35 $C_{30}H_{54}ClN_3O_8$ requires $[MH]^+$, 620.37.

1,4-*Bis*(*t*-butoxycarbonylmethyl)-6-[*bis*(*t*-butoxycarbonylmethyl)]amino-6-(prop-2-yn-1-ylamino)methylperhydro-1,4-diazepine **(110)**.

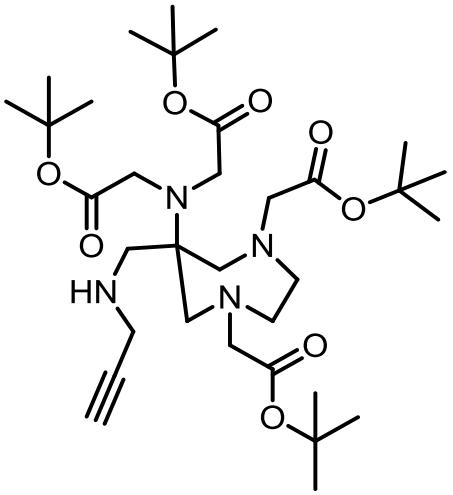

To a crude suspension of 1,4-*bis*(*t*-butoxycarbonylmethyl)-6-[*bis*(*t*-butoxycarbonylmethyl)]amino-6-chloromethylperhydro-1,4-diazepine **(106)** (103 mg, 0.16 mmol, 1 equiv) magnesium sulfate (200 mg) and triethylamine (40 mg, 0.21 mmol, 1.25 equiv) in acetonitrile (5 mL), propargyl amine (13 mg, 0.27 mmol, 1.6 equiv) was added. The solution was then stirred overnight at room temperature under a nitrogen atmosphere. Water (5 mL) was then added to the suspension and extracted with dichloromethane (3 x 5 mL), dried over magnesium sulphate and concentrated *in vacuo*. The residue was then purified using column chromatography (PE/EtOAc, 8/2-6/4) to yield the alkyne as a pale yellow oil **(110)**. Adapted from Gugliotta *et al.* [79] (37 mg, 35%).

δ_H (400 MHz; $CDCl_3$): 1.43 (9H, s, C(C*H*$_3$)$_3$), 1.44 (9H, s, C(C*H*$_3$)$_3$), 1.45 (18H, s, C(C*H*$_3$)$_3$), 2.13 (1H, t, *J* = 2.2 Hz, CC*H*), 2.35-3.60 (16H, m, C*H*$_2$C*H*$_2$, C*H*$_2$CO), 2.89 (2H, d, *J* = 16.2 Hz, C*H*$_2$C), 3.04 (2H, d, *J* = 16.2 Hz, C*H*$_2$C); δ_C (100 MHz $CDCl_3$): 28.1, 28.1, 28.2 (C(*C*H$_3$)$_3$), 38.1 (*C*H$_2$CCH), 48.0, 51.5, 53.2,

56.8, 57.3, 60.3 (CH_2CH_2, CH_2C, CH_2CO, CH_2NH), (CH_2CCH), 80.7, 80.8, 80.8 ($C(CH_3)_3$), 81.0 (CH_2CCH), 169.8, 171.2, 171.3 (C=O); HRMS *m/z* (+ ESI): Found $[MH]^+$, 639.4324 $C_{33}H_{58}N_4O_8$ requires $[MH]^+$, 639.4327.

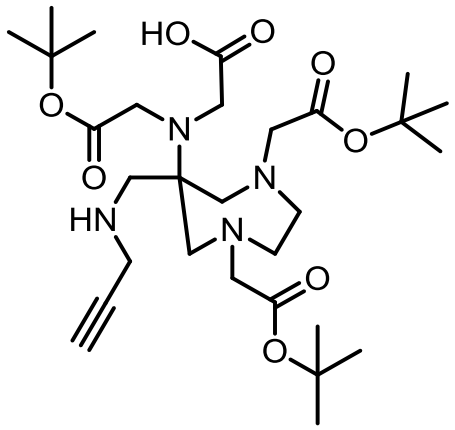

To a crude suspension of 1,4-*bis*(*t*-butoxycarbonylmethyl)-6-[*bis*(*t*-butoxycarbonylmethyl)]amino-6-chloromethylperhydro-1,4-diazepine **(106)** (1.52 g, 2.5 mmol, 1 equiv) magnesium sulfate (1 g) and triethylamine (596 mg, 4.4 mmol, 1.8 equiv) in acetonitrile (50 mL), propargyl amine (324 mg, 5.8 mmol, 2.4 equiv) was added. The solution was then stirred overnight at room temperature under a nitrogen atmosphere. Water (50 mL) was then added to the suspension and extracted with dichloromethane (3 x 50 mL), dried over magnesium sulphate and concentrated *in vacuo*. The residue was then purified using column chromatography (PE/EtOAc, 8/2-1/1) to yield the alkyne as a yellow oil (566 mg, 40%).

δ_H (400 MHz; $CDCl_3$): 1.38 (9H, s, $C(CH_3)_3$), 1.39 (18H, s, $C(CH_3)_3$), 2.12 (1H, t, *J* = 2.5 Hz, CCH), 2.50-2.90 (6H, m, CH_2CH_2, CH_2NH), 2.62 (2H, d, *J* = 13.3 Hz, CH_2C), 2.77 (2H, d, *J* = 13.3 Hz, CH_2C), 3.26 (4H, s, CH_2CO), 3.28 (2H, s, CH_2CO), 3.34 (2H, s, CH_2CO), 3.99 (2H, dd, *J* = 5.5, 2.5 Hz, CH_2CCH), 8.10 (1H, t, *J* = 5.4 Hz, NH); δ_C (100 MHz $CDCl_3$): 28.1, 28.1 ($C(CH_3)_3$), 28.5

(CH_2CCH), 55.8, 59.2, 60.3, 61.0, 61.7, 62.6, 63.5 (CH_2CH_2, CH_2C, CH_2CO, CH_2NH), 70.9 (CH_2CCH), 80.0 (CH_2CCH), 81.2, 81.3 ($C(CH_3)_3$), 170.8, 171.0, 171.5 (*C*=O); HRMS *m/z* (+ ESI): Found $[MH]^+$, 583.3687 $C_{29}H_{51}N_4O_8$ requires $[MH]^+$, 583.3701.

1,4-*Bis*(*t*-butoxycarbonylmethyl)-6-[*bis*(*t*-butoxycarbonylmethyl)]amino-6-(prop-2-yn-1-ylcarbamate)methylperhydro-1,4-diazepine **(114)**.

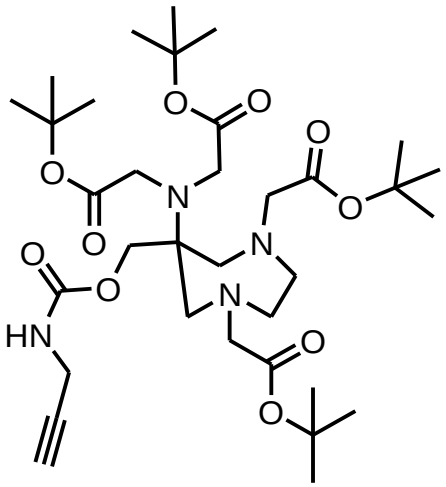

A suspension of 1,4-*bis*(*t*-butoxycarbonylmethyl)-6-[*bis*(*t*-butoxycarbonylmethyl)]amino-6-(prop-2-yn-1-ylamino)methylperhydro-1,4-diazepine **(105)** (4.10 g, 6.8 mmol, 1 equiv), dimethylaminopyridine (2.50 g, 21.8 mmol, 3.2 equiv) and triphosgene (0.81 g, 2.7 mmol, 0.4 equiv) in anhydrous dichloromethane (250 mL) is stirred at room temperature under nitrogen for 10 min. Propargyl amine (0.69 g, 6.8 mmol, 1 equiv) was then added and the suspension was stirred overnight. The reaction was then quenched with ice water (100 mL), and extracted with dichloromethane (3 x 100 mL) before concentration *in vacuo*. The residue was the purified using column

chromatography (PE/EtOAc, 8/2) to yield the product as a sticky pale yellow oil **(114)**. Adapted from Deshmukh *et al.* [133] (1.48 g, 32%).

δ_H (400 MHz; $CDCl_3$): 1.44 (36H, s, C(C*H*$_3$)$_3$), 2.23 (1H, dt, *J* = 8.3, 2.5 Hz, CC*H*), 2.60-2.85 (4H, m, C*H*$_2$C*H*$_2$), 2.73 (2H, d, *J* = 14.4 Hz, C*H*$_2$C), 3.09 (2H, d, *J* = 14.4 Hz, C*H*$_2$C), 3.26 (2H, s, C*H*$_2$) 3.27 (2H, s, C*H*$_2$), 3.69 (4H, s, C*H*$_2$), 3.95 (2H, dd, *J* = 5.4, 2.5 Hz, C*H*$_2$CCH), 4.16 (2H, s, C*H*$_2$), 5.14 (1H, t, *J* = 5.4 Hz, N*H*); δ_C (100 MHz $CDCl_3$): 28.1, 28.2 (C(*C*H$_3$)$_3$), 30.8 (*C*H$_2$CCH), 51.4, 53.4, 58.8, 59.0, 59.3, 62.1, 62.3, 63.2, 68.1 (*C*H$_2$*C*H$_2$, CH$_2$C, *C*H$_2$CO, *C*H$_2$NH), 71.5 (CH$_2$C*C*H), 79.7 (CH$_2$*C*CH), 80.5, 80.8 (*C*(CH$_3$)$_3$), 155.8, 170.8, 172.7 (*C*=O); HRMS *m/z* (+ ESI): Found $[MH]^+$, 683.4229 $C_{34}H_{58}N_4O_{10}$ requires $[MH]^+$, 683.4226.

1,4-*Bis*(carboxymethyl)-6-[*bis*(carboxymethyl)]amino-6-(prop-2-yn-1-yl carbamate)methyl perhydro-1,4-diazepine .4TFA **(115)**.

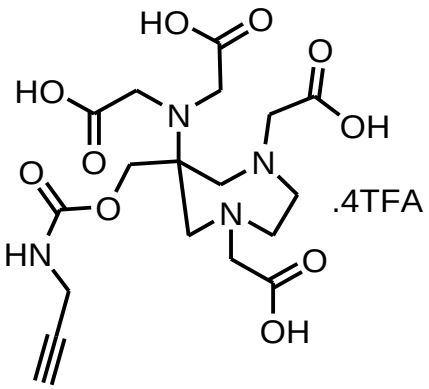

A solution of 1,4-*bis*(*t*-butoxycarbonylmethyl)-6-[*bis*(*t*-butoxycarbonylmethyl)] amino-6-(prop-2-yn-1-ylcarbamate)methylperhydro-1,4-diazepine **(114)** (1.42 g, 2.1 mmol, equiv) in trifluoroacetic acid (20 mL) was stirred overnight at room temperature under a nitrogen atmosphere, before concentration *in vacuo*, to

yield the trifluoroacetic acid salt as a sticky brown oil **(115)**. Adapted from Green *et al.* [122] (0.94 g, 98%).

ν_{max} ($CHCl_3$)/cm^{-1},3279 (OH), 2997 (CH), 1760 (C=O); δ_H (400 MHz; MeOD): 2.57 (1H, dt, *J* = 18.0, 2.1 Hz, CC*H*), 3.35-4.19 (20H, m, CH_2); δ_C (100 MHz MeOD): 29.7 (*C*H_2CCH), 50.2, 51.5, 53.2, 53.3, 57.6, 58.1, 61.8, 65.8, 70.5 (*C*H_2*C*H_2, CH_2C, *C*H_2CO, *C*H_2NH), 70.9 (CH_2C*C*H), 79.5 (CH_2*C*CH), 169.5, 175.5, 175.7 (*C*=O); HRMS *m/z* (+ ESI): Found $[MH]^+$, 459.1716 $C_{18}H_{26}N_4O_{10}$ requires $[MH]^+$, 459.1722.

1,4-*Bis*(carboxymethyl)-6-[*bis*(carboxymethyl)]amino-6-(prop-2-yn-1-yl carbamate)methyl perhydro-1,4-diazepine europium **(CA4-Eu)**.

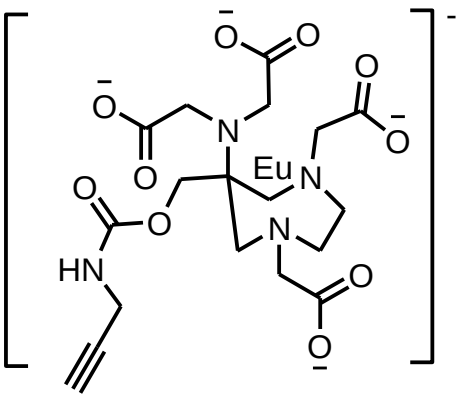

To a solution of 1,4-*bis*(carboxymethyl)-6-[*bis*(carboxymethyl)]amino-6-(prop-2-yn-1-yl carbamate)methyl perhydro-1,4-diazepine .4TFA **(115)** (274 mg, 0.3 mmol, 1 equiv) in water (2 mL), europium (III) chloride hexahydrate (124 mg, 0.3 mmol, 1 equiv) was added. The pH was then adjusted to pH 9 using potassium hydroxide (1 M), and the reaction was stirred for 2 h before freeze drying. The residue was then centrifuged and the supernatant, was

concentrated *in vacuo* to yield the final product as a pale brown solid **(CA4-Eu)**. Adapted from Viguier *et al.* [74] (166 mg, 90%).

ν_{max} ($CHCl_3$)/cm^{-1}, 3436 (OH), 2929 (CH), 1685, 1606 (C=O); HRMS *m/z* (+ ESI): Found $[MH]^-$, 607.0550 $C_{18}H_{22}N_4O_{10}{}^{152}Eu$ requires $[MH]^-$, 607.0554.

1,4-*Bis*(carboxymethyl)-6-[*bis*(carboxymethyl)]amino-6-(prop-2-yn-1-yl carbamate)methyl perhydro-1,4-diazepine gadolinium **(CA4)**.

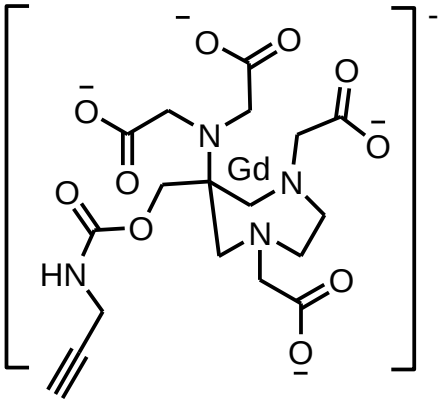

To a solution of 1,4-*bis*(carboxymethyl)-6-[*bis*(carboxymethyl)]amino-6-(prop-2-yn-1-yl carbamate)methyl perhydro-1,4-diazepine .4TFA **(115)** (274 mg, 0.3 mmol, 1 equiv) in water (2 mL), gadolinium (III) chloride hexahydrate (126 mg, 0.3 mmol, 1 equiv) was added. The pH was then adjusted to pH 9 using potassium hydroxide (1 M), and the reaction was stirred for 2 h before freeze drying. The residue was then centrifuged and the supernatant was concentrated *in vacuo* to yield the final product as a pale brown solid **(CA4)**. Adapted from Viguier *et al.* [74] (182 mg, 99%).

ν_{max} ($CHCl_3$)/cm^{-1}, 3416 (OH), 2977 (CH), 1683, 1608 (C=O); HRMS *m/z* (+ ESI): Found $[MH]^-$, 612.0591 $C_{18}H_{22}N_4O_{10}{}^{158}Gd$ requires $[MH]^-$, 612.0582.

2-Nitroimidazole **(117)**.

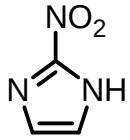

A solution of 2-aminoimidazole hemisulfate **(116)** (418 mg, 3.1 mmol, 1 equiv) in 40 % fluoroboric acid (2.5 mL) and distilled water (4.1 mL) was stirred at -10 °C. Sodium nitrite (1.09 g, 15.8 mmol, 5 equiv) in distilled water (2.5 mL) was then added dropwise below the surface and stirred for 30 min. To solution of copper sulfate pentahydrate (2.18 g, 8.7 mmol, 3 equiv) and 4-dimethylamino pyridine (252 mg, 2.1 mmol, 0.7 equiv) in water (33.6 mL) the 2-aminoimidazole solution was added dropwise, followed by a second addition of sodium nitrite (1.09 g, 15.8 mmol, 5 equiv) before being brought to ambient temperature and stirred for 2 h. The pH was then adjusted to pH 2 using hydrochloric acid, and the product extracted into ethyl acetate (6 x 40 mL). The ethyl acetate layer was dried over magnesium sulfate, filtered and concentrated to produce a yellow solid. The solid was then recrystallised in ethanol to yield 2-nitroimidazole as yellow crystals **(117)**. Repeated from Takuma *et al*. [134] (249 mg, 70 %).

mp, 284-286 °C (Lit: 287-288 °C[172]); ν_{max} ($CHCl_3$)/cm^{-1}, 3420 (NH), 1538 (NO_2); δ_H (400 MHz; D_2O): 7.3 (2H, s, C*H*); HRMS *m/z* (+ EI): Found $[MH]^+$, 113.0215, $C_3H_3N_3O_2$ requires $[MH]^+$, 113.0220

1-(2-Nitro-imidazol-1-yl)-propan-1-ol **(119b)**.

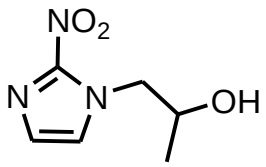

A suspension of 2-nitroimidzole **(117)** (50 mg, 0.44 mmol, 1 equiv), caesium carbonate (161 mg, 0.48 mmol, 1.1 equiv), propene oxide (33.6 mg, 0.58 mmol, 1.3 equiv) in acetonitrile (7 mL) and water (3 mL) was placed in a sealed tube. The sealed tube was heated in a microwave at 100 °C for 10 min, left to cool for 5 min, before being heated at 100 °C for a further 10 min. The reaction was then purified using column chromatography (DCM/MeOH, 9/1) to yield the product as a yellow solid **(119b)**. Adapted from Kim *et al.* [175] (20 mg, 26%).

ν_{max} ($CHCl_3$)/cm^{-1}, 3162 (OH), 2973 (CH), 1520, 1345 (NO_2); δ_H (400 MHz; MeOD): 0.94 (1H, d, *J* = 2.4 Hz, O*H*), 1.24 (3H, d, *J* = 6.2 Hz, CH_3), 4.08 (1H, m, C*H*), 4.29 (1H, dd, *J* = 13.8, 8.5 Hz, CH_2), 4.58 (1H, dd, *J* = 13.8, 3.2 Hz, CH_2), 7.14 (1H, d, *J* = 1.1 Hz, C*H*Ar), 7.45 (1H, d, *J* = 1.1 Hz, C*H*Ar); δ_C (100 MHz MeOD): 19.3 (*C*H_3), 56.0 (*C*H_2), 65.8 (*C*H), 126.6 (*C*HAr), 127.7 (*C*HAr).
HRMS *m/z* (+ EI): Found $[MH]^+$, 171.0642, $C_6H_9N_3O_3$ requires $[MH]^+$, 171.0638

1-(2-Nitro-1H-imidazol-1-yl)propan-2-yl methanesulfonate **(121)**.

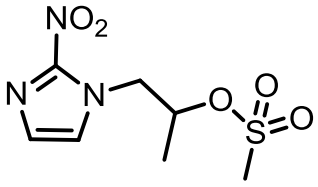

To a solution of 2-(2-nitro-imidazol-1-yl)-propan-1-ol **(119b)** (50 mg, 0.3 mmol, 1 equiv) in anhydrous dichloromethane (5 mL) methanesulfonyl chloride (22 µL, 0.3 mmol, 1 equiv) and diisopropylamine (104 µL, 0.6 mmol, 2 equiv) were

added. The solution was then stirred for 4 hours under a nitrogen atmosphere at room temperature before concentration *in vacuo*. The residue was then purified using column chromatography (DCM/MeOH, 95/5) to yield the primary alcohol as a pale yellow oil **(121)**. Adapted from Zheng *et al.* [131] (6 mg, 8%).

δ_H (400 MHz; MeOD): 1.50 (3H, d, *J* = 6.4 Hz, C*H*$_3$), 2.91 (3H, s, SC*H*$_3$), 4.55 (1H, dd, *J* = 14.5, 9.0 Hz, C*H*$_2$), 4.80 (1H, dd, *J* = 14.5, 2.8 Hz, C*H*$_2$), 5.13 (1H, m, C*H*), 7.15 (1H, d, *J* = 1.2 Hz, C*H*Ar), 7.48 (1H, d, *J* = 1.2 Hz, C*H*Ar).

2-Nitro-1-(2-*p*-toluenesulfonyloxyethyl)-1*H*-imidazole **(122)**.

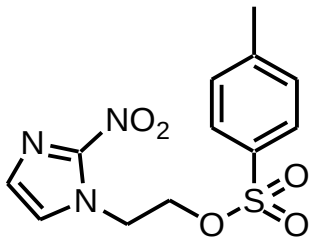

To a solution of 2-nitroimidazole **(117)** (1.00 g, 8.8 mmol, 1 equiv) and triethylamine (5.1 mL, 35.4 mmol, 4 equiv) in dimethylformamide (20 mL), ethylene glycol *bis*-*p*-toluenesulfonate (6.56 g, 17.7 mmol, 2 equiv) was added. The suspension was then stirred under a nitrogen atmosphere at room temperature for 4 days. Water was then added to the reaction before extraction with dichloromethane (3 x 40 mL), the organic layers were then washed with brine (80 mL) before drying over magnesium sulfate and concentration *in vacuo*. The remaining residue was then purified using column chromatography (DCM - MeOH/DCM 0.5/99.5) to yield the product as pale yellow crystals **(122)**. Repeated from Lin *et al.* [114] (2.5 g, 86%).

δ_H (400 MHz; $CDCl_3$): 2.45 (3H, s, C*H*$_3$), 4.39 (2H, t, *J* = 4.8 Hz, NCH$_2$C*H*$_2$), 4.67 (2H, t, *J* = 4.8 Hz, NC*H*$_2$CH$_2$), 7.14 (1H, d, *J* = 1.0 Hz, C*H*Ar $_{imidazole}$), 7.15 (1H, d, *J* = 1.0 Hz, C*H*Ar $_{imidazole}$), 7.30 (2H, dd, *J* = 8.4, 0.5 Hz, C*H*Ar $_{tosyl}$), 7.61 (2H, d, *J* = 8.4 Hz, C*H*Ar $_{tosyl}$); δ_C (100 MHz $CDCl_3$): 21.7 (*C*H$_3$), 49.1 (N*C*H$_2$CH$_2$), 67.2 (NCH$_2$*C*H$_2$), 127.4 (*C*HAr $_{imidazole}$), 127.7 (*C*HAr $_{tosyl}$), 128.5 (*C*HAr $_{imidazole}$), 130.1 (*C*HAr $_{tosyl}$), 131.6 (*C*Ar $_{tosyl}$), 145.8 (*C*Ar $_{tosyl}$); HRMS *m/z* (+ ESI): Found $[MH]^+$, 312.0639 $C_{12}H_{13}N_3O_5S$ requires $[MH]^+$, 312.0649.

1-(2-Azidoethyl)-2-nitro-*1H*-imidazole **(TV1)**.

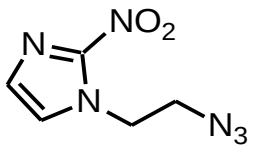

To a solution of 2-nitro-1-(2-*p*-toluenesulfonyloxyethyl)-1*H*-imidazole **(122)** (170 mg, 0.54 mmol, 1 equiv) in dimethylformamide (4 mL), sodium azide (134 mg, 2.18 mmol, 4 equiv) was added. The suspension was then stirred overnight at room temperature under a nitrogen atmosphere, before drying under a stream of nitrogen. The residue was then filtered through a pad of silica (MeOH/,DCM 2/98) and concentrated *in vacuo* to yield the product as a yellow oil **(TV1)**. Repeated from Lin *et al.* [114] (90 mg, 96%).

ν_{max} ($CHCl_3$)/cm^{-1}, 3090 (CHAr), 2094 (N_3), 1537, 1356 (NO_2); δ_H (400 MHz; $CDCl_3$): 3.80 (2H, t, *J* = 5.5 Hz, CH$_2$C*H*$_2$N$_3$), 4.56 (2H, t, *J* = 5.5 Hz, C*H*$_2$CH$_2$N$_3$), 7.16 (11H, d, *J* = 1.1 Hz, C*H*Ar), 7.19 (1H, d, *J* = 1.1 Hz, C*H*Ar); δ_C (100 MHz $CDCl_3$): 49.2 (*C*H$_2$CH$_2$N$_3$), 50.8 (CH$_2$*C*H$_2$N$_3$), 126.9 (*C*HAr), 128.6 (*C*HAr).

tert-Butyl-dimethy-(2-nitro-benzyloxy)-silane **(124)**.

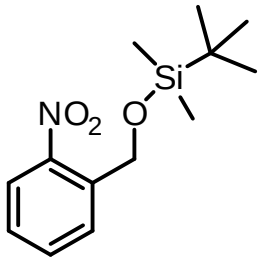

To a stirred solution of 2-nitrobenzyl alcohol **(123)** (153 mg, 1 mmol, 1 equiv) and *tert*-butyl-chloro-dimethyl-silane (180 mg, 1.2 mmol, 1.2 equiv) in dimethylformamide (7 mL), imidazole (170 mg, 2.5 mmol, 2.5 equiv) in dimethylformamide (0.5 mL) was added dropwise. The reaction was then stirred for 2 h at room temperature under a nitrogen atmosphere, before being concentrated *in vacuo*. The remaining residue was then purified with column chromatography (DCM) to yield the protected alcohol as a yellow oil **(124)**. Adapted from Corey *et al.* [176] (256 mg, quantitative).

ν_{max} ($CHCl_3$)/cm^{-1}, 1530, 1342 (NO_2); δ_H (400 MHz; $CDCl_3$): 0.15 (6H, s, CH_3), 0.97 (9H, s, C(CH_3)$_3$), 5.12 (2H, s, CH_2), 7.40 (1H, dd, *J* = 7.8, 1.1 Hz, C*H*Ar), 7.66 (1H, dd, *J* = 7.8, 1.1 Hz, C*H*Ar), 7.91 (1H, dd, *J* = 7.8, 1.1 Hz, C*H*Ar), 8.08 (1H, dd, *J* = 7.8, 1.1 Hz C*H*Ar); δ_C (100 MHz $CDCl_3$): -5.3 (*C*H_3), 18.5 (C(*C*H_3)$_3$), 26.0 (*C*(CH_3)$_3$), 62.2 (*C*H_2), 124.6, 127.5, 128.1. 133.9 (*C*HAr), 138.4, 146.6 (*C*Ar); HRMS *m/z* (+ ESI): Found $[MNa]^+$, 290.1177 $C_{13}H_{21}N_1O_3SiNa$ requires $[MNa]^+$, 290.1183.

1-(4-Nitrophenyl)prop-2-en-ol **(129)**.

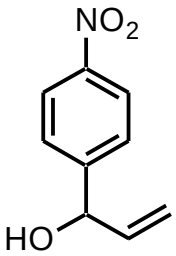

To a solution of 4-nitrobenzaldehyde **(127)** (855 mg, 5.6 mmol, 1 equiv) in anhydrous THF (20 mL), vinylmagnesium bromide (1 M in THF, 6.8 mL, 1.2 equiv) was added dropwise at -78 °C. The solution was then stirred at -50 °C for 40 min under a nitrogen atmosphere before quenching with saturated ammonium chloride (10 mL). Ethyl acetate (2 x 60 mL) was then added before the organic layer was washed with brine (100 mL), dried over magnesium sulfate and concentrated *in vacuo*. The residue was then purified using column chromatography (PE/EtOAc, 8/2) to yield the product as a yellow oil **(129)**. Repeated from Jiang *et al.* [116] (775 mg, 76%).

ν_{max} ($CHCl_3$)/cm^{-1}, 3300 (OH), 1519, 1347 (NO_2); δ_H (400 MHz; $CDCl_3$): 3.16 (1H, bs, O*H*), 5.15-5.38 (3H, m, C*H*CH_2), 5.88-5.99 (1H, m, C*H*OH), 7.48 (2H, d, *J* = 8.9 Hz, C*H*Ar_b), 8.09 (2H, d, *J* = 8.9 Hz, C*H*Ar_a); δ_C (100 MHz $CDCl_3$): 74.4 (*C*HOH), 116.6 (*C*H_2CH), 123.6 (CH_2*C*H), 127.0 (*C*HAr_b), 139.0 (*C*HAr_a), 147.0 (*C*Ar), 150.0 (*C*NO_2Ar); HRMS *m/z* (+ ESI): Found $[MNa]^+$, 202.0468 $C_9H_9NNaO_3$ requires $[MNa]^+$, 202.0475.

1-Methoxymethoxy-1-(4-nitrophenyl)-2-propene **(131)**.

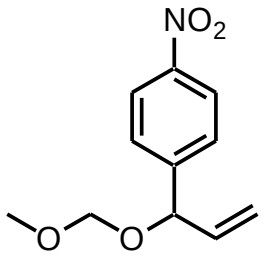

A stirred solution of 1-(4-nitrophenyl)prop-2-en-ol **(129)** (200 mg, 1.1 mmol, 1 equiv) in anhydrous dichloromethane (4 mL) was cooled to 0 °C, before addition of diisopropylethylamine (1.1 mL, 6.3 mmol, 6 equiv). Chloromethyl methyl ether (0.5 mL, 6.6 mmol, 6 equiv) was then added dropwise and the reaction was allowed to reach room temperature and stirred for 24 h under a nitrogen atmosphere. The reaction was then quenched with saturated sodium bicarbonate, before concentration *in vacuo*. The residue was then taken up in diethyl ether (3 x 20 mL), washed with brine (20 mL), dried over magnesium sulfate and concentrated *in vacuo* to yield the product as a yellow oil **(131)**. Repeated from Jiang *et al.* [116] (249 mg, quant).

ν_{max} ($CHCl_3$)/cm^{-1}, 2932 (CH), 1522, 1347 (NO_2); δ_H (400 MHz; $CDCl_3$): 3.35 (3H, s, C*H*$_3$), 4.61 (1H, d, *J* = 6.8 Hz, C*H*$_2$OCH$_3$), 4.77 (1H, d, *J* = 6.8 Hz, C*H*$_2$OCH$_3$), 5.16 (1H, d, *J* = 7.2 Hz, C*H*O), 5.32 (2H, m, CHC*H*$_2$), 5.94 (1H, m, C*H*CH$_2$), 7.53 (2H, d, *J* = 8.8 Hz, C*H*Ar$_b$), 8.18 (2H, d, *J* = 8.8 Hz, C*H*Ar$_a$); δ_C (100 MHz $CDCl_3$): 55.6 (*C*H$_3$), 77.5 (*C*HO), 93.9 (O*C*H$_2$O), 118.2 (*C*H$_2$CH), 123.7 (CH$_2$*C*H), 127.6 (*C*HAr$_b$), 136.9 (*C*HAr$_a$), 147.4 (*C*Ar), 148.2 (*C*NO$_2$Ar); HRMS *m/z* (+ ESI): Found $[MNa]^+$, 246.0727 $C_{11}H_{13}NNaO_4$ requires $[MNa]^+$, 246.0737.

3-Methoxymethoxy-3-(4-nitrophenyl)propan-1-ol **(133)**.

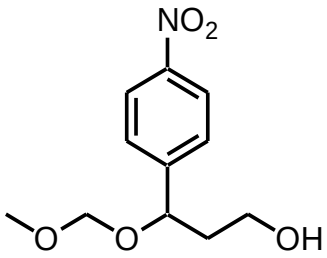

A solution of 1-methoxymethoxy-1-(4-nitrophenyl)-2-propene **(131)** (3.70 g, 17 mmol, 1 equiv) in anhydrous tetrahydrofuran (100 mL) was cooled to 0 °C, borane (1M in THF, 17 mL, 1.0 equiv) was then added dropwise, and then stirred overnight at 0 °C under a nitrogen atmosphere. Sodium hydroxide (3M, 17 mL) was then added followed by dropwise addition of hydrogen peroxide (30%, 17 mL), before stirring for 30 min at 0 °C. The reaction was then quenched with a saturated sodium bisulfite solution (25 mL) and ethyl acetate (50 mL) was added. The organic layer was then washed with sodium hydrogen carbonate (50 mL) and brine (50 mL), before concentration *in vacuo*. The residue was then purified using column chromatography (PE/EtOAc, 2/1-1/1) to yield the primary alcohol as a yellow oil **(133)**. Repeated from Jiang *et al.* [116] (2.21 g, 55%).

ν_{max} ($CHCl_3$)/cm^{-1}, 3416 (OH), 1520, 1347 (NO_2);δ_H (400 MHz; $CDCl_3$): 1.92-1.96 (1H, m, C*H*$_2$CH$_2$OH), 1.98-2.08 (1H, m, C*H*$_2$CH$_2$OH), 2.18 (1H, bs, O*H*), 3.38 (3H, s, C*H*$_3$), 3.71-3.76 (1H, m, CH$_2$C*H*$_2$OH), 3.80-3.86 (1H, m, CH$_2$C*H*$_2$OH), 4.51 (1H, d, *J* = 6.8 Hz, C*H*$_2$OCH$_3$), 4.61 (1H, d, *J* = 6.8 Hz, C*H*$_2$OCH$_3$), 4.95 (1H, dd, *J* = 8.9, 4.4 Hz, C*H*OMOM), 7.51 (2H, d, *J* = 8.8 Hz, C*H*Ar$_b$), 8.21 (2H, d, *J* = 8.8 Hz, C*H*Ar$_a$); δ_C (100 MHz $CDCl_3$): 40.5 (*C*H$_2$CH$_2$OH), 55.9 (*C*H$_3$), 59.6 (CH$_2$*C*H$_2$OH), 75.7 (*C*HOMOM), 94.9 (O*C*H$_2$O),

123.8 (*C*HAr$_b$), 127.4 (*C*HAr$_a$), 147.5 (*C*Ar), 149.5 (*C*NO$_2$Ar); HRMS *m/z* (+ ESI): Found [MNa]$^+$, 264.0835 $C_{11}H_{15}NNaO_5$ requires [MNa]$^+$, 264.0842.

1-Azido-3-methoxymethyl-3-(4-nitrophenyl) propane **(135)**.

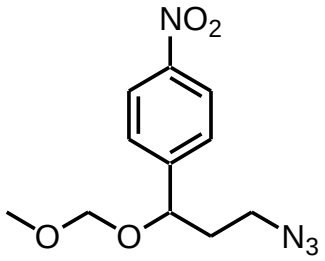

To a solution of 3-methoxymethoxy-3-(4-nitrophenyl)propan-1-ol **(133)** (1.00 g, 4.1 mmol, 1 equiv) in tetrahydrofuran (30 mL), diphenyl phosphorylazide (2.28 g, 8.2 mmol, 2 equiv) and 1,8-diazabicycloundec-7-ene (1.89 g, 12.3 mmol, 3 equiv) were added. The solution was then stirred overnight at room temperature under a nitrogen atmosphere. Sodium azide (1.35 g, 20.5 mmol, 5 equiv) and 15-crown-5 (80 mg, 0.4 mmol, 0.1 equiv) were then added to form a suspension that was refluxed for 4 h. The suspension was then filtered, and the filtrate concentrated *in vacuo*. The remaining residue was then purified using column chromatography (PE/EtOAc, 8/2) to yield the azide as a pale yellow oil **(135)**. Adapted from Liu *et al.* [143] (1.07 g, 97%).

ν_{max} ($CHCl_3$)/cm^{-1}, 2099 (N_3), 1519, 1345 (NO_2); δ_H (400 MHz; $CDCl_3$): 1.83-1.94 (1H, m, C*H*$_2$CH$_2$N$_3$), 1.99-2.10 (1H, m, C*H*$_2$CH$_2$N$_3$), 3.35 (3H, s, C*H*$_3$), 3.36-3.42 (1H, m, CH$_2$C*H*$_2$N$_3$), 3.45-3.53 (1H, m, CH$_2$C*H*$_2$N$_3$), 4.50 (1H, d, *J* = 7.0 Hz, C*H*$_2$OCH$_3$), 4.59 (1H, d, *J* = 7.0 Hz, C*H*$_2$OCH$_3$), 4.82 (1H, dd, *J* = 8.9, 4.5 Hz, C*H*OMOM), 7.50 (2H, d, *J* = 8.7 Hz, C*H*Ar$_b$), 8.21 (2H, d, *J* = 8.7 Hz, C*H*Ar$_a$); δ_C (100 MHz $CDCl_3$): 37.0 (CH$_2$*C*H$_2$N$_3$), 47.7 (*C*H$_2$CH$_2$N$_3$), 56.0 (*C*H$_3$), 74.3 (*C*HOMOM), 94.8 (O*C*H$_2$O), 123.9 (*C*HAr$_b$), 127.4 (*C*HAr$_a$), 147.6 (*C*Ar),

149.0 (*C*NO_2Ar); HRMS *m/z* (+ ESI): Found $[MNa]^+$, 289.0908 $C_{11}H_{14}N_4NaO_4$ requires $[MNa]^+$, 289.0907.

3-Azido-1-(4-nitrophenyl)propan-1-ol **(137)**.

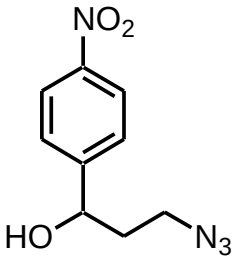

To an emulsion of 1-azido-3-methoxymethyl-3-(4-nitrophenyl) propane **(135)** (1 g, 3.8 mmol, 1 equiv) in tetrahydrofuran (3 mL) and water (5 mL), hydrochloric acid (5 mL) was added. The emulsion was then stirred at 50 °C for 8 h, before extraction with ethyl acetate (2 x 20 mL). The organic layer was then dried over magnesium sulphate and concentrated *in vacuo*. The residue was then purified using column chromatography (PE/EtOAc, 8/2) to yield the alcohol as a pale yellow oil **(137)**. Adapted from Meyers *et al.* [177] (572 mg, 69%).

ν_{max} ($CHCl_3$)/cm^{-1}, 3399 (OH), 2100 (N_3), 1518, 1348 (NO_2); δ_H (400 MHz; $CDCl_3$): 1.88-2.04 (2H, m, C*H*$_2$CH_2N_3), 2.52 (1H, bs, O*H*), 3.40-3.62 (2H, m, CH_2C*H*$_2N_3$), 4.98 (1H, dd, *J* = 8.0, 4.8 Hz, C*H*OH), 7.53 (2H, d, *J* = 8.6 Hz, C*H*Ar$_b$), 8.21 (2H, d, *J* = 8.6 Hz, C*H*Ar$_a$); δ_C (100 MHz $CDCl_3$): 37.9 (CH_2*C*H_2N_3), 48.2 (*C*H_2CH_2N_3), 70.9 (*C*HOH), 123.9 (*C*HAr$_b$), 126.5 (*C*HAr$_a$), 147.4 (*C*Ar), 151.2 (*C*NO_2Ar); HRMS *m/z* (+ ESI): Found $[MNa]^+$, 245.0645 $C_9H_{10}N_4NaO_3$ requires $[MNa]^+$, 245.0644.

1-(3-Azido-1-chloropropyl)-4-nitrobenzene **(TV3)**.

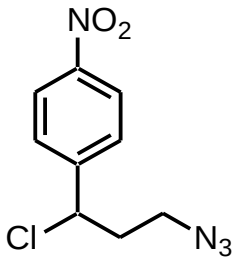

A solution of 3-azido-1-(4-nitrophenyl)propan-1-ol **(137)** (100 mg, 0.45 mmol, 1 equiv) in anhydrous dichloromethane (5 mL) was cooled to 0 °C under a nitrogen atmosphere. Thionyl chloride (5 mL) was then added dropwise and the solution was left to stir at room temperature for 6 h. The reaction was then concentrated *in vacuo* and the residue was purified using column chromatography (PE/EtOAc, 8/2) to yield the product as a pale yellow oil **(TV3)**. Adapted from Nakamura *et al.* [178] (65 mg, 60%).

ν_{max} ($CHCl_3$)/cm^{-1}, 3112, 3079 (CHAr), 2100 (N_3), 1520, 1347 (NO_2); δ_H (400 MHz; $CDCl_3$): 2.13-2.26 (1H, m, C*H*$_2$CH$_2$N$_3$), 2.26-2.37 (1H, m, C*H*$_2$CH$_2$N$_3$), 3.42-3.51 (1H, m, CH$_2$C*H*$_2$N$_3$), 3.57-3.66 (1H, m, CH$_2$C*H*$_2$N$_3$), 5.08 (1H, dd, *J* = 9.4, 5.1 Hz, C*H*Cl), 7.58 (2H, d, *J* = 8.8 Hz, C*H*Ar$_b$), 8.24 (2H, d, *J* = 8.8 Hz, C*H*Ar$_a$); δ_C (100 MHz $CDCl_3$): 38.9 (*C*H$_2$CH$_2$N$_3$), 48.4 (CH$_2$*C*H$_2$N$_3$), 58.4 (*C*H), 124.1 (*C*HAr$_b$), 127.9 (*C*HAr$_a$), 147.7 (*C*Ar), 147.9 (*C*NO$_2$Ar); HRMS *m/z* (+ ESI): Found $[MNa]^+$, 263.0303 $C_9H_9ClN_4NaO_2$ requires $[MNa]^+$, 263.0306.

1-(2-Nitrophenyl)prop-2-en-1-ol **(130)**.

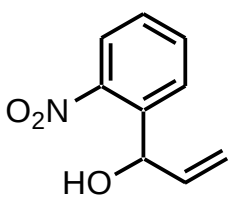

A solution of 2-nitrobenzaldehyde **(128)** (5.00 g, 33 mmol, 1 equiv) in tetrahydrofuran (20 mL) was cooled to 0 °C before dropwise addition of vinyl magnesium bromide (1 M in THF, 33 mL, 1 equiv). The solution was then stirred at room temperature under a nitrogen atmosphere for 2 h before quenching with saturated ammonium chloride (50 mL). Ethyl acetate (50 mL) was then added and the reaction was washed with saturated sodium bicarbonate (50 mL) and brine (50 mL) before concentration *in vacuo.* The residue was then purified using column chromatography (PE/EtOAc, 9/1), to yield the product as a yellow oil **(130)**. Adapted from Jiang *et al.* [116] (1.54 g, 26%).

ν_{max} ($CHCl_3$)/cm^{-1}, 3406 (OH), 1525, 1349 (NO_2); δ_H (400 MHz; $CDCl_3$): 1.63 (1H, bs, O*H*), 5.27 (1H, dt, *J* = 10.4, 1.4 Hz CHCH_{2y}), 5.42 (1H, dt, *J* = 17.3, 1.4 Hz CHCH_{2z}), 5.80 (1H, dt, *J* = 5.2, 1.4 Hz, C*H*OH), 6.08 (1H, ddd, *J* = 17.3, 10.4, 5.2 Hz C*H*CH_2), 7.45 (1H, ddd, *J* = 8.2, 7.7, 1.5 Hz, C*H*Ar_c), 7.64 (1H, td, *J* = 7.7, 1.2 Hz, C*H*Ar_b), 7.77 (1H, dd, *J* = 7.7, 1.5 Hz, C*H*Ar_a), 7.92 (1H, dd, *J* = 8.2, 1.2 Hz, C*H*Ar_d); δ_C (100 MHz $CDCl_3$): 69.9 (*C*HOH), 116.0 (*C*H_2CH), 124.4 (*C*HAr_d), 128.4 (*C*HAr_a), 128.6 (*C*HAr_c), 133.6 (*C*HAr_b), 137.7 (*C*Ar) 138.1 (CH_2*C*H), 148.0 (*C*NO_2Ar).

1-[1-(Methoxymethoxy)prop-2-en-1-yl]-2-nitrobenzene **(132)**.

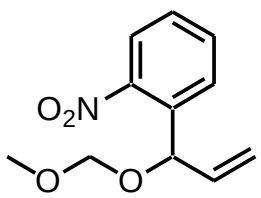

A solution of 1-(2-nitrophenyl)prop-2-en-1-ol **(130)** (3.89 g, 21 mmol, 1 equiv) in anhydrous dichloromethane (50 mL) was cooled to 0 °C before dropwise addition of diisopropylamine (11.0 mL, 63 mmol, 3 equiv). Chloromethyl methyl ether (5.0 mL, 66 mmol, 3.1 equiv) was then added dropwise and the reaction was allowed to reach room temperature and stirred for 24 h under a nitrogen atmosphere. The reaction was then quenched with saturated sodium bicarbonate, before concentration *in vacuo*. The residue was then taken up in diethyl ether (3 x 20 mL), washed with brine (20 mL), dried over magnesium sulfate and concentrated *in vacuo*. The residue was then purified using column chromatography (PE/EtOAc, 8/2), to yield the product as a yellow oil **(132)**. Adapted from Jiang *et al.* [116] (3.00 g, 62%).

ν_{max} ($CHCl_3$)/cm^{-1}, 3083 (CHAr), 1528, 1355 (NO_2); δ_H (400 MHz; $CDCl_3$): 3.29 (3H, s, CH_3), 4.57 (1H, d, *J* = 6.6 Hz, CH_2O), 4.70 (1H, d, *J* = 6.6 Hz, CH_2O), 5.21 (1H, dt, *J* = 10.4, 1.4 Hz, CHCH_{2y}), 5.34 (1H, dt, *J* = 17.2, 1.4, Hz, CHCH_{2z}), 5.75 (1H, d, *J* = 6.1 Hz, C*H*O), 5.94 (1H, ddd, *J* = 17.1, 10.3, 6.1 Hz, C*H*CH_2), 7.40 (1H, ddd, *J* = 7.9, 7.7, 1.4 Hz, C*H*Ar_b), 7.61 (1H, ddd, *J* = 8.0, 7.9, 1.4 Hz, C*H*Ar_c), 7.75 (1H, dd, *J* = 7.7, 1.4 Hz, C*H*Ar_a), 7.86 (1H, dd, *J* = 8.0, 1.4 Hz, C*H*Ar_d); δ_C (100 MHz $CDCl_3$): 55.7 (*C*H_3), 73.3 (*C*HO), 94.5 (O*C*H_2O), 117.2 (*C*H_2CH), 124.2 (*C*HAr_d), 128.3 (*C*HAr_a), 128.7 (*C*HAr_c), 133.2 (*C*HAr_b), 136.2 (*C*Ar), 136.5 (CH_2*C*H), 148.4 (*C*NO_2Ar); HRMS *m/z* (+ ESI): Found $[MNa]^+$, 246.0740 $C_{11}H_{13}NNaO_4$ requires $[MNa]^+$, 246.0737.

3-(2-Nitrophenyl)-3-(methoxymethoxy) propan-1-ol **(134)**.

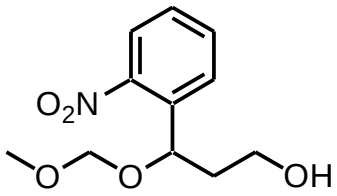

A solution of 1-[1-(methoxymethoxy)prop-2-en-1-yl]-2,4-dinitrobenzene **(132)** (1.83 g, mmol, 1 equiv) in anhydrous tetrahydrofuran (50 mL) was cooled to 0 °C, borane (1M in THF, 7.4 mL, equiv) was then added dropwise, and stirred overnight at 0 °C under a nitrogen atmosphere. Sodium hydroxide (3M, 7.5 mL) was then added followed by dropwise addition of hydrogen peroxide (30%, 7.5 mL), before stirring for 30 min at 0 °C. The reaction was then quenched with a saturated sodium bisulfite solution (20 mL) and ethyl acetate (50 mL) was added. The organic layer was then washed with sodium hydrogen carbonate (50 mL) and brine (50 mL), before concentration *in vacuo*. The residue was then purified using column chromatography (PE/EtOAc, 7/3) to yield the primary alcohol as a brown oil **(134)**. Adapted from Jiang *et al.* [116] (1.10 g, 56%).

ν_{max} ($CHCl_3$)/cm^{-1}, 3425 (OH), 1526, 1346 (NO_2); δ_H (400 MHz; $CDCl_3$): 1.85-2.08 (2H, m, C*H*$_2$CH$_2$OH), 3.21 (3H, s, C*H*$_3$), 3.71-3.76 (2H, m, CH$_2$C*H*$_2$OH), 4.36 (1H, d, *J* = 6.7 Hz, C*H*$_2$OCH$_3$), 4.47 (1H, d, *J* = 6.7 Hz, C*H*$_2$OCH$_3$), 5.28 (1H, dd, *J* = 9.1, 3.4 Hz, C*H*OMOM), 7.33 (1H, ddd, *J* = 8.2, 7.5, 1.2 Hz, C*H*Ar$_b$), 7.56 (1H, ddd, *J* = 8.0, 7.5, 1.3 Hz, C*H*Ar$_c$), 7.67 (1H, dd, *J* = 8.2, 1.3 Hz, C*H*Ar$_a$), 7.80 (1H, dd, *J* = 8.0, 1.2 Hz, C*H*Ar$_d$); δ_C (100 MHz $CDCl_3$): 40.1 (*C*H$_2$CH$_2$OH), 55.8 (*C*H$_3$), 59.8 (CH$_2$*C*H$_2$OH), 71.9 (*C*HOMOM), 95.2 (O*C*H$_2$O), 124.3 (*C*HAr$_d$), 128.2 (*C*HAr$_a$), 128.5 (*C*HAr$_c$), 133.4 (*C*HAr$_b$), 138.0 (*C*Ar),

148.2 (*C*NO_2Ar); HRMS *m/z* (+ ESI): Found $[MNa]^+$, 264.0843 $C_{11}H_{15}NNaO_5$ requires $[MNa]^+$, 264.0842.

1-[Azido-1-(methoxymethoxy)propyl]-2-nitrobenzene **(136)**.

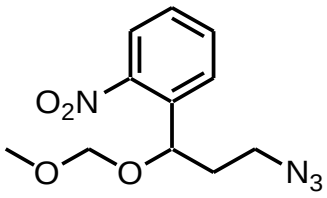

To a solution of 3-(2-nitrophenyl)-3-(methoxymethoxy) propan-1-ol **(134)** (200 mg, 1 equiv) in tetrahydrofuran (30 mL), diphenyl phosphorylazide (456 mg, 2 equiv) and 1,8-diazabicycloundec-7-ene (378 mg, 3 equiv) were added. The solution was then stirred overnight at room temperature under a nitrogen atmosphere. Sodium azide (270 mg, 5 equiv) and 15-crown-5 (16 mg, 0.1 equiv) were then added to form a suspension that was refluxed for 4 h. The suspension was then filtered, and the filtrate concentrated *in vacuo*. The remaining residue was then purified using column chromatography (PE/EtOAc, 8/2) to yield the azide as a pale yellow oil (taken on with some slight impurities) **(136)**. Adapted from Liu *et al.* [143]

ν_{max} ($CHCl_3$)/cm^{-1}, 2098 (N_3), 1526, 1345 (NO_2); δ_H (400 MHz; $CDCl_3$): 1.96-2.06 (1H, m, C*H*$_2$$CH_2N_3$), 2.14-2.24 (1H, m, C*H*$_2$$CH_2N_3$), 3.33 (3H, s, C*H*$_3$), 3.51-3.57 (2H, m, CH_2C*H*$_2$$N_3$), 4.47 (1H, d, *J* = 6.8 Hz, C*H*$_2$$OCH_3$), 4.57 (1H, d, *J* = 6.8 Hz, C*H*$_2$$OCH_3$), 5.32 (1H, dd, *J* = 9.2, 3.1 Hz, C*H*OMOM), 7.44 (1H, ddd, *J* = 8.2, 7.4, 1.4 Hz, C*H*Ar_b), 7.65 (1H, ddd, *J* = 8.0, 7.4, 1.3 Hz, C*H*Ar_c), 7.75 (1H, dd, *J* = 8.2, 1.3 Hz, C*H*Ar_a), 7.95 (1H, dd, *J* = 8.0, 1.4 Hz, C*H*Ar_d).

3-Azido-1-(2-nitrophenyl)propan-1-ol **(138)**.

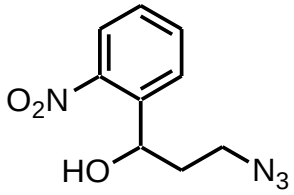

To an emulsion of crude 1-azido-3-methoxymethyl-3-(4-nitrophenyl) propane **(136)** (300 mg, 1 equiv) in tetrahydrofuran (1 mL) and water (2 mL), hydrochloric acid (2 mL) was added. The emulsion was then stirred at 50 °C for 8 h, before extraction with ethyl acetate (2 x 20 mL). The organic layer was then dried over magnesium sulphate and concentrated *in vacuo*. The residue was then purified using column chromatography (PE/EtOAc, 8/2) to yield the alcohol as a pale yellow oil **(138)**. Adapted from Meyers *et al.* [177] (46 mg, 25% over 2 steps).

ν_{max} ($CHCl_3$)/cm^{-1}, 3431 (OH), 2099 (N_3), 1524, 1346 (NO_2); δ_H (400 MHz; $CDCl_3$): 1.88-1.99 (1H, m, C*H*$_2$CH$_2$N$_3$), 2.04-2.14 (1H, m, C*H*$_2$CH$_2$N$_3$), 2.95 (1H, d, *J* = 3.2 Hz, O*H*), 3.55 (2H, dd, *J* = 7.0, 6.3 Hz, CH$_2$C*H*$_2$N$_3$), 5.34 (1H, dd, *J* = 9.0, 3.2 Hz, C*H*OH), 7.43 (1H, ddd, *J* = 8.2, 7.5, 1.3 Hz, C*H*Ar$_b$), 7.65 (1H, ddd, *J* = 8.0, 7.5, 1.2 Hz, C*H*Ar$_c$), 7.81 (1H, dd, *J* = 8.2, 1.2 Hz, C*H*Ar$_a$), 7.91 (1H, dd, *J* = 8.0, 1.3 Hz, C*H*Ar$_d$); δ_C (100 MHz $CDCl_3$): 36.9 (CH$_2$*C*H$_2$N$_3$), 48.7 (*C*H$_2$CH$_2$N$_3$), 67.3 (*C*HOH), 124.5 (*C*HAr$_d$), 128.0 (*C*HAr$_a$), 128.4 (*C*HAr$_c$), 133.8 (*C*HAr$_b$), 139.6 (*C*Ar), 147.5 (*C*NO$_2$Ar); HRMS *m/z* (+ ESI): Found $[MNa]^+$, 245.0644 $C_9H_{10}N_4O_3$ requires $[MNa]^+$, 245.0645.

1-(3-azido-1-chloropropyl)-2-nitrobenzene **(TV4)**.

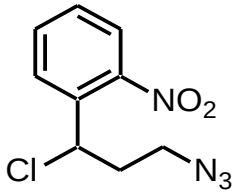

A solution of 3-azido-1-(2-nitrophenyl)propan-1-ol **(138)** (221 mg, 1.8 mmol, 1 equiv) in anhydrous dichloromethane (5 mL) was cooled to 0 °C under a nitrogen atmosphere. Thionyl chloride (5 mL) was then added dropwise and the solution was left to stir at room temperature for 6 h. The reaction was then concentrated *in vacuo* and the residue was purified using column chromatography (PE/EtOAc, 8/2) to yield the product as a pale yellow oil **(TV4)**. Adapted from Nakamura *et al.* [178] (104 mg, 43%).

ν_{max} ($CHCl_3$)/cm^{-1}, 2100 (N_3), 1525, 1349 (NO_2); δ_H (400 MHz; $CDCl_3$): 2.38-2.46 (2H, m, C*H*$_2$CH_2N_3), 3.59-3.63 (2H, m, CH_2C*H*$_2N_3$), 5.69 (1H, dd, *J* = 9.8, 3.9 Hz, C*H*Cl), 7.48 (1H, ddd, *J* = 8.2, 7.6, 1.3 Hz, C*H*Ar$_b$), 7.68 (1H, ddd, *J* = 8.3, 7.6, 1.3 Hz, C*H*Ar$_c$) 7.48 (1H, dd, *J* = 8.2, 1.3 Hz, C*H*Ar$_a$), 8.24 (1H, dd, *J* = 8.3, 1.3 Hz, C*H*Ar$_d$); δ_C (100 MHz $CDCl_3$): 39.0 (*C*H_2CH_2N_3), 48.6 (CH_2*C*H_2N_3), 54.5 (*C*H), 124.5 (*C*HAr$_d$), 129.3 (*C*HAr$_a$), 129.7 (*C*HAr$_c$), 133.6 (*C*HAr$_b$), 135.8 (*C*Ar), 147.7 (*C*NO_2Ar); HRMS *m/z* (+ ESI): Found $[MNa]^+$, 263.0303 $C_9H_9ClN_4NaO_2$ requires $[MNa]^+$, 263.0306.

1-(2-Nitrophenyl) propane-1,3-diol **(139)**. [114] [149]

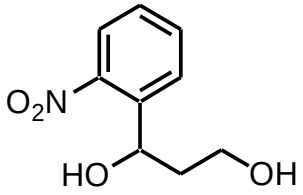

A solution of 1-(2-nitrophenyl)prop-2-en-1-ol **(130)** (1.70 g, 9.5 mmol, 1 equiv) in anhydrous tetrahydrofuran (40 mL) was cooled to 0 °C, borane (1M in THF, 9.5 mL) was then added dropwise, and stirred overnight at 0 °C under a nitrogen atmosphere. Sodium hydroxide (3M, 9.5 mL) was then added followed by dropwise addition of hydrogen peroxide (30%, 9.5 mL), before stirring for 30 min at 0 °C. The reaction was then quenched with a saturated sodium bisulfite solution (20 mL) and ethyl acetate (50 mL) was added. The organic layer was then washed with sodium hydrogen carbonate (50 mL) and brine (50 mL), before concentration *in vacuo*. The residue was then purified using column chromatography (PE/EtOAc, 8/2-1/1 gradient) to yield the primary alcohol as a brown oil **(139)**. Adapted from Jiang *et al.* And Matteucci *et al.* [116], [151] (870 mg, 47%).

ν_{max} ($CHCl_3$)/cm^{-1}, 3367 (OH), 1523, 1346 (NO_2); δ_H (400 MHz; $CDCl_3$): 1.83-2.10 (2H, m, C*H*$_2$CH$_2$OH), 3.01 (1H, bs, CHO*H*), 3.82-3.96 (2H, m, CH$_2$C*H*$_2$OH), 4.05-4.13 (1H, m, CH$_2$O*H*), 5.44 (1H, d, *J* = 7.8 Hz, C*H*OH), 7.39 (1H, ddd, *J* = 8.2, 7.6, 1.3 Hz, C*H*Ar$_b$), 7.63 (1H, ddd, *J* = 8.2, 7.6, 1.2 Hz, C*H*Ar$_c$), 7.85 (1H, dd, *J* = 8.2 1.2 Hz, C*H*Ar$_a$), 7.89 (1H, dd, *J* = 8.2, 1.3 Hz, C*H*Ar$_d$); δ_C (100 MHz $CDCl_3$): 39.5 (*C*H$_2$CH$_2$OH), 61.7 (CH$_2$*C*H$_2$OH), 69.5 (*C*HO), 124.4 (*C*HAr$_d$), 128.1 (*C*HAr$_a$), 128.2 (*C*HAr$_c$), 133.7 (*C*HAr$_b$), 139.9 (*C*Ar), 147.3 (*C*NO$_2$Ar); HRMS *m/z* (+ ESI): Found $[MNa]^+$, 220.0596 $C_9H_{11}NNaO_4$ requires $[MNa]^+$, 220.0580.

3-Hydroxy-3-(2-nitrophenyl)propyl-4-methylbenzene sulfonate **(140)**.

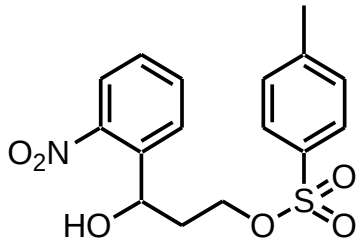

To a solution of 1-(2-Nitrophenyl) propane-1,3-diol **(139)** (837 mg, 4.2 mmol, 1 equiv) in anhydrous dichloromethane (20 mL) toluenesulfonyl chloride (810 mg, 4.2 mmol, 1 equiv) and diisopropylamine (1.5 mL, 8.4 mmol, 2 equiv) were added. The solution was then stirred overnight under a nitrogen atmosphere at room temperature before concentration *in vacuo*. The residue was then purified using column chromatography (PE/EtOAc, 8/2-7/3 gradient) to yield the primary alcohol as a pale yellow oil **(140)**. Adapted from Elban *et al.* [179] (492 mg, 33%). ν_{max} ($CHCl_3$)/cm^{-1}, 3520 (OH), 1524, 1349 (NO_2); δ_H (400 MHz; $CDCl_3$): 1.97-2.08 (1H, m, C*H*$_2$CH$_2$OTs), 2.16-2.28 (1H, m, C*H*$_2$CH$_2$OTs), 2.45 (3H, s, C*H*$_3$), 2.59 (1H, dd, *J* = 4.2, 0.7 Hz, CHO*H*), 4.21-4.29 (1H, m, CH$_2$C*H*$_2$OTs), 4.34-4.44 (1H, m, CH$_2$C*H*$_2$OTs), 5.32 (1H, ddd, *J* = 9.4, 4.2, 3.0 Hz, C*H*OH), 7.36 (2H, d, *J* = 8.2 Hz, C*H*Ar$_{Ts}$), 7.43 (1H, ddd, *J* = 8.2, 7.5, 1.4 Hz, C*H*Ar$_b$), 7.64 (1H, ddd, *J* = 7.8, 7.5, 1.2 Hz, C*H*Ar$_c$), 7.77 (1H, dd, *J* = 8.2, 1.2 Hz, C*H*Ar$_a$), 7.81 (2H, d, *J* = 8.2 Hz, C*H*Ar$_{Ts}$), 7.92 (1H, dd, *J* = 7.8, 1.4 Hz, C*H*Ar$_d$); δ_C (100 MHz $CDCl_3$): 21.7 (*C*H$_3$), 36.9 (*C*H$_2$CH$_2$OTs), 66.1 (CH$_2$*C*H$_2$OH), 67.4 (*C*HO), 124.6 (*C*HAr$_d$), 127.9 (*C*HAr$_{Ts}$), 128.0 (*C*HAr$_a$), 128.5 (*C*HAr$_c$), 129.9 (*C*HAr$_{Ts}$), 132.9 (*C*Ar$_{Ts}$) 133.8 (*C*HAr$_b$), 139.0 (*C*Ar), 144.9 (*C*Ar$_{Ts}$), 147.6 (*C*NO$_2$Ar); HRMS *m/z* (+ ESI): Found $[MNa]^+$, 374.0668 $C_{16}H_{17}NNaO_6S$ requires $[MNa]^+$, 374.0669.

3-Azido-1-(2-nitrophenyl)propan-1-ol **(138)**.

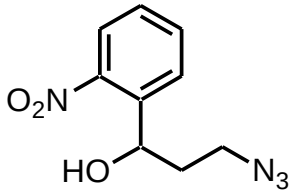

To a solution of 3-hydroxy-3-(2-nitrophenyl)propyl-4-methylbenzene sulfonate **(140)** (492 mg, 1.4 mmol, 1 equiv) in dimethylformamide (3 mL), sodium azide (456 mg, 7.0 mmol, 5 equiv) was added. The suspension was then stirred overnight at room temperature under a nitrogen atmosphere. The suspension was filtered before purification using column chromatography (PE/EtOAc, 8/2) to yield the alcohol as a pale yellow oil **(138)**. Adapted from Meyers *et al.* [177] (198 mg, 64%).

ν_{max} ($CHCl_3$)/cm^{-1}, 3431 (OH), 2099 (N_3), 1524, 1346 (NO_2); δ_H (400 MHz; $CDCl_3$): 1.88-1.99 (1H, m, C*H*$_2$CH$_2$N$_3$), 2.04-2.14 (1H, m, C*H*$_2$CH$_2$N$_3$), 2.95 (1H, d, *J* = 3.2 Hz, O*H*), 3.55 (2H, dd, *J* = 7.0, 6.3 Hz, CH$_2$C*H*$_2$N$_3$), 5.34 (1H, dd, *J* = 9.0, 3.2 Hz, C*H*OH), 7.43 (1H, ddd, *J* = 8.2, 7.5, 1.3 Hz, C*H*Ar$_b$), 7.65 (1H, ddd, *J* = 8.0, 7.5, 1.2 Hz, C*H*Ar$_c$), 7.81 (1H, dd, *J* = 8.2, 1.2 Hz, C*H*Ar$_a$), 7.91 (1H, dd, *J* = 8.0, 1.3 Hz, C*H*Ar$_d$); δ_C (100 MHz $CDCl_3$): 36.9 (CH$_2$*C*H$_2$N$_3$), 48.7 (*C*H$_2$CH$_2$N$_3$), 67.3 (*C*HOH), 124.5 (*C*HAr$_d$), 128.0 (*C*HAr$_a$), 128.4 (*C*HAr$_c$), 133.8 (*C*HAr$_b$), 139.6 (*C*Ar), 147.5 (*C*NO$_2$Ar); HRMS *m/z* (+ ESI): Found $[MNa]^+$, 245.0644 $C_9H_{10}N_4O_3$ requires $[MNa]^+$, 245.0645.

1-(2,4-Dinitrophenyl)prop-2-en-1-ol **(142)**.

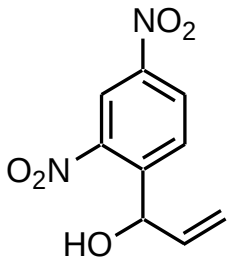

A solution of 2,4-dinitrobenzaldehyde **(141)** (100 mg, 0.5 mmol, 1 equiv) in tetrahydrofuran (5 mL) was cooled to 0 °C before dropwise addition of vinyl magnesium bromide (1 M in THF, 0.6 mL, 1.2 equiv). The solution was then stirred at room temperature under nitrogen for 3 h before quenching with saturated ammonium chloride. Ethyl acetate (10 mL) was then added and the reaction was washed with saturated sodium bicarbonate (10 mL) and brine (10 mL) before concentration *in vacuo.* The residue was then purified using column chromatography (PE/EtOAc, 8/2), to yield the product as a brown oil **(142)**. Adapted from Jiang *et al.* [116] (59 mg, 51%).

ν_{max} ($CHCl_3$)/cm^{-1}, 3542 (OH), 3108 (CHAr), 1534, 1348 (NO_2); δ_H (400 MHz; $CDCl_3$): 3.34 (1H, bs, O*H*), 5.24 (1H, dt, *J* = 10.3, 1.1 Hz CHCH_{2y}), 5.37 (1H, dt, *J* = 17.1, 1.1 Hz CHCH_{2z}), 5.88 (1H, d, *J* = 5.8 Hz, C*H*OH), 5.92-6.04 (1H, m C*H*CH_2), 8.05 (1H, d, *J* = 8.7 Hz, C*H*Ar_a), 8.41 (1H, dd, *J* = 8.7, 2.3 Hz, C*H*Ar_b), 8.65 (1H, d, *J* = 2.3 Hz, C*H*Ar_c); δ_C (100 MHz $CDCl_3$): 69.7 (*C*HOH), 117.8 (*C*H_2CH), 120.1 (*C*HAr_c), 127.5 (*C*HAr_b), 130.2 (*C*HAr_a), 136.9 (CH_2*C*H), 144.1 (*C*Ar), 147.1 (*C*NO_2Ar), 147.9 (*C*NO_2Ar).

1-[1-(Methoxymethoxy)prop-2-en-1-yl]-2,4-dinitrobenzene **(143)**.

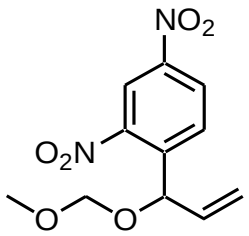

A solution of 1-(2,4-dinitrophenyl)prop-2-en-1-ol **(142)** (150 mg, 0.67 mmol, 1 equiv) in anhydrous dichloromethane (5 mL) was cooled to 0 °C before dropwise addition of diisopropylethylamine (0.72 mL, 4.0 mmol, 6 equiv). Chloromethyl methyl ether (0.30 mL, 4.0 mmol, 6 equiv) was then added dropwise and the reaction was allowed to reach room temperature and stirred for 24 h. The reaction was then quenched with saturated sodium bicarbonate, before concentration *in vacuo*. The residue was then taken up in diethyl ether (3 x 10 mL), washed with brine (10 mL), dried over magnesium sulfate and concentrated *in vacuo*. The residue was then purified using column chromatography (PE/EtOAc, 9/1), to yield the product as a yellow oil **(143)**. Adapted from Jiang *et al.* [116] (99 mg, 55%).

ν_{max} ($CHCl_3$)/cm^{-1}, 3108 (CHAr), 1536, 1348 (NO_2); δ_H (400 MHz; $CDCl_3$): 3.29 (3H, s, CH_3), 4.60 (1H, d *J* = 6.8 Hz, CH_2O), 4.76 (1H, d *J* = 6.8 Hz, CH_2O), 5.28 (1H, d, *J* = 10.1 Hz, CHCH_{2y}), 5.39 (1H, d, *J* = 16.8, Hz, CHCH_{2z}), 5.79-5.93 (2H, m C*H*O, C*H*CH_2), 8.04 (1H, d, *J* = 8.7 Hz, C*H*Ar_a), 8.44 (1H, dd, *J* = 8.7, 2.3 Hz, C*H*Ar_b), 8.72 (1H, d, *J* = 2.3 Hz, C*H*Ar_c); δ_C (100 MHz $CDCl_3$): 55.9 (*C*H_3), 73.3 (*C*HO), 94.8 (O*C*H_2O), 118.7 (*C*H_2CH), 119.9 (*C*HAr_c), 127.3 (*C*HAr_b), 130.4 (*C*HAr_a), 135.1 (CH_2*C*H), 143.2 (*C*Ar), 147.0 (*C*NO_2Ar), 148.0 (*C*NO_2Ar); HRMS *m/z* (+ ESI): Found $[MNa]^+$, 291.0579 $C_{11}H_{12}N_2NaO_6$ requires $[MNa]^+$, 291.0588.

3-(2,4-Dinitrophenyl)-3-(methoxymethoxy) propan-1-ol **(144)**.

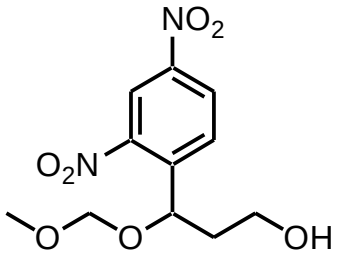

A solution of 1-[1-(methoxymethoxy)prop-2-en-1-yl]-2,4-dinitrobenzene **(143)** (100 mg, 0.3 mmol, 1 equiv) in anhydrous tetrahydrofuran (2 mL) was cooled to 0 °C, borane (1M in THF, 0.4 mL, 1 equiv) was then added dropwise, and then stirred overnight at 0 °C under a nitrogen atmosphere. Sodium hydroxide (3M, 0.4 mL) was then added followed by dropwise addition of hydrogen peroxide (30%, 0.4 mL), before stirring for 30 min at 0 °C. The reaction was then quenched with a saturated sodium bisulfite solution (5 mL) and ethyl acetate (5 mL) was added. The organic layer was then washed with sodium hydrogen carbonate (5 mL) and brine (5 mL), before concentration *in vacuo*. The residue was then purified using column chromatography (PE/EtOAc, 2/1-1/1) to yield the primary alcohol as a brown oil **(144)**. Adapted from Jiang *et al.* [116] (43 mg, 41%).

ν_{max} ($CHCl_3$)/cm^{-1}, 3425 (OH), 3109 (CHAr), 1535, 1348 (NO_2); δ_H (400 MHz; $CDCl_3$): 1.90-2.02 (1H, m, C*H*$_2$CH$_2$OH), 2.08-2.19 (1H, m, C*H*$_2$CH$_2$OH), 3.31 (3H, s, C*H*$_3$), 3.81-3.93 (2H, m, CH$_2$C*H*$_2$OH), 4.49 (1H, d, *J* = 6.8 Hz, C*H*$_2$OCH$_3$), 4.64 (1H, d, *J* = 6.8 Hz, C*H*$_2$OCH$_3$), 5.48 (1H, dd, *J* = 9.3, 3.3 Hz, C*H*OMOM), 8.03 (1H, d, *J* = 8.6 Hz, C*H*Ar$_a$), 8.47 (1H, dd, *J* = 8.6, 2.4 Hz, C*H*Ar$_b$), 8.79 (1H, d, *J* = 2.4 Hz, C*H*Ar$_c$); δ_C (100 MHz $CDCl_3$): 40.0 (*C*H$_2$CH$_2$OH), 56.3 (*C*H$_3$), 59.7 (CH$_2$*C*H$_2$OH), 72.4 (*C*HOMOM), 90.1 (O*C*H$_2$O),

120.1 (*C*HAr$_c$), 127.4 (*C*HAr$_b$), 130.4 (*C*HAr$_a$), 145.5 (*C*Ar), 147.0 (*C*NO$_2$Ar), 147.8 (*C*NO$_2$Ar).

1-[3-azido-1-(Methoxymethoxy)propyl]-2,4-dinitrobenzene **(145)**.

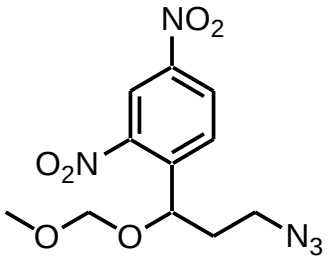

To a solution of 3-(2,4-dinitrophenyl)-3-(methoxymethoxy) propan-1-ol **(144)** (200 mg, 0.7 mmol, 1 equiv) in tetrahydrofuran (5 mL), diphenyl phosphorylazide (385 mg, 1.4 mmol, 2 equiv) and 1,8-diazabicycloundec-7-ene (319 mg, 2.1 mmol, 3 equiv) were added. The solution was then stirred overnight at room temperature under a nitrogen atmosphere. Sodium azide (228 mg, 3.5 mmol, 5 equiv) and 15-crown-5 (15 mg, 0.07 mmol, 0.1 equiv) were then added to form a suspension that was refluxed for 4 h. The suspension was then filtered, and the filtrate concentrated *in vacuo*. The remaining residue was then purified using column chromatography (PE/EtOAc, 8/2) to yield the azide as a pale yellow oil **(145)**. Adapted from Liu *et al.* [143] (107 mg, 49%).

ν_{max} ($CHCl_3$)/cm^{-1}, 3107 (CHAr), 2099 (N_3), 1535, 1348 (NO_2); δ_H (400 MHz; $CDCl_3$): 1.92-2.02 (1H, m, C*H*$_2$CH$_2$N$_3$), 2.11-2.21 (1H, m, C*H*$_2$CH$_2$OH), 3.30 (3H, s, C*H*$_3$), 3.53-3.59 (2H, m, CH$_2$C*H*$_2$N$_3$), 4.49 (1H, d, *J* = 6.9 Hz, C*H*$_2$OCH$_3$), 4.62 (1H, d, *J* = 6.9 Hz, C*H*$_2$OCH$_3$), 5.37 (1H, dd, *J* = 9.3, 3.0 Hz, C*H*OMOM), 8.01 (1H, d, *J* = 8.6 Hz, C*H*Ar$_a$), 8.48 (1H, dd, *J* = 8.6, 2.3 Hz, C*H*Ar$_b$), 8.82 (1H,

d, *J* = 2.3 Hz, C*H*Ar$_c$); δ_C (100 MHz $CDCl_3$): 36.6 (*C*H_2CH_2N$_3$), 47.8 (CH$_2$*C*H$_2$N$_3$), 56.3 (*C*H$_3$), 71.5 (*C*HOMOM), 96.1 (O*C*H$_2$O), 120.3 (*C*HAr$_c$), 127.5 (*C*HAr$_b$), 129.9 (*C*HAr$_a$), 145.1 (*C*Ar), 147.2 (*C*NO$_2$Ar), 147.9 (*C*NO$_2$Ar).

3-Azido-1-(2,4-dinitrophenyl)propan-1-ol **(146)**.

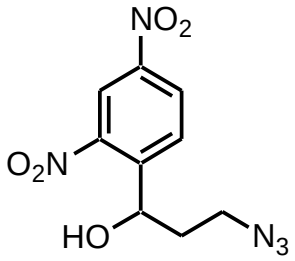

To a suspension of 1-[3-azido-1-(methoxymethoxy)propyl]-2,4-dinitrobnzene in **(145)** (213 mg, 0.7 mmol, 1 equiv) in tetrahydrofuran (2 mL) and water (5 mL), hydrochloric acid (11.8 M, 5 mL) was added. The suspension was then stirred at 70 °C for 5 h. The suspension was cooled and ethyl acetate was added. The organic layer was separated, dried and concentrated *in vacuo*. The residue was then purified using column chromatography (PE/EtOAc, 8/2) to yield the product as a yellow oil **(146)**. Adapted from Meyers *et al.* [177] (111 mg, 65%).

δ_H (400 MHz; $CDCl_3$): 1.84-1.95 (1H, m, C*H*$_2$CH$_2$N$_3$), 2.06-2.17 (1H, m, C*H*$_2$CH$_2$OH), 3.06 (1H, bs, O*H*), 3.64 (2H, dd, *J* = 6.6, 6.1 Hz, CH$_2$C*H*$_2$N$_3$), 5.52 (1H, dd, *J* = 9.2, 2.2 Hz, C*H*OH), 8.15 (1H, d, *J* = 8.7 Hz, C*H*Ar$_a$), 8.48 (1H, dd, *J* = 8.7, 2.3 Hz, C*H*Ar$_b$), 8.80 (1H, d, *J* = 2.3 Hz, C*H*Ar$_c$).

1-(3-Azido-1-chloropropyl)-2,4-dinitrobenzene **(TV5)**.

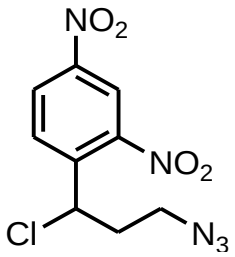

A solution of 3-azido-1-(2,4-dinitrophenyl)propan-1-ol **(146)** (368 mg, 1.4 mmol, 1 equiv) in anhydrous dichloromethane (5 mL) was cooled to 0 °C under a nitrogen atmosphere. Thionyl chloride (5 mL) was then added dropwise and the solution was left to stir at room temperature for 6 h. The reaction was then concentrated *in vacuo* and the residue was purified using column chromatography (PE/EtOAc, 8/2) to yield the product as a pale yellow oil **(TV5)**. Adapted from Nakamura *et al.* [178] (46 mg, 12%).

ν_{max} ($CHCl_3$)/cm^{-1}, 2101 (N_3), 1527, 1348 (NO_2); δ_H (400 MHz; $CDCl_3$): 2.12-2.43 (2H, m, C*H*$_2$CH$_2$N$_3$), 3.15-3.68 (2H, m, CH$_2$C*H*$_2$N$_3$), 6.18-6.24 (1H, m, C*H*Cl), 8.06 (1H, d, *J* = 8.7 Hz, C*H*Ar$_a$), 8.45 (1H, dd, *J* = 8.7, 2.3 Hz, C*H*Ar$_b$) 8.74 (1H, d, *J* = 2.3 Hz, C*H*Ar$_c$); δ_C (100 MHz $CDCl_3$): 37.6 (*C*H$_2$CH$_2$N$_3$), 48.5 (CH$_2$*C*H$_2$N$_3$), 56.2 (*C*HCl), 121.0 (*C*HAr$_c$), 126.6 (*C*HAr$_b$), 129.3 (*C*HAr$_a$), 144.3 (*C*Ar), 146.9 (*C*NO$_2$Ar), 147.8 (*C*NO$_2$Ar).

1-*N*-Methyl-2-amino imidazole-5-carboxylic acid ethyl ester **(149)**.

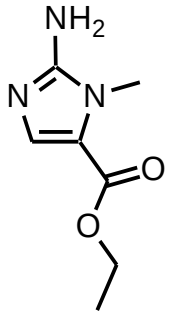

To a suspension of sarcosine methyl ester hydrochloride **(147)** (5 g, 35.8 mmol, 1 equiv), potassium carbonate (5 g, 36.2 mmol, 1.1 equiv) in ethanol (50 mL), ethyl formate (22 mL) was added. The suspension was stirred for 48 h at room temperature, filtered and the filtrate concentrated *in vauco*. Water was then added and extracted with ethyl acetate (3 x 20 mL), dried over magnesium sulfate and concentrated *in vacuo*. The residue was then dissolved in ethyl formate (16 mL) and cooled to 0 °C, before portionwise addition of sodium hydride (1.6 g, 66 mmol, 1.9 equiv) over 1 hour. The suspension was then left to stir overnight at room temperature before being triturated twice with hexane (2 x 20 mL). The residue was then dissolved in ethanol (15 mL) and concentrated hydrochloric acid (11.8 M, 6 mL), and heated to 110 °C for 1 hour. The suspension was then filtered and washed with ethanol before the filtrate was concentrated *in vacuo* to produce a thick brown oil. Acetic acid in water (10%, 20 mL), cyanamide (3.5 g, 83 mmol, 2.3 equiv) and sodium acetate (15 g, 110 mmol, 3.1 equiv) were then added to the residue, before being stirred at 95 °C for 1 hour. The reaction was then adjusted to pH 9 using sodium hydrogen carbonate and a pale yellow precipitate was filtered to yield the imidazole as a yellow powder **(149)**. Repeated from Matteucci *et al.* [151] (4.17 g, 75%).

ν_{max} ($CHCl_3$)/cm^{-1}, 3391 (NH), 3132 (CHAr), 1651 (C=O); δ_H (400 MHz; DMSO): 1.23 (3H, t, *J* = 7.1 Hz, CH_2CH_3), 3.52 (3H, s, NCH_3), 4.15 (2H, q, *J* = 7.1 Hz, CH_2CH_3), 6.16 (2H, d, *J* = 5.2 Hz, NH_2), 7.27 (1H, s, CHAr); δ_C (100 MHz DMSO): 14.8 (CH_2CH_3), 30.7 (NCH_3), 59.3 (CH_2CH_3), 117.3 (CAr), 136.6 (CHAr), 154.8 (CAr), 160.2 (C=O); HRMS *m/z* (+ ESI): Found $[MH]^+$, 170.0925 $C_7H_{11}N_3O_2$ requires $[MH]^+$, 170.0924.

1-*N*-Methyl-2-nitroimidazole-5-carboxylic acid ethyl ester **(150)**.

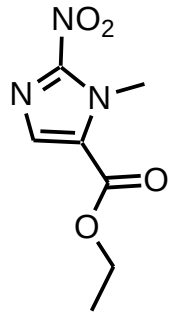

A suspension of 1-*N*-methyl-2-amino imidazole-5-carboxylic acid ethyl ester **(149)** (500 mg, 2.9 mmol, 1 equiv), sodium nitrite (4.5 g, 65.2 mmol, 22 equiv) and water (25 mL) was cooled to 0 °C and sulphuric acid (7%, 22.5 mL) was added dropwise keeping the temperature below 5 °C. The solution was then stirred for 30 min before being raised to room temperature and stirred for a further 2 h. The solution was then extracted with chloroform (6 x 50 mL) and dried with magnesium sulfate before concentration *in vacuo.* The residue was then stirred in ether and filtered, the filtrate was then washed with ice water, and concentrated *in vacuo*, to yield the product as a red/brown solid **(150)**. Repeated from Asato *et al.* [155] (255 mg, 43%).

ν_{max} ($CHCl_3$)/cm^{-1}, 3132 (CHAr), 2984 (CH), 1727 (C=O), 1553, 1368 (NO_2); δ_H (400 MHz; MeOD): 1.39 (3H, t, *J* = 7.1 Hz, CH_2CH_3), 4.30 (3H, s, NCH_3), 4.39 (2H, q, *J* = 7.1 Hz, CH_2CH_3), 7.72 (1H, s, CHAr); δ_C (100 MHz MeOD): 13.0 (CH_2CH_3), 34.5 (NCH_3), 61.4 (CH_2CH_3), 126.5 (CAr), 133.3 (CHAr), 158.9 (C=O); HRMS *m/z* (+ EI): Found $[MH]^+$, 199.0593 $C_7H_9N_3O_4$ requires $[MH]^+$, 199.0588.

1-Methyl-2-nitro-1*H*-imidazole-5-carboxylic acid **(153)**.

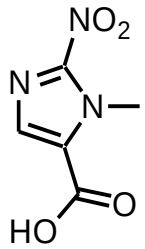

A suspension of 1-*N*-methyl-2-nitroimidazole-5-carboxylic acid ethyl ester **(150)** (2.66 g, 13.4 mmol, 1 equiv) in sodium hydroxide solution (3M, 100 mL) was stirred overnight at room temperature or until dissolution. The solution was then adjusted to pH 3 using hydrochloric acid (1M) before extraction with ethyl acetate (3 x 50 mL). The organic layer was then concentrated *in vacuo* to yield the product as a pale brown solid **(153)**. Repeated from Matteucci *et al.* [151] (1.71 g, 75%).

ν_{max} ($CHCl_3$)/cm^{-1},2856 (CH), 1714 (C=O), 1560, 1364 (NO_2); δ_H (400 MHz; MeOD): 4.30 (3H, s, C*H*$_3$), 5.03 (1H, bs, O*H*), 7.69 (1H, s, C*H*Ar); δ_C (100 MHz MeOD): 34.5 (*C*H$_3$), 127.0 (*C*Ar), 133.4 (*C*HAr), 160.2 (*C*=O).

(1-Methyl-2-nitro-1*H*-imidazol-5-yl)methanol **(152)**.

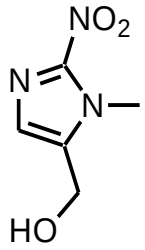

A stirred solution of 1-methyl-2-nitro-1*H*-imidazole-5-carboxylic acid **(153)** (200 mg, 1.17 mmol, 1 equiv) in tetrahydrofuran (2 mL) was cooled to 0 °C, before dropwise addition of borane (1M in THF, 0.24 mL, 1.2 equiv). The reaction was

then stirred at room temperature under a nitrogen atmosphere for 5 h before addition of methanol and concentration *in vacuo*. The residue was then purified using column chromatography (DCM/MeOH 95/5), to yield the product as a pale yellow solid **(152)**. Adapted from Yoon *et al.* [180] (83 mg, 45%).

ν_{max} ($CHCl_3$)/cm^{-1}, 3391 (OH), 2922 (CH), 1546, 1349 (NO_2); δ_H (400 MHz; DMSO): 3.92 (3H, s, C*H*$_3$), 4.23 (1H, bs, O*H*), 4.55 (2H, s, C*H*$_2$), 7.69 (1H, s, C*H*Ar); δ_C (100 MHz DMSO): 34.6 (*C*H_3), 56.4 (*C*H_2), 127.0 (*C*HAr), 139.1 (*C*Ar).

2-Nitro-*1H*-imidazole-5-carbaldehyde **(155)**.

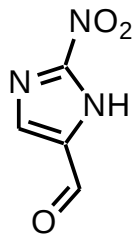

A solution of 1*H*-imidazole-4-carbaldehyde **(154)** (100 mg, 1.0 mmol, 1 equiv) in nitric acid (2 mL) was stirred at room temperature for 30 min before concentration *in vacuo*. This yielded the product as a pale yellow solid **(155)**. Repeated from Baliani *et al.* [160] (147 mg, quant).

δ_H (400 MHz; DMSO): 8.51 (1H, s, C*H*Ar), 9.18 (1H, s, N*H*), 9.84 (1H, s, C=O*H*); δ_C (100 MHz DMSO): 128.9 (*C*HAr), 132.9 (*C*CHO), 138.8 (*C*NO_2), 181.7 (*C*=O); HRMS *m/z* (+ EI): Found $[MH]^+$, 141.0169 $C_4H_3N_3O_3$ requires $[MH]^+$, 141.0169.

1-Methyl-2-nitro-1*H*-imidazole-5-carbaldehyde **(151)**.

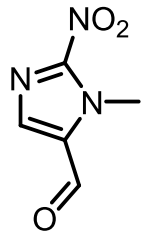

A solution of 1-methyl-1*H*-imidazole-5-carbaldehyde **(156)** (100 mg, 1.0 mmol, 1 equiv) in nitric acid (2 mL) was refluxed for 30 min before concentration *in vacuo*. This yielded the product as a pale yellow solid **(151)**. Adapted from Baliani *et al.* [160] (135 mg, 96%).

δ_H (400 MHz; DMSO): 3.73 (3H, s, C*H*$_3$), 8.53 (1H, s, C*H*Ar), 9.16 (1H, s, N*H*), 9.85 (1H, s, C=O*H*); δ_C (100 MHz DMSO): 28.9 (*C*H$_3$), 128.8 (*C*HAr), 133.1 (*C*CHO), 138.7 (*C*NO$_2$), 182.3 (*C*=O); HRMS *m/z* (+ EI): Found $[MH]^+$, 155.1124 $C_5H_5N_3O_3$ requires $[MH]^+$, 155.1121.

EG180 3-(Acetamino)-2-oxo-2*H*-chromen-7-yl acetate **(159)**.

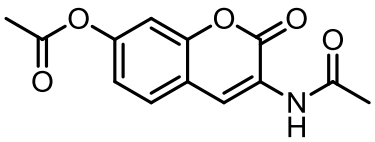

A solution of 2,4-dihydroxybenzaldehyde **(158)** (2.76 g, 20.0 mmol, 1 equiv), N-acetylglycine (2.34 g, 20.0 mmol, 1 equiv) and anhydrous sodium acetate (4.94 g, 60.0 mmol, 3 equiv) in acetic anhydride (100 mL) was heated at reflux (150 °C) for 4 h. The solution was then poured over ice to form a precipitate. The suspension was then filtered and washed with ice water to yield the product as a fluffy yellow solid **(159)**. Repeated from Sivakumar *et al.* [162] (549 mg, 11%)

ν_{max} ($CHCl_3$)/cm^{-1}, 3341 (NH), 1759, 1720, 1681 (C=O); δ_H (400 MHz; $CDCl_3$): 2.24 (3H, s, NHCOC*H*$_3$), 2.34 (3H, s, OCOC*H*$_3$), 7.07 (1H, dd, *J* = 8.5, 2.2 Hz, C$_h$*H*Ar), 7.13 (1H, d, *J* = 2.2 Hz, C$_f$*H*Ar), 7.51 (1H, d, *J* = 8.5 Hz, C$_i$*H*Ar), 8.03 (1H, bs, N*H*), 8.67 (1H, s, C$_c$*H*Ar); δ_C (100 MHz $CDCl_3$): 21.1 (NHCO*C*H$_3$), 24.7 (OCO*C*H$_3$), 110.1 (*C*$_f$HAr), 117.6 (*C*$_d$Ar), 119.1 (*C*$_h$HAr), 122.8 (*C*$_b$Ar), 123.6 (*C*cHAr), 128.4 (*C*$_i$HAr), 150.1 (*C*$_e$Ar), 151.4 (*C*$_g$Ar), 158.5 (*C*$_a$Ar), 168.9, 169.4 (*C*=O); HRMS *m/z* (+ ESI): Found $[MNa]^+$, 284.0529 $C_{13}H_{11}NNaO_5$ requires $[MNa]^+$, 284.0529.

3-Azido-7-hydroxy-2*H*-chromen-2-one **(DYE1)**.

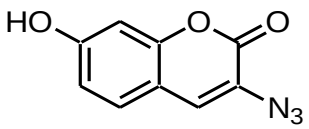

A solution of 3-(acetamino)-2-oxo-2*H*-chromen-7-yl acetate **(159)** (549 mg, 1.6 mmol, 1 equiv) in ethanol (10 mL) and hydrochloric acid (11.8M, 20 mL) was heated at reflux for 1 hour. Ice water was then added and the solution was allowed to cool to <5 °C, before addition of sodium nitrite (1.3 g, 18.8 mmol. 11.8 equiv). The solution was then stirred for 5 min before portion wise addition of sodium azide (1.5 g, 23.1 mmol, 14.4 equiv), before stirring for a further 15 min. A precipitate was formed and this was filtered and washed with ice water to yield the azide as a brown powder **(DYE1)**. Repeated from Sivakumar *et al.* [162] (363 mg, 85%).

ν_{max} ($CHCl_3$)/cm^{-1}, 3418 (OH), 2116 (N_3), 1695 (C=O); δ_H (400 MHz; DMSO): 6.76 (1H, d, *J* = 2.2 Hz, C$_f$*H*Ar), 6.81 (1H, dd, *J* = 8.5, 2.2 Hz, C$_h$*H*Ar), 7.48 (1H, d, *J* = 8.5 Hz, C$_i$*H*Ar), 7.60 (1H, s, C$_c$*H*Ar); δ_C (100 MHz DMSO): 102.5 (*C*$_f$HAr),

111.8 (C_dAr), 114.3 (C_hHAr), 121.6 (C_bAr), 128.3 (C_cHAr), 129.6 (C_iHAr), 153.2 (C_eAr), 157.8 (C_gAr), 160.8 (C_aAr); HRMS *m/z* (+ EI): Found $[MH]^+$, 203.0329 $C_9H_5N_3O_3$ requires $[MH]^+$, 203.0325.

Synthesis of all 'click' products.

A solution of targeting vector (1.8 equiv, 0.077 mmol) in methanol (1.0 mL), was added to a solution of contrast agent (1 equiv, 0.042 mmol) in water (0.5 mL) and under nitrogen. To this a solution of copper sulphate (0.1 equiv, 0.0042 mmol) and sodium ascorbate (0.2 equiv, 0.0084 mmol) in water (0.5 mL) was added. The resulting suspension was then stirred for 24 hours under nitrogen, before concentration in vacuo. The residue was then purified using reverse phase silica chromatography (MeOH – H_2O) before freeze drying the water fraction. The residue was then dissolved in MeOH and centrifuged, before the supernatant taken and concentrated in vacu to produce the final product as a colourless or off white solid.

All analytical HPLC of the final compounds was run using the following method: 0-0% B over 7 minutes, 0-100% B over 15 minutes before returning to 0% B.

Compound	Data
C1 – 42%	HRMS *m/z* (+ ESI): Found $[MH]^+$, 779.1848 $C_{24}H_{35}N_{11}O_9Gd$ requires $[MH]^+$, 779.1855. Rf on HPLC 1.39 min.
C2 – 8%	HRMS *m/z* (+ ESI): Found $[MNa]^+$, 859.1539

	$C_{28}H_{37}N_9O_9ClGdNa$ requires $[MNa]^+$, 859.1536. Rf on HPLC 1.56 min.
C3 – 21%	HRMS *m/z* (+ ESI): Found $[MH]^+$, 837.1693 $C_{28}H_{38}N_9O_9Gd$ requires $[MH]^+$, 837.1717. Rf on HPLC 1.38 min.
CA1 + dye – 19%	HRMS *m/z* (+ ESI): Found $[MNa]^+$, 822.1444 $C_{28}H_{35}N_8O_9GdNa$ requires $[MNa]^+$, 822.1459. Rf on HPLC 1.26 min.

NMR Relaxivity Testing

The NMR experiments were carried out by Dr Walter Köckenberger at the Sir Peter Mansfield Magnetic Resonance Centre, School of Physics and Astronomy, University Park, University of Nottingham. The field strength used was 20 MHz at 298 K. Nine NMR tubes 500 µL, containing the following concentrations of contrast agent were made up in milli q water, 0.1, 0.4, 0.6, 0.8, 1.0, 1.2, 1.6, 2.0, 2.5 mM. Inversion recovery experiments were carried out acquiring 128 x 128 pixel images with a field of view of 3cm. A conventional spin echo experiment was used, and the 180 inversion pulse was an adiabatic hyperbolic secant pulse with inversion recovery delays set at 20, 40, 60, 80, 100, 150, 200, 250, 300, 400, 500, 700, 1000, 1800, 2500 ms. Signal intensity in each NMR tube was averaged over a region of 11 x 11 pixels.

Enzymatic Assay

Aerobic Assay.

To a solution of Xanthine (0.45 mL, 0.5mM) in PBS buffer (50mM), a solution of azole (0.45 mL, 0.25 mM) in PBS buffer (50Mm) was added. This was heated in an incubator at 37 °C for >30 minutes before addition of *xanthine oxidase* (30 µL, 0.003 U/mL) in PBS buffer (50mM). The cuvette was then monitored every 15 minutes by UV spectroscopy and kept in an incubator at 37 °C between each run.

Bibliography

1. http://missionscience.nasa.gov/ems/11_xrays.html. [Online] 2009

2. D.W. McRobbie, E.A. Moore, M.J. Graves, M.R. Prince. *MRI from picture to proton*. 2nd. Edition : Cambridge University Press, New York, 2007.

3. Lauterbur, P.C. *Nature.* **1973**, *242*, 190.

4. http://www.med.nagasaki-u.ac.jp/radiology/MRI%20of%FOOT/MRI-CDNUH/nf-history.html. [Online] 2009

5. Hunter, J.K.M. Sanders B.K. *Modern NMR Spectroscopy: A guide for chemists.* 2nd. Edition : OUP, Oxford, 2003.

6. Hore, P.J. *Nuclear Magnetic Resonance (Oxford Chemistry Primers)*. 1st. Edition : OUP, Oxford, 1995.

7. http://en.allexperts.com/q/Biology-664/2008/2/water-human-body.htm. [Online] 2009

8. Gaillard, L. PhD, University of Nottingham, 2008.

9. Damadian, R. Minkoff, L. Goldsmith, M. *Physiol Chem Phys*. **1977**, *10*, 561.

10. Strijkers, G.J. Mulder, W.J. van Tilborg, G.A. Nicolay, K. *Anticancer Agents Med Chem.* **2007**, *7*, 291.

11. Provenzale, J.M. Ison, C. Delong, D. *Am J Roentgenol.* **2009**, *193*, W515.

12. Hanaoka, K. *Chem Pharm Bull*. **2010**, *58*, 1283.

13. http://imaging.bayerhealthcare.com/html/magnevist/index.html. [Online] 2009.

14. http://md.gehealthcare.com/omniscan/. [Online] 2009.

15. http://www.drugs.com/pro/prohance.html. [Online] 2009.

16. http://www.emea.europa.eu/pdfs/human/press/pus/4974107en.pdf. [Online] 2009.

17. Aime, S. Botta, M. Crich, S.G. Giovenzana, G. Pagliarin, R. Sisti, M. Terreno, E. *Magn Reson Chem*. **1998**, *36*, S200.

18. Reilly, R.F. *Clin J Am Soc Nephrol.* **2008**, *3*, 747.

19. Grobner, T. *Nephrol Dial Transpl*. **2006**, *21*, 1104.

20. Prince, M.R. Zhang, H.L. Roditi, G.H. Leiner, T. Kucharczyk, W. *J Magn Reson Imaging.* **2009**, *30*, 1298.

21. Raymond, K.N. Pierre. V.C. *Bioconjugate Chem.* **2005**, *16*, 3.

22. Bolskar, R.D. Benedetto, A.F. Husebo, L.O. Price, R.E. Jackson, E.F. Wallace, S. Wilson, L.J. Alford, J.M. *J Am Chem Soc.* **2003**, *125*, 5471.

23. Shu, C.Y. Corwin, F.D. Zhang, J.F. Chen, Z.J. Reid, J.E. Sun, M.H. Xu, W. Sim, J.H. Wang, C.R. Fatouros, P.P. Esker, A.R. Gibson, H.W. Dorn, H.C. *Bioconjugate Chem.* **2009**, *20*, 1186.

24. Mulder, W.J.M. Stijkers, G.J. Griffieon, A.W. van Bloois, L. Molema, G. Storm, G. Koning, G.A. Nicolay, K. *Bioconjugate Chem.* **2004**, *15*, 799.

25. van Tilborg, G.A.F. Mulder, W.J.M. Deckers, N. Storm, G. Reutelingsperger, C.P.M. Strijkers, G.J. Nicolay, K. *Bioconjugate Chem.* **2006**, *17*, 741.

26. Winter, P.M. Caruthers, S.D. Kassner, A. Harris, T.D. Chinen, L.K. Allen, J.S. Lacy, E.K. Zhang, H.Y. Robertson, J.D. Wickline, S.A. Lanza, G.M. *Cancer Res.* **2003**, *63*, 5838.

27. Langereis, S. Dirksen, A. Hackeng, T.M. van Genderen, M.H.P. Meijer, E.W. *New J Chem.* **2007**, *31*, 1152.

28. Kobayashi, H. Kawamoto, S. Jo, S.K. Bryant, H.L. BrechbielL, M.W. Star, R.A. *Bioconjugate Chem*. **2003**, *14*, 388.

29. Costa, J. Toth, E. Helm, L. Merbach, A.E. *Inorg Chem.* **2005**, *44*, 4747.

30. Costa, J. Ruloff, R.Burai, L. Helm, L. Merbach, A.E. *J Am Chem Soc.* **2005,** *127*, 5147.

31. Duimstra, J.A. Femia, F.J. Meade, T.J. *J Am Chem Soc.* **2005**, *127*, 12847.

32. Que, E.L. Chang, C.J. *J Chem Soc Rev.* **2010**, *39,* 51.

33. Moats, R.A. Fraser, S.E. Meade, T.J. *Angew Chem Int Edit.***1997**, *36*, 726.

34. Marais, R. Spooner, R.A. Light, Y. Martin, J. Springer, C.J. *Cancer Res.* **1996**, *56*, 4735.

35. Urbanczyk-Pearson, L.M. Fernia, F.J. Smith, J. Parigi, G. Duimstra, J.A. Eckermann, A.L. Luchinat, C. Meade, T.J. *Inorg Chem.* **2008**, *47*, 56.

36. Hanaoka, K. Kikuchi, K. Terai, T. Komatsu, T. Nagano, T. *Chem Eur J.* **2008**, *14*, 957.

37. Que, E.L. Gianolio, E. Baker, S.L. Aime, S. Chang, C.J. *Dalton Trans.* **2010**, *39*, 469.

38. Que, E.L. Gianolio, E. Baker, S.L. Wong, A.P. Aime, S. Chang, C.J. *J Am Chem Soc.* **2009**, *131*, 8527.

39. Li, W.S. Luo, J.A. Chen, Z.N. *Dalton Trans.* **2011**, *40*, 484.

40. Li, W.H. Fraser, S.E. Meade, T.J. *J Am Chem Soc.* **1999**, *121*, 1413.

41. Mishra, A. Fouskova, P. Angelovski, G. Balogh, E. Mishra, A.K. Logothetis, N.K. Toth, E. *Inorg Chem.* **2008**, *47*, 1370.

42. Youn, J.H. McDonough, A.A. *Annu Rev Physol.* **2009**, *71*, 381.

43. Hifumi, H. Tanimoto, A. Citterio, D. Komatsu, H. Suzuki, K. *Analyst.* **2007**, *132*, 1153.

44. Paris, J. Gamiero, C. Humblet, V. Mohapatra, P.K. Jacques, V. Desreux, J.F. *Inorg Chem.* **2006**, *45*, 5092.

45. Aime, S. Fedeli, F. Sanino, A. Terreno, E. *J Am Chem Soc*. **2006**, *128*, 11326.

46. Lowe, M.P. Parker, D. Reany, O. Aime, S. Botta, M. Castellano, G. Gianolio, E. Pagliarin, R. *J Am Chem Soc.* **2001**, *123*, 7601.

47. Gianolio, E. Maciocco, L. Imperio, D. Giovenzana, G.B. Simonelli, F. Abbas, K. Bisi, G. Aime, S. *Chem Commun.* **2011**, *47*, 1539.

48. Martinelli, J. Fekete, M. Tei, L. Botta, M. *Chem Commun.* **2011**, *47*, 3144.

49. Raghunand, N. Guntle, G.P. Gokhale, V. Nichol, G.S. Mash, E.A. Jagadish, B. *J Med Chem.* **2010**, *53*, 6747.

50. Iwaki, S. Hanaoka, K. Piao, W. Komatsu, T. Ueno, T. Terai, T. Nagano, T. *Bioorg Med Chem Lett.* **2012**, *22*, 2798.

51. Renshaw, P.F. Owen, C.S. Mclaughlin, A.C.. Frey, T.G Leigh, J.S. *Magn Reson Imaging.* **1986**, *3*, 217.

52. Bulte, J.W.M. Kraitchman, D.L. *NMR Biomed.* **2004**, *17*, 1017.

53. Aime, S. Frullano, L. Crich, S.G. *Angew Chem Int Edit.* **2002**, *41*, 1017.

54. Hennequin, B. Turyanska, L. Ben, T. Beltran, A.M. Molina, S.I. Li, M. Mann, S. Patane, A. Thomas, N.R. *Ad Mater.* **2008**, *20*, 3592.

55. Yoo, D. Lee, J.H. Shin, T.H. Cheon, J. *Accounts Chem Res.* **2011,** *44*, 863.

56. Yu, M.K. Park, J. Jon, S. *Drug Deliv Tansl Res.* **2012**, *2*, 3.

57. Ling, Y. Wei, K. Luo, Y. Guo, X. Zhong, S.Z. *Biomat.* **2011**, *32*, 7139.

58. Medarova, Z. Pham, W. Farrar, C. Petkova, V. Moore, A. *Nat Med.* **2007**, *13*, 372.

59. Aoki, I. Ebisu, T. Tanaka, C. Katsuta, K. Fujikawa, A. Umeda, M. Fukunaga, M. Takegami, T. Shapiro, E.M. Naruse, S. *Magn Res Med.* **2003**, *50*, 7.

60. Bertin, A. Steibel, J. Michou-Gallani, A.I. Gallani, J.L. Felder-Flesch, D. *Bioconjugate Chem.* **2009,** *20*, 760.

61. Federle, M. Chezmar, J. Rubin, D.L. Weinreb, J. Freeny, P. Schmiedl, U.P. Brown, J.J. Borrello, J.A. Lee, J.K Semelka, R.C. Mattrey, R. Dachman, A.H. Saini, S. Harms, S.E. Mitchell, D.G. Anderson, M.W. Halford, H.H. Bennett, W.F. Young, S.W. Rifikin, M. *J Magn Reson Imaging.* **2000**. *12*, 689.

62. Mertzmann, J.E. Kar, S. Lofland, S. Fleming, T. Van Keuren, E. Tong, Y.Y. Stoll, S.L. *Chem Commun.* **2009,** 788.

63. Sherry, A.D. Woods, M. *Ann Rev Biomed Eng.* **2008,** *10,* 391.

64. http://www.guerbet.hk/index.php?id=4459. [Online] 2009.

65. Benetollo, F. Bombieri, G. Calabi, L. Aime, S. Botta, M. *Inorg Chem.* **2003**, *42*, 148.

66. Magerstadt, M. Gansow, O.A. Brechbiel, M.W. Colcher, D. Baltzer, L. Knop, R.H Girton, M.E. Naegele, M. *Magn Reson Med.* **1986**, *3*, 808.

67. Esqueda, A.C. Lopez, J.A. Andreu-De-Riquer, G. Alvarado-Monzon, J.C. Ratnakar, J. Lubag, A.J.M. Sherry, A.D. De Leon-Rodriguez, L.M. *J Am Chem Soc.* **2009**, *131,* 11387.

68. Mamedov, I. Taborsky, P. Lubal, P. Laurent, S, Elst, L.V. Mayer, H.A. Logothetis, N.K. Angelovski, G. *Eur J Inorg Chem.* **2009**, 3298.

69. Dunand, F.A. Aime, S. Merbach, A.E. *J Am Chem Soc.* **2000,** *122*, 1506.

70. Burai, L. Hietapelto, V. Kiraly, R. Toth, E. Brucher, E. *Magn Reson Med.* **1997**, *38*, 146.

71. Magerstadt, M. Gansow, O.A. Brechbiel, M.W. Colcher, D. Baltzer, L. Knop, R.H Girton, M.E. Naegele, M. *Magn Reson Med.* **1986**, *3*, 808.

72. Richman, J.E. Atkins, T.J. *J Am Chem Soc.* **1974**, *96*, 2268.

73. Machitani, K. Sakamoto, H. Nakahara, Y. Kimura, K. *Anal Sci.* **2008**, *24*, 463.

74. Viguier, R.F.N. Hulme, A.N. *J Am Chem Soc.* **2006**, *128*, 11370.

75. Sengar, R.S. Nigam, A. Geib, S.J Weiner, E.C. *Polyhedron.* **2009,** *28*, 1525.

76. Z. Baranyai, Z. Uggeri, F. Giovenzana, G.B. Benyeu, A. Brucher, E. Aime, S. *Chem Eur J.* **2009**, *15*, 1696.

77. Aime, S. Bombieri, G. Cavallotti, C. Giovenzana, G.B. Imperio, D. Marchini, N. *Inorg Chim Acta.* **2008**, *361*, 1534.

78. Gianolio, E. Giovenzana, G.B. Longo, D. Longo, I. Menegotto, I. Aime, S. *Chem Eur J.* **2007**, *13*, 5785.

79. Gugliotta, G. Botta, M. Giovenzana, G.B. Tei, L. *Bioorg Med Chem Lett.* **2009**, *19*, 3442.

80. Aime, S. Calabi, L, Cavallotti, C. Gianolio, E. Giovenzana, G.B. Losi, P. Maiocchi, A. Palmisano, G. Sisti, M. *Inorg Chem.* **2004**, *43*, 7588.

81. Krohn, K.A. Link, J.M. Mason, R.P. *J Nucl Med.* **2008**, *49*, 129s.

82. Mees, G. Dierekx, R. Vangestel, C. van de Wiele, C. *Eur J Nucl Med Mol Imaging.* **2009**, *36*, 1674.

83. Postema, E.J. McEwan, A.J.B. Riauka, T.A. Kumar, P. Richmond, D.A. Abrams, D.N. Wiebe, L.I. *Eur J Nucl Med Mol Imaging.* **2009**, *36*, 1565.

84. Everett, S.A. Naylor, M.A. Patel, K.B. Stratford, M.R.L. Wardman, P. *Bioorg Med Chem Lett.* **1999,** *9*, 1267.

85. Ware, D.C. Palmer, B.D. Wilson, W.R. Denny, W.A. *J Med Chem.* **1993**, *36*, 1839.

86. Mallia, M.B. Subramanian, S. Mathur, A. Sarma, H.D. Venkatesh, M. Banerjee, S. *J Labelled Compd Rad.* **2008**, *51*, 308.

87. Le Bars, D. *J Fluorine Chem.* **2006**, *127*, 1488.

88. K.L Bennewith, K.L. Raleigh, J.A. Durand, R.E. *Cancer Res.* **2002**, *62*, 6827.

89. Evans, S.M. Judy, K.D. Dunphy, I. Jenkins, W.T. Nelson, P.T. Collins. R. Wileyto, E.P. Jenkins, K. Hahn, S.M. Stevens, C.W. Judkins, A,R. Phillips, P. Geoerger, B. Koch, C.J. *Cancer Res.* **2004**, *64*, 1886.

90. Seddon, B.M. Payne, G.S. Simmons, L. Ruddle, R. Grimshaw, R. Tan, S. Turner, A. Raynaud, F. Halbert, G. Leach, M.O. Judson, I. Workman, P. *Clin Cancer Res.* **2003**, *9*, 5101.

91. Vavere, A.L. Lewis, J.S. *Dalton Trans.* **2007**, 4893.

92. Hockel, M. Knoop, C. Schlenger, K. Vorndran, B. Baussmann, E. Mitze, M. Knapstein, P.G. Vaupel, P. *Radiother Oncol.* **1993**, *26*, 45.

93. Palmer, B.D. Wilson, W.R. Cliffe, S. Denny, W.A. *J Med Chem.* **1992**, *35*, 3214.

94. Damen, E.W.P. Nevalainen, T.J. van der Bergh. T.J.M. de Groot, F.M.H. Scheeren, H.W. *Bioorg Med Chem.* **2002**, *10*, 71.

95. Denny, W.A. Wilson, W.R. *J Med Chem.* **1986**, *29*, 879.

96. Denny, W.A. *Eur J Med Chem.* **2001,** *36*, 577.

97. Brown, J.M. *Cancer Res.* **1999**, *59*, 5863.

98. Hicks, K.O. Flemming, Y. Siim, B.G. Koch, C.J. Wilson, W.R. *Int J Radiat Oncol Biol Phys.* **1998**, *42*, 641.

99. Monge, A. Martinezcrespo, F.J.Decerain, A.L. Palop, J.A. Narro, S. Senador, V. Marin, A. Sainz, Y. Gonzalez, M. Hamilton, E. Barker, A.J. *J Med Chem.* **1995**, *38*, 4488.

100. Urquiola, C. Vietes, M. Torre, M.H. Cabrera, M. Lavaggi, M.L. Cerecetto, H. Gonzalez, M. de Cerain, A.L. Monge, A. Smircich, P. Garat, B. Gambino, D. *Bioorg Med Chem.* **2009**, *17*, 1623.

101. Tomasz, M. Palom, Y. *Pharmacol Ther.* **1997**, *76*, 73.

102. Beall, H.D. Winski, S.I. *Front Biosci.* **2000**, *5*, D639.

103. Blower, P.J. Dilworth, J.R. Maurer, R.I. Mullen, G.D. Reynolds, C.A. Zheng, Y.F. *J Inorg Biochem.* **2001**, *85*, 15.

104. Urquiola, C. Vieites, M. Torre, M.H. Cabrera, M. Lavaggi, M.L. Cerecetto, H. Gonzalez, M. Cerain, A.L. Monge, A. Smircich, P. Garat, B. Gambino, D. *Bioorg Med Chem.* **2009**, *17*, 1623.

105. Ahn, G.O. Botting, K.J. Patterson, A.V. Ware, D.C. Tercei, M. Wilson, W.R. *Biochem Pharmacol.*2006, Vol. 71, p. 1683.

106. Ware, D.C. Brothers, P.J. Clark, G.R. Denny, W.A. Palmer, B.D. Wilson, W.R. *J Chem Soc Dalton Trans.* **2000**, 925.

107. Wang, Q. Chan, T.R. Hilgraf, R. Fokin, V.V. Sharpless, K.B. Finn, M.G. *J Am Chem Soc.* **2003**, *125*, 3192.

108. Rostovtsev, V.V. Green, L.G. Fokin, V.V. Sharpless, K.B. *Angew Chem Int Edit.* **2002,** *41*, 2596.

109. Prasuhn, D.E. Yeh, R.M. Obenaus, A. Manchester, M. Finn, M.G. *Chem Commun.* **2007,** 1269.

110. Powell, D.H. Pubanz, D. Helm, L. Lebedev, Y.S. Sclaepfer, W. Merbach, A.E. *J Am Chem Soc.* **1996**, *118*, 9333.

111. Elemento, E.M. Parker, D. Aime, S. Gianolio,E. Lattuada, L. *Org Biomol Chem.* **2009**, *7*, 1120.

112. Wang, X.Y. Jin, T.Z. Comblin, V. Lopezmut, A. Merciny, E. Desreux, J.F. *Inorg Chem.* **1992**, *31*, 1095.

113. Dubois, L. Landuyt, W. Cloetens, L. Bol, A. Bormans, G. Haustermans, K. Labar. D. Nuyts, J. Gregoire, V. Mortelmans, L. *Eur J Nucl Med Mol Imaging.* **2009**, *36*, 209.

114. Lin, Z. Fenghua, D. Yajing, L. Novel F-triazole ring-polyethyleneglycol-2-nitroimidazole compound and preparation method there of. China Patent, 101624392 2009, January 13, 2010.

115. M.I. Walton, M.I. Sugget, N. Workman, P. *Int J Radiat Oncol Biol Phys.* **1992**, 22, p. 643.

116. Jiang, Y.Y. Han, J.Y. Yu, C.Z. Vass, S.O. Searle, P.F. Browne, P. Knox, R.J. Hu, L.Q. *J Med Chem.* **2006**, *49*, 4333.

117. D. Spence: PhD, Univeristy of Nottingham, 2009.

118. Bejot, R. Fowler, T. Carroll, L. Boldon, S. Moore, J.E. Declerck, J. Gouverneur, V. *Angew Chem Int Edit.* **2009,** *48*, 586.

119. Song, Y. Kohlmeir, E.K. Meade, T.J. *J Am Chem Soc.* **2008**, *130*, 6662.

120. De Leon-Rodriguez, L.M. Kovacs, Z. Esqueda-Oliva, A.C. Miranda-Vera, A.D. *Tetraherdron Lett.* **2006**, *47*, 6937.

121. Wangler, C. Wangler, B. Eisenhut, M. Haberkorn, U. Mier, W. *Bioorg Med Chem.* **2008**, *16*, 2606.

122. Green, T.W. Wuts, P.G.M. *Protective Groups in Organic Synthesis.* 3rd.Edition: John Wiley & Sons inc. New York, 1999.

123. Heppeler, A. Froidevaux, HS. Macke, H.R. Jermann, E. Behe, M. Powel, P. Hennig, M. *Chem Eur J.* **1999**, *5*, 1974.

124. Knorr, R. Trzeciak, A. Bannwarth, WD. Gillessen, D. *Tetrahedron Lett.* **1989**, *30*, 1927.

125. Mani, T. Tircso, G. Zhao, P.Y. Sherry, A,D. Woods, M. *Inorg Chem.* **2009**, *48*, 10338.

126. Ferreira, M.F. Martins, A.F. Martins, J.A. Ferreira, P.M. Toth, E. Geraldes, C.F.G.C. *Chem Commun.* **2009**, 6475.

127. Reibenspies, J.H. *Acta Crystallogr, Sect C: Crys Struct Commun.* **1992**, *C48*, 1717.

128. Onisko, B.C. Tambling, D.R. Gorder, G.W. Diaz, D.G. Ericson, J.L. Prisbylia, M.P. Spilner, C.J. *J Agri Food Chem.* **2002**, *50*, 1922.

129. Zhu, Y.F. Yamazaki, T. Tsang, J.W. Lok, S. Goodman, M. *J Org Chem.* **1992,** *57,* 1074.

130. Gug, F. Bach, S. Blondel, M. Vierfond, J.M. Martin, A.S. Galons, H. *Tetrahedron.* **2004**, *60*, 4705.

131. Zheng, W.W. Hsieh, Y.H. Chiu, Y.C. Cai, S.J. Cheng, C.L. Chen, C.P. *J Mater Chem.* **2009**, *19*, 8432.

132. W. Drewe: PhD, University of Nottingham, 2008.

133. A.R.A.S. Deshmukh, V.K. Gumaste. Process for preparing alkyl/aryl chloroformates. US6919471 B2 2005, US patent 19th July, 2005.

134. Y. Takuma, Y. Kasuga, Y. Mizuho, T. Murakami. Preparation and extraction of 2-nitroimidazole. JP2001122861 2001, Japan Patent, 27th Oct, 2001.

135. Chu, T.W. Li, Z.J. Wang, X.Y. *Bioorg Med Chem Lett.* **2009**, *19*, 658.

136. Sen, S.E. Roach, S.L. *Synthesis.* **1995,** 756.

137. Palmer, B.D. Wilson, W.R. Anderson, R.F. Boyd, M. Denny, W.A. *J Med Chem.* **1996**, *39*, 2518.

138. Patterson, A.V. Ferry, D.M. Edmunds, S.J. Gu, Y.C. Singleton, R.S. Patel, K. Pullen, S.M. Hicks, K.O. Syddall, S.P. Atwall, G.J. Wang, S.J. Denny, W.A. Wilson, W.R. *Clinical Cancer Res.* **2007**, *13*, 3922.

139. Shyam, K. Penketh, P.G. Shapiro, M. Belcourt, M.F. Loomis, R.H. Rockwell, S. Sartorelli, A.C. *J Med Chem.* **1999,** *42*, 941.

140. Teicher, B.A. Sartorelli, A.C. *J Med Chem.* **1980**, *23*, 955.

141. Seow, H.A. Penketh, P.G. Shayam, K. Rockwell, S. Sartorelli, A.C. *Proc Natl Acad Sci USA.* **2005**, *102*, 9282.

142. Palmer, B.D. Vanzijl, P Denny, W.A. Wilson, W.R. *J Med Chem.* **1995**, *38*, 1229.

143. Liu, F. Austin, D.J. *J Org Chem.* **2001**, *66*, 8643.

144. Appel, R. *Angew Chem Int Edit.* **1975**, *14*, 801.

145. Lee, C.C. Zohdi, H.F. Sallam, M.M.M. *J Org Chem.* **1985**, *50*, 705.

146. Helsby, N.A. Ferry, D.M. Patterson, A.V. Pullen, S.M. Wilson, W.R. *Br J Cancer.* **2004**, *90*, 1084.

147. Anlezark, G.M. Melton, R.G. Sherwood, R.F. Coles, B. Friedlos, F. Knox, R.J. *Biochem Pharmacol.* **1992**, *44*, 2289.

148. Knox, R.J, Friedlos, F. Sherwood, R.F. Melton, R.G. Anelzark, G.M. *Biochem Pharmacol.* **1992,** 44, 2297.

149. Boland, M.P. Knox, R.J. Roberts, J.J. *Biochem Pharmacol.* **1991**, *41*, 867.

150. Knox, R.J. Boland, M.P. Friedlos, F. Coles, B. Southan, C. Roberts, J.J. *Biochem Pharmacol.* **1988**, *37*, 4671.

151. M. Matteucci, J.X. Duan, H. Jiao, J. Kaizerman, S. Ammons. Phosphoramidate alyklator prodrugs**.** WO2007/002931 2007, US patent, 4th January 2007.

152. M.R. Matteucci, J.X. Duan. Compositions and methods for treating cancer. WO2004/087075 2004, US patent, 14th October 2004.

153. Cavaller, B. Ballotta, R. Lancini, G.C. *J Hetercyclic Chem.* **1972**, *9*, 979.

154. Lancini, G.C. Lazzari, E. Arioli, V. Bellani, P. *J Med Chem.* **1969**, *12*, 775.

155. Asato, G. Berkelhammer, G. *J Med Chem.* **1972**, *15*, 1086.

156.Tochtrop, G.P. Sadhukhan, S. Han, Y. Zhang, G.F. Brunengraber, H. *J Am Chem Soc.* **2010,** *132*, 6309.

157. Taber, D.F. Guo, P.F. Guo, N. *J Am Chem Soc.* **2010,** *132*, 11179.

158. Yoon, N.M. Cho, B.T. *Tetrahedron Lett.* **1982**, *23*, 2475.

159. Hay, M.P. Sykes, B.M. Denny, W.A. Wilson, W.R. *Bioorg Med Chem Lett.* **1999**, *9*, 2237.

160. Ballani, A. Peal, V. Gros, L. Brun, R. Kaiser, M. Barrett, M.P. Gilbert, I.H. *Org Biomol Chem.* **2009**, *7*, 1154.

161. Mindt, T.L. Muller, C. Stuker, F. Salazar, J. Hohn, A. Mueggler, T. Rudin, M. Schibil, R. *Bioconjugate Chem.* **2009**, *20*, 1940.

162. Sivakumar, K. Xie, F. Cash, B.M. Long, S. Barnhill, H.N. Wang, Q. *Org Lett.* **2004**, *6*, 4603.

163. Chan, T.R. Hilgraf, R. Sharpless, K.B. Fokin, V.V. *Org Lett.* **2004**, *6*, 2853.

164. Aime, S. Bombieri, G. Cavallotti, C. Giovenzana, G.B. Imperio, D. Marchini, N. *Inorg Chim Acta.* **2008**, *361*, 1534.

165. Bejot, R. Kersemans, V. Kelly, C. Carroll, L. King, R. Gouverneur, V. *Nucl Med Biol. R.* **2010**, *37*, 1013.

166. Hille, R. *Eur J Inorg Chem.* **2006**, 1913.

167. Clarke, E. Goulding, K. Wardman, P. *Biochem Phamacol.* **1982**, *31*, 3237.

168. Tatsumi, K. Kitamura, S. Yoshimura, H. Kawazoe, Y. *Chem Pharm Bull.* **1978**, *26*, 1713.

169. Clarke, E. Wardman, P. Goulding, K. *Biochem Pharmacol.* **1980**, *29*, 2684.

170. Benniston, A.C. Gunning, P. Peacock, R.D. *J Org Chem.* **2005,** *70*, 115.

171. Jagadish, B. Brickert-Albracht, G. Nichol, G. Mash, E. Raghunand, N. *Tetrahedron Lett.* **2011**, *52*, 2058.

172. Montalbetti, C.A.G.N. Falque, V. *Tetrahedron.* **2005**, *61*, 10827.

173. Thomas, N.R. Quin-Yang, Y. Drewe, W. Biomolecular Labelling Using Multifunctional Biotin Analogues, 20120083599 2012, US patent, 5th April 2012.

174. Molteni, M. Volonterio, A. Fossati, G. Lazzari, P. Zanda, M. *Tetrahedron Lett.* **2007**, *48*, 589.

175. Kim, P. Zhang, L. Manjunatha, U.H. Singh, R. Patel, S. Jiricek, J. Keller, T. Boshoff, H.I. Barry, C.E. Dowd, C.S. *J Med Chem.* **2009**, *52*, 1317.

176. Corey, E.J. Venkateswarlu, A. *J Am Chem Soc.* **1972**, *94*, 6190.

177. Meyers, A.I. Durandetta, J.L. Munavu, R. *J Org Chem.* **1975**, *40*, 2005.

178. Nakamura, H. Usui, T. Kuroda, H. Ryu, I. Matsubara, H. Yasuda, S. Curran, D.P. *Org Lett.* **2003**, *5*, 1167.

179. Elban, M.A. Hecht, S.A. *J Org Chem.* **2008**, *73*, 785.

180. Yoon N. M, Cho B. T. *Tetrahedron Lett.* **1982**, *23*, 2475.